INVESTIGATION OF THE ABSORPTION PATHWAYS OF SOME POORLY ABSORBED DRUGS USING HUMAN INTESTINAL (CACO-2) CELL MONOLAYERS

ROY FOX

Doctor of Philosophy

ASTON UNIVERSITY

January 1999

ASTON UNIVERSITY

INVESTIGATION OF THE ABSORPTION PATHWAYS OF SOME POORLY ABSORBED DRUGS USING HUMAN INTESTINAL (CACO-2) CELL MONOLAYERS

Roy Fox

Doctor of Philosophy

January 1999

THESIS SUMMARY

Absorption across the gastro-intestinal epithelium is *via* two pathways; the transcellular and paracellular pathway. Caco-2 cells, when cultured on polycarbonate filters, formed a confluent monolayer with many properties of differentiated intestinal epithelial cells. As a model of human gastro-intestinal tract epithelia they were used to elucidate and characterise the transepithelial transport of two protein kinase C inhibitors, N-(3-chlorophenyl)-4-[2-(3-hydroxypropylamino)-4-pyridyl]-2-pyrimidinamin (CHPP) and N-benzoyl-staurosporine (NBS), and the polypeptide, human calcitonin.

Lanthanum ions are proposed as a paracellular pathway inhibitor and tested with D-mannitol permeability and transepithelial electrical resistance measurements. The effect La^{3+} has on the carrier-mediated transport of D-glucose and Sodiun taurocholate as well as the vesicularly transcytosed horseradish peroxidase was also investigated.

As expected, 2 mM apical La^{3+} increases transepithelial electrical resistance 1.5-fold and decreases mannitol permeability by 63.0 % ± 1.37 %. This inhibition was not repeated by other cations. Apical 2 mM La^{3+} was found to decrease carrier-mediated D-glucose and taurocholate permeability by only 8.7 % ± 1.6 %, 26.3 % ± 5.0 %. There was no inhibitory effect on testosterone or PEG 4000 permeability observed with La^{3+}. However, for horseradish peroxidase and human calcitonin permeability was decreased by 98.7 % ± 11.7 %, and 96.2 % ± 0.8 % respectively by 2 mM La^{3+}. Indicating that human calcitonin could also be transported by vesicular transcytosis.

The addition of 2 mM La^{3+} to the apical surface of Caco-2 monolayers produces a paracellular pathway inhibition. Therefore, La^{3+} could be a useful additional tool in delineating the transepithelial pathway of passive drug absorption.

Keywords: Lanthanum, tight junctions, paracellular pathway, transcellular pathway, transcytosis, protein kinase C inhibitors, polypeptide, human calcitonin, gastrointestinal, *in vitro*.

ACKNOWLEDGEMENTS

My grateful thanks to Dr John Hastewell, Dr Nick Lowther and Professor Bill Irwin, my supervisors for all their assistance and encouragement. Thanks also to the staff of the Novartis Horsham Research Centre for their assistance and support throughout the project.

Also Angela, my long suffering wife, without whose support none of this would have happened.

LIST OF CONTENTS

LIST OF TABLES AND FIGURES

CHAPTER ONE INTRODUCTION

1.1 GENERAL INTRODUCTION

Gastro-intestinal (GI) absorption of solutes, including therapeutic drugs, involves the passage from the intestinal lumen across the intestinal mucosa into the systemic circulation, either directly or *via* the lymphatics. The small intestine is considered the major site of solute absorption in humans and has evolved to maximise its absorptive surface area. The small intestinal surface area has been reported to be 120-200 m^2; in comparison, the colon is very much smaller at 0.25 to 0.3 m^2. The presence of folds of Kerckring, villi and microvilli result in a 600-fold increase in surface area compared to a simple tube (Figure 1.1). To aid digestion of complex food stuffs into constituent sugars, fats, and amino acids there are secretions from the liver and pancreas, as well as surface hydrolases. The liver produces bile salts and acids stored in the gallbladder and secreted into the duodenum to solubilise fats. The pancreas releases digestive juices into the duodenum which contains hydrolytic enzymes for the break down of carbohydrate, fats and proteins. Terminal digestion is carried out by hydrolytic enzymes associated with the brush border of the absorptive epithelial cell, the enterocyte (Caspary, 1992). Underlying the monolayer of epithelial cells that line the GI tract is the lamina propria, which is supported by a layer of smooth muscle, the muscularis mucosa. Together the three layers- epithelium, lamina propria, and muscularis mucosa are called the intestinal mucosa.

Epithelia protect all external surfaces of the body which is reflected in the generation of polarity at the interface. This polarity serves to maintain the composition of the compartments either side of the epithelium. In the GI tract, this polarity is demonstrated in the monolayer of epithelial cells that covers the inner surface of the stomach and intestine. The polarized epithelial cell phenotype is characterised by; 1) neighbouring cells connected to each other by intercellular junctional domains and to the basement membrane, 2) the distribution of plasma membrane proteins and lipids to three distinct surface domains apical, lateral, and basal, 3) the polarised distribution of cytoplasmic organelles and the cytoplasmic and cortical cytoskeleton.

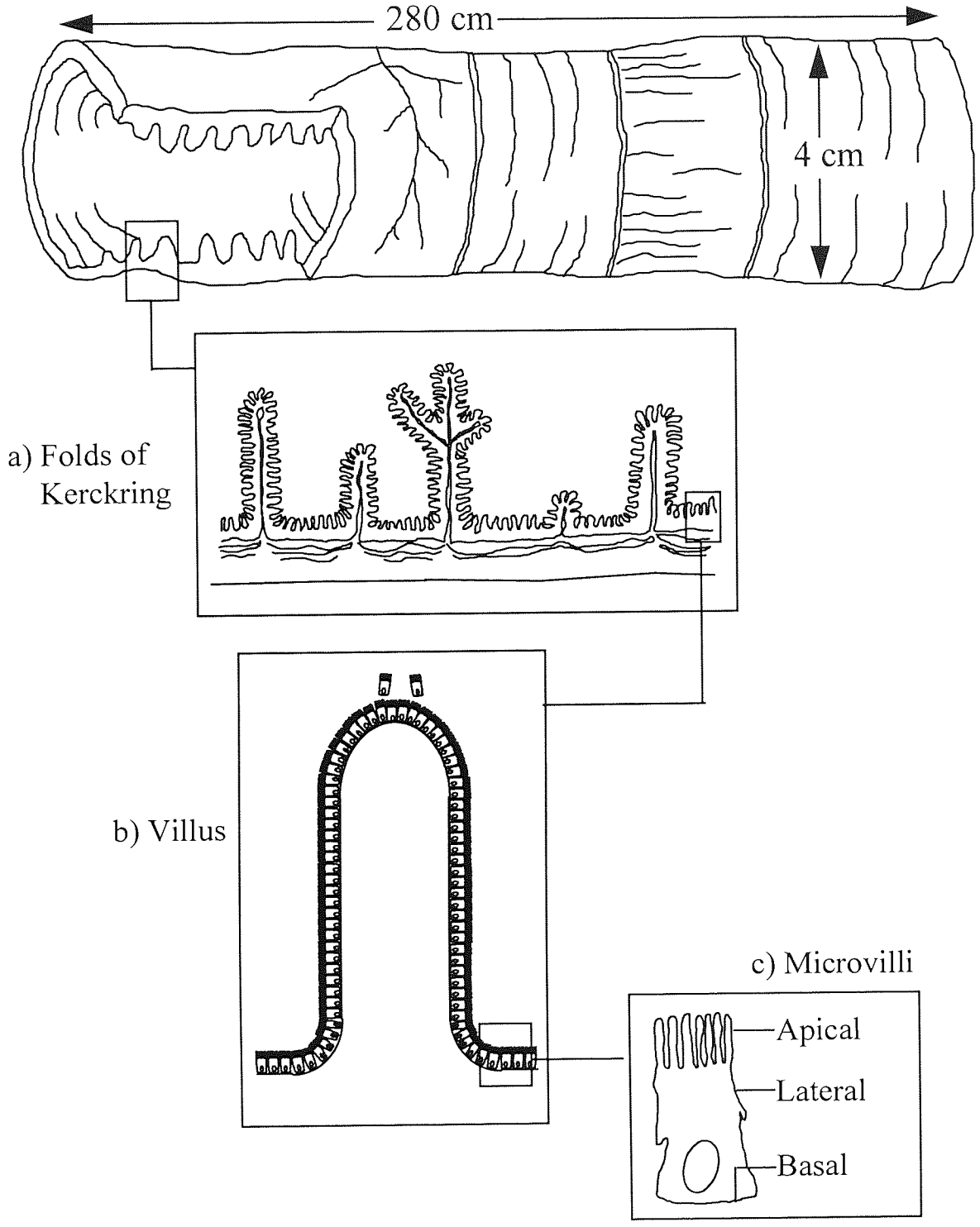

Figure 1.1 Morphological structures of the small intestinal mucosa. The presence of A) Folds of Kerckring, B) villi with proliferating and maturing epithelial cells travelling up the villi, to be lost at the tip, and C) microvilli on epithelial cells increases contact of digested food with the enzymes and transport carriers of the apical brush-border membrane. Whereas the lateral and basal membranes form cell-cell contacts and with the substratum respectively (adapted from Caspary, 1992).

The characteristic apical 'brush-border' of enterocytes, is the regular array of microvilli on the apical surface of the enterocyte (Figure 1.1c). These microvilli are approximately 1 μm in length and 0.1 μm in diameter and coated with the glycocalyx . The apical membrane of human enterocytes possess highly active enzymes plus numerous transport systems. In addition, enterocytes have a large number of mitochondria, a well-developed smooth and rough endoplasmic reticulum and Golgi system with many lysosomes and endosomes indicating they are highly active cells. Within the GI epithelium there are different cell types performing absorptive, secretive and protective functions which work in concert to maintain intestinal function (Mackay *et al.*, 1991). The GI tract epithelial cells are one of the most rapidly differentiating and renewing cell population. Within their life-span of approximately 5 days, they proliferate and differentiate from crypt cells into mature epithelial cells lost from the tip of the villi into the lumen of the intestine (Figure 1.1b). However, the continuity of the epithelium and its absorptive and protective barrier function is maintained. But this process may also give rise to the pores that allow macromolecular absorption.

1.2 INTESTINAL ABSORPTION

Absorption from the intestinal lumen across the GI epithelial monolayer into the body is *via* two potential routes. Transepithelial absorption is achieved either by going around the cell *via* the intercellular junctions (paracellular) or crossing the cell (transcellular) (Figure 1.2). The passive diffusion of molecules through the paracellular pathway is restricted by the tight junctional complex limiting the transport to ions, small solutes with calculated Stokes radius less than 11Å and water (Madara and Dharmsathaphorn, 1985). The transcellular pathway is of major importance to an absorbing epithelium. This is where the selective and regulative nature of the absorbing epithelium is exhibited, through the expression of different transporters or receptors on the apical surface of the cell. However, for drug absorption, passive diffusion across the intestine *via* the apical and basolateral membranes is considered to be the most important route. In the apical membrane of intestinal cells carrier-mediated absorption is performed by; 1) facilitated diffusion which aids in the passive diffusion of a number of essential nutrients in to the cell, 2) secondary active where the absorption of solute is linked to the energy supplied by the movement of another solute, usually Na^+, into or out of the cell, synport or antiport transporters. The

only active transport carrier-mediated protein that has been discovered to date in the apical membrane is the P-glycoprotein efflux pump which may constitute a barrier to drug absorption (see section 1.3.1.3). Vesicular endocytosis, either clathrin or caveolin coated, is also a selective process for nutrient uptake which could lead to transcytosis of molecules across the epithelium (see section 1.2.2.3). Liberation across the basolateral membrane into the body is *via* a different set of transporters which may have similar transport characteristics but different energy requirements.

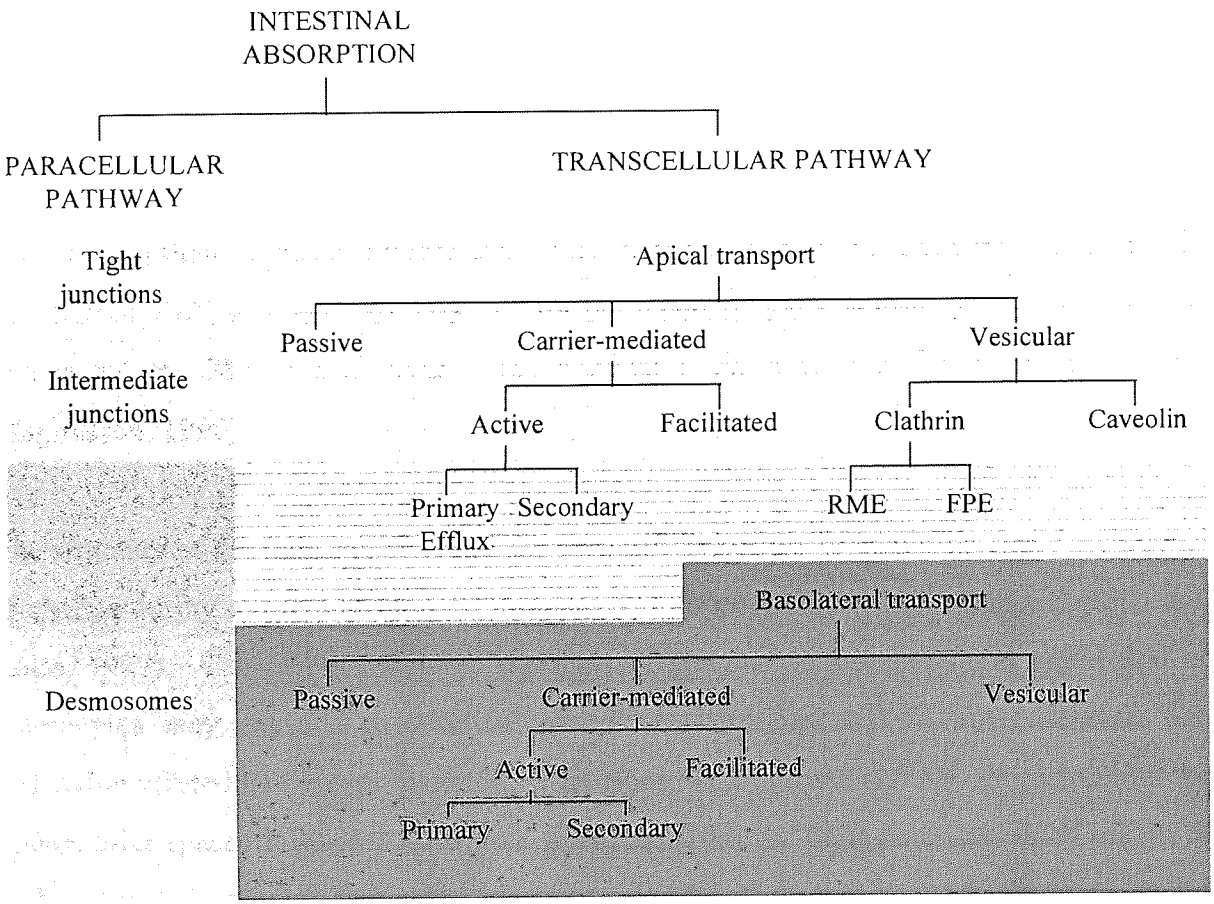

Figure 1.2 Schematic of the transport pathways and absorption processes available to intestinal epithelia. The two pathways are the paracellular pathway (grey) and the transcellular pathway with the processes that are required to cross the apical (light grey) and basolateral membrane (dark grey). RME = receptor mediated endocytosis; FPE = fluid phase endocytosis.

1.2.1 THE PARACELLULAR PATHWAY

The GI tract epithelium is not a continuous lipid bilayer, but has divisions between the cells called junctional complexes. The junctional complex is a major characteristic of

absorptive and secretory epithelia and contributes to the function of the transepithelial permeability barrier. Tight junction structure and function has been recently reviewed (Anderson and Van Itallie, 1995; Lutz and Siahaan, 1997; Denker and Nigam, 1998).

There is growing evidence that tight junctions are dynamic structures (Hill and Shachar-Hill, 1993) that influence and regulate paracellular transport (Cereijido *et al.*, 1981, 1988; Gumbiner, 1987; Madara *et al.*, 1987; Madara 1988, 1989). Factors which influence the tight junction are cytochalasin D (Madara *et al.*, 1986), hormones (Coleman and Kan, 1990) and drugs that affect the intracellular concentration of cAMP (Bentzel *et al.*, 1980, 1991; Duffey *et al.*, 1981; Balda, 1991; Balda *et al.*, 1991) and protein kinase C (Stenson *et al.*, 1993). It is also known that the tight junctions are connected to the cytoskeleton of the cell and that changes in this may have an influence on the shape of the tight junction and therefore on their permeability (Madara, 1987; Madara *et al.*, 1987; Schnittler *et al.*, 1990). In addition, Ca^{2+} and Mg^{2+} are required for the integrity and functioning of tight junctions (Meza *et al.*, 1980; Pitelka *et al.*, 1983; Gonzalez-Mariscal *et al.*, 1990; Artursson and Magnusson, 1990).

The structure of the tight junction and the permeability of the intercellular space are known to change during nutrient absorption (Madara and Pappenheimer, 1987; Pappenheimer and Reiss, 1987). The carrier-mediated transport of glucose across the apical membrane of enterocytes may cause a cytoskeletal contractile response that in turn decreases the restriction offered by the tight junction. This along with glucose and Na^{+} extrusion into the intercellular space, develops an osmotic gradient across the tight junction which results in high solvent drag. Madara (1991) suggests that solvent drag through the paracellular pathway is the principal route for intestinal transepithelial transport of glucose after a meal. However, Diamond (1991) does not agree with their conclusions because two studies have estimated that intestinal luminal glucose concentrations were 6- to 60-fold lower (50 to 0.5 mM) and, further, the absorption of unabsorbable sugars, L-glucose and D-mannitol were negligible in the presence and in the absence of D-glucose. He also stated that it would lead to poor discrimination by the paracellular pathway allowing toxic substances of small molecular size to pass and intoxicate the organism.

1.2.2 THE TRANSCELLULAR PATHWAY

1.2.2.1 PASSIVE DIFFUSION ACROSS THE MEMBRANE

The epithelial cell is limited in its ability to exert any control over transcellular passive absorption. The physico-chemical characteristics of the drug molecule dictate if molecules diffuse across the epithelial cell barrier. Passive diffusion is modelled by Fick's law of diffusion which states that the rate of diffusion is proportional to the concentration gradient. The linear relationship between rate of transport and concentration shows no evidence of saturation and the slope of the line being the diffusion constant.

In general, it is thought that for conventional drug molecules, a strong correlation exists between the partition coefficient and absorption. The partition coefficient measures relative lipophilicity of a molecule and has long been recognised as one of the major determinants in membrane permeability of drugs (Leo *et al.*, 1971; Ho *et al.*, 1983). This led to the development of more lipophilic drugs in the attempt to improve permeability. But the relationship between lipophilicity and membrane permeability is parabolic (Kararli, 1989; Nook *et al.*, 1988). This was corroborated by Wils *et al.* (1994) using the intestinal HT-29 and Caco-2 cell lines. They found that for a series of drugs with log D (pH 7.4) between -3.1 and 5.2 that log D values lower than 3.5, the apparent permeability coefficient (P_{app}) increased with increasing lipophilicity. But for Log D values above 3.5, P_{app} decreased demonstrating the parabolic relationship. Alcorn *et al.* (1993) measured the partition and distribution coefficients into rat small intestine BBMV for a variety of ionisable *e.g.* atenolol and non-ionisable drugs *e.g.* naphthylsulphonamide. Brush-border membrane vesicle partition coefficients of greater than 3 were not observed, even for solutes with Log P values in model solvents that were greater than 5. They explained the apparent discrepancy by a "surfactant-like" orientation of the drug into the membrane and an interaction of the ionized drug with the charged phospholipid head groups. Solute partition/distribution coefficients in model solvents is only one factor among many and should not be used in isolation as a predictor of intestinal absorption. Studies have shown that a simple relationship between partition coefficient and membrane permeability is not reliable for a broad class of compounds (Artursson, 1990; Rubas *et al.*, 1993) and the test is not sufficiently reliable to replace *in-vivo* studies (Alcorn *et al.*, 1991; Nook *et al.*, 1988; Collado *et al.*, 1988).

Lipophilicity and aqueous solubility are interrelated and often share a compensatory relationship; highly lipophilic compounds will typically have low aqueous solubility and *vice versa*. Aqueous solubility will dictate the amount of drug in solution and hence the amount available for absorption. A compound with a balance between these two properties presents the best case for achieving high absorption. For compounds containing highly polar groups, *e.g.* protein, peptides and some peptidomimetics, desolvation and the breaking of H-bonds may be the rate-limiting step, for a solute in the external aqueous phase to become incorporated into the hydrophobic bilayer and transfer across the epithelium (Burton *et al.*, 1992; Kim *et al.*, 1993).

Size is another important determinant for passive transcellular absorption, as measured by molecular weight (M_r), the higher the M_r the lower the absorption. For example the β-blockers alprenolol and propanolol with Log D (at pH 7.4) 1.38 and 1.55 and M_r of 249.3 Da and 259.3 Da respectively are completely absorbed (Artursson and Karlsson, 1991). Whereas, for the neutral lipophilic (Log D 3.6) endecapeptide Cyclosporin-A with a M_r of 1202 is incompletely absorbed. Approximately 40 % of an oral dose is absorbed; of that oral dose, approximately 30 % is bioavailable the reduced systemic availability is due to first-pass metabolism in the intestine and liver (Wood *et al.*, 1983).

1.2.2.2 NON-VESICULAR CARRIER-MEDIATED CELL UPTAKE

Transport systems can be described in a functional sense according to the number of molecules moved and the direction of movement. A uniport system moves one type of molecule bidirectionally. In cotransport systems, the transfer of one solute depends upon the stoichiometric simultaneous or sequential transfer of another solute. A symport moves these solutes in the same direction e.g. Na^+-glucose transporter and Na^+-amino acid transporter. Antiport system moves 2 molecules or ions in opposite directions e.g. Na^+/Ca^{2+} exchanger. The following features are characteristic of carrier-mediated transport processes that are generally considered sufficient, and often, necessary criteria for the implication of carriers in the transport of a given solute:-

1) All carriers appear to display a high degree of structural specificity with regard to the substance they will bind and transport. For example a high degree of selectivity within the

class of molecules the pyrimidines exists, with uracil and thymine being absorbed to a much greater degree than cytosine (Bronk and Hastewell, 1987). Also, transporters exhibit stereoselectivity in the case of sugars and amino acids; dextrorotary glucose is preferentially transported but not levorotary glucose whereas the L-stereoisomers but not D-stereoisomer amino acids are transported.

2) All carrier-mediated transport processes exhibit saturation kinetics: that is, the rate of transport gradually approaches a maximum as the concentration of solute transported by the carrier increases. Plots of the rate of transport against concentration often closely resemble the hyperbolic plots characteristic of Michaelis-Menten enzyme kinetics (Figure 1.3a). The kinetics of the mediated transport process can be described by defining the maximum transport rate (J_{max}) and the substrate concentration at which the transport rate is half maximum (K_t).
Thus;

$$J_i=[J_{max}(C_i)/(K_t+C_i)]$$

where C_i is the substrate concentration. In contrast, transport due to simple diffusion, as predicted by Fick's law, is linear (Figure 1.3b).

Fick's first law of diffusion;

$$J_i=D \cdot A\ (C_o-C_i/dx)$$

where, the transport rate J_i, with a diffusion coefficient D, crossing an area A is proportional to a concentration difference (C_o-C_i) over a distance dx.

There are two types of carrier-mediated transport processes; facilitated diffusion and active transport. Facilitated diffusion is a carrier-mediated process only capable of transferring a substance from a region of high concentration to one of a lower concentration. Although facilitative diffusion has similarities to active transport: 1) a specific binding site for the solute, 2) the carrier is saturable, 3) there is a binding constant (K_m), and 4) structurally

similar competitive inhibitors block transport. The major differences are: 1) facilitated diffusion can transport in either direction, whereas active transport is usually driven in one direction, 2) active transport of a solute is the movement of that solute up its electrochemical potential gradient which requires energy to be expended. The classic example of facilitated diffusion, is glucose transport across the membranes surrounding many animal cells, such as erythrocytes, striated muscle and adipocytes. The carrier GLUT (1-5) promotes the transport of glucose down a concentration gradient with the transport rate increasing with increasing glucose concentration, but ultimately approaches a maximum rate.

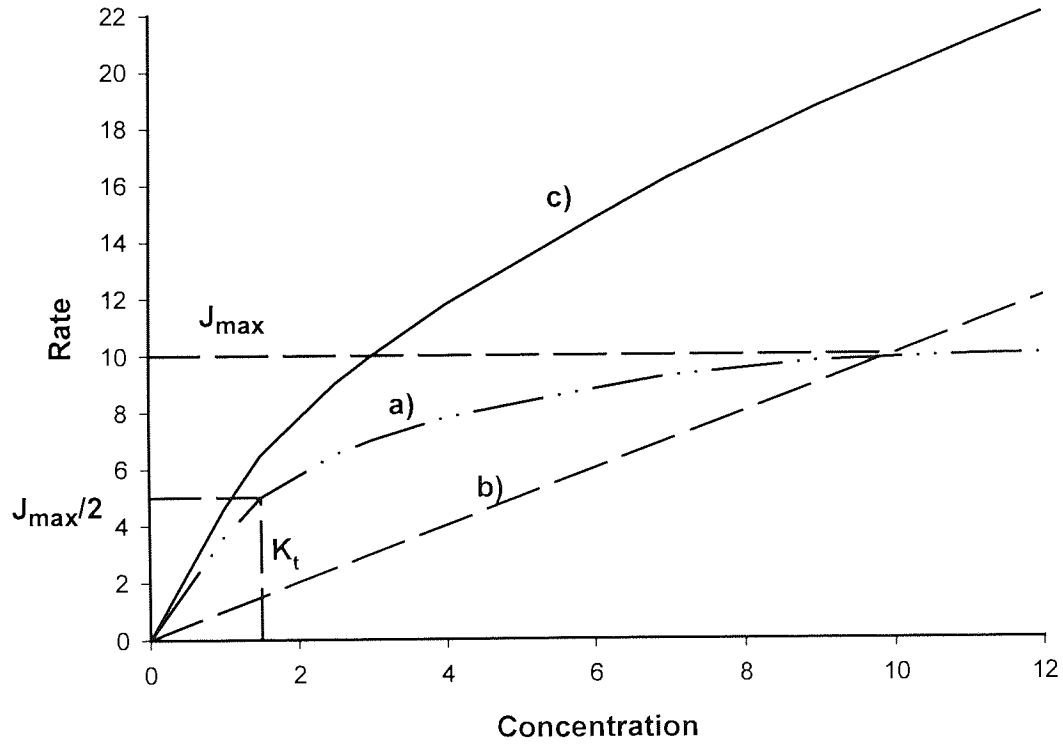

Figure 1.3 Relationship between flux and concentration for passive and carrier-mediated transport processes. a) Relationship between flux (J_i) and concentration (C_i) for a saturable process illustrating J_{max} and K_t the concentration at which J_i is one-half J_{max} (dash-dot-dot line). b) Linear relation between flux and concentration characteristic of diffusional processes (dashed line). c) Combination of both processes as possibly seen for a compound that is absorbed by both mechanisms (solid line).

Active carrier-mediated transport is capable of net transfer of an uncharged solute from a region of low concentration to one of higher concentration, or the transfer of a charged solute against the combined chemical and electrical gradients. There are two types of active transport processes, termed primary active transport and secondary active transport, differing in the ways they derive (or are coupled to) a supply of energy. Primary active transport implies that the carrier mechanism responsible for the movement of a solute is directly coupled to metabolic energy namely adenosine triphosphate (ATP). Three examples and the best studied primary active transport processes in animal cells are Na^+/K^+-ATPase (Skou and Norby, 1979), Ca^{2+}-ATPase (Carafoli, 1991) and H^+-ATPase (Mego *et al.*, 1972). Secondary active transport mediates the uphill movement of solutes but is not directly coupled to metabolic energy. Instead, the energy required is derived from the coupling to the downhill movement of another solute, cotransport *e.g.* the Na^+-coupled cotransport of D-glucose and L-amino acid uptake across the apical membrane of small intestinal cells. Two examples of secondary active countertransport are Na^+-H^+ exchanger (Murer *et al.*, 1976) and Na^+-Ca^{2+} exchanger (Affolter and Carafoli, 1980). In both instances, H^+ and Ca^{2+} are extruded from the cell coupled to the downhill influx of Na^+ into the cell.

1.2.2.3 VESICULAR PROCESSES

Vesicular transcytosis is a multi-step process involving endocytosis, transport across polarised epithelium and exocytosis at a different cell surface domain (Figure 1.4). In epithelial cells, studied so far, endocytosis proceeds from both cell surface domains with comparable kinetics, and the internalised molecules initially accumulate in distinct apical and basolateral early endosomes. These early endosomes undergo sorting, fusion with intracellular organelles, modification and recycling of plasma membrane. Tracer studies indicate that the content of early endosomes from both cell surfaces can be delivered to common late endosomes (Hughson and Hopkins, 1990). In some cells, however, recycling of fluid-phase or membrane proteins, ligands, and their receptors can occur from late endosomes (Bomsel *et al.*, 1989). Therefore, there is a possible route for vesicular transcytosis. How molecules move from one early endocytic pathway to the common late endosome and be exocytosed at the opposite cell surface domain remains unclear.

There are two types of endocytosis, fluid-phase endocytosis or pinocytosis (non-specific endocytosis) and absorptive endocytosis (specific endocytosis). Non-specific endocytosis is the vesicular uptake of extracellular fluid containing dissolved solutes. Specific endocytosis is solute binding to the cell membrane followed by internalization. Receptor-mediated endocytosis is a special case of absorptive endocytosis. Phagocytosis, vesicular uptake of large particles (0.5 μm) or molecular complexes, is also considered a form of endocytosis. However, this process is limited to specialised cells such as macrophages and granulocytes. Non-specific endocytosis differs from specific endocytosis in the following aspects:- 1) solute uptake varies linearly with its concentration in the medium, showing no evidence of saturation over a large concentration range; 2) uptake of labelled solute is not reduced in the presence of unlabelled solutes, and 3) when two or more solutes are tested their uptake rates are similar.

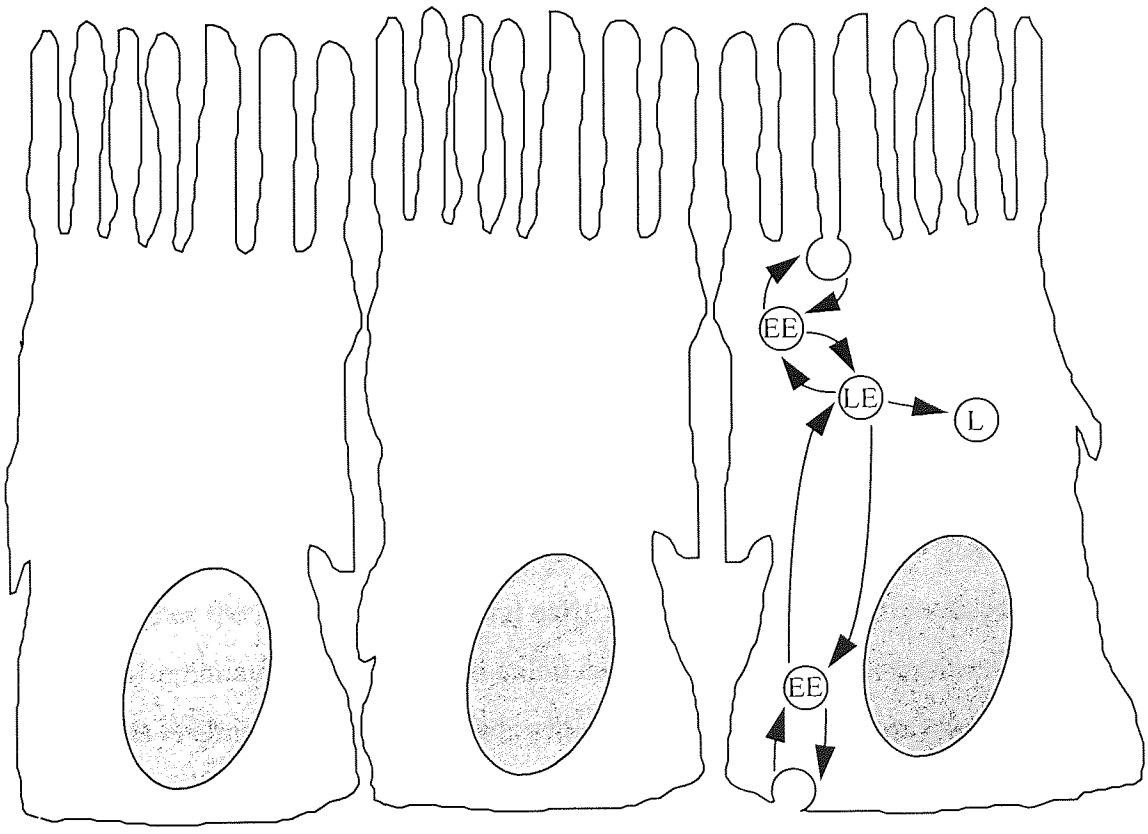

Figure 1.4 A diagram to show the potential fate of endocytosed material in intestinal epithelial cells. EE = early endosomes, LE = late endosomes, L = lysosome.

In epithelial cells, non-specific endocytosis is negligible compared with specific endocytosis, since the protein uptake rate of specific endocytosis can be 100-1000 times higher than that of non-specific endocytosis (Steinman *et al.*, 1983).

a) Receptor-mediated endocytosis

Russell-Jones (1996) described four ways receptor-mediated endocytosed material is processed within a cell. The fate of endocytosed receptor after it has bound its ligand depends on whether; 1) the receptor is recycled *e.g.* asialoglycoprotein (Mostov and Simister, 1985) or degraded *e.g.* epidermal growth factor receptor, after dissociation from its ligand through acidification of the early endosome. The dissociated ligand and/or the receptor are then routed to the lysosome for degradation. 2) the receptor-ligand complex is unaffected by the acidification and the complex is directly routed to the lysosome for degradation *e.g.* insulin receptor (Féger *et al.*, 1994). 3) the endocytosis of transferrin-bound iron and the recycling of transferrin to the plasma membrane. 4) the endocytosed material that is transcytosed across the polarised epithelial cell. The absorption of vitamin-B_{12} (cobalamin, Cbl) neonatal immunoglobulin and iron use receptor-mediated transcytosis to enter the body (Russell-Jones, 1996). Also, many viruses (Daniels *et al.*, 1985), plant lectins (King *et al.*, 1980) and toxins gain entry into the body via receptor-mediated endocytosis (Olsnes *et al.*, 1974).

b) Fluid-phase endocytosis

The kinetics and mechanisms of fluid-phase transcytosis has been analysed mainly in intestinal and kidney cultured cell lines grown on permeable supports. The fluid-phase marker enters either the apical or basolateral early endosomes but their fate depends on the cell type. In differentiated HT-29 human colon carcinoma cells, the content of basolateral early endosomes is almost entirely recycled, while less than 10 % is transcytosed (Godefroy *et al.*, 1990).

In Madin-Darby canine kidney (MDCK) cells the rates of internalisation from the apical or basolateral surface are identical, but the fate of the molecules internalised from the apical and basolateral domains differ. Using horseradish peroxidase (HRP) as tracer, it was observed that early apical endosomes distributed only 10 % of their fluid-phase content to

late endosomes. While the other 90 % was released from the cell, 45 % by transcytosis to the basolateral membrane and 45 % by recycling to the apical membrane. In contrast, about 75 % of the HRP that entered basolateral early endosomes was directed to the late endocytic compartment, and only 15 % was transcytosed to the apical membrane (Bomsel *et al.*, 1989).

Whereas, in MDCK cells the apical to basolateral transcytotic pathway is dominant, in Caco-2 cells, apical to basolateral transcytosis of HRP was visualised (Hildago *et al.*, 1989; Ma *et al.*, 1993) and detected (Heyman *et al.*, 1990) but others have not detected it (Hughson and Hopkins, 1990). Heyman *et al.* (1982) demonstrated *in vitro* with segments of rabbit jejunum that HRP transport is *via* two transcellular routes, direct and degradative. The amount of HRP travelling *via* each of the routes in the mucosal-to-serosal direction is 3 % and 97 % respectively. Whereas, in the opposite direction they observed 12 % and 88 %.

Thus, it appears that transcytosis in different cell types has distinct rates and directionality. Furthermore, transcytosis in cultured "model" cell monolayers may not accurately reflect transport activity in the corresponding cell *in vivo* (Heyman *et al.*, 1988; Heyman *et al.*, 1990). Heyman *et al.* (1990) compared the rate of transcytosis across jejunum of healthy children and under the same conditions in Caco-2 cells. Taking into account the increase in surface area of the jejunum over the Caco-2 monolayers, they indicated that the Caco-2 cells have a larger capacity, about 5-times, for transcytosis than intact intestine. Although these conditions are inherent to the models used, they give an indication of the mechanism and amount that is possible to transcytose across an epithelium. Also, giving the researcher an indication of qualitative and quantitative differences in this route of absorption and its potential to drug delivery.

1.3 BARRIERS TO INTESTINAL DRUG ABSORPTION

The biological barrier of the intestinal mucosa consists of a physical and an enzymatic component. The physical barrier consists of cellular components; the lipid bilayer of the apical and basolateral cell membrane, the multidrug efflux pump in the apical membrane, the intercellular tight-junctions and the combination of the glycocalyx and the mucus

secreted from the intestinal epithelium. The intra- and extracellular enzymatic component of the barrier arises from enzymes associated with the different physical barriers (Figure 1.5).

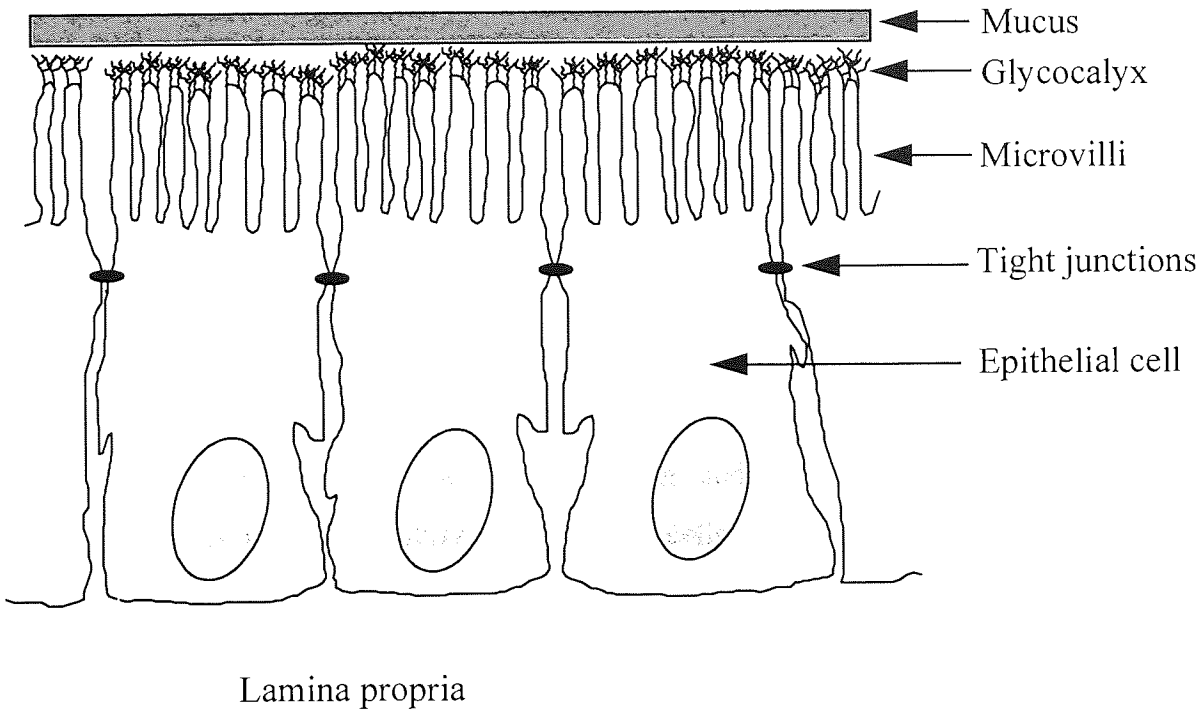

Figure 1.5 Epithelial cell and its related structures

1.3.1 PHYSICAL BARRIERS

In the intestinal lumen, pancreatic and biliary juices, intestinal motility, mucus, glycocalyx and resident microflora interact to limit the amount of time substances and entero-pathogens come into contact with the intestinal epithelium, the main barrier to drug absorption. Although not part of the epithelium, mucus on the surface of the intestinal mucosa, shields the epithelial cells from direct contact with the luminal contents and thus can potentially be a diffusional barrier.

1.3.1.1 UNSTIRRED WATER LAYER

In order to cross the epithelial layer a drug must first diffuse through the unstirred water layer (USWL) which consists of the glycocalyx, mucus, and a stationary layer of water before absorption across the epithelium is possible. The glycocalyx is a series of glycosylated proteins protruding from the apical membrane of the epithelial cell, supporting the mucus on top of the epithelial cell and forming the basis of the USWL (Thomson and Dietschy, 1977). Movement through this USWL has been regarded as a

simple diffusion process dependent on the thickness of the layer. The USWL was thought to be 600 μm in depth (Read *et al.*, 1977) and would represent a major barrier to diffusion. It now appears from work carried out in dogs, that the maximum thickness of the USWL is only 40 μm (Strocchi and Levitt, 1991), achieved by efficient stirring within the GI lumen through peristalsis and contractile movement of villi and microvilli. The composition of the USWL changes along with varying amounts and composition of mucus in different regions of the GI tract (Procter, 1973; Sakakurra, 1983; Rhodes, 1990). Both quoted values 40 μm and 600 μm seem to be relevant in human intestine, as the range of mucus thickness reported in the human intestine (MacAdam, 1993). It still implies that this layer constitutes an appreciable barrier to compounds that permeate by diffusion.

The mucus layer also helps in the formation and maintenance of an acid micro-environment trapped directly above the epithelial cells (Lucas and Blair, 1978). This acidic micro-environment, which sometimes measures a full pH unit lower than the bulk luminal contents, can also act as a barrier or enhance drug absorption depending on drug solubility and ionisation. As a consequence, the charged state of the drug at the epithelial surface rather than in the bulk phase of the lumen is the significant factor (Schanker *et al.*, 1985). The blanket of mucus covering the entire length of the GI tract is essential to its physiological function. The balance of mucus secretion by goblet cells in the epithelium and loss by enzymatic degradation and physical erosion, along with its buffering capacity, gives the mucus layer its ability to protect the underlying epithelium. The gel protects against autodigestion of the GI tract by presenting a diffusional barrier to the enzymatic macromolecules, pepsin, trypsin *etc.* present in the luminal contents.

The mucus layer is a layer of glycoprotein gel with the potential for interaction with drugs and the consequent retardation of diffusion through the mucus. Therefore, two important aspects of drug interactions with mucus should be considered; that of drug binding to mucus and the effects of mucus on drug diffusion (MacAdam, 1993). The drug tetracycline hydrochloride has been well investigated with regard to its binding with mucus. Mucus, will be neutral below pH 2 and negatively charged above pH 2. Thus, maximal binding of tetracycline will occur at approximately pH 3, in the stomach, where the tetracycline is positively charged and the mucus is negatively charged, due to the

ionisation of the sialic acid and sulphate residues. Above pH 3, tetracycline becomes neutral and at pH 7, in the small intestine, negatively charged leading to low mucus binding. Any binding at higher pH's is possibly as a result of hydrophobic interactions with the globular protein region or with lipid associated with the glycoprotein, or as a result of hydrogen bonding with sugar residues.

There are reports indicating that the rate-limiting step to the absorption of lipophilic solutes is their transfer across the aqueous diffusion barrier. But, in one study, testosterone was shown to bind extensively to gastric and small intestine mucus possibly as a result of interaction with the hydrophobic regions of the glycoprotein. Thus mucus may form a drug reservoir (Hughes 1988). Several studies have revealed that the presence of mucus, both native and purified, may produce up to a 5-fold reduction in the diffusion rate of hydrogen ions, water, and certain drugs *e.g.* benzylpenicillin (Cheema *et al.*, 1984; Sarosiek *et al.*, 1984: Turner *et al.*, 1985). It is difficult to know whether this is due to drug binding to mucus or the diffusional barrier posed by the USWL and mucus. It is possible that decreasing the pH of mucus, by the addition of an acidic drug, increases intermolecular interactions of the glycoprotein molecule resulting in a more tortuous path for drug diffusion through the gel. However, there are drugs which do not bind to, or increase, mucus viscosity, yet still have decreased perfusion through mucus *e.g.* caffeine (MacAdam, 1993). It would appear that the mucus itself acts as a diffusional barrier by virtue of its gel matrix increasing the USWL. Mucus type has also been shown to be a factor influencing drug diffusion, which is slower in the small intestine mucus compared to gastric mucus. This was explained by the more expanded macromolecular structure due to electrostatic repulsion forces from the higher sialic acid content. Such an expanded structure could again result in an effective increase in the USWL and tortuosity of the diffusion path.

Winne and Verheyen (1990) compared the diffusion coefficients of 6 compounds; urea, benzoic acid, antipyrine, aminopyrine, α-methyl-glucoside and L-phenyl-alanine and found in rat intestinal mucus a 50-60 % reduction compared to buffer solutions. They concluded, that compared to free water the mucus represents a considerable hinderance to the passage of certain compounds. In contrast, Desai and Vadgama (1991) showed little retardation of low-molecular-weight uncharged solutes through gastric mucus compared with higher

molecular-weight compounds which were markedly retarded. Charged solutes with low molecular-weight diffused much slower than similar uncharged compounds which indicates the involvement of ionic interactions in the diffusion process. Other factors may also affect drug diffusibility through mucus, increased mucus secretion increasing the depth of the mucus layer, or changes in the glycoprotein content affecting the viscosity or porosity of the mucus layer.

1.3.1.2 EPITHELIAL CELLS

Knowledge of the organisation, turnover, and differentiation of the intestinal epithelium is central to the understanding of its barrier function. Intestinal cell proliferation is at least in part constitutive, allowing fine tuning of proliferation by a number of stimulatory and inhibitory factors *e.g.* TGF-β or essential energy substrates. Proliferation is increased during regeneration, or accelerated cell death, or exposure to mitogenic factors. Cell differentiation is also primarily constitutive, all the factors that up- or down-regulate the rate of differentiation are still unknown in the normal adult intestine. Cell death is initiated in the intestinal epithelium before they are lost from the villus. This may occur by three mechanisms: 1) cell shedding, the cells at the tip of the villus are lost either singularly or in sheets. This is through loose attachment to the basement membrane and are easily dislodged by mechanical forces through intestinal motility and luminal contents. 2) Necrosis or cell lysis is the result of cell injury through cellular or soluble factors. Finally, 3) apoptosis or programmed cell death which results in membrane-bound apoptotic bodies. These bodies can be either shed into the lumen or phagocytosed. Injury to the intestinal epithelium may occur as part of normal physiological processes or as a result of physical or chemical injury. The epithelium response to injury, initially involves mucus secretion to cover the exposed wound. Followed by, phenotypic, secretory, and biochemical changes in enterocytes to seal the epithelium wound with cell migration (restitution), and accelerated epithelial cell regeneration.

The epithelial monolayer of the GI tract constitutes the major barrier to drug absorption. The selective nature of nutrient absorption in the small intestine is created by the polarity of protein expression of carrier-mediated nutrient transporters or receptors for receptor-mediated endocytosis. The passive transport of molecules across the cell barrier relies on

the physico-chemical properties of the molecule rather than any control by the epithelial cell. Yet metabolic processes within the cell may still act as an effective barrier to absorption. To take advantage of the transcellular route, a drug must either have the structural characteristics of the naturally transported substrate or have the physicochemical properties that will allow passive absorption across the cellular barrier (Amidon *et al.*, 1980).

1.3.1.3 P-GLYCOPROTEIN

The multi-drug resistance 1 (MDR1) gene product P-glycoprotein, a multidrug efflux pump, was first recognised in tumour cell lines displaying cross-resistance to various anticancer agents (colchicine, anthracyclines, epipodophyllotoxines and vinca alkaloids) (Juliano and Ling, 1976). The P-glycoprotein has been shown to act as an ATP-dependent pump that expels drugs out of cells or reduces the transcellular flux of a wide variety of drugs (Chin *et al.*, 1993). Its location in many elimination organs suggests that it plays a significant role in detoxification processes (Thiebaut *et al.*, 1987). P-glycoproteins location in the tip of villi enterocytes may form a significant barrier to drug absorption. Also, its shared location within the intestinal epithelium with the major phase I metabolising enzyme cytochrome P_{450} 3A (CYP3A) and the large number of substrates and inhibitors they have in common (Wacher *et al.*, 1995), indicate that intestinal drug metabolism and counter-transport processes are potentially a major determinant of oral drug bioavailability and variability (Wacher *et al.*, 1996).

1.3.1.4 TIGHT JUNCTION

The GI tract lumen and the paracellular space between epithelial cells are continuous and therefore a more significant route for hydrophilic molecules, despite their small surface area. The paracellular pathway gated by the tight junctions allows ions and small molecules, up to approximately 900 Da, to pass through (Gumbiner, 1987). The paracellular spaces are considered "pores". The pore radius of the rat intestinal mucosa is 4 Å for lipid-insoluble non-eletrolytes (Burton *et al.*, 1991) big enough to allow D-mannitol through (182 Da, 3.6 Å molecular radius). The calculated effective pore radii of the human small intestinal epithelium are about 3-4 Å for ileum and 7-9 Å for jejunum (Madara, 1991).

It has also been demonstrated that the intestinal permeability of substances of different molecular weights in rabbit intestines varies inversely to their molecular weights (Loehry *et al.*, 1970). Donovan *et al.* (1990) and Artursson *et al.* (1993) demonstrated using the homogenous series of compounds, polyethylene glycols (PEG's) of different molecular weights that absorption from the GI tract decreases with molecular size. Hussain (1998) concluded that factors such as size of the molecule and the ability of the compound (in the case of peptides) to hydrogen bond with components of the membrane are more important than lipophilicity and ionisation in determining permeability. For example the *in vivo* rate of absorption of the highly lipophilic drug progesterone is similar to that observed for sodium benzoate, and the *in vivo* rate of absorption of benzoic acid is independent of the pH of the medium.

Tight junction permeability has been shown to be sensitive to a host of factors (section 1.2.1). Therefore, the tight junctions appear to be a potential site for the action of absorption enhancers (van Hoogdalem *et al.* 1989). Absorption enhancers can generally be split into two classes a) calcium chelators or b) surfactants which when present open tight junctions, after their removal the process is revered. The application of enhancers is usually necessary to increase the flux of therapeutic peptides and proteins such as human calcitonin.

1.3.2 ENZYMATIC BARRIER

Drugs and other xenobiotics that gain access to the body may undergo one or more of 4 distinct fates:- i) elimination unchanged, ii) retention unchanged, iii) spontaneous chemical transformation iv) enzymatic metabolism; each of these fates is of importance. In quantitative terms it is enzymatic metabolism, often also referred to as biotransformation, that predominates. The metabolism of drugs usually results in loss of efficacy. The main site of metabolism of foreign compounds is considered to be the liver, although extraheptic tissues, frequently at the site of entry to or excretion from the body, *e.g.* GI mucosa, lungs, kidneys, also play a role in the metabolism of drug. This view is now being challenged since the finding that enzymes of the CYP3A sub-family considered the major phase I drug metabolising enzymes in humans (Wacher *et al.*, 1995; Watkins, 1994) are expressed at high levels in mature enterocytes of the small intestine. This level constitutes

approximately 70 % of CYP content in human enterocytes (Watkins *et al.*, 1987; Kolars *et al.*, 1992) while in the liver it is only 30 % of total human hepatic CYP content (Shimanda *et al.*, 1994). Therefore, an important consideration in the oral absorption of drugs is their pre-systemic metabolism following oral administration.

The scope of drug metabolism is immense, and this is reflected in the range of chemical reactions that are involved in the metabolism of substrates, including oxidation, reduction, hydrolysis, hydration, conjugation and condensation. Typically, the process of drug metabolism is biphasic whereby the compound first undergoes a functionalisation reaction (oxidation, reduction, or hydrolysis), which introduces or uncovers a functional group, *e.g.* -OH, $-NH_2$, -SH suitable for subsequent conjugation with an endogenous conjugating agent. The metabolism of most compounds is enzymatic, therefore any factor that can influence the activity of these enzymes can alter metabolism (Table 1.1) (Caldwell *et al.*, 1995).

Table 1.1 Physicochemical, endogenous, and exogenous factors affecting the rate and extent of metabolism of drugs *in vivo* (adapted from Caldwell *et al.*, 1995).

Physicochemical	**Endogenous**	**Exogenous**
Electrophilicity	Age	Dose
Nucleophilicity	Sex	Nutrition
Lipophilicity	Species	Route of administration
pH	Strain	Time of day
Polarity	Pathology	Enzyme inhibition
Protein binding	Genetic deficiencies	Enzyme induction
Conformation	Cofactor availability	
Concentration	Activating ions	

It has been estimated that an orally administered peptide or protein might encounter in excess of 40 different peptidase enzymes during the passage across the GI tract (Woodley, 1994). Contained in the secretions of the stomach and pancreas, bound to the brush-border, and contained in the cytosol of the epithelial cell along with the degradative

enzyme systems of the lysosome. Table 1.2 summarizes the proteases encountered by a peptidomimetic and peptide drug and the major site of action.

Proteases are divided into four classes according to their mechanism of action, serine, metallo-, cysteine, and aspartic. Protein degradation starts in the stomach with pepsins. The major intestinal degrading proteases are trypsin, α-chymotrypsin, elastase and carboxypeptidases A and B, their products being polypeptides. The brush-border peptidases are active mainly against tri-, tetra-, and oligopeptides up to ten amino acids, while intracellular peptidases are active predominantly against dipeptides.

Table 1.2 Typical substrates of intestinal peptidases.

Type	Enzyme	Site of action	Specificity
Endopeptidase	Pepsin	S	Phe, Trp, Tyr, Met, Leu
	Trypsin	P	Arg, Lys
	α-Chymotrypsin	P	Phe, Tyr, Trp
	Elastase	P	Ala, Gly, Leu, Val, Ileu
	Endopeptidase-24.11	BB	Hydrophobic
	Endopeptidase-24,18	BB	aromatic
	Endopeptidase-3	BB	Arg-Arg ?
	Enteropeptidase	BB	$(Asp)_4$-Lys
Exopeptidase, NH_2 terminus	Aminopeptidase N	BB	Many amino acids
	Aminopeptidase A	BB	Asp or Glu
	Aminopeptidase P	BB	Pro
	Aminopeptidase	BB	Trp, Tyr, Phe
	Dipeptidylpeptidase IV	BB	Pro, Ala
	γ-Glutamyltranspeptidase	BB	γ-Glu
Exopeptidase, COOH terminus	Carboxypeptidase A	P	Tyr, Phe, Ileu, alsoThr, Glu, His, Ala
	Carboxypeptidase B	P	Lys, Arg, hydroxyLys, Ornithine
	Angiotensin-converting enzyme	BB	Many amino acids
	Carboxypeptidase P	BB	Pro, Ala, Gly,
	Carboxypeptidase M	BB	Lys, Arg
	γ-Glutamyl carboxypeptidase	BB	γ-Glu
Exopeptidase dipeptidase	Microsomal dipeptidase	BB	Many amino acids

S = stomach, P = pancreas and BB = brush-border.

The qualitative information on these enzymes is useful if trying to predict stability/resistance of a therapeutic peptidomimetic drug or peptide. The regional distribution of intestinal protease activity varies along the GI tract. Bai (1994a) showed in rat and rabbit intestine that the activity of aminopeptidase P and W increases down the GI tract reaching its highest levels in the ileum. The lowest activities were found at the ileo-caecal junction. Similar results were found in rabbit and humans for aminopeptidase N and dipeptidylpeptidase IV. In contrast the activities of cytosolic peptidases show no regional variation (Sterchi, 1981). Lysosomal peptidase enzymes seem to have their highest activities in the caecum (Bai, 1994b). However, if peptidomimetic drugs, peptides and proteins are delivered to the colon, an advantage may be gained in increased absorption as this segment of the GI tract has fewer proteases than the small intestine (Ritschel, 1991). For the majority of peptides and proteins under investigation for chronic administration, a non-parenteral route would have the greatest patient compliance (Mackay *et al.*, 1997).

1.4 ABSORPTION MODELS

Investigation of the absorption of poorly absorbed drugs requires the choice of suitable intestinal models. A number of *in vivo*, *in situ* and *in vitro* models have been used to investigate the extent and mechanism of intestinal absorption (Gardner, 1988). With *in vivo*, and *in vitro* intestinal preparations, along with some GI tract epithelial cell lines all displaying structural polarity. Although the *in vitro* preparations, brush-border membrane vesicles (BBMV) and basolateral membrane vesicles (BLMV), are a result of polarity they have been used extensively in measuring drug uptake and efflux. The application of each preparation in measuring drug absorption depends upon their different qualities, the merits of each preparation available to measure intestinal absorption are shown in Table 1.3.

1.4.1 *IN VIVO* MODELS

1.4.1.1 THIRY-VELLA FISTULA

Absorption studies using the Thiry-Vella fistula model are performed after a period of post-operative recovery, commonly in dogs. However, a similar chronic intestinal resection method has been performed in rats (Poelma and Tukker, 1987). This procedure gives the closest preparation to normal GI tract function after recovery from surgery, with normal blood supply and innervation allowing reuse of the fistula.

Table 1.3 Table of intestinal preparations available to investigate mechanisms of absorption with some utility parameters.

Intestinal preparation	**Flexibility of preparation**	**Viability**	**Polarity of process**	**Information relating to specific transport processes**						**Elucidation of pathway/ mechanism**	**Complexity**
				Apical transport	Basolateral transport	Luminal metabolism	Metabolism I	Metabolism E	Bulk absorption		
IN VIVO Thiry-vella fistula	Low	Weeks	+	-	-	-	+①	-	+	+/-①	High
IN SITU Intestinal loop (perfusions)	Medium	hours	+	-	-	-*	+①	-	+	+/-①	High
IN VITRO Intestinal perfusions	Medium	hours	+	-	-	-*	+①	-	+	+/-①	Medium
Intestinal sheets (with muscle)	High	4 h	+	+	+/-	-*	+	-	+	+/-①	Medium
Epithelial sheets	High	4 h	+	+	+/-①	-*	-	+	+	+	Medium
Everted sacs	High	5 min	+	+/-①	+/-①	-*	+	-	+	+/-	Low
Intestinal rings	High	10-20 min	+	+/-①	+/-①	-	+	-	-	+/-	Low②
Cell culture monolayers③	High	weeks	+	+	+	-*	-	+	+	+	Low②
Isolated cells	High	2 h	-	+/-①	+/-①	-	-	+	-	+/-①	Low②
Vesicles	High	2-4 h	+	+	+	+	-	-	-	+	Low②

+ = can be shown, - = cannot be shown, +/- = may be shown, * = defined experimentally, I = intestinal, E = epithelial

① = by using specific inhibitors, ② = by using radioactive substrates, ③= dependent on the processes expressed

Although absorption and bioavailability are measured, mechanistic studies to determine absorption pathway or luminal metabolism are difficult to do.

1.4.1.2 *IN SITU* MODELS

The advantages of the *in situ* intestinal loop method are that the intestinal segment still has its own blood supply and nervous innervation along with all the barriers to drug absorption (Section 1.3). Although the *in situ* rat intestinal method of Doluisio *et al.* (1969) represents a very powerful tool for assessing the factors of importance in drug absorption, it also has its disadvantages. Highly lipid soluble drugs were found to be stored significantly in the membrane due to decreased intestinal blood supply caused by anaesthesia (Doluisio *et al.*, 1970). Therefore, there is no direct relation between the disappearance of a highly lipophilic drug from the intestinal lumen and its absorption. Whereas, directly measuring the amount of drug that reaches the blood rather than the loss of drug from the intestinal lumen adds to the power of the *in situ* model (Hanson and Parsons, 1976; Hastewell *et al.*, 1992).

1.4.2 *IN VITRO* MODELS

1.4.2.1 EVERTED SACS

The everted sac technique was developed by Wilson and Wiseman (1954). The major advantage of the open everted intestinal sac, over the closed everted sacs, is that it permits sequential sampling from the serosal compartments. The surrounding muscle layer of the GI tract forms a barrier to drug absorption *in vitro*, which is not the case *in vivo*, because of the intact circulation system. Wolfe *et al.* (1973) showed that stripping the muscle layer off, doubled the transport of salicylate across the intestinal mucosa.

The ease of preparation without the need of specialized equipment, has led to everted sacs being used extensively to study transport of nutrients and drugs across the intestinal mucosa (Tomita *et al.*, 1988; Shaw *et al.*, 1983; Middleton, 1990; Leese and Mansford, 1971; Elsenhans *et al.*, 1983). However, great care is needed when handling the segments, because everting and filling the sacs distends them causing damage to the tissue. Once the sacs are prepared they are difficult to maintain, since the tissue needs to be constantly oxygenated, especially the serosal side which is not well oxygenated even with stripped

segments. This gives rise to the major disadvantage of this *in vitro* technique which lies in the short-lasting integrity of everted sacs. After 5 min there is loss of morphology, after 30 min 50 to 75 % of epithelial cells are distorted, and after 60 min there is total disruption of the epithelial brush border (Levine *et al.*, 1970). Therefore, everted sacs are only good for short absorption experiments, which is true of most *in vitro* intestinal preparations.

1.4.2.2 INTESTINAL RINGS

Everted intestine is cut into rings and suspended in oxygenated medium containing the compound of interest. This is a good model to study passive and active mechanisms of drug uptake. Since all surfaces are exposed to the incubation medium it is not possible to demonstrate transport or polarity of uptake. Intestinal rings are further restricted by their limited viability, 10 to 20 min (Plumb *et al.*, 1987).

Generally, radiolabelled substrates are used because they offer greater sensitivity in detection. If non-radioactive substrates are used, analysis could become the rate-limiting step in the study of the compound, as the drug has to be extracted from the tissue and measured with high sensitivity and specificity. Despite these limitations intestinal rings have been used to study the intestinal uptake of 5-fluorouracil (Bronk and Hastewell, 1987) and peptides (Addison *et al.*, 1972).

1.4.2.3 INTESTINAL SHEETS

Absorption across intestinal sheets can be studied using Ussing chambers (Ussing and Zerahn, 1951). A mixture of 95 % O_2 and 5 % CO_2 is continuously bubbled through the incubation media, at 37°C, of each chamber to ensure tissue oxygenation and minimise USWLs. Viability of intestinal preparations in Ussing chambers is commonly assessed by transepithelial potential difference or short-circuit current (Hillgren *et al.*, 1995). The compound of interest is introduced to the mucosal chamber and the rate of appearance in the serosal chamber is determined giving a measurement of drug flux across the particular segment of intestine.

The Ussing chamber technique allows easy manipulation of conditions. Using intestinal sheets (with muscle) or epithelial sheets (without muscle) from different regions of the GI

tract allows absorption and metabolism to be tested. A limitation of the *in vitro* Ussing chamber system is the relatively short viability, usually no longer than 4 h which compares unfavourably with cell culture models but better than some of the other *in vitro* preparation (Table 1.3).

1.4.2.4 MEMBRANE VESICLES

Brush-border membrane vesicles (BBMV) and basolateral membrane vesicles (BLMV) allow detailed characterisation of transport mechanisms at the plasma membrane level not available with *in vivo* techniques (Milovic *et al.*, 1994). They have been successfully used to characterise the nature and mechanisms of membrane transport processes present in the plasma membranes of several epithelia, including small intestine, renal tubule and parotid gland (Lash and Jones, 1984; Dyer *et al.*, 1990; Tarpey *et al.*, 1992; Mullins *et al.*, 1992). Conditions can be controlled accurately with respect to media composition, pH, ion concentration, osmolality and, the presence of inhibitors inside or outside of the vesicle. Thus mechanistic studies and the transport of drugs using transporter proteins in the plasma membrane can be investigated and assessed (Hashimoto *et al.*, 1994).

The use of membrane vesicles gives a better indication of drug uptake in the *in vivo* situation than perhaps some of the other *in vitro* preparations *e.g.* intestinal rings. Also, membrane vesicles can be prepared and stored from different regions of the GI tract, from different species including humans (Pinches *et al.*, 1993). However, membrane vesicles have disadvantages, they are prepared by a long procedure and alterations in membrane permeability and/or inactivation of transport systems can occur. The measurement of partition and distribution coefficient into rat small intestine BBMV is complicated by the distribution of the solute into the membrane. With BBMV partition coefficients of greater than 3 not observed even with solutes with Log P values in model solvents that were greater than 5 (Alcorn *et al.*, 1993). Also, the use of oily formulations and micro-emulsions may cause surfactant-like solubilisation of the vesicles making it extremely difficult to separate them from the formulation for drug uptake measurement (Sanyal *et al.*, 1992). Measurement of drug uptake needs to have in place a sensitive assay for measurement, the usual method being by radiolabelled drug.

1.4.2.5 ISOLATED ENTEROCYTES

Isolated enterocytes seem to be only viable for 1 to 2 h, and do not readily attach to substrates and are not suited to sub-culture, therefore they are used in suspension. This allows only for uptake and metabolism studies to be determined and not transport or absorption of compounds to be investigated. Although, a few cases of intestinal enterocytes maintained in culture can be found (Goodwin *et al.*, 1993; Moyer, 1983). The isolation procedures tend to lack reproducibility with large variability in viability, number, and character of cells obtained. The different harvesting techniques, either proteolytic enzymes, chelating agents, or mechanical dissociation can vary the yield and quality of the cells, with the optimum technique also varying with different species (Hartmann *et al.*, 1982; Kremski *et al.*, 1977; Kimmich 1990). Proteolytic enzymes damage external proteins on the membrane and decrease viability, chelating agents increase permeability of the membrane to ion flow, and mechanical dissociation damages external proteins and weakens cell membranes (Kimmich, 1990).

An advantage of isolated enterocyte uptake and metabolism experiments is the relatively large number of compounds and different conditions that can be tested, from different regions of the GI tract from one animal. Also, villus enterocytes can be separated from crypt cells during isolation and the roles of the different cell types in uptake can be determined (Iglesias *et al.*, 1988). But the major disadvantage of isolated enterocytes is that uptake studies are predominantly studying the basolateral membrane.

Membrane vesicles are a cleaner system than isolated enterocytes as they indicate if the compound will be transported by either the basolateral or apical membrane. They do not indicate the fate of the compound once inside the cell as can isolated enterocytes. To understand the transport of a compound through intestinal enterocytes, it needs to be put through a polarised system which mimics the intestine.

1.4.3 CELL CULTURE MODELS

In order to mimic successfully the monolayer of polarised epithelial cells lining the GI tract with an *in vitro* cell culture system, the selection of the cell line becomes particularly

important. Thus far, all attempts to obtain primary differentiated cell cultures have been unsuccessful with low viability, monolayer formation, and differentiation.

The immortalised human intestinal cell lines have provided the system to study absorption, metabolism and differentiation in enterocytes. Twenty intestinal adenocarcinoma cell lines have recently been classified into four groups according to their degree of differentiation (Chantret *et al.*, 1988; Chantret *et al.*, 1994). Type 1; undergo spontaneous differentiation under cell culture conditions, this group contains only one cell line, the Caco-2's. Type 2; do not differentiate spontaneously, however, they can be induced to differentiate when the cell culture conditions are altered. An example is the cell-line HT-29 where replacement of glucose with galactose in the cell culture medium initiates differentiation. Type 3; are organised into polarised monolayers with formation of domes but are otherwise undifferentiated *i.e.* no significant expression of brush border hydrolases. Type 4; grow in multilayers without any signs of differentiation.

The cell culture system has proven invaluable in the elucidation of the fundamental biochemical pathways and regulatory steps involved in intestinal differentiation and function. When seeded on microporous filters, immortalised tumour epithelial cell lines like Caco-2, HT-29 and T84 are able to form a polarised monolayer through the formation of intercellular tight junctions. In these systems, the filter supporting the cell monolayer is contained within a filter insert which separates culture medium on the apical and basolateral side of the cell monolayer (Figure 1.6).

Intestinal epithelial cell cultures have much longer viability, along with using less compound compared with *in vivo*, *in situ* and other *in vitro* techniques. Manipulation of their environment, *e.g.*, pH, sodium and ion concentration, metabolic inhibitors, temperature and USWL, allows mechanisms of absorption, transport and metabolism to be more easily probed. An important advantage is the isolation of specific cells, enterocyte, crypt cell or goblet cell giving an opportunity to study their effect on transport across the intestinal epithelium. The most obvious disadvantage of the cell culture system is that the cells are of tumour origin and not normal intestinal epithelial cells. However, they show absorption, transport and metabolism properties of normal intestinal epithelium.

Therefore, cell lines mimicking intestinal mucosa appear to be a very good method for the study of absorption, transport and metabolism of drugs.

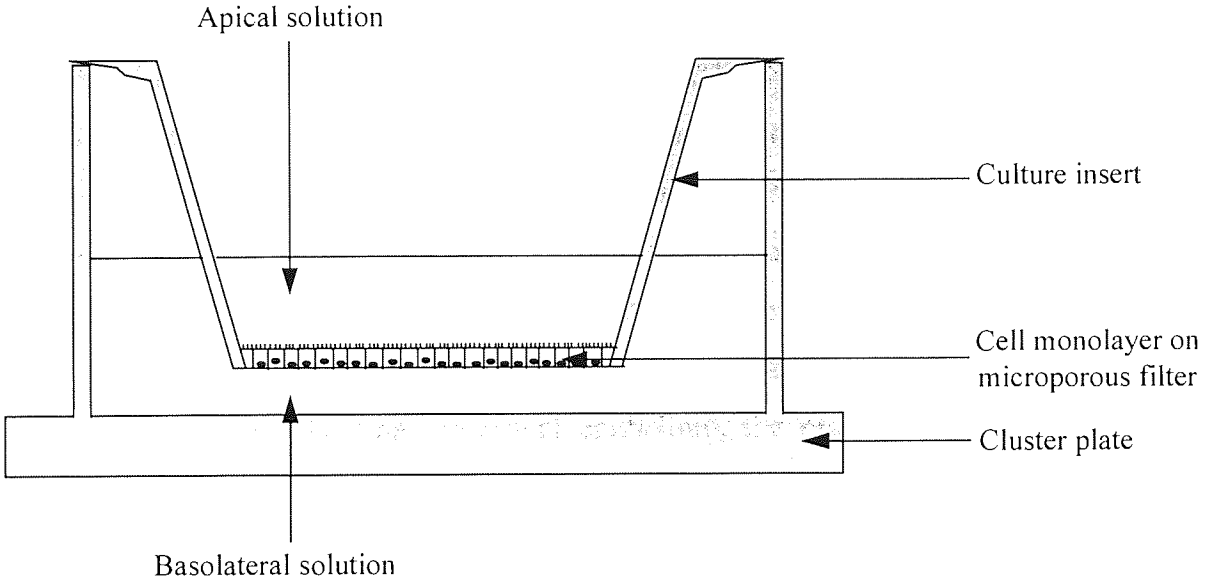

Figure 1.6 Diagram of filter grown polarised epithelial cell monolayer.

1.5 CACO-2 CELLS

The Caco-2 cell line was isolated from a human colonic adenocarcinoma from a 72 year old patient (Fogh *et al.*, 1977). When grown on permeable supports they mimic the digestive, absorptive, and morphological characteristics of a small intestinal absorptive cell.

At confluency, Caco-2 cells spontaneously differentiate, initiated by the formation of tight apical junctions giving rise to the polarised distribution of membrane components e.g. brush-border membrane hydrolases (Pinto *et al.*, 1983), Na^+-dependent membrane transporters (Mohrmann *et al.*, 1986) di- and tripeptide transporters (Inui *et al.*, 1992) and lipid molecules, leading to the formation of apical and basolateral domains and brush border cytoskeleton. They are known to express nutrient carrier-mediated transport systems for amino acids, bile salts, calcium, dipeptides and dipeptide analogues, folate, hexoses, inorganic phosphate, iron, and cobalamin (Dix *et al.*, 1990; Blais *et al.*, 1987; Riley *et al.*, 1991; Hidalgo and Borchardt, 1990; Hu and Borchardt, 1992; Nicklin *et al.*, 1992b; Dantzig and Bergin, 1990; Inui *et al.*, 1992) all of which are found *in vivo*. These are consistent with a small intestine phenotype, particularly those related to the distal ileum

in vivo (Pinto *et al.*, 1983; Inui *et al.*, 1992; Nicklin *et al.*, 1992a and reviewed by Neutra and Louvard, 1989; Artursson, 1991).

However, Caco-2 monolayers have increased TER values ranging from 300 to 1400 Ω cm^2, equivalent to their colonic origin (Woodcock *et al.*, 1991; Nicklin *et al.*, 1992a; Lu *et al.*, 1995). Despite their colonic origin this cell line should be considered as an important intestinal absorption model because they express many of the receptors, transporters and enzymes expressed are found *in vivo* in the distal ileum. As screening for drug carrier interactions is not feasible *in vivo*, it is important to use a relevant intestinal human cell line. They are therefore a very useful model to investigate, the most abundent single cell type (enterocyte) of the small intestinal epithelium, the properties and mechanisms of nutrient and drug absorption.

1.5.1 HETEROGENEITY

Caco-2 cells proliferate and differentiate on cell-to-cell contact, forming junctional complexes and maturing into polarised enterocyte-like cells with a well developed microvillar membrane. Caco-2 cells were observed to be morphologically heterogeneous, and cloning experiments have yielded clones with varying hydrolase expression, transepithelial electrical resistance, mannitol permeabilities and taurocholic acid transport rates (Woodcock *et al.*, 1991; Chantret *et al.*, 1994; Caro *et al.*, 1995). Furthermore, they represent the only cell line known to express endogenous lactase as well as sucrase-isomaltase and are the only model that exhibits temporal, differentiation-dependent lactase and sucrase-isomaltase, gene expression (van Beers *et al.*, 1995).

Cell culture conditions play an important role in establishing a reproducible system along with the different types of membrane support material, which have shown differences in cell density and transepithelial electrical resistance (Nicklin *et al.*, 1992a; Sergent-Engelen *et al.*, 1990). Also, the effect of various hormones contained within the serum supplement to the cell culture medium has an effect on growth characteristics, viability, cell activity and morphology. This has been shown by a number of groups using serum-free media supplemented with the molecule of choice (Hashimoto *et al.*, 1995; Oguchi *et al.*, 1995; Herold *et al.*, 1995; Halline *et al.*, 1994; Jumarie *et al.*, 1996).

Walter and Kissel (1995) have investigated differences in transepithelial resistance and mannitol permeabilities from Caco-2 lines from other laboratories, and tried to relate them to growth characteristics, morphological heterogeneity, viability and metabolic activity in Caco-2 cells. Their conclusions were that the variations seen in each of the laboratories, was probably the result of a selection process promoted by the culture conditions, giving a variable composition of Caco-2 clones in each of the heterogeneous parent population in the laboratories.

1.5.2 CACO-2 TRANSPORT MODEL

The Caco-2 transport model (Figure 1.6) of the GI tract epithelium gives a means of isolating the intestinal cell barrier from the underlying mucosal tissues. They have been used to measure the apparent permeability of drug across Caco-2 monolayers with a variety of drugs (Artursson, 1990; Hu and Borchardt, 1990; Wilson *et al.*, 1990; Conradi *et al.*, 1991; Inui *et al.*, 1992 Ranaldi *et al.*, 1992).

A good correlation between drug absorption in Caco-2 monolayers and percent absorbed in man was established by Artursson and Karlsson (1991). Artursson *et al.* (1993) further concluded that "both excised ileal and colonic segments from the rat and monolayers of Caco-2 cells have permeability profiles that are comparable to those found in normal human intestine *in vivo*". Using drugs from different therapeutic classes, Rubas *et al.* (1995) show that Caco-2 monolayers may be a predictive tool for solute permeabilities across rabbit and human colon. It has also been shown, using the Caco-2 model, that it may be a good predictor of intestinal permeabilities of peptides and peptide analogues *e.g.* the renin inhibitor peptides (Kim *et al.*, 1993; Conradi *et al.*, 1993). Stewart *et al.* (1995) using reference compounds and peptidomimetics showed the highest correlation between Caco-2 cell monolayers and rat single-pass intestinal perfusion with fraction absorbed in humans.

1.5.3 TRANSCELLULAR TRANSPORT

1.5.3.1 PASSIVE TRANSPORT

The traditional concept of a positive correlation between drug absorption and lipophilicity has been shown in numerous *in vitro* studies (Martin, 1981; Artursson and Karlsson, 1991;

Wils *et al.*, 1993; van Bree *et al.*, 1988). Artursson and Karlsson (1991) showed a sigmoid correlation of percent absorbed in humans to the apparent permeability coefficient across Caco-2 cell monolayers for passively absorbed drugs. This relationship holds for a series of compounds, but lipophilicity is not the sole predictor. Charge on the molecule, M_r and the potential for hydrogen bonding has a significant effect on permeability across the intestinal epithelium. Wils *et al.* (1994) have shown in Caco-2 and HT29-18-C cells, that Log D versus apparent permeability is a parabolic correlation; with increases in Log D up to 3.5, the transepithelial permeability coefficient increased with the lipophilicity. But for Log D values above 3.5 the transepithelial permeability coefficient decreased with increasing lipophilicity. The other major concern is, that there are two pathways by which passive drug diffusion can occur, transcellular and paracellular, and this is not shown through this correlation.

1.5.3.2 CARRIER-MEDIATED TRANSPORT

The polarised morphology and ability to form domes, led Pinto *et al.* (1983) to propose Caco-2 monolayers as an *in vitro* model of a transporting epithelium. Over the last decade Caco-2 cells have been demonstrated to express a series of carrier-mediated intestinal ion and nutrient transport systems detected *in vivo* (see section 1.5.2).

Investigations range from determining the Michaelis-Menten kinetic parameters and inhibitor affinities to detection, and cloning of the transport protein in question. Mahraoui *et al.* (1994) has shown that clones of Caco-2 cells isolated from early and late passages of the Caco-2 cell line express differently the glucose facilitative transport protein GLUT1, GLUT2, GLUT3, GLUT5, and Na^+-dependent glucose transport protein SGLT1 mRNA's. Their level of expression and presence vary from clone to clone and from one transporter to another in relation to the phase of cell growth and the rates of glucose consumption. In the small intestine, hexose transport proteins are coded by the SGLT1 gene, the products of which are the Na^+-dependent glucose cotransporter and the family of facilitative hexose transporters referred to as GLUT1-GLUT5. In the small intestine, the Na^+-dependent glucose cotransporter and GLUT5 are associated with the brush-border membrane of enterocytes, and GLUT2, associated with the basolateral membrane. Whereas, in malignant epithelial cells including colonic cells, GLUT1 and GLUT3 are mainly

expressed. Caco-2 cells express Na^+-dependent glucose cotransporter, GLUT1 and GLUT3 and the fructose transporter GLUT5. Therefore, as cancer cells expressing GLUT1 and GLUT3 they display an altered and generally increased utilisation of glucose.

Tien *et al.* (1993) have used the Ca^{2+} sensitive dye Fura-2 to show that Caco-2 cells do not express the L-type, voltage-dependent Ca^{2+} channel. However, there does appear to be a $1,25(OH)_2D_3$-sensitive La^{3+} inhibitable cation influx pathway in Caco-2 cells. Giuliano and Wood (1991) characterised calcium transport in differentiated Caco-2 cells grown on permeable filter inserts. Calcium transport was increased in a dose-dependent manner by $1,25(OH)_2D_3$. The maximum rate of saturable calcium transport was increased by 4.3-fold in cells treated with 10 nM $1,25(OH)_2D_3$. The treatment increased the apparent buffer calcium concentration that results in half-maximal velocity from 0.4 to 1.3 mM with no significant effect on nonsaturable calcium transport.

Caco-2 cells have been shown to actively transport bile acids in the apical to basolateral direction and shown to be Na^+- and glucose-dependent (Hidalgo and Borchardt, 1990). Apical-to-basolateral (Ap-to-Bl) transport of taurocholic acid was saturable and temperature-dependent. The kinetic parameters J_{max} and K_t for transport were 13.7 pmol mg protein^{-1} min^{-1} and 49.7 μM, respectively. The transport of [^{14}C]taurocholic acid was competitively inhibited by apical co-administration of unlabelled taurocholic acid or deoxycholic acid. Chandler *et al.* (1993) corroborated these findings with an apparent Michaelis-Menten constant for [^{3}H] taurocholic acid transport of approximately 65 μM, and maximal transport rate approximately 800 pmol min^{-1} mg protein^{-1}. Taurocholic acid transport was inhibited by lower temperature, metabolic inhibitors and unlabelled bile acids, indicating that the Caco-2 cell model is appropriate to study the transport of bile acids, similar to that found *in vivo* in the ileum.

1.5.3.3 RECEPTOR-MEDIATED TRANSPORT

Caco-2 monolayers grown on permeable supports bind and internalise intrinsic factor-vitamin B_{12} (cobalamin, Cbl) complexes and after 14-28 days in culture this binding is exclusively located to the apical membrane. Transcobalamin II is synthesised and secreted after 20 days in culture from the basolateral side. Transcellular transport of [^{57}Co]Cbl also

occurs between day 20 and 28 day in culture (Dix *et al.*, 1990). Dan and Cutler (1994) investigated the fate of the intrinsic-factor-Cbl complex following receptor-mediated endocytosis and transcytosis across the Caco-2 monolayer. They found, following internalisation of the complex, intrinsic factor is degraded with a half-life of 4 h. Co-administration of leupeptin causes a partial block in the degradation of intrinsic factor, an intracellular accumulation of Cbl bound to intrinsic factor, and a decrease in the transcytosis of Cbl was observed.

Caco-2 cell monolayer express transferrin receptors. Hughson and Hopkins (1990), using the receptor as a marker for the basolateral route along with radiolabelled transferrin and transferrin-peroxidase conjugate, showed 95 % efficiency for recycling of ligand back to the basolateral surface. They delineated an early basolateral endocytic pathway/compartment that mixed with the apical endocytic route labelled with Concanavalin A complexed to gold particles. Indicating that the apical and basolateral endocytic pathways meet in an endocytic compartment that can recycle transferrin.

1.5.3.4 FLUID-PHASE ENDOCYTOSIS

Intrinsic-factor-Cbl complexes show that receptor-mediated endocytosis can occur from the apical pole in Caco-2 cells and that the apical and basolateral endocytic pathways meet. However, these receptors, are not expressed in sufficient numbers for morphological studies and no other mobile receptor population in high enough copy number has yet been identified on the apical membrane of Caco-2 cells. Therefore, for morphological studies of endocytosis in Caco-2 cells, fluid-phase tracers *e.g.* horseradish peroxidase (HRP) (Heyman *et al.*, 1988; Heyman *et al.*, 1990) or ligands of broad specificity such as plant lectins (Shurety and Luzio, 1995), are used.

The HRP data, indicates that approximately 5 % of the dose is internalised and is transported across the Caco-2 monolayer delivering intact HRP to the basolateral surface. Caillard and Tome (1995) have confirmed this, measuring β-lactoglobulin and α-lactalbumin transport across Caco-2 monolayers; both the transport and release from the cells were measured following different incubation times. Labelled material was analysed by either trichloroacetic acid precipitation or HPLC. The overall mechanism followed

approximately the same pattern for both proteins and that of HRP. Intact internalised protein was recycled (10-15 %) or transcytosed (approximately 5 %). The intracellular degradation pathway of proteins recycled 70 % of the degraded protein to the apical surface, whereas approximately 30 % was transcytosed to the basolateral chamber. Moreover 5-10 % of endocytosed protein was retained intracellularly. Even though a direct transcytotic Ap-to-Bl pathway may not exist in adult enterocytes, it may be possible to exploit the fact that apical ligands reach the same compartment as membrane protein recycled to the basolateral membrane.

1.5.3.5 EFFLUX TRANSPORT

Caco-2 cells express the multidrug-resistance (MDR) gene product P-glycoprotein at the apical surface leading to a polarised secretion of MDR substrates such as vinblastine. Inhibitors of P-glycoprotein, *e.g.,* verapamil, nifedipine and dideoxyforskolin, enhance vinblastine absorption, demonstrating a potential mechanism for enhancing absorption of some drugs (Hunter *et al.*, 1993).

1.5.4 PARACELLULAR TRANSPORT

The intercellular tight junction of intestinal epithelia is a barrier that restricts the flow of solutes through the paracellular pathway and thus contributes to the epithelial barrier. Caco-2 cells spontaneously exhibit various small intestine enterocyte characteristics, including the brush-border enzymes, nutritional transporter activities, and apical tight junctions. However, the electrical resistance of their tight-junctions seem to be different, adhering more tightly than small intestinal epithelium (Woodcock *et al.*, 1991). This might explain the low permeability of this epithelium to hydrophilic drugs that permeate the intestinal epithelium mainly through the tight-junctional route. Tanaka *et al.* (1995) elucidated a linear relationship between drug permeability and chloride ion conductance for Caco-2 monolayer, rat jejunum and colon. The correlation was interpreted as the effective pore radius of the three epithelia to be essentially the same. With the differences in TER and drug permeability not due to the differences in tightness of the junctional pathway, but a structural difference of the epithelia. The jejunal epithelia has a specific villous structure, that increases the effective surface area for absorption, whereas, Caco-2 monolayer is flat. Therefore the differences in drug permeability and TER which was calculated on the basis

of unit area of membrane might be different because of the difference in effective area. With the number of junctions per unit area being higher in the jejunum than in Caco-2 monolayers. This suggests that the permeability of drug per unit of chloride ion conductance is similar in the three areas, and indicates that the size of the tight junctional pathway is similar in all three membranes. Also, when Caco-2 monolayers were treated with EDTA, the electrical resistance was reduced to the same level as the jejunum, increasing the permeability significantly.

Artursson and Magnusson (1990) showed a sigmoid relationship of Log D versus apparent permeability coefficient across Caco-2 monolayers with a range of β-blockers which increased with the chelation of extracellular calcium by EDTA especially for the more hydrophilic β-blockers practolol and atenolol (Artursson and Magnusson, 1990).

For thyrotropin-releasing hormone, predominantly paracellular transport was indicated by Thwaites *et al.* (1993) and Gan *et al.* (1993) but Walter and Kissel (1994) and Nicklin and Irwin (1991) indicated a significant carrier-mediated component. The Thwaites *et al.* (1993) and Gan *et al.* (1993) data were obtained at pH 7.4, conditions which might favour passive paracellular transport. Their conditions may not reflect the pH at the apical surface of the small intestinal epithelium, around pH 5.5-6.3 (Shimada and Hoshi, 1988; Lucas *et al.*, 1975) and therefore the other groups may indicate the presence of a tri-peptide carrier system in the apical membrane of the Caco-2 cell monolayer.

1.5.5 ENZYME ACTIVITY AND METABOLISM

Caco-2 cells develop mature microvilli and show characteristics of mature differentiated small intestine epithelial cells (Hilgers *et al.*, 1990). The apical membrane of Caco-2 cells have the activities of brush-border membrane exo- and endopeptidases. Thus, they provide a plausible model for *in vitro* evaluation and characterisation of absorption and intestinal-wall metabolism of drugs (Howell *et al.*, 1992; Dantzig *et al.*, 1994; Borchardt *et al.*, 1995).

Various researchers have demonstrated the presence of CYP1A1, CYP2A, and CPY3A gene subfamilies found in human liver and in Caco-2 cells (Boulenc *et al.*, 1992;

Rosenberg and Leff, 1993; Sergent-Engelen *et al.*, 1993). Their expression parallels the differentiation process with higher levels at late confluency. Caro *et al.* (1995) positively tested the Caco-2 parental population and a Caco-2 clone expressing higher activities of various enzymatic reactions including cytochrome P_{450} monooxygenases and UDP-glucuronyl transferase. It has also been demonstrated that Caco-2 cells have the machinery for phase II biotransformations. Peters and Roelofs (1989) investigated the expression of glutathione-S-transferase and demonstrated that during exponential growth they expressed the placental π-isoform, which decreased during the stationary phase of growth. The decrease in π-isoform was associated with the appearance and continuous increase in the α-isoform.

Howell *et al.* (1992) measured the presence of eight peptidases on Caco-2 cells (passage 82-88) and HT-29 cells (passage 176-179). They were aminopeptidase N, dipeptidyl peptidase IV, peptidyl dipeptidase A (angiotensin-converting enzyme), aminopeptidase P, aminopeptidase W, endopeptidase-24.11, γ-glutamyl transpeptidase and membrane dipeptidase. The activities of aminopeptidase P, peptidyl dipeptidase A and alkaline phosphatase, and membrane dipeptidase reached a plateau and then began to decline after 15 days in culture. In contrast, aminopeptidase N, dipeptidyl peptidase IV and endopeptidase-24.11 activities were still rising after 26 days in culture. This study was carried out on flask-grown cells and not filter-grown cells which influences the differentiation of the cells (Nicklin *et al.*, 1992).

Early knowledge of drug absorption and metabolism has a major impact on the potential for drug discovery. Successful prediction of drug absorption or metabolism could be used as an integral part of drug development. The Caco-2 transport model gives a means of isolating the intestinal cell barrier and thus a chance at elucidating the transport pathways of new chemical entities and their role in oral bioavailability studies. Also, the transport studies offer the opportunity of rapid assessment using human cells under controlled conditions.

1.6 AIM OF THIS THESIS

The aim of this thesis is to investigate paracellular drug absorption across Caco-2 monolayers. This will be accomplished by evaluating La^{3+} as an inhibitor of the paracellular pathway. La^{3+} ions will be administered to Caco-2 monolayers to block the paracellular pathway, if inhibition occurs a rise in transepithelial electrical resistance and a reduction in mannitol and PEG 4000 permeability across Caco-2 monolayers would be expected. Using La^{3+} and other transport inhibitors, the absorption pathways across Caco-2 monolayers will be characterised for; NBS and CHPP, both low molecular weight, highly lipophilic organic compounds and human calcitonin, a high molecular weight hydrophilic polypeptide. The Caco-2 absorption model will be considered as a predictive tool of CHPP absorption and compared with animal absorption studies.

CHAPTER TWO MATERIALS AND METHODS

2.1 CHEMICALS

Human calcitonin (hCT), N-(3-chlorphenyl)-4-[2-(3-hydroxypropylamino)-4-pyridyl]-2-pyrimidinamin (CHPP), N-benzoyl-staurosporine (NBS) and [^{14}C]NBS (32.03 mCi mg^{-1}) were provided by Novartis Ltd., Basle, Switzerland. Klucel HF, hydroxypropylcellulose, (Honeywell and Stein Ltd., Sutton, Surrey, UK), Pluronic PE6800 (BASF, Cheadle, Cheshire, UK) and Gelucire 44/14 (Alpha Chemicals Ltd., Bracknell, Berkshire, UK) were all pharmaceutical grade excipients. All cell-culture media-components and reagents were purchased from Gibco BRL (Paisley, UK). Radiochemicals were purchased from Amersham (Amersham, Bucks, UK) or Dupont (New England Nuclear, Stevenage, Herts, UK) unless specified. All cell-culture plasticware were purchased form Costar (High Wycombe, Bucks, UK). All chemicals were cell-culture grade or the highest purity available from Sigma Chemical Company (Poole, Dorset, UK) unless otherwise specified. All reagents were used as received without further purification.

2.2 ANALYTICAL METHODS

2.2.1 GAMMA COUNTING

^{125}Iodine was quantified using gamma-radiation spectrophotometry. Samples were counted for 1 min using a LKB-Wallac Multigamma II gamma-counter (EG & G Instruments Ltd., Milton Keynes, UK) and expressed as CPM.

2.2.2 LIQUID SCINTILLATION COUNTING

Beta-emitting radionuclides [^{14}C]- and [^{3}H]- were quantified using liquid scintillation spectrophotometry. Two methods were employed;

A) Sample + 5 ml Lumagel (Lumac, Netherlands),
   Beckman LS1801 liquid scintillation analyser,
   5 min count-time.

B) Sample + 5 ml Ultima Gold XR (Packard Instrument Co., UK),
   Beckman LS1801 liquid scintillation analyser,
   5 min count-time.

In both cases, counts per minute (CPM) were converted to decays per minute (DPM) by comparison to standard quench-correction curves.

2.2.3 HORSERADISH PEROXIDASE ASSAY

Horseradish peroxidase (HRP) (Type II, 150-200 units mg^{-1}) levels were determined by the method of Gallati and Pract (1985). Briefly, 10 µl of standard, 25-125 pM HRP in transport buffer or sample, was placed into a well of a 96-well microtitre plate (Nunc, UK). Followed by 100 µl of substrate solution, containing 1 mM tetramethylbenzidine in 20 ml of 0.21 mM potassium citrate buffer with 7.2 µl of 30 % (v/v) hydrogen peroxide. The reaction was quenched by the addition of 100 µl of 1 M sulphuric acid. The colour was read on a MRX plate reader (Dynatech Laboratories, UK) at 450 nm. The mean of duplicate standard and sample analyses was calculated and a standard curve was constructed and the unknown samples were read off the standard curve (Figure 2.1).

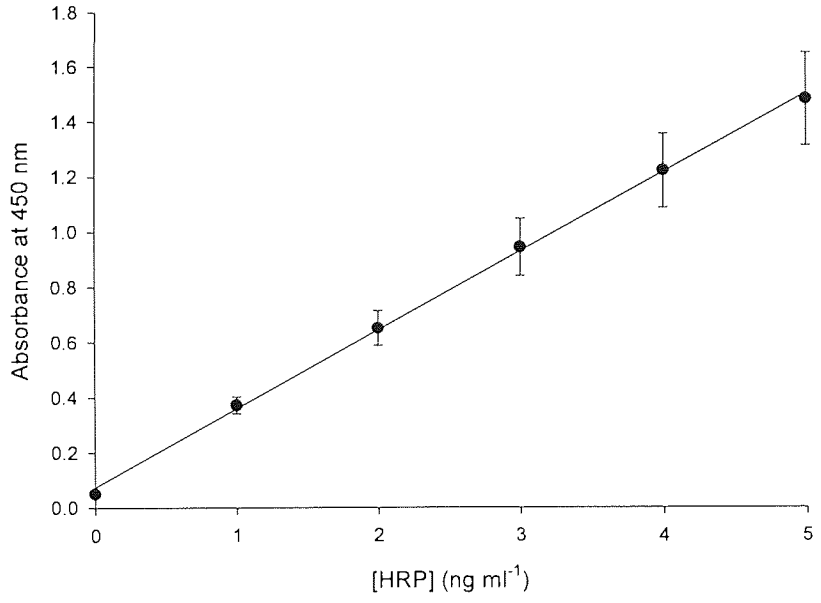

Figure 2.1 A typical horseradish peroxidase standard curve. The plot of absorbance at 450 nm against HRP concentration (0 to 5 ng ml^{-1}), the line represents the best fit by linear regression, $y=0.285x+0.0728$ $R^2=0.999$, to the standard concentration values (mean ± SEM n=5).

2.2.4 HUMAN CALCITONIN RADIOIMMUNOASSAY

Human calcitonin was quantified by radioimmunoassy (RIA) for the measurement of the effect of hCT concentration on the rate of hCT transport. The RIA protocol is summarised in table 2.1. For transport studies, the receiver-solution was assayed for hCT content. Therefore transport medium was used as the assay-medium for the calibration standards.

Table 2.1 Human calcitonin radioimmunoassay protocol. All quantities are in µl.

Tube	**Standard (Std)**	**Transport medium**	**Sample**	**Antibody**	**[^{125}I]hCT**	**Assay buffer**
Total	-	-	-	-	50	-
NSB	-	100	-	-	50	150
Zero Std	-	100	-	50	50	100
Std	100	-	-	50	50	100
Sample	-	-	100	50	50	100

Tubes 1 and 2 (polyethylene LP3, Luckman, UK) represent the total counts, tubes 3 and 4 represent the effect of non-specific binding. Tube 5 through 28 constitute a standard curve (0 to 1000 ng ml^{-1}). Two additional tubes were required for a duplicate assay of each hCT sample. Briefly, 100 µl of standard or sample were added to the appropriate tubes, 50 µl of [^{125}I]hCT was added to each tube followed by 50 µl of diluted hCT-antiserum (Rabbit anti-hCT IgG, Dako, UK) to the appropriate tubes. The tubes were vortexed and incubated overnight at 4°C. The hCT bound to the primary antibody was separated from unbound hCT by specifically precipitated the hCT-primary antibody complex with 1.0 ml of Amerlex-M (Donkey anti-rabbit IgG linked to magnetic beads). Each tube was vortexed and incubated at 22C for 15 min. All tubes were centrifuge at 1500 rpm for 15 min at 4°C (Mistral 3000, MSE, UK) to pellet the precipitate. The supernatant (containing the unbound hCT fraction) was removed by aspiration. The [^{125}I] content of each pellet (represented the bound [^{125}I]hCT) was determined by gamma counting (see section 2.2.1). A line function ($y=((B_0\text{-NSB}/(x^n/K+1))+\text{NSB}$) could be fitted to the standard curve of pellet associated CPM versus log hCT concentration profile (Figure 2.2). Sample concentration were calculated using the equation which described the best fit through the standard curve data.

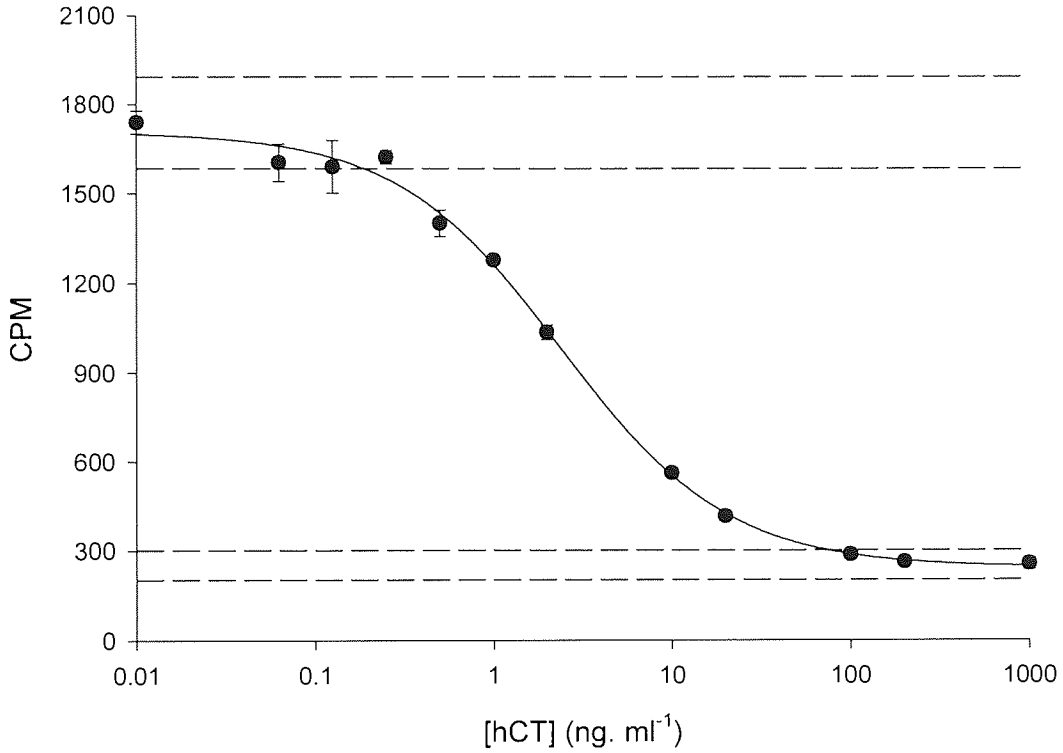

Figure 2.2 Human calcitonin radioimmunoassay standard curve. A semi logarithmic plot of CPM against hCT concentration. The curve represents the best fit of the line function, $y=((B_o\text{-NSB}/(x^n/K+1))+\text{NSB})$ to the standard concentration values (mean ± SEM n=4). The dashed lines represent 2 standard deviation spread on the zero analyte concentration and the non-specific binding values.

2.2.5 HUMAN CALCITONIN IMMUNORADIOMETRIC ASSAY

The effect of peptidase inhibitors and absorption modulators on hCT flux across Caco-2 monolayers was measured using a commercially available solid-phase two-site immunoradiometric assay (IRMA), ELSA-hCT (CIS (UK) Ltd., High Wycombe, Bucks, UK). Two monoclonal antibodies, one recognising amino acid region 24-32 and the other the 11-17 region, allowing the assay of hCT monomer. One is used to coat the ELSA™ fixed to the bottom of the tube and the second is ^{125}I-radiolabelled and used as a tracer in

excess. The hCT present in the standards or samples are sandwiched between the two antibodies (Figure 2.3).

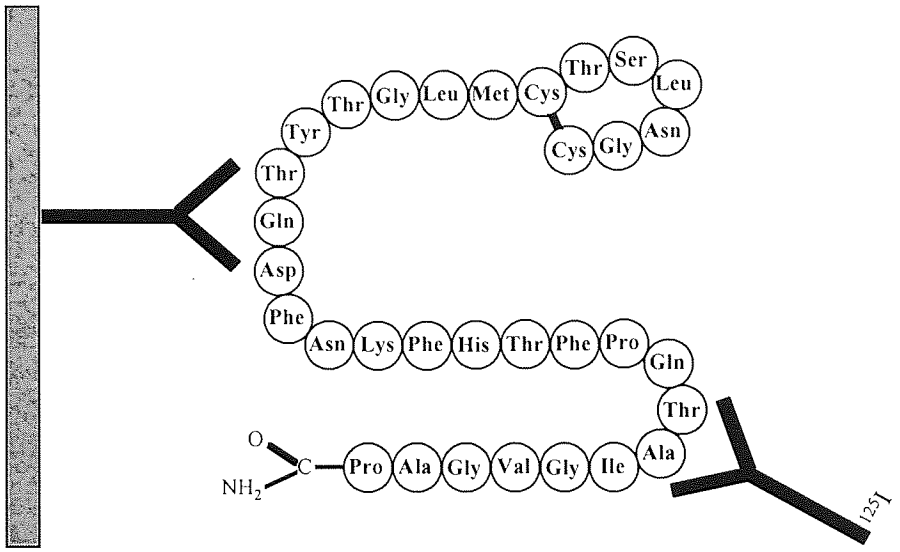

Figure 2.3 A diagram of the ELSA-hCT assay. The assay uses two monoclonal antibodies with precise immunoreactive sites to measure the physiologically active mature hCT. One monoclonal antibody is attached to the solid-phase and the other is radiolabelled.

Following the formation of the coated antibody/hCT/iodinated antibody-complex, the excess tracer is removed with a washing step. The amount of radioactivity bound to the tube is proportional to the concentration of hCT present in the sample.

All the reagents were brought to room temperature (18-25°C) at least 30 min before use. Dispensing of reagents into the ELSA™ tubes were carried out at room temperature. The assay was performed in duplicate for standards (9-10,000 pg ml^{-1}) and samples. The order in which the reagents are added is shown in Table 2.2.

Following the dispensing of 50 µl of standard or sample into the corresponding tube, 150 µl of 4.5 % (w/v) human serum albumin (HSA) to block non-specific binding of hCT, was added followed by 100 µl of monoclonal anti-hCT tracer into all ELSA™ tubes. Each tube was gently mixed on a Vortex mixer and incubated for 20-24 h at room temperature (18-25°C).

Table 2.2 ELSA-human calcitonin assay protocol. All quantities are in µl

Tubes	Standards	Samples
Standards	50	-
Samples	-	50
4.5 % HSA	150	150
Anti-hCT ^{125}I	100	100
Mix and incubate		
Wash and count		

Washing the ELSA™ tubes is a crucial step to obtain reliable and reproducible results; therefore, following the manufacturers protocol was important. The contents of the tube were aspirated completely and 3 ml of washing solution added to each ELSA™ tube, followed by a 5 min incubation and then the contents aspirated. This process was repeated twice. The radioactivity bound to the ELSA™ tubes was measured by gamma scintillation counter (Section 2.2.1).

Concentrations of duplicate samples were determined from the standard curve (Figure 2.4). The minimum detectable concentration of hCT was 9 pg ml^{-1}, the intraassay coefficient of variation 4-8 %, and the interassay coefficient of variation 3-36 % for values between 9 and 10,000 pg ml^{-1}. Recovery of hCT added to transport buffer was 100 %.

2.2.6 HPLC ANALYSIS OF CHPP

Samples were analysed on a Kontron HPLC system (UV 279 nm) with a reversed-phase column (Nucleosil 5C18 column 25 cm x 4.6 mm). The injection volume was 130 µl, with a total run time for each sample of 27 min. Chromatograms were developed by gradient elution (solution A, 20 mM phosphate buffer pH 7.4/MeCN HPLC grade acetonitrile (Rathburn Chemicals Ltd. Walkerburn, UK); A = 90/10 and solution B, MeCN), with a flow rate of 1 ml min^{-1}.

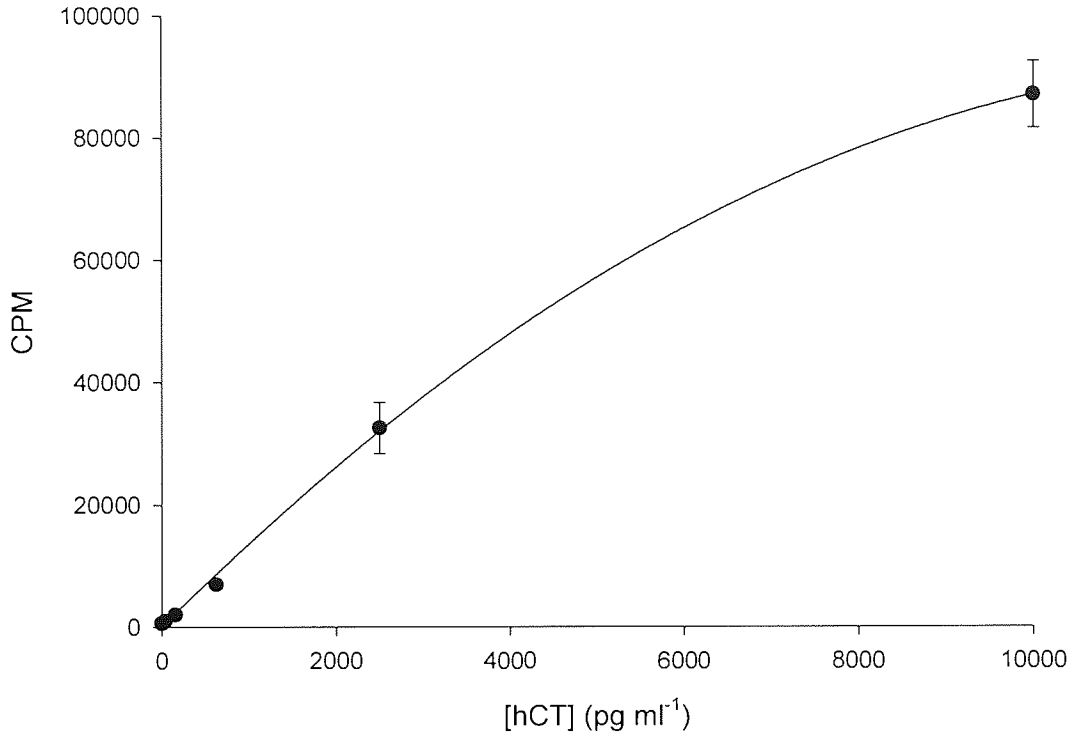

Figure 2.4 Human calcitonin standard curve. The plot of CPM against hCT concentration (0 to 10,000 pg ml^{-1}), the line represents the best fit of the line function $y=14.15x+41.02x^2-0.000543$, $R^2=0.9995$, to the standard concentration values (mean ± SEM, n=4).

The peak areas for the compound in the Ap and Bl chambers were recorded and used to calculate the apparent permeability coefficient in Caco-2 experiments. Quantitation was by the external standard method. A stock ethanolic 11.25 mM CHPP standard was prepared, and diluted in either 2.9 % (v/v) ethanol in transport buffer or rat plasma to construct a standard curve (0.3-10.0 μM CHPP). Peak areas were used to determine the concentration of CHPP by reference to a standard curve. The standard curve was linear up to 10 μM in both rat plasma and 2.9 % (v/v) ethanol in transport buffer (Figure 2.5). Rat plasma samples were prepared for HPLC analysis as described in section 2.11.3. The minimum detectable concentration of CHPP in rat plasma was 0.3 μM, the intraassay coefficient of variation 2.1-8.5 %, and the interassay coefficient of variation 6.5-31.6 % for values between 0.3 and 10.0 μM. Recovery of CHPP added to rat plasma (1 μM) was 100 %.

The minimum detectable concentration of CHPP in 2.9 % (v/v) ethanol in transport buffer was 0.3 μM, the intraassay coefficient of variation 3.1-8.4 %, and the interassay coefficient of variation 4.5-11.6 % for values between 0.3 and 10.0 μM. Recovery of CHPP added to 2.9 % (v/v) ethanol in transport buffer was 95.0 % ± 7.2 %.

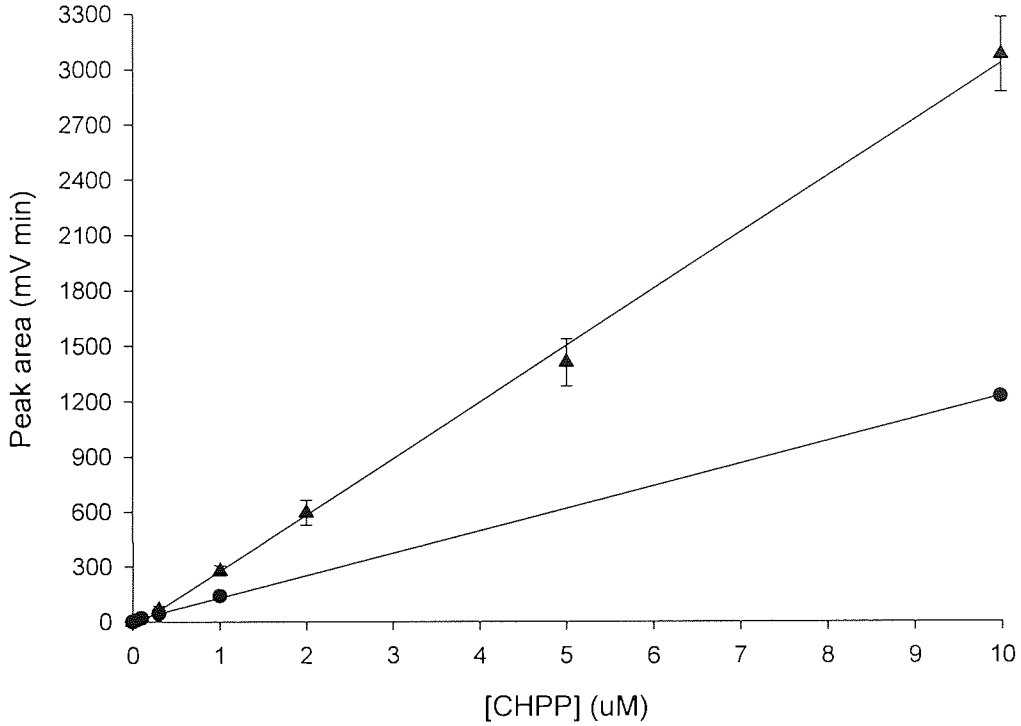

Figure 2.5 Standard curve for CHPP. The plot of peak area against CHPP concentration (0 to 10 μM); in rat plasma (▲) the line represents the best fit by linear regression, y=306.95x-31.13 R^2=0.998, to the standard concentration values (mean ± SEM, n=4); in 2.9 % (v/v) ethanol in transport buffer (●) the line represents the best fit by linear regression, y=122.036x+6.3 R^2=0.999, to the standard concentration values (mean ± SEM, n=4).

2.3 CACO-2 CELL CULTURE

The preparation of culture media and the maintenance of stock cultures, together with the preparation of Caco-2 monolayers for experiments, are described below.

2.3.1 CULTURE MEDIA

Two media were prepared to culture Caco-2 cells. A maintenance medium was used to maintain stock cultures in plastic 162 cm^2 T-flasks and a filter medium was used to cultivate cells on permeable polycarbonate filters in polystyrene culture-inserts (Transwell™ Costar, UK) for transport experiments. Maintenance medium comprised Dulbecco's modification of Eagle's medium (DMEM) supplemented with (final concentrations) 10 % (v/v) foetal bovine serum (FBS), 1 % (v/v) non-essential amino acids (NEAA). Filter medium comprised of maintenance medium supplemented with 1 % (v/v) penicillin and streptomycin (PS), final concentration.

Foetal bovine serum (GibcoBRL 10108-066), 10,000 units ml^{-1} penicillin and 10,000 μg ml^{-1} streptomycin (GibcoBRL 15140-031) were stored at -20°C and thawed according to the manufacturer's directions immediately prior to use. DMEM (GibcoBRL 41965-039) and NEAA (GibcoBRL 11140-035) were stored at 4°C. Maintenance and filter media were prepared aseptically from pre-sterilised components and were used without further sterilisation. They were stored at 4°C and used within 14 d.

2.3.2 STOCK CULTURES

The Caco-2 cell line was a generous gift from Professor Colin Hopkins, MRC unit, University of London, UK. Cells were used for experiments between passage 87-105. Cells were cultured in 162 cm^2 plastic T-flasks with maintenance medium. They were incubated at 37°C in a humidified (95 %) atmosphere of 10 % CO_2 in air. The maintenance medium was renewed every 48 h. Stock cultures were passaged (1:3) weekly by trypsinisation with a solution containing 0.25 % (w/v) trypsin and 0.2 % (w/v) disodium ethylenediamine tetraacetate in phosphate-buffered saline, pH 7.2 (PBS; Oxoid, UK).

2.3.2.1 FREEZING AND THAWING CACO-2 CELL STOCKS

Frozen stocks of Caco-2 cells (2-4 x 10^6 cells, passage 87-100) were stored in a liquid nitrogen cell bank in 1.5 ml plastic screw-capped cryovials (Costar, UK) using a freezing medium comprising maintenance medium and 10 % (v/v) dimethyl sulphoxide. Cells were revived from frozen stocks by thawing in a 37°C water bath and immediately washing once

in 10 ml maintenance medium to remove the dimethyl sulphoxide. The cells were cultured for at least two passages before they were used for experiments.

2.3.2.2 MYCOPLASMA TESTING

The Caco-2 cells were regularly monitored for mycoplasma-contamination using the Gen-probe® mycoplasma T.C. rapid detection system (Gen-probe Inc. USA). Maintenance medium from stock Caco-2 cells cultured in 162 cm^2 flasks was routinely used. The kit uses a ^3H-labelled single-stranded DNA probe complementary to mycoplasma ribosomal RNA. After the ribosomal RNA is released from the organism, the [^3H]DNA probe combines with mycoplasma ribosomal RNA to form a stable DNA-RNA hybrid. The labelled DNA-RNA complex is separated from non-hybridised DNA probe by hydroxyapatite in buffered solution. Scintillation solution is added to the labelled hybrids and counted in a scintillation counter (section 2.2.1). Positive and negative controls supplied with the kit, as well as test results are calculated as a percentage of total counts hybridized. A percentage hybridisation greater than, or equal, to 0.4 % is positive for the presence of mycoplasma. The Caco-2 cell line was mycoplasma-negative throughout the work described here.

2.3.3 CULTURES FOR TRANSEPITHELIAL ELECTRICAL RESISTANCE AND TRANSPORT STUDIES

For transepithelial electrical resistance (TER) and transport studies, Caco-2 cells were cultured in Transwell™ culture-inserts, a polycarbonate permeable support in a polystyrene housing. Briefly, 2-3 d post confluent stock cultures were trypsinised and resuspended in filter medium. The viable cell density was measured by haemocytometry using a trypan blue exclusion test and reduced to 1.0 x 10^6 cells ml^{-1} by dilution. The apical (Ap) chambers of each culture-insert were seeded with 2 ml of the cell suspension (2.0 x 10^6 cells) and 3 ml of filter-medium was added to the basolateral (Bl) chamber. The inserts were not disturbed for the first 24 h, thereafter, the filter medium was replaced on alternate days. The monolayers received their final change of filter medium 24 h prior to experimentation.

Caco-2 cells develop a highly polarised morphology when cultured on permeable-supports (Hidalgo *et al.*, 1989; Wilson *et al.*, 1990; Cogburn *et al.*, 1991 and Nicklin *et al.*, 1992a). Their apical brush-border of microvilli projects into the inner-chamber of the culture-insert and their Bl membranes are in contact with the solution in the outer chamber. The inner- and outer-compartments are referred to as the apical (Ap) and basolateral (Bl) chambers, respectively.

2.3.4 CULTURES FOR CYTOTOXICITY ASSAY

For cytotoxicity studies, Caco-2 cells were cultured on flat-bottom tissue culture-treated 96-well cell culture clusters (Costar, UK). Briefly, 2-3 d post-confluent stock-cultures were trypsinised and resuspended in maintenance medium. The viable cell density was measured by haemocytometry using a trypan blue exclusion test which was reduced to 2.5 x 10^5 cells ml^{-1} by dilution with further maintenance medium. Each well was seeded with 200 µl of the diluted cell-suspension (5.0 x 10^4 cells). The 96-well clusters were incubated at 37°C in a humidified atmosphere (95 %) of 10 % carbon dioxide in air. Maintenance medium was renewed every day. The monolayers received their final change of maintenance medium 24 h prior to an experiment unless otherwise specified.

2.4 TRANSPORT MEDIA

Transport buffer (TB) was used for the majority of transport studies. It comprised Hanks' balanced salt solution (HBSS) containing 0.1 % (w/v) BSA (Fraction V), 5.5 mM D-glucose and buffered with 25 mM HEPES (pH 7.0, 7.2 and 8.0) or MES (pH 5.5, 6.0, 6.5). These media were adjusted to the appropriate pH using sodium hydroxide (potassium hydroxide for sodium-free solutions) or hydrochloric acid (BDH, Poole, Dorset, UK), as appropriate. They were filter sterilized using a bottle-top filter system (Costar, UK) and stored at 4°C. After the addition of acids or bases in quantities that displaced the pH of these buffered transport media, the correct pH was restored by the addition of 1 M sodium hydroxide, 1 M potassium hydroxide or 1 M hydrochloric acid, as appropriate. Transport buffer adjusted to pH 7.2 was used unless stated otherwise.

A sodium-free version was prepared by equimolar substitution of NaCl with choline chloride ($TB_{Choline}$). Similarly, a glucose-free version ($TB_{Glucose}$) was prepared by omitting

glucose from the above formula. TB_{NoBSA} comprised Hanks' balanced salt solution, 5.5 mM D-glucose and was buffered to pH 7.2 with 25 mM HEPES.

TB_{EtOH} was used for NBS and CHPP transport experiments (Chapter Four). It comprised transport buffer plus ethanol (0-5 % v/v) (AnalaR BDH, Poole, Dorset, UK) at the stated concentrations.

2.5 TRANSEPITHELIAL ELECTRICAL RESISTANCE

Transepithelial electrical resistance (TER) was measured using pre-warmed TB added to the Ap (3 ml) and Bl (3 ml) chambers and allowed to equilibrate to 37°C for 15 min. At the time points indicated, the six-well cluster was removed from the incubator and placed on a hot-plate that maintained the medium at 37°C while measuring TER. The TER of each monolayer was measured with an epithelial voltmeter using STX2 'chopstick' electrodes (EVOM, World Precision Instruments, Stevenage, Herts, UK).

The positioning of the electrode was critical in achieving consistent and reliable TER measurements. The 'chopstick' electrode was arranged with its longest electrode in the Bl chamber, against the base of the six-well cluster, and its shorter electrode in the Ap chamber. The mean TER for each monolayer was calculated from three measurements at discrete positions. The intrinsic resistance of the system (permeable-support alone) was subtracted from the total resistance (cell monolayer + permeable-support) to calculate the resistance of the monolayer. The resistance was corrected for surface area of the Transwell™ polycarbonate permeable-support (4.71 cm^2) and the TER expressed in ohms cm^2.

As can be seen in Figure 2.6 the TER increases to a plateau of approximately 500 ohms cm^2 after confluency at day 4, which shows no change up to 21 d when cultured on Transwell™ inserts. This is in agreement with Karlsson *et al.* (1993) and Artursson (1990) explaining the increase in TER is due to the formation of intercellular tight junctions and differentiation of the Caco-2 monolayer.

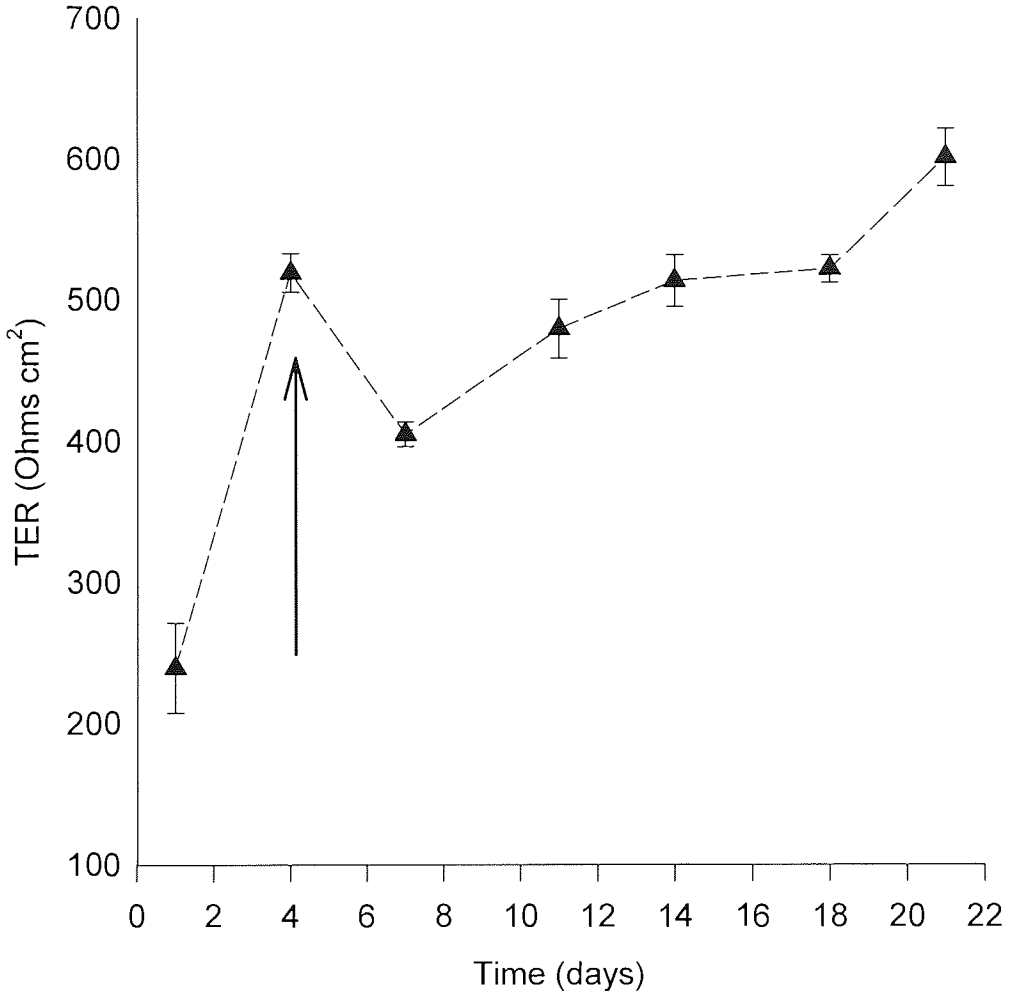

Figure 2.6 The effect of days in culture on the transepithelial electrical resistance (TER) of Caco-2 monolayers grown on Transwell™ inserts. Transepithelial electrical resistance of Caco-2 monolayers in TB at 37°C in air was measured as described in section 2.5. The arrow indicates when confluency was reached by the monolayers. Each point is the mean ± SEM (n=3).

2.6 TRANSPORT STUDIES

Throughout the work described here, a variety of media have been used for transport experiments. The most frequently employed media are detailed in section 2.4. Standard protocols for transport experiments are given in section 2.6.2. This general method was

subject to minor adaptations as appropriate for each experiment. Such modifications are described in the relevant sections.

2.6.1 TRANSPORT ACROSS OPEN TRANSWELL™

Transwell™ inserts were conditioned for 15 min in TB at 37°C. The conditioning buffer was removed before incubation with TB containing radiochemical:- either [^{125}I]human calcitonin, D-[^{14}C]mannitol, [^{14}C]PEG 4000, [^{14}C]taurocholic acid, [4-^{14}C]testosterone and D-[^{14}C]glucose (all Amersham, Bucks, UK). Transport experiments across open Transwell™ were conducted for 1 h at 37°C, after the incubation period, Transwell™ were transferred to a cold table (0-4°C). The incubation solutions were collected and their radioactive content was determined by liquid scintillation counting (see section 2.2.1). Each Transwell™ was carefully rinsed (3 x 2 ml Ap and 3 ml Bl x 5 min) with ice-cold PBS-sodium azide 0.04 % (w/v) (PBS-N_3). Following the final PBS-N_3 wash, the filters were removed from the filter insert using a scalpel. The residual [^{3}H] and [^{14}C] radioactivity on the permeable-supports was measured by liquid scintillation counting (see section 2.2.1 A or B). Residual [^{125}I] was determined by gamma counting (see section 2.2.2). The radioactivity associated with the permeable support was expressed as a percentage of the total radioactivity in the incubation chamber. Also the transport of the radiochemicals across open Transwell™ was calculated (Table 2.3).

2.6.2 TRANSPORT EXPERIMENTS

The Caco-2 monolayer transport model comprises a cell monolayer, cultured on a permeable-support, separating a donor chamber from a receiver chamber (Figure 1.6).

Transport studies were performed over 180 min at 37°C in air. Typically, the donor solution is placed in the Ap chamber of the culture insert and the receiver solution in the outer Bl chamber. In this way, the apical-to-basolateral (Ap-to-Bl) flux of a compound can be investigated as described below.

Table 2.3 Transport and adsorption of radiochemicals across conditioned Transwell™ filters. Each value is the mean ± SEM (n=3)

Radiochemical probe	Apical concentration (M)	Flux (%/h)	P_{app}[a] ($cm\ s^{-1} \times 10^{-6}$)	Adsorption to filter (%)
[^{125}I]hCT	5.0×10^{-14}	5.16 ± 0.268	16.6 ± 0.085	3.84 ± 0.263
D-[^{14}C]mannitol	4.0×10^{-6}	17.09 ± 0.758	20.2 ± 0.894	0.00 ± 0.00
[^{14}C]PEG 4000	1.34×10^{-5}	3.69 ± 0.083	1.1 ± 0.025	1.61 ± 0.05
[^{14}C]taurocholic acid	3.5×10^{-6}	7.14 ± 0.494	21.9 ± 1.51	0.01 ± 0.001
D-[^{14}C]glucose	8.17×10^{-7}	9.53 ± 0.326	20.6 ± 0.698	0.002 ± 0.001
[4-^{14}C]testosterone	3.0×10^{-6}	13.60 ± 1.52	20.6 ± 2.303	1.98 ± 0.388

a=P_{app}, Apparent permeability coefficient is defined as $P_{app}=dQ/dt \times 1/(A.C_o)$ (see section 2.6.2).

Plate medium was aspirated from the Ap and Bl chambers and the monolayers washed once with 2 ml (Ap) and 3 ml (Bl) of TB for 15 min at 37°C. The washing and incubation solutions, in the donor and receiver chambers may or may not be identical depending on experimental requirements. The transport experiment was initiated by aspirating the washing solutions and applying a donor solution (2 ml) of incubation medium containing an appropriate concentration of the radiochemical being studied plus transport modulators/inhibitors. The culture insert and donor solution were immediately transferred to a chamber containing 3 ml of receiver solution. All washing and incubation solutions were equilibrated to 37°C prior to use. Ap-to-Bl transport kinetics were followed by sequentially transferring the culture insert, complete with its donor solution, into a new receiver chamber at, 30, 60, 90, 120, and 180 min. After the final receiver sample had been collected, monolayers were transferred to a cold-table (0-4°C) and the Ap donor solutions were collected and their radiochemical concentration determined. The radiochemical flux into the receiver solution for each time interval was corrected for dilution and specific radiochemical activity to express total solute flux. Transport in the reverse direction (*ie:* Bl-to-Ap) was also determined. In this case, the rate of radiochemical flux into the Ap chamber from a Bl donor solution was monitored. The amount of absorbed marker versus

time showed a linear relationship for all probes over the time period 30 to 120 min. The apparent permeability coefficient P_{app} was determined according to the following equation

$$P_{app} = dQ/dt \times 1/(A.C_o)$$

where dQ/dt is the permeability rate (steady-state flux, moles s^{-1}), C_o is the initial concentration in the donor chamber (moles ml^{-1}) and A is the surface area of the membrane (cm^2). Apparent permeability coefficient values were calculated for time intervals during which < 10 % of the marker drug had been transported (*i.e.* under sink conditions). Since the effects of some compounds on permeability were time dependent, the P_{app} values were calculated for each time point separately. In addition a "mean" P_{app} was calculated for the 90 min period between the first time point at 30 min and 120 min of the experiment for comparison of the data.

2.6.2.1 D-[^{14}C]MANNITOL TRANSPORT

Caco-2 monolayers were washed with 2 ml (Ap), and 3 ml (Bl) of respective TB for 15 min at 37°C in air. The wash solutions were removed and D-[^{14}C]mannitol (0.225 μCi ml^{-1}; 4 μM) in the chosen TB with either added transport inhibitors or modulators were applied to the Ap chamber of Transwell™ inserts in the presence of a Caco-2 monolayer. Stock solutions of transport inhibitors or modulators in either ethanol or DMSO, were diluted to give final solvent concentrations of <0.2 % (v/v) in TB. Ap-to-Bl transport kinetics were followed as described previously (see section 2.6.2). D-[^{14}C]mannitol is regarded as a paracellular marker and therefore an indicator of the integrity of tight junctions within a monolayer (Artursson, 1990). Figure 2.7 shows the decrease in D-[^{14}C]mannitol permeability following the formation of tight junctions and the polarisation of the Caco-2 monolayer cultured on Transwell™ inserts for up to 21 d.

2.6.2.2 [^{14}C]PEG 4000 TRANSPORT

Following the removal of the wash solutions from Caco-2 monolayers [^{14}C]PEG 4000 (0.225 μCi ml^{-1}; 13.4 μM) in TB was added to the Ap or Bl chamber of culture inserts and transport kinetics followed as in section 2.6.2 above.

2.6.2.3 D-[^{14}C]GLUCOSE TRANSPORT

Caco-2 monolayers were washed (1 x (2 ml Ap + 2 ml Bl) x 15 min) with TB containing the respective glucose concentration before D-[^{14}C]glucose (0.25 μCi ml^{-1}; 817 nM) in TB was added to either the Ap or Bl chamber. Transport kinetics were followed as in section 2.6.2 above.

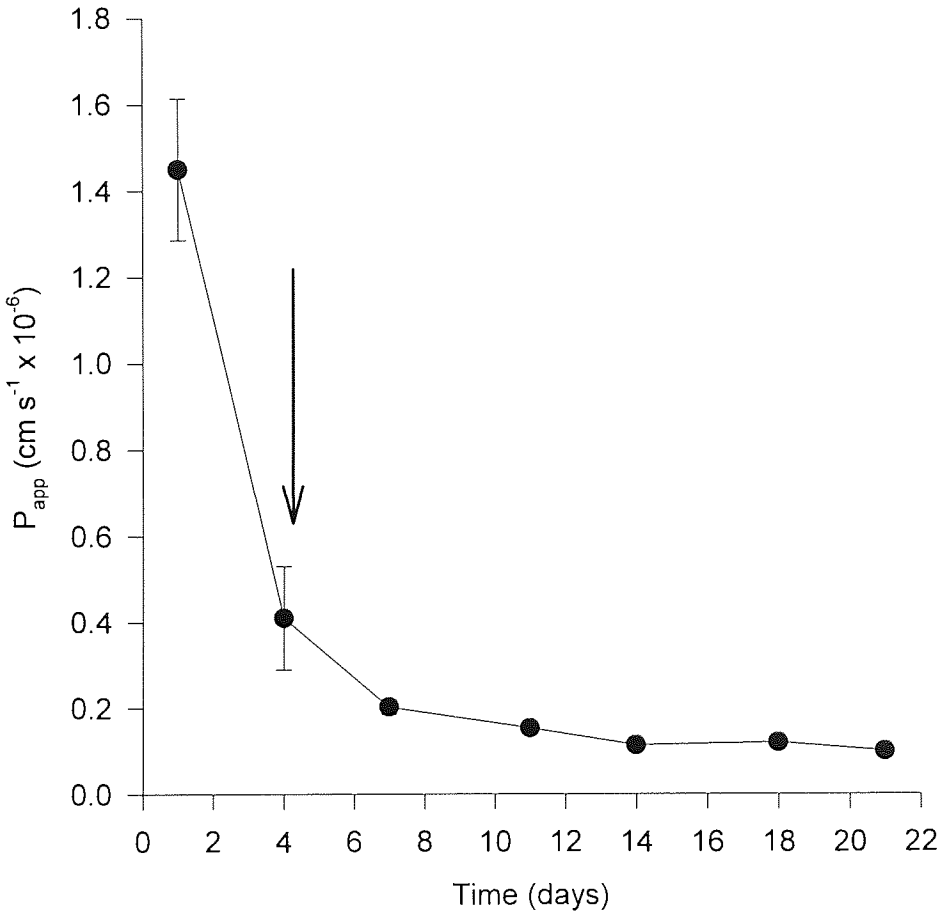

Figure 2.7 The apical to basolateral apparent permeability coefficients (P_{app}) for [^{14}C]mannitol across Caco-2 monolayers versus days in culture on Transwell™ inserts. P_{app} was calculated from Ap-to-Bl D-[^{14}C]mannitol flux in TB at 37°C in air over 120 min. The arrow indicates when confluency was reached by the monolayers. Each point is the mean ± SEM (n=3).

At the end of the experiment, the inserts were transferred to a cold-table (0-4°C), the Ap and Bl media collected and assayed for [^{14}C]-content by liquid scintillation counting. The appearance of [^{14}C] in the receiver chamber represented total (saturable + non-saturable) Ap-to-Bl transport. The non-saturable transport component was estimated by measuring transport in the presence of a 1.0 x 10^5 molar excess of D-glucose. The saturable transport was calculated by subtraction of the total and non-saturable transport components.

2.6.2.4 [4-^{14}C]TESTOSTERONE TRANSPORT

Caco-2 monolayers were washed (1 x (2 ml Ap + 2 ml Bl) x 15 min) with TB before [4-^{14}C]testosterone (0.25 μCi ml^{-1}; 3 μM) in TB was added to either the Ap or Bl chamber. Transport kinetics were followed as in section 2.6.2. At the end of the experiment at 37°C, the inserts were transferred to a cold-table (0-4°C), the Ap and Bl media collected and assayed for [^{14}C]-content by LSC (see section 2.2.1). The appearance of [^{14}C] in the receiver chamber represented total (saturable + non-saturable) Ap-to-Bl transport. The non-saturable transport component was estimated by measuring transport in the presence of a 3333-fold molar excess of testosterone.

2.6.2.5 [^{14}C]TAUROCHOLIC ACID TRANSPORT

Caco-2 monolayers were washed with TB (1 x (2 ml Ap + 3 ml Bl) x 15 min) before [^{14}C]taurocholic acid (0.1 μCi ml^{-1}; 3.5 μM) in TB was added to the Ap or Bl chamber. They were incubated at 37°C in air. Transport kinetics were followed by sequential transfer of the culture insert into fresh receiver solution at 30 min intervals. At the end of each transport experiment the culture inserts were transferred to a cold table (0-4°C), the Ap and Bl transport media were collected and the monolayers washed three times with ice-cold PBS-N_3. The [^{14}C]-content of each sample was measured by LSC (see section 2.2.1). The appearance of [^{14}C] at the opposite side of the monolayer gave total (saturable + non-saturable) transport. The non-saturable transport component was estimated by measuring transport in the presence of a 1,000-fold molar excess (3.5 mM) of unlabelled taurocholic acid. Saturable transport was calculated by subtraction of the total and non-specific transport components.

2.6.2.6 HORSERADISH PEROXIDASE TRANSPORT

Horseradish peroxidase (HRP) Type II was dissolved in TB up to 250 μM (10 mg ml^{-1}) and brought to 37°C in a water-bath. The transport experiments were carried out as in section 2.6.2. Samples were taken at the timepoints indicated and stored at -20°C until analysis by the HRP assay (section 2.2.3).

2.6.2.7 HUMAN CALCITONIN TRANSPORT

Caco-2 cells were washed in TB at 37°C in air for 15 min. Transport experiments were started when the hCT dose solution (0.1 to 5 mg ml^{-1}) in TB was placed in either the Ap or Bl chamber with the other chamber already filled. The transport experiments were carried out as in section 2.6.2. Samples were taken at 0, 30, 60, 90, 120, and 180 min and stored at -20°C until analysis by hCT-IRMA.

In transport experiments with protease inhibitors and transport enhancers, Caco-2 cells were washed with TB. Experiments were initiated by the addition of mixtures of inhibitors or enhancers and 0.1 mg ml^{-1} hCT. At the end of the experiment, following the last sample, the cells were transferred to a cold-tray (0-4°C) and the Ap and Bl solutions were removed and stored at -20°C before analysis of the residual hCT was measured by two-site hCT-IRMA (section 2.2.6). The cell monolayers were washed 3 times with ice-cold PBS-N_3 (2 ml Ap and 3 ml Bl). Following the last wash 0.5 ml of lysis buffer (see section 2.6.2.5 for composition) was added to the Ap chamber. After shaking for 30 min at room temperature the cell extracts were centrifuged at 15,000 rpm in an Eppendorf centrifuge at 4°C. The supernatants were removed and stored at -20°C until analysis by hCT-IRMA (section 2.2.6).

2.6.2.8 NBS AND CHPP TRANSPORT

Both NBS and CHPP, two drug candidates, have limited aqueous solubility which hindered their use in the Caco-2 transport model. To use [^{14}C]NBS and NBS, the concentration range was limited by the aqueous solubility of the drug 0.068 mg l^{-1}. To increase the amount of soluble drug available, a co-solvent, ethanol, was used. Ethanol was also used as a co-solvent for CHPP, as it also has limited aqueous solubility (0.4 mg l^{-1}). To overcome this problem both drugs were made up into stock ethanol solutions, CHPP 11.25

mM and for NBS 35.05 mM and then diuted into TB_{EtOH}. This resulted in the highest drug concentration, 100 μM, in TB containing 2.9 % (v/v) ethanol as a co-solvent.

Caco-2 cell monolayers for this work was carried out on 14 d old cells because Caco-2 monolayers were considered a tight monolayer with all the morphological characteristics of the small intestine (Artursson, 1990) and as these candidate drugs are highly lipophilic with Log D of >5.5 for NBS and 4.1 for CHPP; the mechanism of transport is likely to be by passive permeation. All transport experiments were carried out as in section 2.6.2 but using the modified transport buffer, 2.9 % (v/v) TB_{EtOH}. To determine the effect of modified transport buffer on Caco-2 monolayer integrity a [^{14}C]mannitol transport assay was carried out (see section 2.6.2.1) along with [^{14}C]PEG 4000 transport (see section 2.6.2.2). Briefly, the medium was replaced with 2 ml of a donor (Ap) solution containing radiolabelled tracer (either [^{14}C]NBS or [^{14}C]mannitol or [^{14}C]PEG 4000) at a concentration of 0.45 μCi ml^{-1} and unlabelled drug at the concentration shown (Chapter 4). Transport kinetics were followed by sequential transfer of the culture insert into fresh receiver solution at 30 min intervals. At the end of each transport experiment the culture inserts were transferred to a cold table (0-4°C), the Ap and Bl transport media were collected and the monolayers washed three times with ice-cold PBS-N_3. For investigations of the effect of inhibitors on the transport of NBS and CHPP, the inhibitors were present in both the donor and receiver chambers. Except when 5 mM La^{3+} or pH 5.5 were tested these were used in the Ap chamber only. The [^{14}C] content of 2.9 % (v/v) TB_{EtOH} and filters were assayed for radioactivity by LSC (section 2.2.1) or in the case of CHPP by HPLC (see Section 2.2.7).

2.7 CELLULAR ASSOCIATION EXPERIMENTS

To allow the comparison of probe molecule cell association/uptake, each filter insert was fed on alternate days for 21 d. The filter medium was aspirated and the filter and monolayer were washed with TB (1 x 2 ml Ap and 3 ml Bl x 15 min). This washing solution was removed, and 3 ml of TB was added to the Bl compartment. To initiate the experiment, 2 ml of TB containing the radiolabelled ligand was applied to the Ap chamber. After the incubation period, monolayers were transferred to a cold-table (0-4°C). The incubation solutions were collected and their radioactive content was determined by liquid

scintillation counting (see section 2.2.1). Each monolayer was carefully rinsed (3 x 2 ml Ap and 3 ml Bl x 5 min) with ice-cold PBS-N_3 to terminate the uptake process and remove trace quantities of extracellular radioligand. Following the final PBS-N_3 wash, the filters containing the cell monolayers were cut out from the filter insert using a scalpel and collected for LSC. This procedure ensured that all the cells were effectively removed, and the associated radioactivity was determined by LSC. The cell-associated radioactivity was corrected for specific radiochemical activity and this correction cancelled fluctuations in cell-associated radioactivities resulting from minor variations in the radiochemical concentrations applied to each monolayer. The cell-associated solute (monolayer + filter) was expressed as moles of solute per insert.

2.8 CACO-2 CYTOTOXICITY ASSAYS

The effect of test compounds on Caco-2 cell integrity was measured by two assays. Release of lactate dehydrogenase (LDH) into the supernatant by cells with damaged cell membranes (Surendran *et al.*, 1995) and the reduction in cleavage of 3-[4,5-dimethylthiazol-2yl]-2,5-diphenyltetrazolium bromide (MTT) by mitochondrial dehydrogenase in living cells to give an insoluble dark blue formazan. Damaged or dead cells show reduced or no dehydrogenase activity (Mosmann, 1983).

Caco-2 cells were seeded at a concentration of 2 x 10^5 cells per well into 96-well tissue-culture plates (Costar UK) and grown for 4 d as described in section 2.3.4. The wells are washed with TB for 15 min at 37°C in air. The TB was removed and replaced with 0.2 ml of TB containing test compound at the stated concentrations. The negative control was TB alone while the positive control was TB containing 0.05 % Triton-X100. After 2 h at 37°C in air, 20 µl aliquots of medium were transferred to a new 96-well microtitre plate to measure LDH activity, section 2.8.1. The cell monolayer was then stained using the MTT assay kit as in section 2.8.2.

2.8.1 LACTATE DEHYDROGENASE ASSAY

To each 20 µl sample aliquot was added 235 µl of a solution containing 0.1 M KH_2PO_4 (pH 7.2), 0.69 mM sodium pyruvate and 0.1 mg ml^{-1} reduced β-nicotinamide adenine dinucleotide (NADH) and the assay was allowed to proceed for 3 min. The reaction was

stopped with 50 µl of oxamic acid and the optical absorbance at 340 nm, blanked on TB, was measured in a MRX plate reader (Dynatech Laboratories, Billingshurst, Sussex, UK). Cells with damaged membranes would show reduced optical absorbances through the release of LDH and therefore decreased amounts of NADH.

2.8.2 MTT ASSAY

The assay was performed as described by Mosmann (1983). Briefly, TB containing the test compounds was removed and to each well 180 µl of fresh TB was added, followed by 20 µl of a 5 mg ml^{-1} solution of MTT in TB. After 2 h at 37° C in air, 200 µl of MTT solubilisation buffer (10 % (v/v) Triton X-100 in acidic isopropanol; 0.02 M HCl/isopropanol, 1:1 solution) was added and the plate was shaken for 30 min to dissolve the precipitate. The optical absorbance of 100 µl aliquots from each well was placed into a microtitre plate and measured against TB alone at 570 nm in a MRX microplate reader. Mitochondrial dehydrogenase readily turns MTT into an insoluble dark blue formazan. Triton X-100 is used to solubilise the Caco-2 monolayer and release the colour. The acidic isopropanol is used to solubilise the colour dark blue formazan crystals. Therefore, if the drug being tested enters the cell and causes cell death, less colour will be produced.

2.9 HUMAN CALCITONIN BINDING EXPERIMENTS

For the cell surface hCT binding experiments, Caco-2 cells were cultured as described for transport studies (section 2.3.3). The monolayers were washed with 2 ml (Ap), and 3 ml (Bl) TB for 15 min at 37°C in air. The wash solution was removed by aspiration and 3 ml TB was placed in the Bl chamber. To initiate the experiment, 2 ml of TB containing trace amount of radiolabelled [^{125}I]hCT with unlabelled hCT was added to the Ap chamber. The cells were incubated at 4°C for 120 min. After incubation, the hCT solution was removed, and the monolayers were washed three times with ice-cold PBS-N_3. The washed cells were permeabilised with 500 µl 0.1 % (v/v) Triton X-100. After 30 min incubation at room temperature, the cell extract was centrifuged at 15,000 rpm in an Eppendorf centrifuge at 4°C. The supernatent was removed and [^{125}I] was determined by gamma counting (see section 2.2.2). No specific binding was observed over the concentration range tested (3 pM - 300 µM).

2.10 HUMAN CALCITONIN DEGRADATION MODEL

Plate medium was aspirated from 21 d Caco-2 cell monolayers cultured on Transwell™ inserts and washed once with 2 ml (Ap) and 3 ml (Bl) of TB for 15 min at 37°C. The washing solutions were removed and the degradation experiment was initiated by adding TB containing 0.1 mg ml^{-1} of hCT in either the Ap or Bl chamber. After incubations for 2, 5, 10, 20, 30, and 60 min the concentrations of hCT in all the solutions was measured by hCT-IRMA (section 2.2.6). In experiments with protease inhibitors, Caco-2 cells were washed with TB, and incubated with mixtures of inhibitors and 0.1 mg ml^{-1} hCT. After a 10 min incubation period the monolayers were transferred to a cold-tray (0-4°C) and the Ap and Bl solutions were removed and stored at -20°C before analysis of the residual hCT was measured by two site hCT-IRMA (section 2.2.6). The cell monolayers were washed 3 times with ice-cold PBS-N_3 (2 ml Ap and 3 ml Bl) and then 0.5 ml lysis buffer (PBS containing 2 mM PMSF, 2 mM benzamidine, 0.5 % SDS, 1 % Triton X-100 and 0.1 mg ml^{-1} aprotinin) was added and shaken for 10 min at room temperature. The cell extract was centrifuged at 15,000 rpm in an Eppendorf centrifuge at 4°C, the supernatent was removed and stored at -20°C before being assayed by two site hCT-IRMA (section 2.2.6). The amount of hCT degraded was calculated by subtracting the value after 10 min contact with the monolayers from the hCT dose.

2.11 *IN VIVO* BIOAVAILABILITY EXPERIMENTS

2.11.1 ANIMALS

Male Wistar rats (248.9 g ± 20.6 g) kept on a 12 h light cycle (07:00 - 19:00) and fed *ad libitum* (Bantin and Kingman rat mouse diet) were used.

2.11.2 TREATMENT OF ANIMALS AND SAMPLE COLLECTION

Micronised CHPP was prepared by Dr. J. Zimmermann, Novartis Ltd., Basle, Switzerland. The compound was formulated as in Table 2.4.

Animals were anaesthetised with an i.m. injection (50 µl) of Hypnorm (Fentanyl 0.315 mg ml^{-1} and fluanisone 10 mg ml^{-1}). An i.v. formulation of CHPP 10 % (v/v) lactic acid in saline or PBS was administered by tail vein (500 µl) and seven oral formulations of CHPP were administered (500 µl), six by gavage and one i.d. Two oral formulations were

administered at higher dosing volumes, 1 ml per 100 g body weight to compare dosing regimes.Blood samples were removed from the tail vein at 5, 15, 30, 60, 120 min after dosing. The samples were mixed with 3 µl (15 U) of heparin (Evans Medical Ltd, Horsham, Sussex, UK) and kept on ice before spinning down in a bench centrifuge. The plasma was removed and stored frozen at -20°C before analysis.

Table 2.4 Formulations of micronised CHPP administered to male Wistar rats

[CHPP] ($mg\ ml^{-1}$)	Route	Formulation	Dose ($mg\ kg^{-1}$)
5	i.v.	10 % (v/v) Lactic acid	10
25	p.o.	3 % (v/v) Lactic acid	50
25	p.o.	Sesame oil + 1 % (w/v) Pluronic PE6800	50
25	p.o.	0.5 % (w/v) Klucel HF	50
25	p.o.	Oleic acid + 1 % (v/v) Tween 80	50
25	i.d.	0.5 % (w/v) Klucel HF	50
25	p.o.	SEDDS 40 % (v/v) Linoleic acid 17 % (v/v) Oleic acid 20 % (v/v) Cremophor RH40 23 % (v/v) Inwitor 988	50
5	p.o.	3 % (w/v) Gelucire 44/14	20

i.v.=intravenous, p.o.=per os, i.d.=intraduodenal

2.11.3 SAMPLE PREPARATION

Extraction and analysis of plasma samples occured on the same day. Plasma samples were aliquoted and vortexed with an equal amount of acetonitrile HPLC grade (Rathburn chemicals Ltd, Walkerburn, UK) and placed on ice for 30 min. After centrifugation the supernatant was removed and assayed by HPLC, see section 2.2.5.

2.12 DATA PRESENTATION

Transport data are expressed by two methods;

A) Amount entering the receiver solution per defined time period,

B) Apparent permeability coefficient (P_{app}) (see section 2.6.2).

Uptake values are presented as the moles of compound becoming associated with the monolayer or 1.0×10^6 cells per defined period of time.

Data are presented as mean values and experimental errors are expressed as standard error of the mean (SEM). When not shown, error bars are smaller than the symbols. Statistical analysis of the data was performed by one way analysis of variance (ANOVA) followed by Dunnett's test to show significance between control and treatment groups using SigmaStat for windows version 2.03 program (SPSSl Inc, USA). Differences with $P<0.05$ were considered significant.

CHAPTER THREE LANTHANUM AS A CACO-2 PARACELLULAR PATHWAY INHIBITOR

3.1 INTRODUCTION

Intestinal absorption of a molecule may be predominately, but not exclusively, *via* a particular transepithelial pathway, either the transcellular or paracellular pathway. As outlined in section 1.2, molecules have physico-chemical properties that predispose them to travel *via* one of the two absorption pathways. For example, biologically relevant peptides and proteins are generally large, charged, and hydrophilic molecules, which favour absorption *via* the paracellular pathway (McMartin, 1989). However, tight junctions display minimal porosity, allowing only small molecules (<11Å) and ions to cross the paracellular pathway. Larger molecules, therefore are not predisposed to use this route and only small amounts are absorbed. The use of paracellular pathway enhancers (Table 3.1) have been used to demonstrate that a particular molecule can potentially be transported by the tight junctional controlled paracellular pathway. This may mean the breakdown of epithelial barrier properties which lead to uncharacteristic intercellular junctions. Therefore, a paracellular inhibitor to block the pathway would give a direct measure of the amount transported by the paracellular pathway, with competent tight junctions.

3.1.1 PARACELLULAR PATHWAY

The intercellular junctional complex in GI tract epithelia consists of zonula occludens (tight junctions), zonula adherens (intermediate junctions), and macula adherens (desmosomes) (Lutz and Siahaan, 1997). The components of the tight junction, are the transmembrane-spanning protein occludin and its associated proteins linked to the cytoskeleton and the various intracellular second messengers. Tight junctions show cation-selectivity because they are lined with fixed negative charges such as COO^-, SO_4^{2-}, and PO_4^{3-} groups present on proteoglycans and glycoproteins on adjacent cell membranes (Schneeberger and Lynch, 1992).

It is believed that the formation of tight junctions is a secondary response to the primary interaction of the Ca^{2+}-dependent cell adhesion molecule E-cadherin (uvomorulin) (Gumbiner *et al.*, 1988). The adheren junctions consist of cell-cell adhesion below the

tight junctions in GI tract epithelia (Boller *et al.*, 1985). The Ca^{2+}-dependent homophilic binding of the glycoprotein E-cadherin, is transmitted across the plasma membrane by a cascade of reactions involving phospholipase C, G-proteins, protein kinase C (PKC) and calmodulin (Balda *et al.*, 1991, 1993).

Table 3.1 Paracellular transport enhancers (from Hochman and Artursson, 1994)

Paracellular transport enhancers	**Time**	**Reference**
PEPTIDE HORMONES		
IGF I or II	4 d	McRoberts and Riley, 1992
TNF	90 min	Mullin and Snock, 1990
INF-γ	2-3 d	Madara and Stafford, 1989
CYTOSKELETAL PERTURBATION		
Cytochalasin B or D	10-30 min	Meza *et al.*, 1980; Meza *et al.*, 1982; Madara *et al.*, 1986
Clostidium difficile toxin A	6-8 h	Hecht *et al.*, 1988
Oxidants	10-30 min	Shasby *et al.*, 1988; Welsh *et al.*, 1985
Na^{+}-dependent nutrient absorption	10 min	Madara and Pappenheimer, 1987
ATP depletion	10-120 min	Mandel *et al.*, 1993
PKA inhibitors	1 h	Rubin *et al.*, 1991
PKC activators	1-3 h	Mullin and O'Brien, 1986
ZO toxin	30 min	Fasano *et al.*, 1991
Ca^{2+} chelators	5-15 min	Martinez-Palomo *et al.*, 1980
Ca^{2+} ionophores	30 min	Martinez-Palomo *et al.*, 1980

Cells with less E-cadherin molecules are generally less adhesive. Also, if calcium is removed from the extracellular environment, cell-cell adhesion loosens or, in some cases, is destroyed. Thus, E-cadherin is crucial for the development and maintenance of GI epithelial intercellular junctions. Studies have demonstrated the effect of extracellular

calcium on the assembly and sealing of tight junctions (Gonzalez-Mariscal *et al.*, 1985; Contreras *et al.*, 1992). When extracellular calcium is removed, the opposing junctional contacts loosen, opening the paracellular pathway, leading to reduced barrier function. This removal of calcium is a reversible process, as subsequent addition of calcium restores normal tight junctions (Artursson and Magnusson, 1990; Nicklin *et al.*, 1995). It is believed that the addition of calcium to the medium initiates E-cadherin interactions which, in turn, induce rapid tight junction formation. Tight junction integrity is therefore an indirect result of the calcium effects on E-cadherin rather than a direct effect on the tight junction.

3.1.2 LANTHANUM

Lanthanum (La) is a white malleable metal, its trivalent cation La^{3+}, is a useful Ca^{2+} probe (Table 3.2). La^{3+} binds primarily by electrostatic interactions, the increased charge to ionic radius ratio of La^{3+} enables it to form stronger complexes facilitating the replacement of Ca^{2+} at the same site (Brittain *et al.*, 1976; Switzer, 1978; Snyder *et al.*, 1990).

Table 3.2 Comparison of some physicochemical properties of calcium and lanthanum

Cation	**La^{3+}**	**Ca^{2+}**
Atomic number	57	20
Atomic size	0.114 nm	0.099 nm
Hydrated ionic radius	0.104 nm	0.106 nm
Ionic molecular mass	138.9 Da	40.1 Da

Solutions containing small quantities of La (1 mM) will be in the ionic form, La^{3+}. Approximately 90 % of the La is in the ionic form La^{3+} and 10 % in the form of $La(OH)^{2+}$ and $La(OH)_2^{+}$. None of the La precipitates as $La(OH)_3$ (Moeller, 1963; Sillen and Martell, 1964).

La^{3+} binds to superficial Ca^{2+} sites on the plasma membrane and to Ca^{2+} channels of a large number of cells (Langer *et al.*, 1979). Schatzki (1971) stated that La^{3+} appears to bind to structures on the surface of well preserved cells but does not enter the cytoplasm. La^{3+} has

been reported to have no effect on tight junction formation in low calcium medium (Gonzalez-Mariscal *et al.*, 1990). Powis *et al.* (1994) demonstrated that La^{3+} enters bovine chromaffin cells *via* the Na/Ca^{2+}-exchanger below 0.9 mM acting as a Ca^{2+} agonist, in catecholamine release, but above 0.9 mM blocks the influx or efflux of Ca^{2+}. The inhibition of cellular Ca^{2+} transport mechanisms by La^{3+} is well known both of Ca^{2+} channels and the Ca^{2+}-ATPase efflux pump (Taylor and Broad, 1998; Carafoli, 1991).

Lanthanum possesses sufficient electron scattering power to produce contrast in electron microscopy. Martinez-Palomo *et al.* (1971) demonstrated that the stratum granulosum of frog skin was impermeable to colloidal La, whereas Whittembury and Rawlins (1971) put forward evidence that ionic La^{3+} was able to cross the tight junctions in perfused toad kidney proximal tubule and form the insoluble $La_2(SO_4)_3$ precipitate in the tight junction. Schatzki (1971) demonstrated La^{3+} passage across tight junctions, this time in rat gallbladder. Machen *et al.* (1972) measured the passage of La^{3+} through the tight junctions of rabbit gallbladder using radioactive $^{140}La^{3+}$. The mucosal-to-serosal fluxes of $^{140}La^{3+}$ was 0.03 ± 0.01 nmol cm^{-2} h compared to Na^+ in fish gallbladder 8.4 μmol cm^{-2} h (Diamond, 1962); the rabbit gallbladder has a very low permeability to La^{3+}. Machen *et al.* (1972) also demonstrated in their report that there was precipitate in the intercellular spaces, which may account for the low permeability of La^{3+}. Along with Fromter and Diamond (1972), Machen *et al.* (1972) proposed a division of epithelia into "leaky" and "tight", depending on the tightness of their junctional complexes. Those that were "leaky" and allowed penetration of La through the tight junction, *e.g.* ileum and gallbladder epithelia, and those of frog skin and toad urinary bladder where La never penetrated to the serosal-side are tight junctions or non-leaky.

Lanthanum chloride has been used to block the tight junctions of lingual epithelium to cations which elicit action potentials from lingual trigeminal nerve fibres by diffusing across tight junctions between epithelial cells and altering the composition of the extracellular space (Sostman and Simon, 1991; Bryant and Moore, 1995). Therefore La^{3+} binding to membrane sites and proteins may cause a redistribution of intracellular Ca^{2+} leading to cell death (Kolbeck and Speir, 1986). However, La^{3+} in certain cases may have a pharmacological or toxic effect, depending on the concentration and treatment period.

3.1.3 LANTHANUM CACO-2 TRANSPORT MODEL

The hypothesis that La^{3+} will inhibit the paracellular pathway is based on the knowledge that; Ca^{2+} is needed to maintain intercellular junctional integrity and cation selectivity in Caco-2 monolayers (Artursson and Magnusson, 1990; Nicklin *et al.*, 1995), La^{3+}, is a known calcium antagonist, with ability to replace calcium at extracellular binding sights (Langer *et al.*, 1979; Schatzki, 1971), and inhibition of the paracellular pathway as indicated by increased transepithelial resistance has been reported in a number of epithelia (Martinez-Palomo *et al.*, 1971; Whittembury and Rawlins, 1971; Machan *et al.*, 1972). La^{3+} was administered to Caco-2 monolayers to block the paracellular pathway, if inhibition occured, a rise in TER and a reduction in mannitol and PEG 4000 flux across Caco-2 monolayers would be expected. Also, to investigate the specificity of La^{3+} paracellular pathway inhibition by measuring the possible effects La^{3+} has on other transepithelial transport systems. The effect of La^{3+} on two carrier-mediated transport system, glucose and taurocholic acid, along with HRP transport will be assessed.

3.2 EXPERIMENTAL

3.2.1 CACO-2 CELL CULTURE

All transport studies in this chapter were performed using 21 d Caco-2 monolayers, passage number 87 to 100, unless otherwise stated. They were cultured on polycarbonate permeable Transwell™ supports as described previously (see section 2.3.3).

3.2.2 TRANSPORT AND TRANSEPITHELIAL ELECTRICAL RESISTANCE STUDIES

For the majority of transport studies and all transepithelial electrical resistance studies, transport buffer (TB) was used (see section 2.4). Where a sodium-free, or a glucose-free version of TB was required $TB_{Choline}$ or $TB_{Glucose}$ was used in both the apical and basolateral chambers (see section 2.4).

The protocols for measuring transepithelial resistance (see section 2.5), transepithelial transport (see section 2.6.2), cellular association (see section 2.7) and cytotoxicity assays (see section 2.8) are described in Chapter 2 Materials and Methods.

3.3 RESULTS

3.3.1 INHIBITION OF PARACELLULAR TRANSPORT

3.3.1.1 TRANSEPITHELIAL ELECTRICAL RESISTANCE

The TER of Caco-2 monolayers at 30 min was 387.8 ± 21.8 ohms cm^2, a decrease of 21.3 ± 4.4 % following replacement of the wash solutions with fresh TB at 0 min. After this time point, 30 min, the TER remained at a new constant value of approximately 370 ohms cm^2 for the duration of the experiment (Figure 3.1). The TER values at 0 min in Figure 3.1 and the TER values in Figure 2.5 show a discrepency of approximately 100 ohms cm^2 for 21 d Caco-2 monolayer TER values. This can be explained by the difference in experimental design, the TER values for different days in culture (Figure 2.5) were measured without a washing step or change of media, whereas for the effect of La^{3+} on TER values, the Caco-2 monolayers were first incubated in TB for 15 min at 37°C and then replaced with fresh media. This would cause the Caco-2 monolayers to re-establish chemical gradients leading to reduced TER values.

Following apical administration of 2 mM and 5 mM La^{3+} there was a significant increase in TER values compared to control monolayers. There was no significant difference in TER values following apical administration of 1 mM La^{3+} compared to control monolayers (Figure 3.1). The administration of 2 mM La^{3+} to the apical chamber significantly increased the TER to 584.0 ± 4.7 ohms cm^2 after 5 min, a value which gradually increased for the duration of the experiment (180 min) to 821.1 ± 73.7 ohms cm^2. For 5 mM La^{3+}, the increase in TER was more dramatic over 5 to 90 min, thereafter it plateaued at approximately 1800 ohms cm^2. The increase in TER was repeated following basolateral administration of La^{3+} (Figure 3.2). No effect was observed with the basolateral administration of 1 mM La^{3+}. However, 2 mM La^{3+} caused the TER to increase to 1141.4 ± 239.2 ohms cm^2 after 5 min. This value remained constant for 90 min and then decreased to 783.4 ± 51.9 ohms cm^2 at 180 min. With 3 mM basolateral La^{3+} the TER increased to 1742.7 ± 98.6 ohms cm^2 at 5 min and remained at approximately that level for the duration of the experiment.

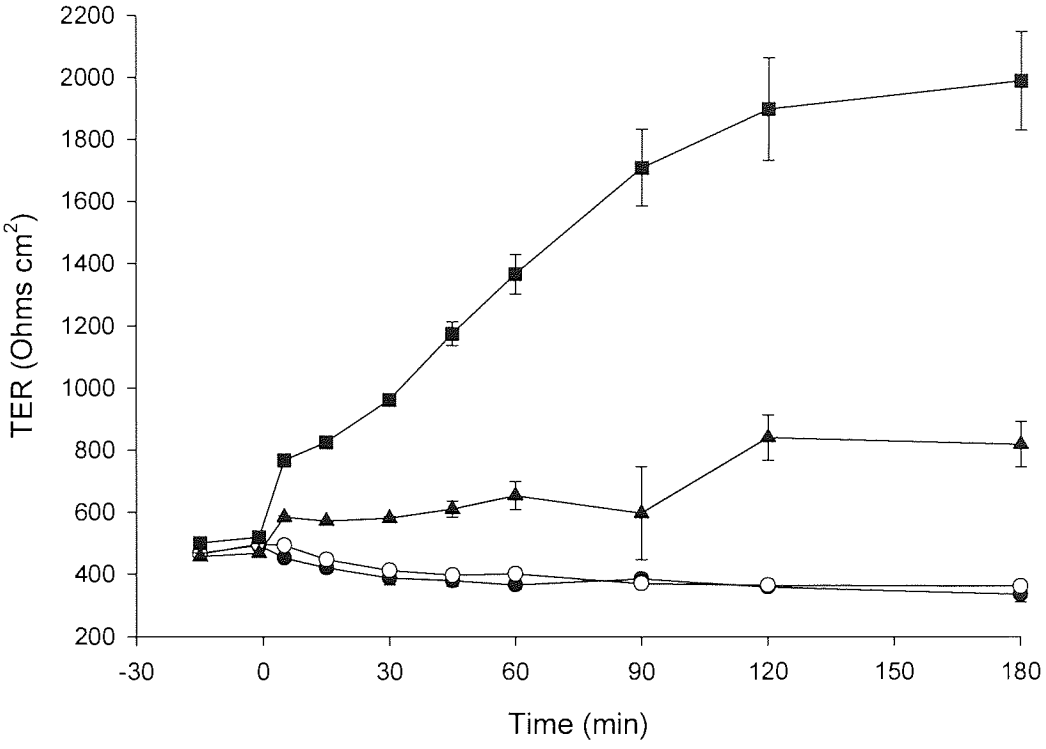

Figure 3.1 The acute effect of apical La^{3+} on transepithelial electrical resistance (TER) of Caco-2 monolayers cultured for 21 d. Monolayers were washed with TB for 15 min at 37°C before La^{3+} was applied to the Ap surface. The TER of each monolayer was measured with an epithelial voltmeter using STX2 'chopstick' electrodes at the time points shown. Control ●; 1 mM apical La^{3+} (○); 2 mM apical La^{3+}(▲); 5 mM apical La^{3+}(■). Data are presented as mean values ± SEM (n=3).

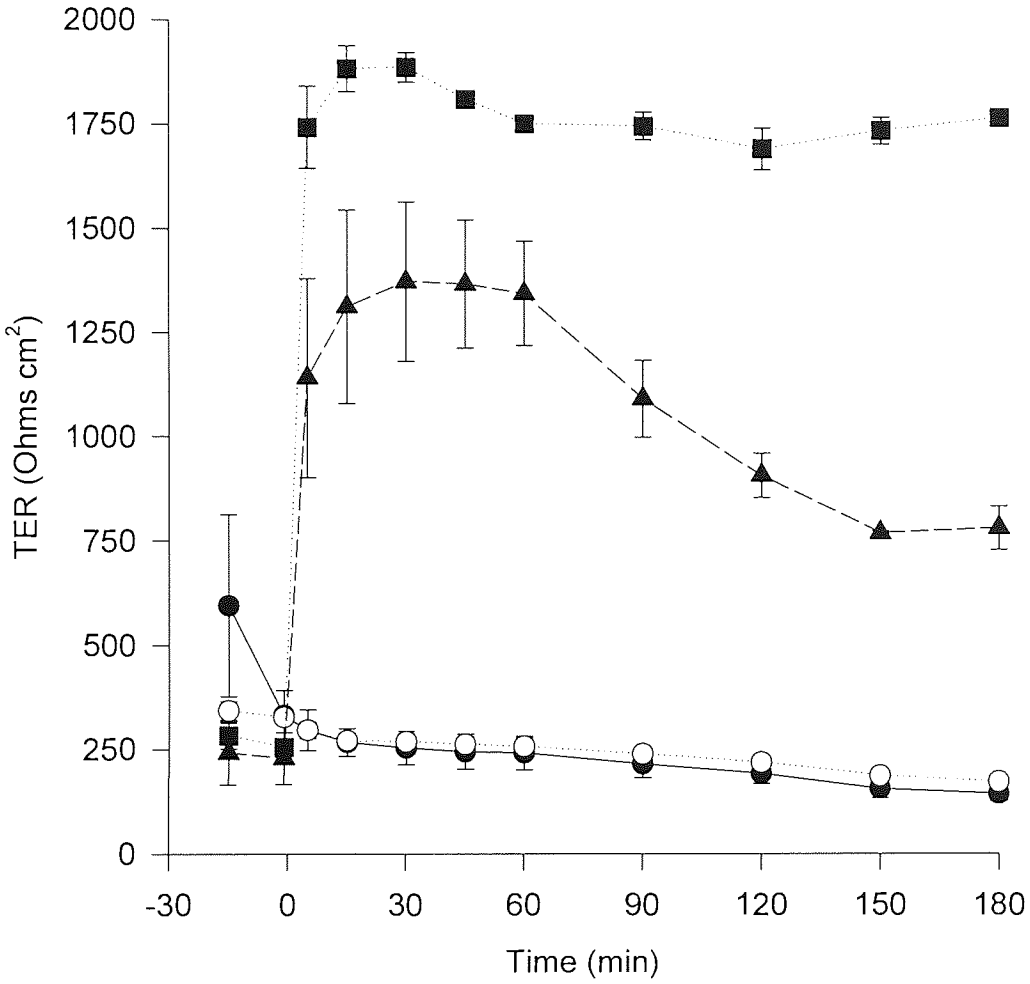

Figure 3.2 The acute effect of basolateral La^{3+} on transepithelial electrical resistance (TER) of Caco-2 monolayers cultured for 21 d. Monolayers were washed with TB for 15 min at 37°C before La^{3+} was applied to the basolateral surface. The TER of each monolayer was measured with an epithelial voltmeter using STX2 'chopstick' electrodes at the time points shown. Control ●; 1 mM basolateral La^{3+} (O); 2 mM basolateral La^{3+}(▲); 3 mM basolateral La^{3+}(■). Data are presented as mean values ± SEM (n=3).

3.3.1.2 [^{14}C]MANNITOL APPARENT PERMEABILITY COEFFICIENT

To assess the functional impact of the increase in TER caused by La^{3+}, the apparent permeability coefficient (P_{app}) of [^{14}C]mannitol across 21 d Caco-2 monolayers was measured. The P_{app} of D-[^{14}C]mannitol across Caco-2 monolayers was $1.05 \pm 0.04 \times 10^{-7}$ cm s^{-1}, this is in agreement with values quoted by various other groups (Knipp *et al.*, 1997; Artursson *et al.*, 1994; Gan *et al.*, 1998; Kotze *et al.*, 1998). The P_{app} was significantly inhibited, by 18.2 ± 3.73 %, on the addition of 1.5 mM apical La^{3+} and by 36.36 ± 0.36 % and 45.45 ± 0.60 % inhibition for 2 mM and 5 mM apical La^{3+} respectively (Figure 3.3). The impact of La^{3+} on the transfer across the polycarbonate filters was investigated. At 2 mM La^{3+} the flux of [^{14}C]mannitol across open filters *i.e.* no cells, was tested in the presence and absence of 2 mM La^{3+}, no significant difference (P=0.656) was observed with P_{app} values of 55.86 ± 2.06 and 57.51 ± 2.75 cm $s^{-1} \times 10^{-6}$ respectively.

The Ap-to-Bl P_{app} of [^{14}C]mannitol across Caco-2 monolayers was inhibited by 63.0 ± 1.37 % to 0.54 ± 0.02 cm $s^{-1} \times 10^{-7}$ by the administration of 2 mM apical La^{3+}. When 2 mM La^{3+} was administered to the basolateral chamber the inhibition was significantly increased to 72.6 ± 0.34 % which gave a [^{14}C]mannitol P_{app} of 0.4 ± 0.003 cm $s^{-1} \times 10^{-7}$ (Figure 3.4). Whereas, P_{app} of [^{14}C]mannitol across Caco-2 monolayers in the Bl-to-Ap direction was 2.16 ± 0.24 cm $s^{-1} \times 10^{-7}$ which was not significantly different from the Ap-to-Bl [^{14}C]mannitol P_{app}. The increased Bl-to-Ap [^{14}C]mannitol P_{app} gave rise to increased percentage inhibition of [^{14}C]mannitol P_{app} when either apical or basolateral 2 mM La^{3+} was administered, 80.6 ± 1.85 % and 79.6 ± 1.39 %, respectively. However, the actual values were not significantly different from the Ap-to-Bl [^{14}C]mannitol P_{app} value for 2 mM basolateral La^{3+}. There is possible sensitivity to La^{3+} administration when measuring Ap-to-Bl [^{14}C]mannitol P_{app}, which is relevant for oral absorption of solutes. Following either apical or basolateral application of 2 mM La^{3+} a significant difference was observed between the Ap-to-Bl [^{14}C]mannitol P_{app} values (Figure 3.4).

The Caco-2 monolayer uptake of [^{14}C]mannitol after 180 min was significantly inhibited by apical concentrations above 2 mM La^{3+} (Figure 3.5). At 2 mM La^{3+} the [^{14}C]mannitol

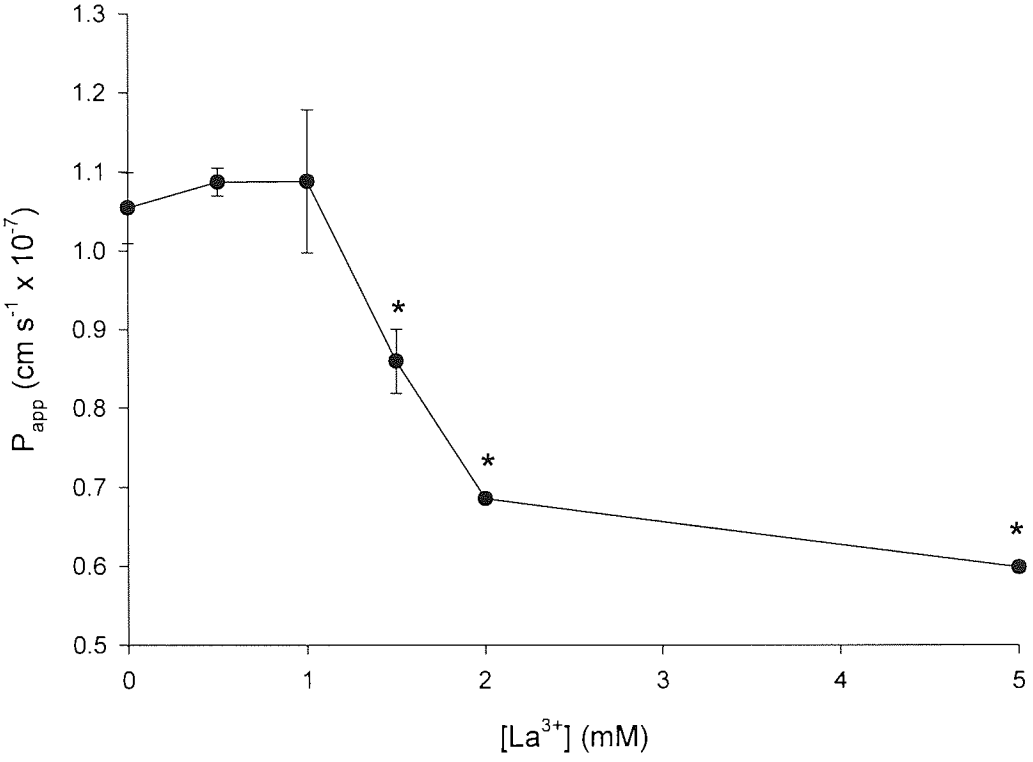

Figure 3.3 The effect of La^{3+} on the apical to basolateral transport of [^{14}C]mannitol across 21 d Caco-2 monolayers. Monolayers were washed with TB for 15 min at 37°C before [^{14}C]mannitol and La^{3+} were applied to the Ap surface. Transport kinetics were followed by sequential transfer of the inserts to fresh medium at 30, 60, 90, 120 and 180 min. The Ap-to-Bl [^{14}C]mannitol P_{app} was determined in the presence of a range of La^{3+} concentrations (0-5 mM). Data are presented as the mean values ± SEM (n=3). * Denotes significant difference from control value at $p<0.05$.

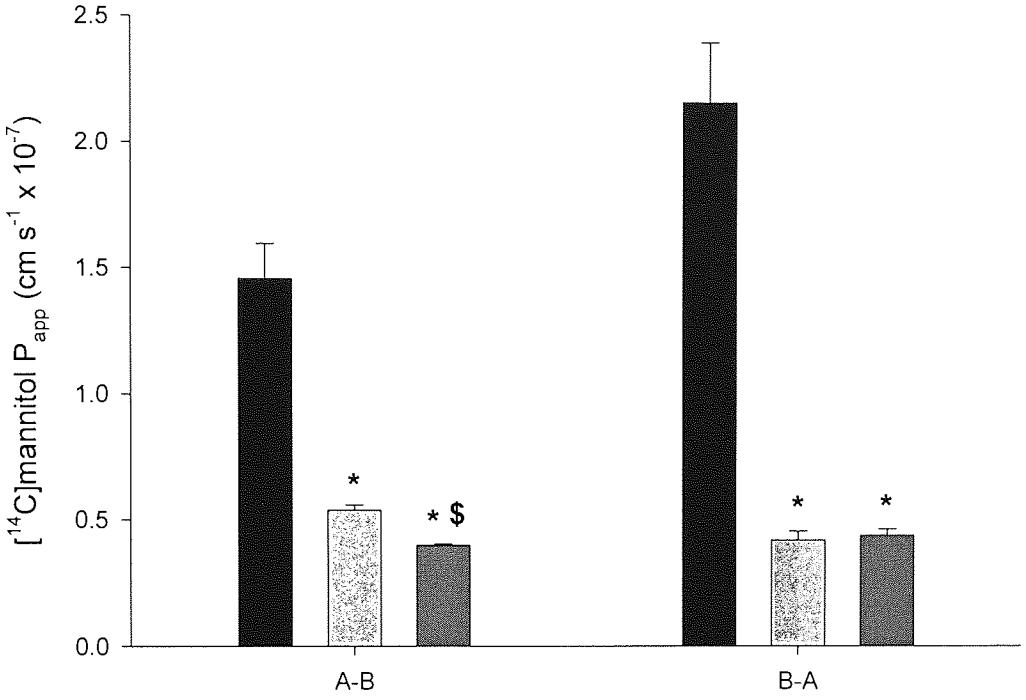

Figure 3.4 The effect of 2 mM La^{3+} on the apical to basolateral and basolateral to apical [^{14}C]mannitol apparent permeability coefficient (P_{app}) across 21 d Caco-2 monolayers. Monolayers were washed with TB for 15 min at 37°C before [^{14}C]mannitol and/or La^{3+} were administered to either the Ap or Bl surface. Transport kinetics were followed by sequential transfer of the inserts to fresh medium or replacement with fresh Ap medium at 30, 60, 90, 120 and 180 min. The Ap-to-Bl or Bl-to-Ap [^{14}C]mannitol P_{app} values were determined with no La^{3+} present (black bar) or in the presence of 2mM La^{3+} administered either apically (light grey bar) or basolaterally (dark grey bar). Data are presented as the mean values ± SEM (n=3). * Denotes significant difference from control value at $p<0.05$. $ denotes significant difference from Ap-to-Bl 2 mM apical La^{3+} value at $p<0.05$.

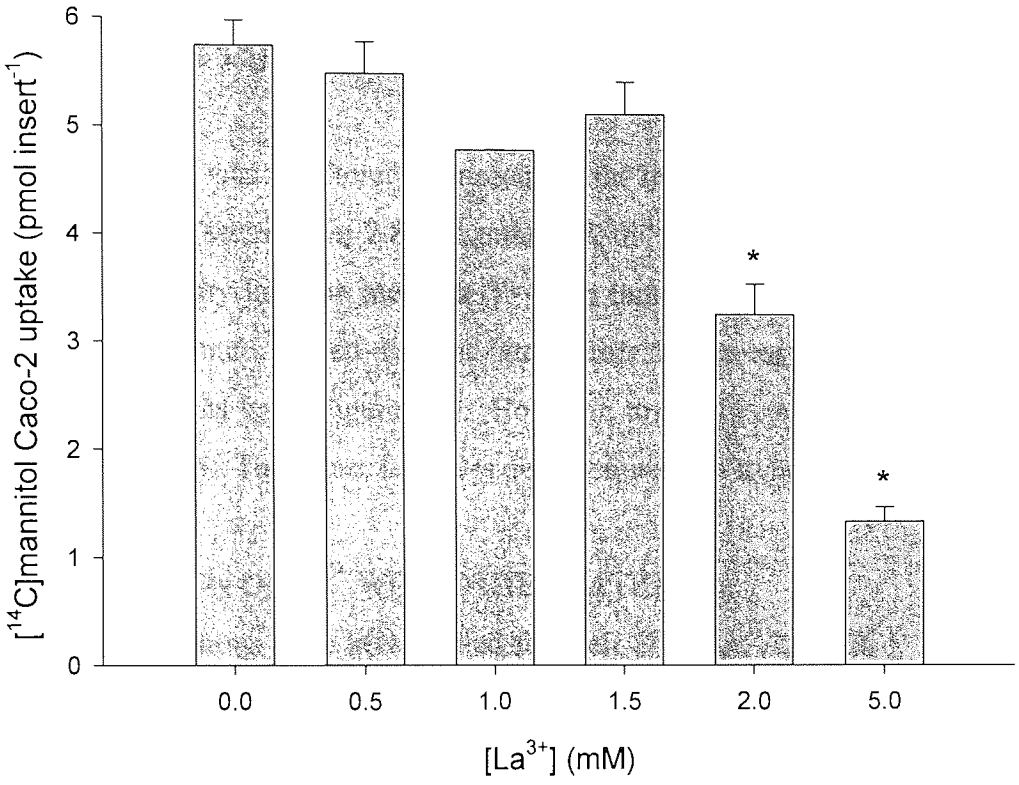

Figure 3.5 The effect of La^{3+} on [^{14}C]mannitol uptake with 21 d Caco-2 monolayers. Monolayers were washed with TB for 15 min at 37°C before [^{14}C]mannitol and La^{3+} were applied to the Ap surface. Following a transport experiment at 37°C in air, monolayer association was measured by removal of the insert into an empty cluster plate and the apical medium removed. The inserts were washed 3 times, each for 5 min, with ice-cold PBS-N_3 at room temperature 20-22 °C. The levels of [^{14}C]mannitol in each monolayer was determined in the presence of a range of La^{3+} concentrations (0-5 mM). Data are presented as the mean values ± SEM (n=3). * Denotes significant difference from control value at $p<0.05$.

uptake was 3.27 ± 0.29 pmol insert^{-1} an inhibition of 43.0 % ± 5.1 % and a maximal inhibition at 5 mM La^{3+} of 76.48 % ± 2.3 %, 1.35 ± 0.13 pmol insert^{-1} compared to the control value of 5.74 ± 0.23 pmol insert^{-1} which represents 0.052 ± 0.002 % of the dose administered (Figure 3.5).

Cytotoxicity of La^{3+} was monitored by measuring the release of LDH and the conversion of MTT to formazan (see section 2.8). Lanthanum did not cause a significant increase in released LDH activity into the medium (P=0.40) indicating no gross damage to the cell membrane. Lanthanum caused a slight but significant increase in formazan production with 1 mM and 2 mM La^{3+} (Figure 3.6). However, toxic effects would yield a decrease in formazan production. Therefore, La^{3+} was demonstrated not to be toxic to Caco-2 cells.

3.3.2 COMPARISON OF La^{3+} WITH OTHER CATIONS

Other polyvalent cations were investigated for their effect on Ap-to-Bl [^{14}C]mannitol P_{app} to see if they mimicked the inhibitory actions of La^{3+}. To quantify any effects an enhancement ratio was calculated, this was the ratio of the [^{14}C]mannitol P_{app} in the presence of 2 mM cation divided by the [^{14}C]mannitol P_{app} for the corresponding control monolayers. The enhancement ratio was increased by 2 mM Cd^{2+}, Cu^{2+}, Hg^{2+}, Ni^{2+}, and Pb^{2+}. Whereas, the enhancement ratio in the presence of 2 mM Al^{3+}, Ba^{2+}, Mg^{2+}, Mn^{2+} and 10 mM Ca^{2+} showed no significant difference from control values (Table 3.3). However, 2 mM apical Zn^{2+} significantly inhibited [^{14}C]mannitol P_{app} with an enhancement ratio of 0.81. This agrees with Lugea *et al.* (1995) and Rodriguez-Yoldi *et al.* (1996) both testing the effect of zinc on sugar and amino acid transport. They found that zinc inhibited the sodium-dependent substrate cotransporters and did not inhibit passive transport of the selected nutrients.

3.3.3 COMPARISON OF La^{3+} WITH OTHER TRANSPORT INHIBITORS

The effect of various transport inhibitors were investigated to see if La^{3+} binding to the Caco-2 plasma membrane altered carrier-mediated transport of Ca^{2+}, Na^{+}, Cl^{-} or glucose to produce the changes in TER and [^{14}C]mannitol P_{app}.

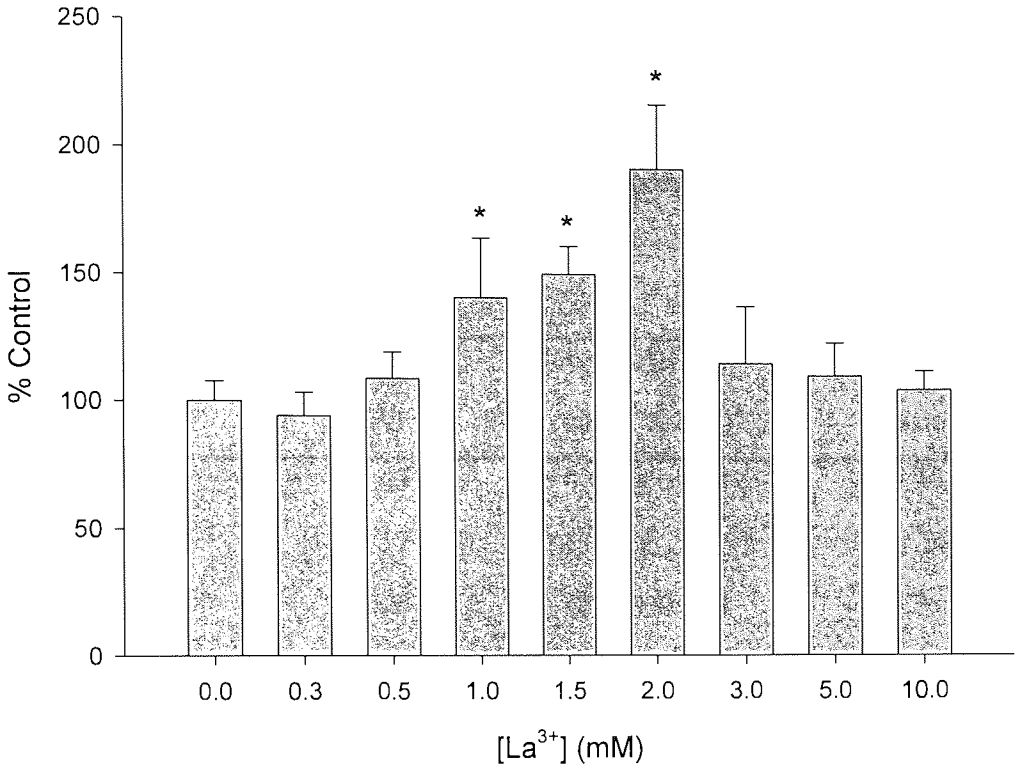

Figure 3.6 The effect of La^{3+} on MTT transformation in Caco-2 monolayers. Monolayers were washed with TB for 15 min at 37°C before La^{3+} in TB was applied to the Caco-2 monolayers. The formation of formazan coloured product was determined in the presence of a range of La^{3+} concentrations (0-10 mM). Data are presented as the mean values ± SEM (n=8). * Denotes significanct difference from control value at $p<0.05$

Table 3.3 The effect of 2 mM cations on the apical to basolateral [^{14}C]mannitol apparent permeability coefficient (P_{app}). Monolayers were washed with TB for 15 min at 37°C before [^{14}C]mannitol and 2 mM cation were applied to the Ap chamber. Transport kinetics were followed by sequential transfer of the inserts to fresh medium at 30, 60, 90, 120 and 180 min. The Ap-to-Bl transport rate for [^{14}C]mannitol was determined in the presence or absence of 2 mM cation. Data are presented as the mean values ± SEM (n=3). * Denotes significant difference from control value at $p<0.05$.

Cations	**Ionic radii (Å)**	**Ap-to-Bl P_{app} ($cm\ s^{-1} \times 10^{-7}$)[a]**	**Enhancement Ratio[b]**
Ba^{2+}	1.43	1.03 ± 0.032	0.97
Pb^{2+}	1.17	105.47 ± 21.15*	81.76
Ca^{2+c}	1.06	0.76 ± 0.013	0.79
La^{3+}	**1.04**	**0.54 ± 0.02***	**0.37**
Cd^{2+}	1.03	66.4 ± 2.99*	51.47
Hg^{2+}	0.97	145.2 ± 6.0*	112.5
Mn^{2+}	0.91	0.774 ± 0.062	1.16
Mg^{2+}	0.78	0.99 ± 0.025	1.08
Cu^{2+}	0.72	17.2 ± 0.75*	14.09
Zn^{2+}	0.69	0.731 ± 0.019*	0.81
Ni^{2+}	0.68	1.67 ± 0.088*	13.69
Fe^{3+}	0.53	1.82 ± 0.33	1.13
Al^{3+}	0.45	1.23 ± 0.084	1.16

a = transport buffer contains 1.26 mM calcium

b = The enhancement ratio was calculated by dividing the [^{14}C]mannitol P_{app} in the presence of 2 mM cation by the [^{14}C]mannitol P_{app} for the corresponding control monolayers.

c= 10mM Ca^{2+} added

3.3.3.1 Ca^{2+} TRANSPORT INHIBITORS

La^{3+} is a well known Ca^{2+} channel blocker (Langer *et al.*, 1979) which can lead to alterations in intracellular Ca^{2+} concentrations signalling changes in TER and [^{14}C]mannitol P_{app}. The calcium channel blockers, nifedipine and verapamil were tested. With nifedipine (0.01 to 1 mM) there was no significant difference (P=0.067) in [^{14}C]mannitol P_{app}, from the control value 1.05 ± 0.035 cm s^{-1} x 10^{-7}. Whereas, above 1 mM, verapamil significantly increased the [^{14}C]mannitol P_{app} value. This increase in [^{14}C]mannitol P_{app} was 1.24-fold and 1.28-fold, at 1 and 2 mM respectively, increasing to 63-fold at 3 mM and 133.8-fold at 10 mM verapamil (Table 3.4).

The Ca^{2+} ionophore A23187 was tested to see if increasing intracellular Ca^{2+} concentration in Caco-2 monolayers produced the inhibitory effect. The lowest concentration tested was 1 μM A23187; this was not significantly different from the control values. Above 2 μM A23187 there is a significant increase in [^{14}C]mannitol P_{app} (Table 3.5). These data show that inhibition of Ca^{2+} channels or changes in intracellular Ca^{2+} concentration do not mimic the decrease in [^{14}C]mannitol P_{app} brought about by La^{3+}.

3.3.3.2 SODIUM AND CHLORIDE TRANSPORT INHIBITORS

The [^{14}C]mannitol P_{app} following apical administration of the Na^{+}-channel inhibitor amiloride (10 nM to 100 μM) and the chloride channel inhibitor DIDS (3 to 300 μM) gave no significant difference from control values (Table 3.6). To examine if La^{3+} was interacting with the basolateral transport proteins Na^{+}/K^{+}ATPase and the $Na^{+}/K^{+}/2Cl^{-}$ cotransporter, the inhibitors ouabain and bumetanide respectively, were tested in the Caco-2 absorption model. Only bumetanide at 3 and 10 mM produce a significant 1.2- and 4.5-fold increase in [^{14}C]mannitol P_{app} (Table 3.7) the opposite of the decrease observed with La^{3+}.

3.3.3.3 GLUCOSE TRANSPORT INHIBITORS

The Na^{+}-dependent glucose cotransporter inhibitor phloridzin was added to the apical chamber of Caco-2 monolayers. Over the phloridizin concentration range tested (10 μM to 1 mM), no significant difference in [^{14}C]mannitol P_{app} from control values was observed (Table 3.8). Whereas, the facilitative glucose transporter inhibitor phloretin, at 1 mM

Table 3.4 The effect of the calcium channel blocker verapamil on [^{14}C]mannitol apparent permeability coefficient (P_{app}). Monolayers were washed with TB for 15 min at 37°C before [^{14}C]mannitol and verapamil were applied to the Ap chamber. Transport kinetics were followed by sequential transfer of the inserts to fresh medium at 30, 60, 90, 120 and 180 min. The Ap-to-Bl transport rate for [^{14}C]mannitol was determined in the presence of verapamil. Data are presented as the mean values ± SEM (n=3). * Denotes significant difference from control value at $p<0.05$.

[Verapamil] (mM)	**P_{app} ± SEM ($cm\ s^{-1} \times 10^{-7}$)**
0	1.501 ± 0.069
1	1.869 ± 0.061*
2	1.922 ± 0.075*
3	94.49 ± 7.046*
5	181.1 ± 12.29*
10	200.9 ± 5.73*

Table 3.5 The effect of the calcium ionophore A23187 on [^{14}C]mannitol apparent permeability coefficient (P_{app}). Monolayers were washed with TB for 15 min at 37°C before [^{14}C]mannitol and A23187 were applied to the Ap chamber. Transport kinetics were followed by sequential transfer of the inserts to fresh medium at 30, 60, 90, 120 and 180 min. The Ap-to-Bl transport rate for [^{14}C]mannitol was determined in the presence of A23187. Data are presented as the mean values ± SEM (n=3). * Denotes significant difference from control value at $p<0.05$.

[A 23187] (μM)	**P_{app} ± SEM (cm s^{-1} x 10^{-7})**
0	0.704 ± 0.030
1	0.756 ± 0.036
2	0.908 ± 0.025
10	1.610 ± 0.098*
30	2.500 ± 0.095*
100	5.170 ± 0.040*

Table 3.6 The effect of Caco-2 apical ion transport inhibitors on [^{14}C]mannitol apparent permeability coefficient (P_{app}). Monolayers were washed with TB for 15 min at 37°C before [^{14}C]mannitol and inhibitor were applied to the Ap chamber. Transport kinetics were followed by sequential transfer of the inserts to fresh medium at 30, 60, 90, 120 and 180 min. The Ap-to-Bl transport rate for [^{14}C]mannitol was determined in the presence of inhibitor. Data are presented as the mean values ± SEM (n=3). * Denotes significant difference from control value at $p<0.05$.

[Amiloride] (μM)	**P_{app} ± SEM (cm s^{-1} x 10^{-7})**
0	1.132 ± 0.121
0.01	1.152 ± 0.204
0.1	1.049 ± 0.136
1	0.984 ± 0.112
10	1.007 ± 0.117
100	0.987 ± 0.084

[DIDS] (μM)	**P_{app} ± SEM (cm s^{-1} x 10^{-7})**
0	1.008 ± 0.004
3	1.258 ± 0.048
10	1.416 ± 0.024
30	1.737 ± 0.032
100	1.816 ± 0.096
300	1.485 ± 0.199

Table 3.7 The effect of Caco-2 basolateral ion transport inhibitors on [^{14}C]mannitol apparent permeability coefficient (P_{app}). Monolayers were washed with TB for 15 min at 37°C before [^{14}C]mannitol and inhibitor were applied to the Ap chamber. Transport kinetics were followed by sequential transfer of the inserts to fresh medium at 30, 60, 90, 120 and 180 min. The Ap-to-Bl transport rate for [^{14}C]mannitol was determined in the presence of inhibitor. Data are presented as the mean values ± SEM (n=3). * Denotes significant difference from control value at $p<0.05$.

[Ouabain] (mM)	**P_{app} ± SEM ($cm\ s^{-1} \times 10^{-7}$)**
0	0.931 ± 0.097
0.01	1.052 ± 0.049
0.1	1.012 ± 0.036
1	1.071 ± 0.043
3	1.059 ± 0.100
10	0.855 ± 0.077
[Bumetanide] (mM)	**P_{app} ± SEM ($cm\ s^{-1} \times 10^{-7}$)**
0	0.608 ± 0.020
0.01	0.698 ± 0.008
0.1	0.616 ± 0.040
1	0.678 ± 0.033
3	0.716 ± 0.006
10	2.727 ± 0.589*

Table 3.8 The effect of glucose transport inhibitors on [^{14}C]mannitol apparent permeability coefficient (P_{app}). Monolayers were washed with TB for 15 min at 37°C before [^{14}C]mannitol and inhibitor were applied to the Ap chamber. Transport kinetics were followed by sequential transfer of the inserts to fresh medium at 30, 60, 90, 120 and 180 min. The Ap-to-Bl transport rate for [^{14}C]mannitol was determined in the presence of inhibitor. Data are presented as the mean values ± SEM (n=3). * Denotes significant difference from control value at $p<0.05$.

[Phloretin] (μM)	**Apical administration**	**Basolateral administration**
	P_{app} ± SEM ($cm\ s^{-1} \times 10^{-7}$)	P_{app} ± SEM ($cm\ s^{-1} \times 10^{-7}$)
0	0.835 ± 0.038	1.061 ± 0.017
10	0.875 ± 0.055	1.108 ± 0.024
100	1.006 ± 0.069	0.868 ± 0.076
300	0.976 ± 0.069	0.872 ± 0.124
1000	1.962 ± 0.198*	1.548 ± 0.222*
[Phloridzin] (μM)		
0	1.478 ± 0.126	ND
10	1.496 ± 0.026	ND
100	1.739 ± 0.103	ND
300	1.457 ± 0.121	ND
1000	1.283 ± 0.068	ND

ND = Not determined

significantly increased [^{14}C]mannitol P_{app} by 2.35-fold. Below 1 mM there was no significant difference from control values (Table 3.8).

3.3.4 OTHER TRANSPORT PROBES

The effect La^{3+} had on other probes; PEG 4000 a larger paracellular marker, testosterone a passive transcellular transport marker, glucose and taurocholate two solutes transported by carrier-mediated processes, and HRP a fluid-phase endocytic marker were also investigated.

3.3.4.1 THE EFFECT OF La^{3+} ON [^{14}C]PEG 4000 TRANSPORT

The transport marker [^{14}C]PEG 4000 is another paracellular pathway marker of higher molecular mass (average 4000 Da). Control Caco-2 monolayers gave a [^{14}C]PEG 4000 P_{app} of 2.05 ± 0.12 cm s^{-1} x 10^{-8}, with the addition of increasing apical concentrations of La^{3+} (1 to 30 mM) there was no significant effect (P=0.733) on Ap-to-Bl [^{14}C]PEG 4000 P_{app} across 21 d Caco-2 monolayers.

3.3.4.2 THE EFFECT OF La^{3+} ON HORSERADISH PEROXIDASE TRANSPORT

Apical 2 mM La^{3+} has a significant effect on Ap-to-Bl HRP transport across 21 d Caco-2 monolayers (Figure 3.7), inhibiting transcytotic HRP transport across Caco-2 monolayers over the concentration range tested (2.5-250 μM). At all HRP concentrations tested there was a significant inhibition of HRP transport *e.g.* at 25 μM HRP the inhibition was 98.7 % ± 11.7%. The residual transport might reflect some extracellular leakage (Heyman *et al.*, 1990).

3.3.4.3 THE EFFECT OF La^{3+} ON TESTOSTERONE TRANSPORT

The P_{app} for testosterone across 21 d Caco-2 monolayers was 2.06 ± 0.23 cm s^{-1} x 10^{-5}, this value is in agreement with other groups (Cogburn *et al.*, 1991; Hilgers *et al.*, 1990). The addition of apical 1 to 10 mM La^{3+} has no significant effect (P= 0.688) on Ap-to-Bl transport of testosterone across 21 d Caco-2 monolayers. Although there was no significant difference in testosterone transport measured this is possibly due to the variability in the data, the testosterone P_{app} with 2 mM apical La^{3+} was 3.27 ± 1.58 cm s^{-1} x 10^{-5}.

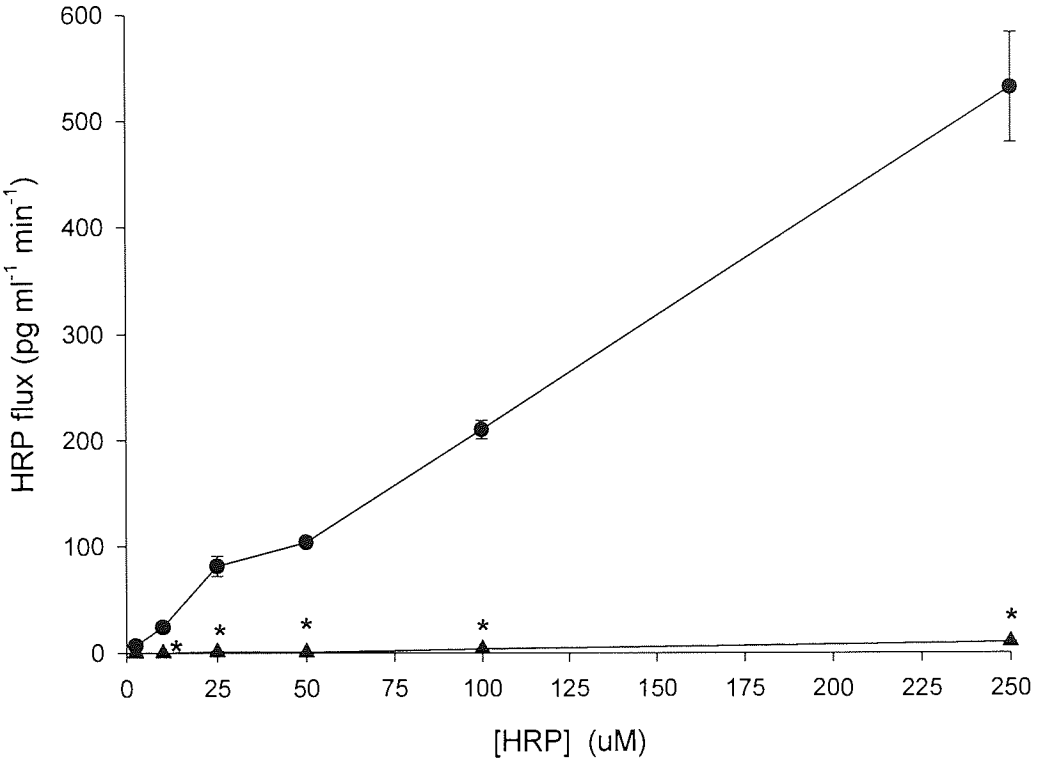

Figure 3.7 The effect of 2 mM La^{3+} on the apical to basolateral horseradish peroxidase (HRP) transport across 21 d Caco-2 monolayers. Monolayers were washed with TB for 15 min at 37°C before HRP and 2 mM La^{3+} were administered to the Ap surface. Transport kinetics were followed by sequential transfer of the inserts to fresh medium at 30, 60, 90, 120 and 180 min. The Ap-to-Bl HRP flux was determined in the presence (▲) or absence (●) of 2mM La^{3+}. Data are presented as the mean values ± SEM (n=3). * Denotes significant difference from control value at $p<0.05$.

3.3.4.4 THE EFFECT OF La^{3+} ON TAUROCHOLATE TRANSPORT

Caco-2 monolayers transport taurocholate by a saturable process in the Ap-to-Bl direction, which is 4.1-fold higher than in the Bl-to-Ap direction showing polarity of transport (Figure 3.8). The transport is energy- and sodium- dependent (Figure 3.8). The application of 1 mM sodium azide and 50 mM 2-deoxyglucose, a metabolic poison and a non-metabolised glucose analogue, respectively demonstrate energy dependence. Whereas, equimolar substitution of NaCl with choline chloride significantly inhibits Ap-to-Bl transport by 95.0 % ± 0.5 % (Figure 3.9).

At 3 μM taurocholate, taurocholate transport is inhibited 26.3 % ± 5.0 %, 53.9 % ± 7.9 % and, 79.5 % ± 3.5 % by 2, 10, and 30 mM La^{3+} respectively. In contrast, the transport of 1 mM taurocholate a 333-fold excess is inhibited 97.1 % ± 0.33 %, 98.5 % ± 0.48 % and, 94.1 % ± 0.37 % by 2, 10, and 30 mM La^{3+} respectively (Figure 3.10). Indicating that La^{3+} may be a passive transport inhibitor with relatively higher taurocholate concentrations.

3.3.4.5 THE EFFECT OF La^{3+} ON GLUCOSE TRANSPORT

Figure 3.11 shows the effect of 2 mM La^{3+} on the saturable Ap-to-Bl transport of glucose across Caco-2 monolayers. The addition of La^{3+} increases the values for J_{max} (98.6 nmol min^{-1} for 2 mM La^{3+} against 74.6 nmol min^{-1} for control) and K_t (10.0 mM for 2 mM La^{3+} against 7.0 mM for control) for glucose transport. Indicating that at 5.5 mM the glucose transport process will be working at non-saturating conditions.

Figure 3.12 shows glucose flux across Caco-2 monolayers, 19.32 ± 0.46 nmol min^{-1}. The transport of glucose is significantly inhibited by 12.9 ± 3.0 %, with the addition of 3 mM La^{3+} (16.82 ± 0.58 nmol min^{-1}). Thereafter, there is a decrease in glucose flux inhibition, 8.7 ± 2.8 %, at 10 mM La^{3+} (17.64 ± 0.55 nmol min^{-1}). This contradictory evidence of the effect of La^{3+} on glucose flux across Caco-2 monolayers suggests no definite effect. However, investigations into the possible mode of La^{3+} inhibition on glucose transport in Caco-2 monolayers were undertaken. Media conditions were changed and the addition of phloridzin, a Na^{+}-dependent glucose transporter inhibitor was tested (Figure 3.13).

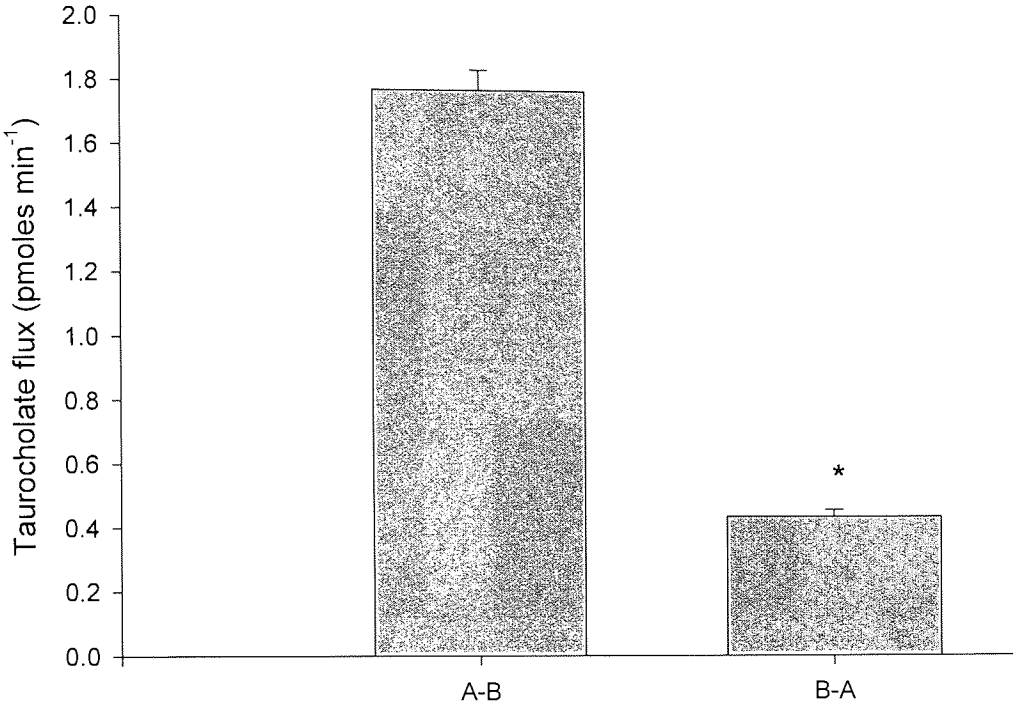

Figure 3.8 The polarity of 4.8 μM [^{14}C]taurocholate transport across 21 d Caco-2 monolayers. Monolayers were washed with TB for 15 min at 37°C before [^{14}C]taurocholate was applied to either the Ap or Bl surface. Transport kinetics were followed by sequential transfer of the inserts to fresh medium or replacement with fresh apical medium at 30, 60, 90, 120 and 180 min. Ap-to-Bl transport (A-B), Bl-to-Ap transport (B-A). Data are presented as the mean values ± SEM (n=3). * Denotes significant difference from Ap-to-Bl transport at $p<0.05$.

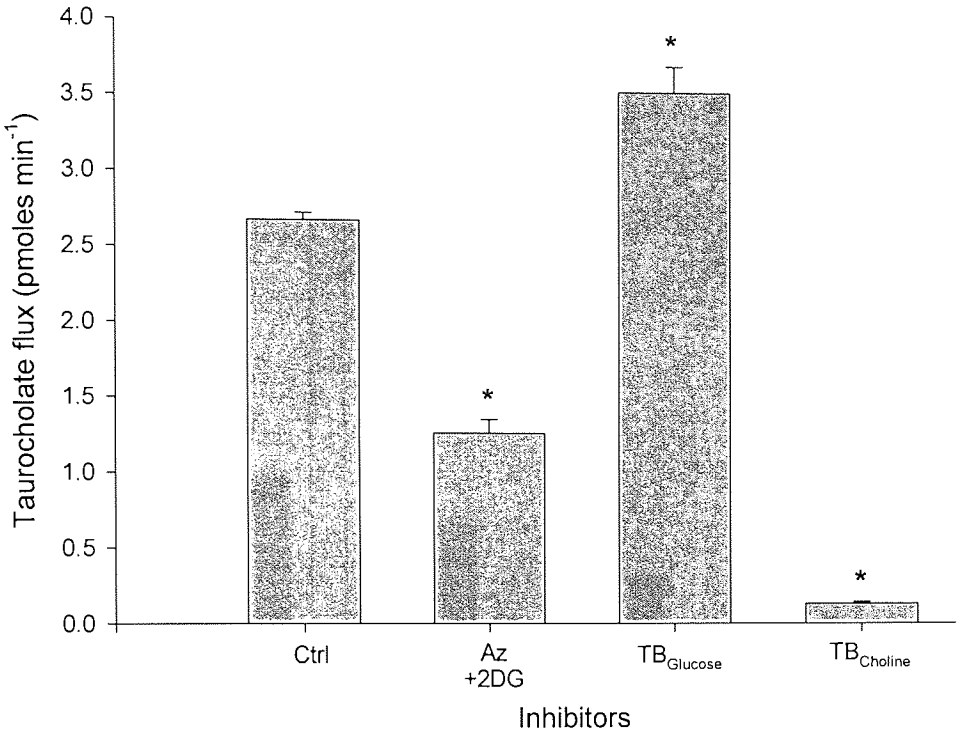

Figure 3.9 The effect of selected inhibitors on the apical to basolateral transport of 4.8 μM sodium taurocholate across 21 d Caco-2 monolayers. Monolayers were washed with TB for 15 min at 37°C in air before inhibitor and [^{14}C]taurocholate were applied to the Ap surface. Transport kinetics were followed by sequential transfer of the inserts to fresh medium at 30, 60, 90, 120 and 180 min. Control (ctrl); 1 mM Azide + 50 mM 2-deoxyglucose (Az+2DG); no glucose in the medium ($TB_{Glucose}$); 136 mM Choline chloride in TB ($TB_{Choline}$). Data are presented as the mean values ± SEM (n=3). * Denotes significant difference from control value at $p<0.05$.

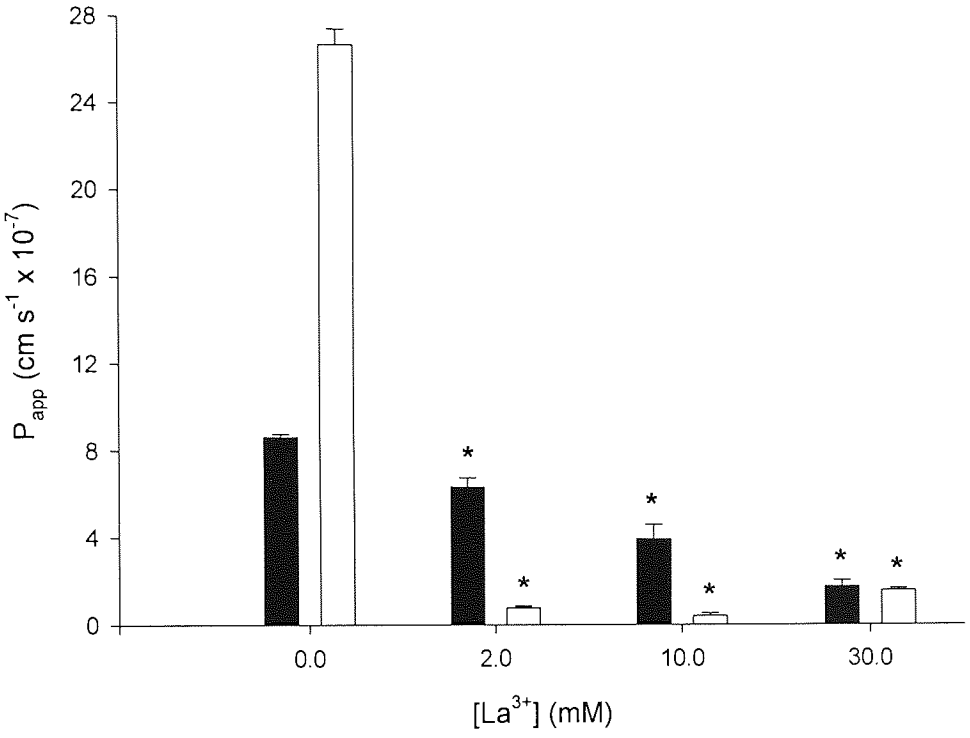

Figure 3.10 The effect of La^{3+} on the apical to basolateral transport of sodium taurocholate across 21 d Caco-2 monolayers. Monolayers were washed with TB for 15 min at 37°C before sodium taurocholate and La^{3+} were applied to the Ap surface. Transport kinetics were followed by sequential transfer of the inserts to fresh medium at 30, 60, 90, 120 and 180 min. The Ap-to-Bl P_{app} were determined for 3 μM (black bar), 1 mM (white bar) sodium taurocholate in the presence of a range of La^{3+} concentrations (0-30 mM). Data are presented as the mean values ± SEM (n=3). * Denotes significant difference from control value at $p<0.05$.

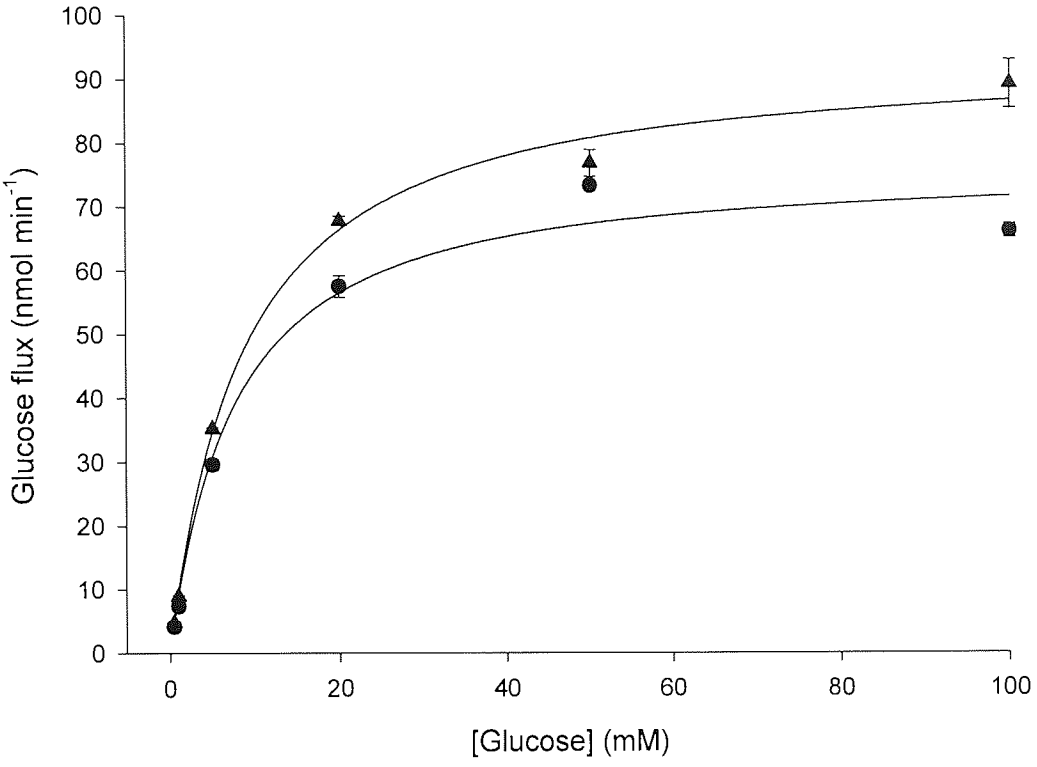

Figure 3.11 Concentration-dependent apical to basolateral transport of D-glucose across 21 d Caco-2 monolayers. Monolayers were washed with TB for 15 min at 37°C before [^{14}C]glucose and D-glucose were applied to the Ap surface. Transport kinetics were followed by sequential transfer of the inserts to fresh medium at 30, 60, 90, 120 and 180 min. The Ap-to-Bl D-glucose transport were determined over a range of apical concentrations (0.5 to 100 mM) in the presence (▲) and absence (●) of 2 mM apical La^{3+}. Data are presented as the mean values ± SEM (n=3).

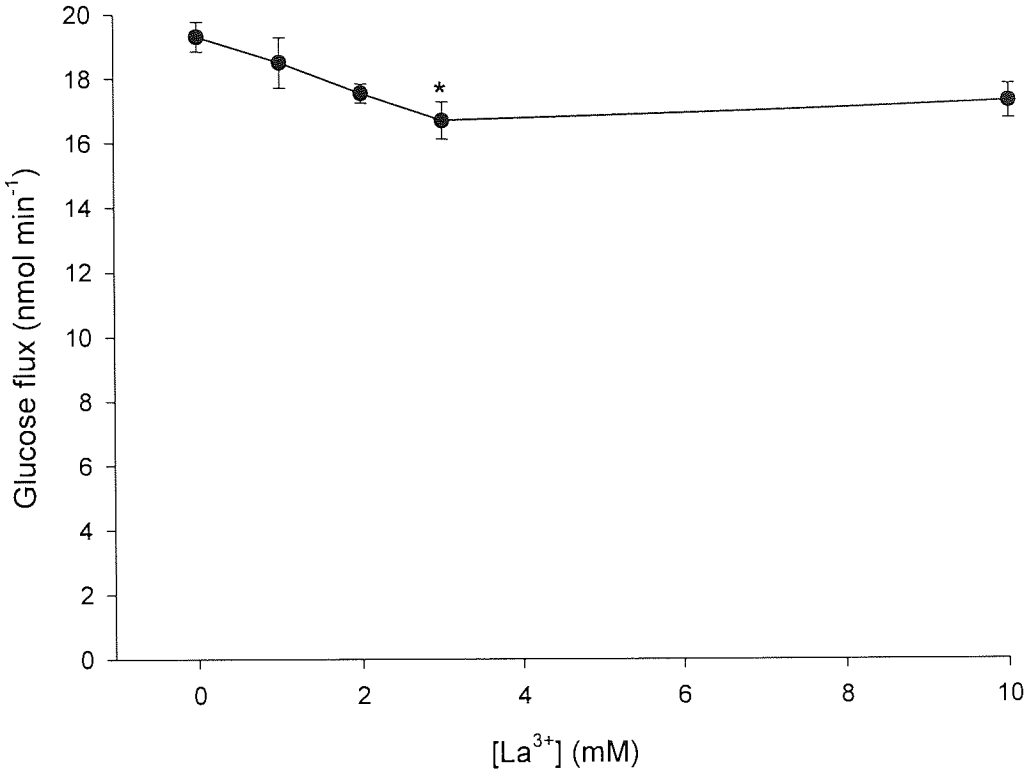

Figure 3.12 The effect of apical La^{3+} on the apical to basolateral transport of 5.5 mM D-glucose across 21 d Caco-2 monolayers. Monolayers were washed with TB for 15 min at 37°C before D-glucose and La^{3+} were applied to the Ap surface. Transport kinetics were followed by sequential transfer of the inserts to fresh medium at 30, 60, 90, 120 and 180 min. The Ap-to-Bl transport rate for D-glucose was determined in the presence of a range of La^{3+} concentrations (0 -30 mM). Data are presented as the mean values ± SEM (n=3). * Denotes significant difference from control value at $p<0.05$.

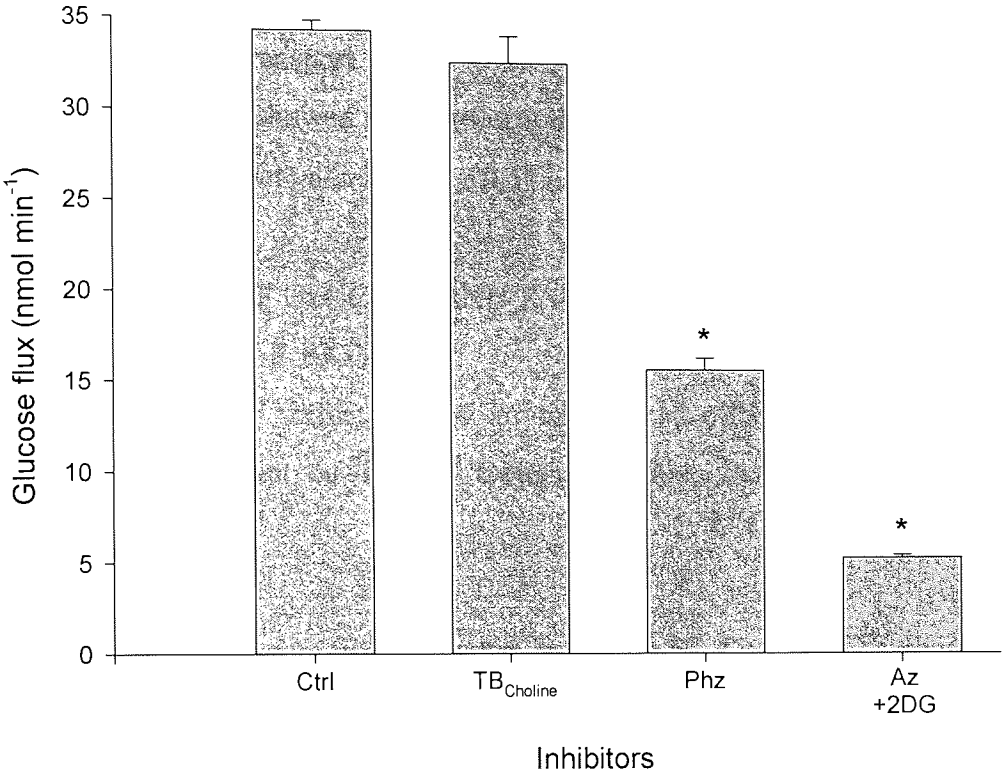

Figure 3.13 The effect of selected inhibitors on the apical to basolateral transport of 5.5 mM D-glucose across 21 d Caco-2 monolayers. Monolayers were washed with TB for 15 min at 37°C before inhibitor and [^{14}C]glucose were applied to the Ap surface. Transport kinetics were followed by sequential transfer of the inserts to fresh medium at 30, 60, 90, 120 and 180 min. TB (ctrl), $TB_{Choline}$ ($TB_{Choline}$), TB containing 1 mM Phloridzin (Phz), TB containing 1 mM Azide + 50 mM 2-deoxyglucose (Az+2DG). Data are presented as the mean values ± SEM (n=3). * Denotes significant difference from control value at $p<0.05$.

The addition of phloridzin produced a 54.2 ± 1.9 % inhibition of glucose transport across Caco-2 monolayers. The addition of the metabolic poison sodium azide (1 mM) and the non-metabolised glucose analogue 2-deoxyglucose (50 mM) produced an 84.5 ± 0.5 % inhibition of glucose transport across Caco-2 monolayers. Whereas, $TB_{Choline}$ medium without sodium present showed no significant difference in glucose transport across Caco-2 monolayers from control values, 34.3 ± 0.53 nmol min^{-1}.

3.3.5 THE EFFECT OF GLUCOSE AND TAUROCHOLATE ON THE PARACELLULAR PATHWAY

To show that the La^{3+} effect is not an artefact of either glucose or taurocholate concentration, their effect on TER, [^{14}C]mannitol flux, and [^{14}C]PEG 4000 flux was examined.

Glucose produced no significant change in TER of Caco-2 monolayers over the concentration range tested, 5.5-100.0 mM (Figure 3.14). Also, 5.5-100.0 mM glucose had no significant effect on [^{14}C]PEG 4000 (P=0.105) and [^{14}C]mannitol (P=0.069) P_{app} values, with control P_{app} values of 2.69 ± 0.58 cm s^{-1} x 10^{-8}. and 0.70 ± 0.01 cm s^{-1} x 10^{-7} respectively.

With 20 mM taurocholate, a significant decrease in TER is produced after 5 min 344.4 ± 3.3 ohms cm^2, decreasing further to 317.7 ± 21.7 ohms cm^2 after 180 min. This was enhanced with 40 mM taurocholate; at zero min the TER was 430.7 ± 15.0 which fell to 39.8 ± 8.2 ohms cm^2 at 180 min (Figure 3.15). The effect of 20 mM and 40 mM taurocholate on Caco-2 monolayer integrity, as indicated by the drop in TER, was corroborated by significant increases in both [^{14}C]mannitol and [^{14}C]PEG 4000 P_{app} values (Figure 3.16 and 3.17). With 20 and 40 mM taurocholate significantly increasing the [^{14}C]mannitol P_{app} above control levels, 4.3-fold (2.44 ± 0.28 cm s^{-1} x 10^{-7}) and 228-fold (130.0 ± 3.08 cm s^{-1} x 10^{-7}) respectively. Also, significantly increasing [^{14}C]PEG 4000 P_{app}, but not to the same level as [^{14}C]mannitol P_{app}, with only 3.0-fold (4.96 ± 0.44 cm s^{-1} x 10^{-8}) and 5.5-fold (8.96 ± 0.2 cm s^{-1} x 10^{-8}) increases following 20 and 40 mM taurocholate administration.

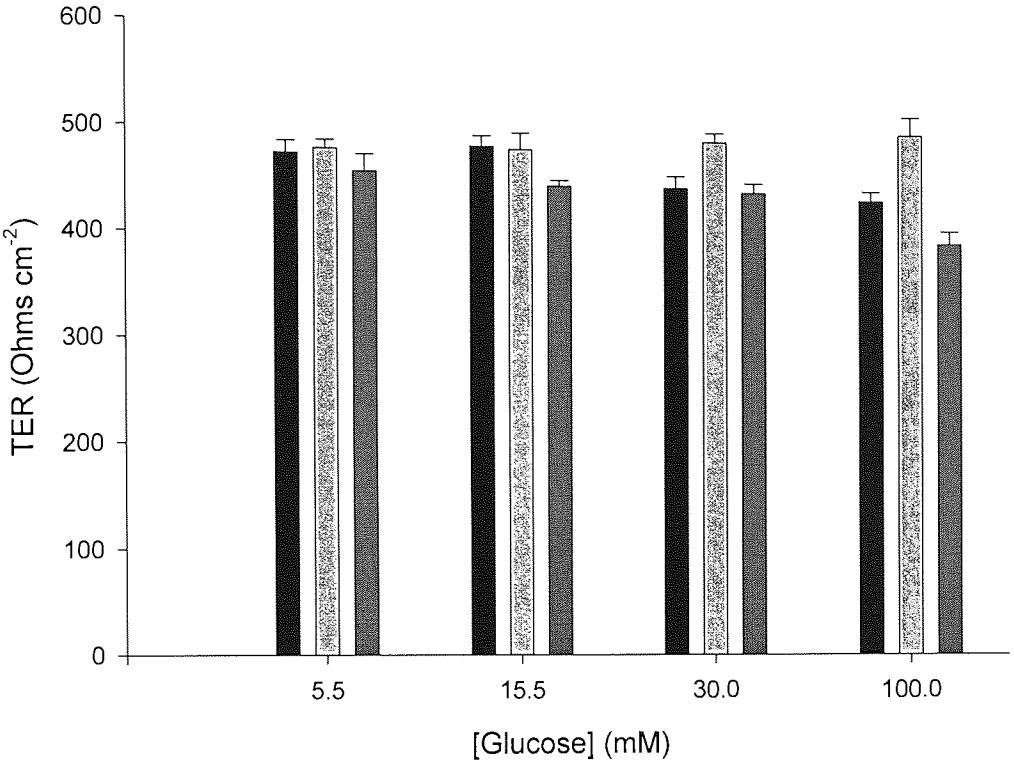

Figure 3.14 The effect of D-glucose on transepithelial electrical resistance (TER) of Caco-2 monolayers cultured over 21 d. Monolayers were washed with TB for 15 min at 37°C before D-glucose was applied to the Ap surface. The TER of each monolayer was measured with an epithelial voltmeter using STX2 'chopstick' electrodes at the time points shown. TER at 0 min (black), 5 min (light grey), 180 min (dark grey). Each bar represents the mean ± SEM (n=3).

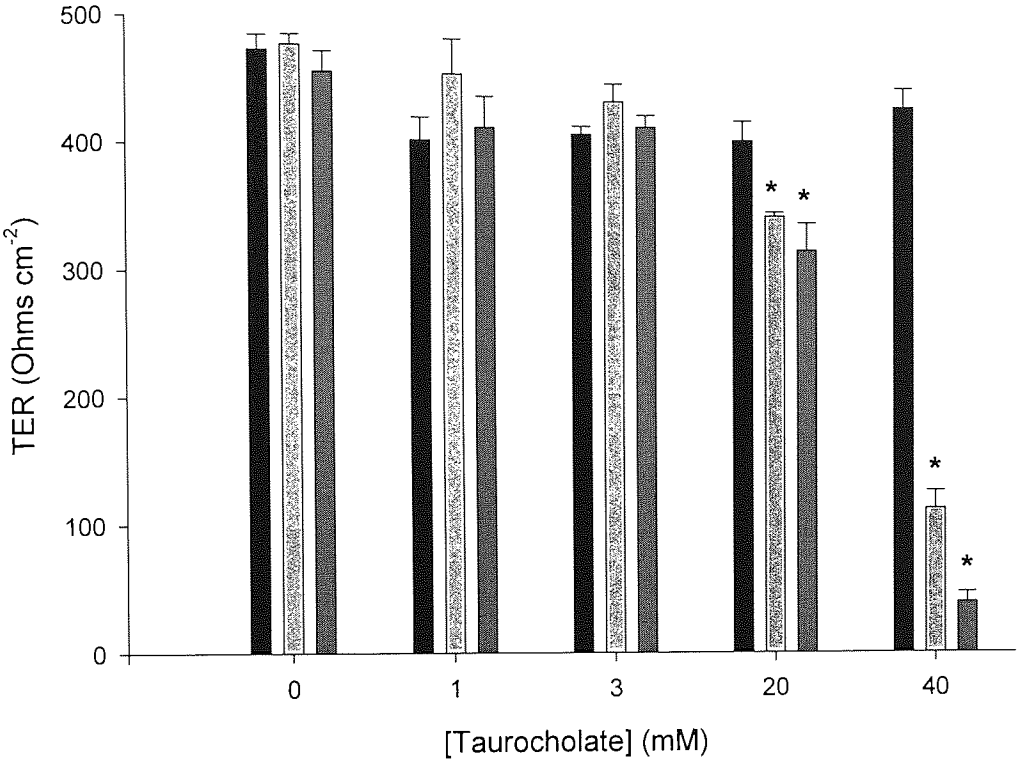

Figure 3.15 The effect of apical sodium taurocholate on transepithelial electrical resistance (TER) of Caco-2 monolayers cultured over 21 d. Monolayers were washed with TB for 15 min at 37°C before sodium taurocholate was applied to the Ap surface. The TER of each monolayer was measured with an epithelial voltmeter using STX2 'chopstick' electrodes at the time points shown. TER at 0 min (black), 5 min (light grey), 180 min (dark grey). Each bar represents the mean ± SEM (n=3). * Denotes significant difference from control value at $p<0.05$.

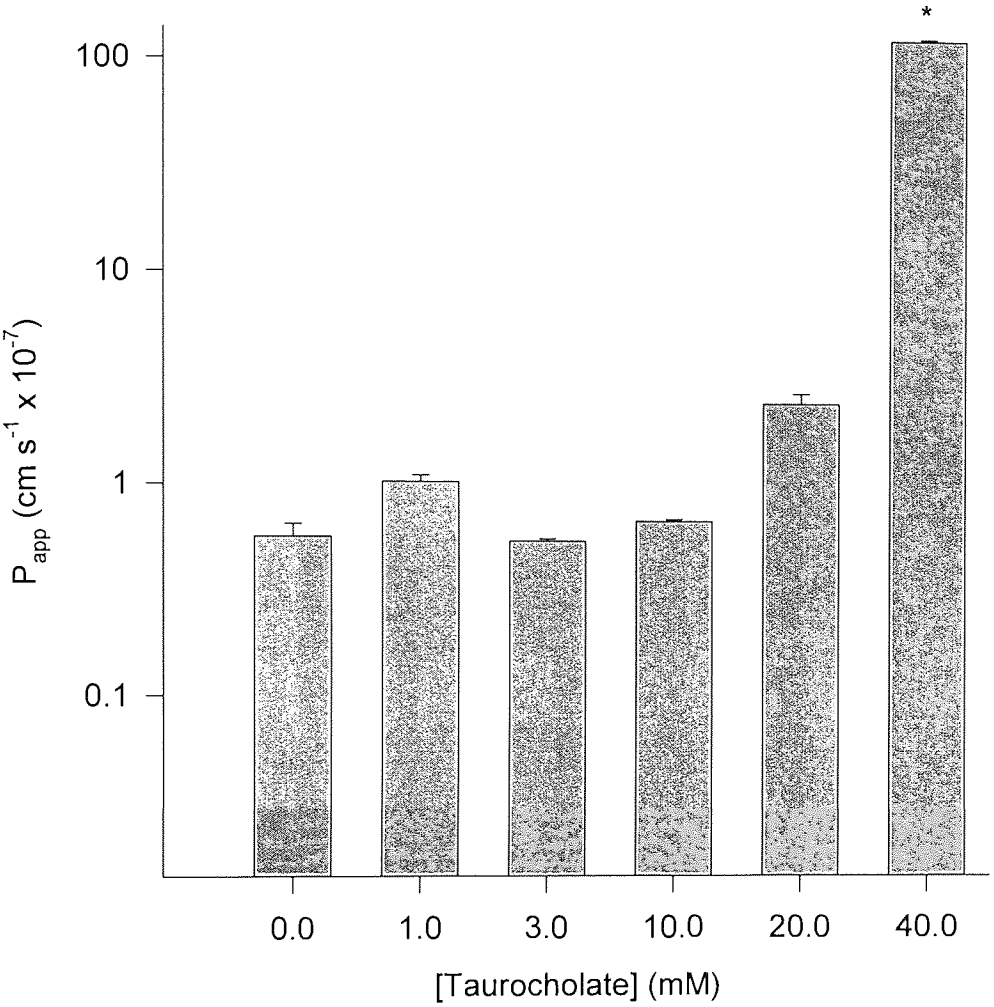

Figure 3.16 The effect of apical sodium taurocholate on the apical to basolateral transport of [^{14}C]mannitol across 21 d Caco-2 monolayers. Monolayers were washed with TB for 15 min at 37°C before [^{14}C]mannitol and sodium taurocholate were applied to the Ap surface. Transport kinetics were followed by sequential transfer of the inserts to fresh medium at 30, 60, 90, 120 and 180 min. The Ap-to-Bl transport rate for [^{14}C]mannitol was determined in the presence of a range of sodium taurocholate concentrations (0-40 mM). Data are presented as the mean values ± SEM (n=3). * Denotes significant difference from control value at $p<0.05$.

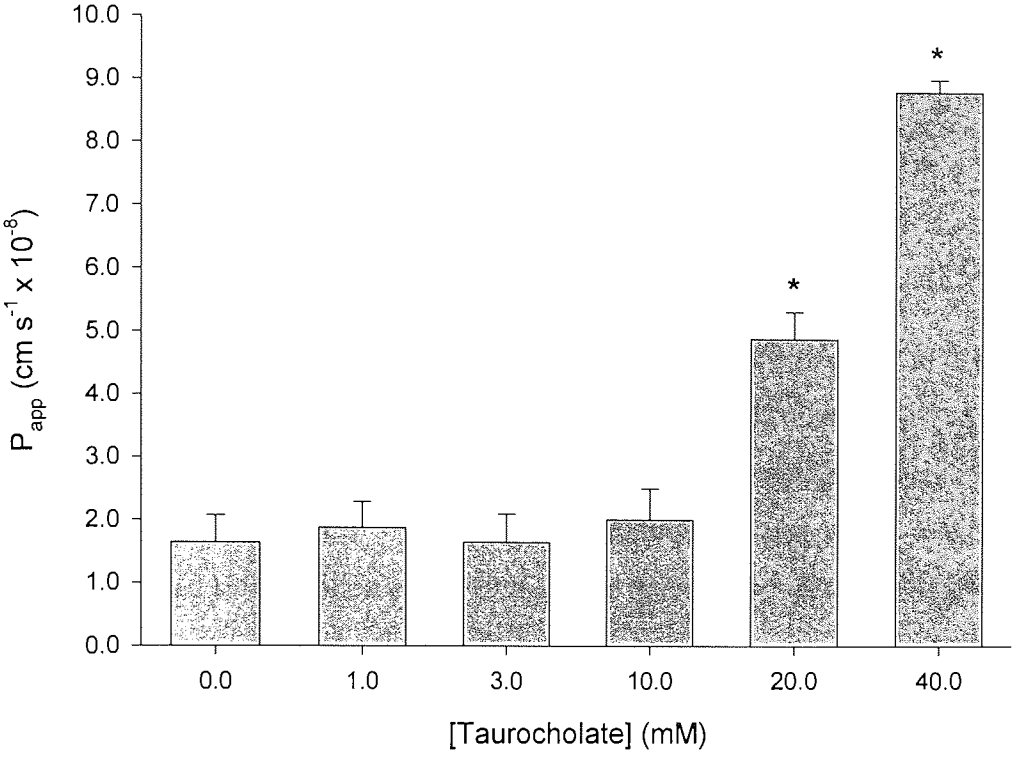

Figure 3.17 The effect of apical sodium taurocholate on the apical to basolateral transport of [^{14}C]PEG 4000 across 21 d Caco-2 monolayers. Monolayers were washed with TB for 15 min at 37°C before [^{14}C]PEG 4000 and sodium taurocholate were applied to the Ap surface. Transport kinetics were followed by sequential transfer of the inserts to fresh medium at 30, 60, 90, 120 and 180 min. The Ap-to-Bl transport rate for [^{14}C]PEG 4000 was determined in the presence of a range of sodium taurocholate concentrations (0-40 mM). Data are presented as the mean values ± SEM (n=3). * Denotes significant difference from control value at $p<0.05$.

The effect of 1.0-40.0 mM taurocholate on Caco-2 monolayer MTT transformation and LDH release was investigated. At 20 and 40 mM taurocholate was shown to be toxic to Caco-2 cells by the MTT assay (Figure 3.18). This was not corroborated by increased LDH release at these taurocholate concentrations, however, the reduced release is probably due to the inhibitory effect of taurocholate on LDH activity (Figure 3.19).

3.4 DISCUSSION

3.4.1 La^{3+} AS A PARACELLULAR PATHWAY INHIBITOR

The hypothesis that La^{3+} ions may inhibit the paracellular pathway was derived from its ability to replace Ca^{2+} at extracellular binding sites, its known Ca^{2+} antagonism, and its use in defining tight junctions in electron micrographs. This knowledge, together with the importance of extracellular Ca^{2+} on tight junction function (Artursson and Magnusson 1990; Nicklin *et al.*, 1995; Collett *et al.*, 1996), gave the basis for the investigation.

This study used La^{3+} in the form of La chloride as a potential inhibitor of the paracellular pathway in Caco-2 monolayers. No cytotoxicity was demonstrated by the measurement of LDH release or the conversion of MTT to a coloured formazan salt. Caco-2 monolayer barrier efficiency was evaluated by measuring TER and mannitol flux, both used as paracellular pathway markers in *in vitro* systems (Yap *et al.*, 1998). Inhibition of mannitol transport and enhanced TER across Caco-2 monolayers was attained with 2 mM La^{3+}, indicating that the tight junctions were blocked, inhibiting both ion and mannitol flow. This agrees with Sostman and Simon (1991) and Bryant and Moore (1995), who used La^{3+} as a tight-junction blocking agent, and Machen *et al.* (1972) who measured an increase in rabbit ileal resistance and decrease in ion flow following La^{3+} administration. However the inhibition of mannitol flux was not total, leaving approximately 40 % of control levels. Explanations for this observation could be that there are intercellular pores that cannot be blocked by La^{3+}, or mannitol has a substantial transcellular transport in Caco-2 monolayers that is maintained when the paracellular pathway is blocked. This may well be corroborated by the inhibition of [^{14}C]mannitol flux by approximately 20 % with the addition of 2 mM apical zinc. Zinc was shown to inhibit both Na^{+}-dependent sugar and amino acid transport by approximately 30 % but not the passive transport in *in vitro* intestinal preparation (Lugea *et al.*, 1995; Rodriguez-Yoldi *et al.*, 1996).

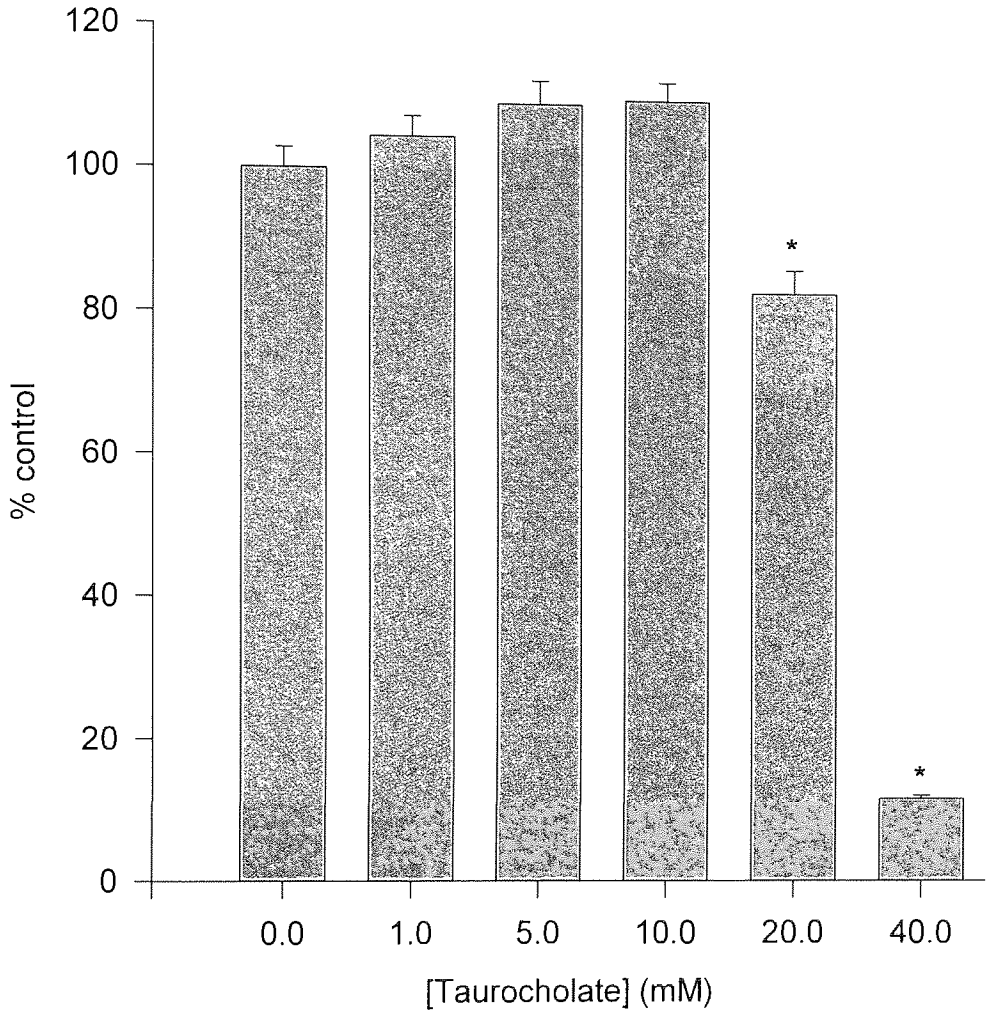

Figure 3.18 The effect of taurocholate on MTT transformation in Caco-2 monolayers. Monolayers were washed with TB for 15 min at 37°C before taurocholate in TB was applied to the Caco-2 monolayers. The formation of formazan coloured product was determined in the presence of a range of taurocholate concentrations (0-40 mM). Data are presented as the mean values ± SEM (n=8). * Denotes significanct difference from control value at $p<0.05$.

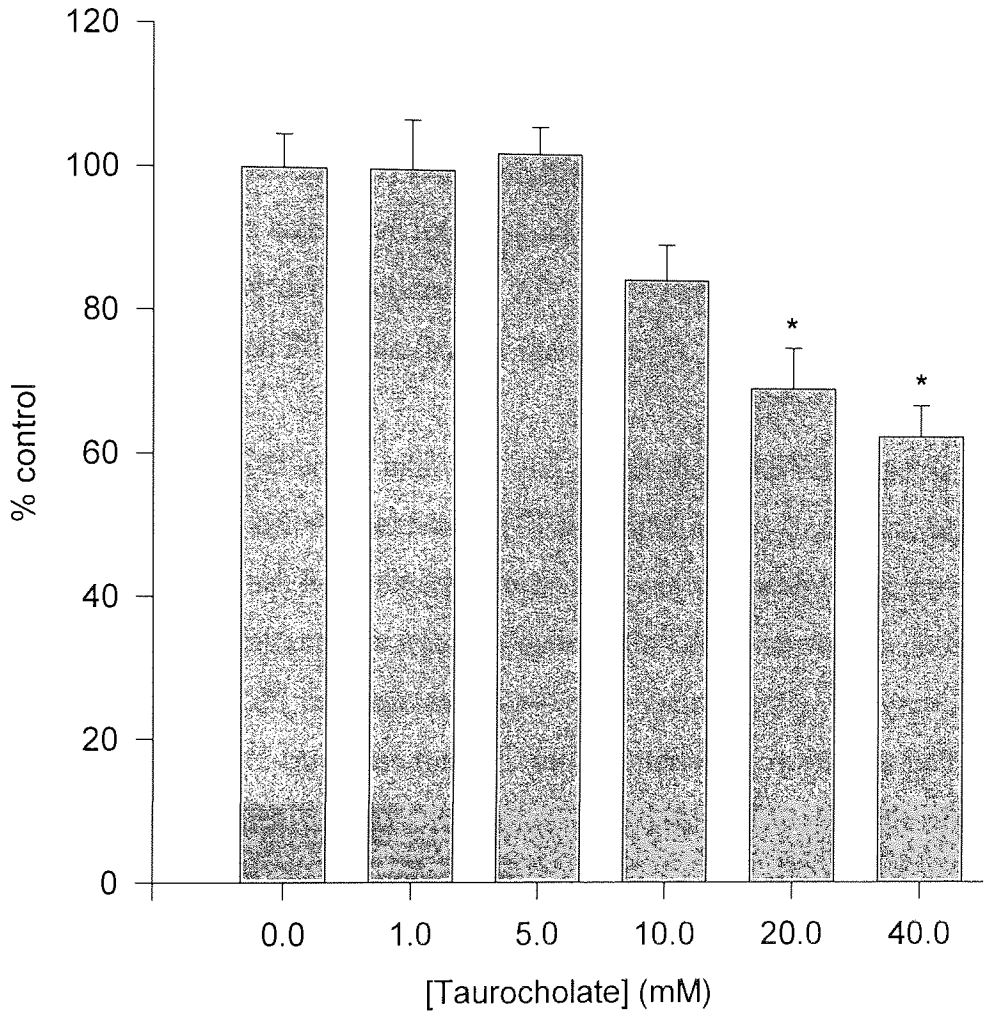

Figure 3.19 The effect of taurocholate on lactate dehydrogenase release from Caco-2 monolayers. Monolayers were washed with TB for 15 min at 37°C before taurocholate in TB was applied to the Caco-2 monolayers. The LDH release was determined in the presence of a range of taurocholate concentrations (0-40 mM). Data are presented as the mean values ± SEM (n=8). * Denotes significanct difference from control value at $p<0.05$.

3.4.2 CATION EFFECTS

The inhibition of [^{14}C]mannitol P_{app} produced by 2 mM La^{3+} was not repeated by other cations tested at 2 mM (Table 3.3). However, 2 mM Zn^{2+} did produce a significant decrease in [^{14}C]mannitol P_{app} as explained in the previous section (section 3.4.1). No effect on passive transport and therefore the paracellular pathway was observed (Lugea *et al.*, 1995; Rodriguez-Yoldi *et al.*, 1996) indicating that [^{14}C]mannitol permeability across Caco-2 monolayers has a significant transcellular component. With no significant effect on [^{14}C]mannitol P_{app} being demonstrated by Al^{3+}, Ba^{2+} Fe^{3+}, Mg^{2+}, and Mn^{2+}. Whereas, Cd^{2+},Cu^{2+}, Hg^{2+}, Ni^{2+}, and Pb^{2+} significantly increased [^{14}C]mannitol P_{app} (Table 3.3).

Nickel, which is a Ca^{2+}-channel inhibitor, and elicits the same response as other Ca^{2+}-channel inhibitors (see below), increased [^{14}C]mannitol P_{app}. Cadmium, also a known Ca^{2+}-channel inhibitor, has been reported to be tight-junction stabilising, interrupting the early phase of the opening process when basolateral Ca^{2+} is removed; this is in contrast to the cytotoxic effect of Cd^{2+} cell accumulation (Lacaz-Vieira, 1997). Whereas, Rossi *et al.* (1996) reported that Cd^{2+} competes for Ca^{2+} influx interfering with tight junction sealing and also fails to trigger junction formation; this is in accord with the increased [^{14}C]mannitol P_{app} across Caco-2 monolayers.

Iron is an essential element, with normal plasma levels of 14 and 21 μM in females and males respectively, and is absorbed from the small intestine (Wien and Van Campen, 1991), and transported by Caco-2 monolayers (Alvarez-Hernandez *et al.*, 1994b). Aluminium has been shown to be transported by Caco-2 monolayers but the mechanism is unknown (Alvarez-Hernandez *et al.*, 1994a). Therefore, aluminium could share intestinal uptake with essential ions, such as iron and calcium. If, Al^{3+} behaves like iron in binding to transferrin and ferritin in Caco-2 cells this would make it unavailable to exert its cytotoxic actions (Greger and Sutherland, 1997) as seen with no difference in [^{14}C]mannitol P_{app} values. Lead, and Cu^{2+}, increase [^{14}C]mannitol P_{app} probably due to the toxicity of cellular accumulation of these metals in Caco-2 monolayers (Rossi *et al.*, 1996). Whereas, Hg^{2+}, also a known toxic heavy metal is also an aquaporin inhibitor (Deen *et al.*, 1997; Carlsson *et al.*, 1996). Therefore, it could disrupt transcellular osmotic water

permeabilities and volume regulation of Caco-2 cells which would lead to loss of Caco-2 monolayer integrity and the increase in [^{14}C]mannitol P_{app}.

This demonstrates that besides La^{3+} and Zn^{2+} other cations do not reduce the [^{14}C]mannitol P_{app} value and only La^{3+} is capable of inhibiting the paracellular pathway. In fact, it shows that the majority of cations tested at 2 mM are cytotoxic and reduce the barrier efficiency of Caco-2 monolayers as demonstrated by the increases in [^{14}C]mannitol P_{app}.

3.4.3 TRANSPORT INHIBITORS

La^{3+} inhibition of the paracellular pathway could result from blocking of specific Ca^{2+} transporters in the plasma membrane. If La^{3+} is blocking Ca^{2+} influx this would be mimicked by Ca^{2+}-channel blockers, however, all the Ca^{2+}-channel blockers tested except nifedipine increased [^{14}C]mannitol P_{app} (Tables 3.3, 3.4), indicating that if La^{3+} was interacting with Ca^{2+} channels to block Ca^{2+} flux it would have an adverse affect on Caco-2 monolayer integrity. If La^{3+} was blocking Ca^{2+} efflux and increasing intracellular Ca^{2+}, or blocking Ca^{2+} entry *e.g.* verapamil (Table 3.4) this could signal the release of intracellular Ca^{2+} stores again increasing intracellular Ca^{2+}. Then the effect of the Ca^{2+} ionophore A-23187 would mimick this process. This has been shown not to be the case, as A-23187 increases [^{14}C]mannitol P_{app} in Caco-2 monolayers (Table 3.4) indicating raised intracellular Ca^{2+} concentrations leads to increased permeability of the epithelial layer. However, to test this hypothesis fully one would need to measure intracellular Ca^{2+} concentration in Caco-2 monolayers, which at present is not feasible.

La^{3+} inhibiting any element of cellular Na^+ or Cl^- transport in the apical or basolateral membranes of Caco-2 monolayers could disturb transcellular osmotic water permeabilities and volume regulation of Caco-2 cells leading to loss of integrity and therefore increased [^{14}C]mannitol P_{app}. All the transport inhibitors tested, none inhibited [^{14}C]mannitol P_{app}. Disruption of Na^+ handling seems unlikely, as amiloride a Na^+ channel inhibitor and ouabain, a Na^+/K^+-ATPase inhibitor, had no effect on [^{14}C]mannitol P_{app}. The Cl^- transport inhibitors, bumetanide and 4, 4'-diisothiocyanatostilbene-2, 2'-disulphonic acid (DIDS) increased [^{14}C]mannitol P_{app} across Caco-2 monolayers. Interaction of La^{3+} with glucose transporters seems unlikely, as phloridzin the Na^+-dependent glucose cotransporter

inhibitor, showed no significant change in [^{14}C]mannitol P_{app} from control values. In contrast, phloretin, the facilitative Na^+-independent glucose transporter inhibitor, increased [^{14}C]mannitol P_{app}, but only following apical administration of 1 mM phloretin. Therefore this initial investigation of the transport inhibitors tested indicates that La^{3+} is not inhibiting one or more of the cellular transport processes as their inhibition would seem to induce loss of Caco-2 monolayer integrity, indicated by the increase in [^{14}C]mannitol P_{app}.

3.4.4 OTHER PROBES

Along with measuring TER and mannitol, other transport probes were used to elucidate La^{3+} inhibition of transepithelial transport. As TER and [^{14}C]mannitol initially indicated that La^{3+} was inhibiting the paracellular pathway, the transport of larger probes were tested to delineate the effect. Transepithelial transport of [^{14}C]PEG 4000 was measured across Caco-2 monolayers, no significant effect (P=0.733) was seen with increasing concentration of La^{3+}. The mechanism by which PEG 4000 is transported across epithelial monolayers is in debate. Because of its M_r and linear configuration it is assumed to travel *via* the aqueous paracellular pathway at very low levels. However, it has also been shown that permeation of PEG across a lipid barrier *in vitro* permeated relatively readily compared with lactulose which did not permeate at all (Iqbal *et al.*, 1993). This suggests that PEG may permeate the intestinal epithelium by direct interaction with the phospholipid wall, in contrast to the largely paracellular permeation of lactulose or mannitol. The results of this study indicate that PEG 4000 is not affected by La^{3+} inhibition of the paracellular pathway. The constant level of PEG 4000 transport may infact be an indication that 13.4 μM PEG 4000 is transcellularly transported across Caco-2 monolayers.

In contrast to PEG 4000, HRP a glycosylated protein is 10-fold larger (40,000 Da) and is transported by energy requiring fluid-phase vesicular transcytosis across Caco-2 monolayers (Heyman *et al.*, 1990). This is almost completely inhibited by La^{3+}, leaving a small flux which might be due to much reduced HRP transcytosis and/or a population of pores in the paracellular pathway of Caco-2 monolayers unable to be inhibited by La^{3+}. This indicates that La^{3+} has an inhibitory effect on transcytotic vesicular transport, possibly affecting membrane endocytosis.

If La^{3+} exerts a membrane effect then other transcellular transport processes could be affected, for example, sodium taurocholate and glucose which are both carrier-mediated solutes. Caco-2 monolayers have been shown to have the Na^{+}-dependent cotransporter for taurocholate. In this study, La^{3+} does inhibit both passive and active processes. The passive transport of 1 mM taurocholate was inhibited by 97.1 % ± 0.3 % by 2 mM La^{3+} whereas the predominantly active transport of 3 μM taurocholate was only inhibited by 26.3 % ± 5.0 % (Figure 3.9), indicating that La^{3+} probably has a membrane effect. The transport disturbances observed here might be explained by changes in taurocholate permeability in relation to alterations of the membrane properties. Aldini *et al.* (1996) found that passive diffusion is higher through a less fluid membrane with a higher cholesterol-to-lipid ratio in the intestinal absorption of bile acids in the rabbit. Therefore, the increased La^{3+} inhibition of taurocholate permeability across Caco-2 monolayers is possibly a combination of La^{3+} stabilising the membrane and the increased proportion of taurocholate being passively transported.

Investigation of the nature of transepithelial glucose transport across Caco-2 monolayers revealed that glucose transport was inhibited by 54.2 ± 1.9 % with phloridzin, a SGLT-1 inhibitor, and 84.5 ± 0.5 % by the addition of the metabolic inhibitors, azide and 2-deoxyglucose. This indicates that glucose transport occurs *via* SGLT-1 and is energy-dependent in Caco-2 cells. However, the fact that La^{3+} does not totally inhibit mannitol transport across Caco-2 monolayers, may be explained because of their oncogenic origin, with the over expression of GLUT-1 and GLUT-3 facilitative hexose transporters. These transporters are also capable of mannitol transport as well as glucose and therefore La^{3+} may not inhibit transcellular mannitol transport (Figure 3.4). The fact that $TB_{Choline}$ medium without sodium present showed no significant difference in glucose transport (Figure 3.13) also corroborates that Na^{+}-independent hexose transport by this mechanism is present in Caco-2 monolayers.

The effect of increasing La^{3+} concentrations on glucose transport, was a small (12.9 %) but significant inhibition of glucose transport observed below 10 mM La^{3+} (Figure 3.12). However, this was not corroborated by the analysis of the saturable concentration-dependent glucose transport across Caco-2 monolayers increasing J_{max} in the presence of 2

mM La^{3+} (Figure 3.11). Indicating 2 mM La^{3+} had no definitive effect on glucose transport across Caco-2 monolayers but would have to be investigated further in the future.

Pappenheimer and Reiss (1987), proposed the hypothesis that transcellular nutrient absorption after a meal caused increased passive transport *via* the paracellular pathway. This was not corroborated with increasing concentration, 5.5-100 mM, of apical glucose on TER, [^{14}C]mannitol and [^{14}C]PEG 4000 permeability with no effect even at 100 mM glucose. This indicates that either Pappenheimer's hypothesis is not correct or the Caco-2 absorption model does not mimic the fluid handling found *in vivo*.

3.4.5 La^{3+} MECHANISM

Transepithelial transport inhibition by La^{3+} is complicated by possibly more than one action on Caco-2 monolayers. Machen *et al.* (1972) suggested that La^{3+} permeability was different depending on the chosen epithelia. In rabbit gallbladder and small intestine, La^{3+} is observed to permeate these epithelia. In contrast, toad urinary bladder and frog skin epithelia do not allow transport. Even in the permeable epithelia, electron-opaque deposits were seen in the intercellular space. Although La^{3+} ions, and not colloidal La, were used in the present studies, this still could be interpreted as deposits of colloidal La or interaction with membrane structures as shown in other morphological studies (Machen *et al.*, 1972; Martinez-Palomo *et al.*, 1971). These deposits could block the tight junctions, bringing about inhibition of the paracellular pathway. If these deposits are colloidal La or insoluble carbonate or hydroxide salts being formed in the intercellular spaces this would possibly lead to disruption of tight junction structure as seen when barium sulphate is selectively precipitated in tight junctions (Lacaz-Vieira and Kachar, 1996). The disruption in tight junction structure would lead to a decrease in TER and increase in [^{14}C]mannitol P_{app}, in contrast, with La^{3+} there is an increase in TER and decrease in [^{14}C]mannitol P_{app}.

La^{3+} interacting with transporter proteins or channels and other membrane components could induce dipole changes, leading to shifts in polarization of the membrane. This would alter electrochemical gradients, causing nonspecific damage or possible opening of a free-solution channel (Machen and Diamond, 1972) that would lead to a decrease in TER and an increase in [^{14}C]mannitol P_{app}. If La^{3+} precipitates on to the Caco-2 monolayers there

would be a non-specific inhibition of all the transepithelial transport probes, not indicated in this study. However, La^{3+} "coating" Caco-2 tight junctions through interaction with the negatively charged proteoglycans or exchange with Ca^{2+} binding sites would lead to changes in ion selectivity of the paracellular pathway (Machen and Diamond, 1972) and a decrease in [^{14}C]mannitol P_{app} and possible affects on other transport probes.

3.5 CONCLUSION

This study has shown that La^{3+} inhibits the paracellular pathway in Caco-2 monolayers as demonstrated by the reduced [^{14}C]mannitol P_{app} and increased TER. This inhibitory action is not reproduced by a selection of cations or transport inhibitors indicating that La^{3+} does not bind to these transporters inhibiting them. However, it does inhibit the transcytotic permeability of HRP across Caco-2 monolayers. Although [^{14}C]mannitol P_{app} is inhibited across Caco-2 monolayers by La^{3+} there is a significant flux which cannot be inhibited by La^{3+} which may be more than 40 % of transepithelial transport by this method. Therefore, La^{3+} as a probe to study paracellular transport in Caco-2 monolayers may need to be used with care.

CHAPTER FOUR TRANSEPITHELIAL TRANSPORT OF TWO PROTEIN KINASE C INHIBITORS

4.1 INTRODUCTION

Protein kinase C (PKC) is an enzyme family with serine/threonine kinase function, consisting of ten isoforms which have been cloned and sequenced and categorised in three families (Nishizuka, 1992). i) The conventional PKCs (PKC-α, -β_1, -β_2, -γ) contain four conserved regions and are activated by Ca^{2+}, diacylglycerols and phorbol esters. ii) The nonconventional forms (PKC-δ, -ε, -η, -θ) are Ca^{2+}-independent, but are still responsive to diacylglycerols and phorbol esters. iii) The atypical forms (PKC- ζ and -λ) have one cysteine-rich zinc finger-like motif and are unresponsive to Ca^{2+}, diacylglycerols and phorbol esters.

PKC is involved in the transduction of signals for cell proliferation and differentiation, where overexpression or activation of PKC may underlie developmental and proliferative diseases such as cancer. They have also been linked with inflammatory diseases, diabetes and central nervous system disorders (Lane *et al.*, 1990; Rasmussen *et al.*, 1990; Represa *et al.*, 1990). Protein kinase C is an intracellular receptor for a number of tumour-promoting agents which are involved in many processes such as apoptosis, exocytosis, proliferation and differentiation. This suggests that alterations in the expression levels and/or deregulation of the activity of PKC members has an important role in the processes relevant to neoplastic transformation, carcinogenesis and tumour cell invasion, making PKC inhibitors a potential anticancer therapy (Caponigro *et al.*, 1997).

4.1.1 PROTEIN KINASE INHIBITORS

Two PKC inhibitors from different chemical classes were evaluated for oral administration as potential anticancer drugs. The first, 4-N-benzoylstaurosporine (NBS) is a derivative of staurosporine while a second, N-(3-chlorophenyl)-4-{2-(3-hydroxypropylamino)-4-pyridyl}-2-pyrimidinamine, (CHPP), is a member of the phenylaminopyrimidine class of drug (Figure 4.1).

NBS has shown reduced protein kinase inhibition, but a higher degree of selectivity towards PKC when assayed for inhibition of different kinases (Meyer *et al.*, 1989; Caponigro *et al.*, 1997). NBS shows broad antiproliferative activity against various tumour and normal cell lines *in vitro* (Ikegami *et al.*, 1996a; Ikegami *et al.*, 1996b; Andrejauskas-Buchdunger and Regenass, 1992), and this antitumour activity is maintained *in vivo* when administered as a single agent against a variety of cell lines transplanted subcutaneously into nude mice (Killion *et al.*, 1995).

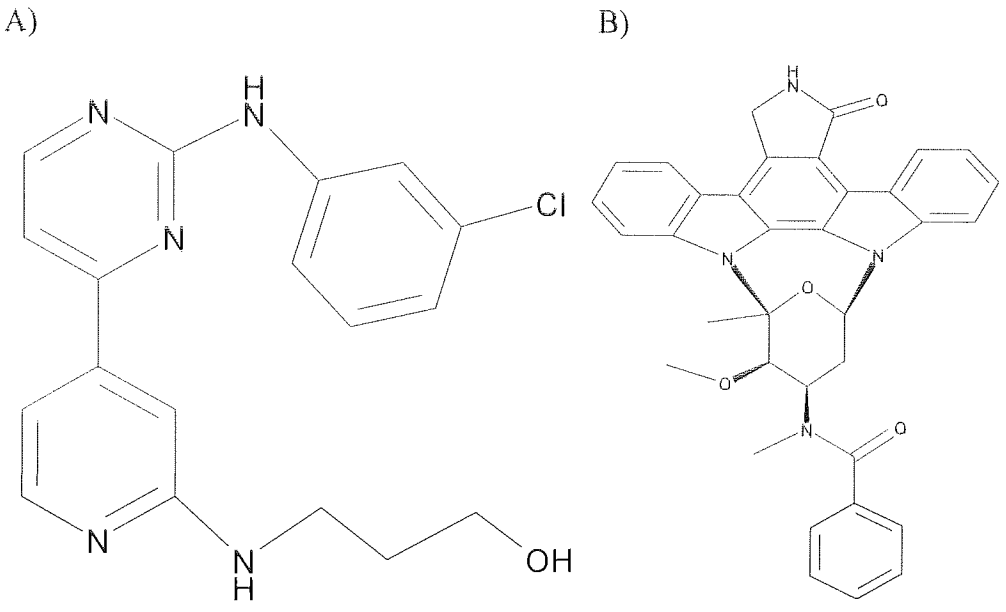

Figure 4.1 The structure of CHPP and NBS, two PKC inhibitors. A) CHPP and B) NBS.

Importantly, NBS has been found to reverse the P-glycoprotein (P-gp) mediated multidrug resistance (MDR) phenotype by inhibiting the function of P-gp and increasing the sensitivity of resistant tumours to anticancer drugs (Killion *et al.*, 1995). Several studies indicate a role for PKC in the regulation of the MDR phenotype, since several PKC inhibitors are able to partially reverse MDR and inhibit P-gp phosphorylatation. The MDR phenotype is also associated with variation in PKC isoenzyme content, in particular with PKC-alpha overexpression and its inhibition is able to reverse the P-gp-mediated MDR of tumour cells *in vitro* (Utz *et al.*, 1994; Beltran *et al.*, 1997; Budworth *et al.*, 1996; Chorvath *et al.*, 1994).

CHPP is a low molecular weight mitogenic signal transduction inhibitor that displays potent inhibitory activity against the serine/threonine-specific protein kinases cdk 1/2 and PKC-α with IC_{50} values in the nM range. This compound exerts potent antiproliferative activity *in vitro* but is poorly active *in vivo*. Both these compounds, CHPP and NBS, would be expected to show antitumour activity *in vitro* and *in vivo* following i.v. administration. Initial *in vitro* absorption studies across Caco-2 monolayers were used to assess the likelihood of further development of these drugs for oral administration.

4.1.2 LOW MOLECULAR WEIGHT DRUG ABSORPTION

It is assumed that the great majority of drugs cross biological barriers by a passive diffusion mechanism. Therefore, with both PKC inhibitors, CHPP and NBS, their high lipophilicity (Table 4.1) will enhance the probability of crossing the plasma membrane to interact with the intracellular enzyme.

Table 4.1 Selected physicochemical characteristics of NBS and CHPP (Ciba internal report)

Phys/chem characteristic	**NBS**	**CHPP**
Molecular weight	570.65	355.5
Log D‡	>5.5	4.1
pK_a	2.1, 3.5, 3.8	5.58,1.10
Aqueous solubility	0.068 mg l^{-1}	0.4 mg l^{-1}
Ethanol solubility	20 g l^{-1}	4.0 g l^{-1}

‡=n-oct/phosphate buffer at pH 7.4

In section 1.2.1.1 it has already been stated that the absorption of low molecular weight drug shows a strong positive correlation with distribution coefficient, but the relationship has been found to be parabolic with an absorption window between log D coefficients of 1.5 and 4.0 at physiological pH. Below log D 1.5, the compounds are relatively polar and do not traverse the cell membrane readily and therefore absorption by the paracellular pathway is perhaps preferred. Above log D 4.0, they are highly lipophilic and should be well transported across cell membranes, but transport is found to be limited; through lack

of dissolution of the drug into the aqueous environment of GI lumen, reducing the concentration gradient and also causing the compound to preferentially partition into the lipophilic environment of the cell membrane and not partition out into the cytoplasm of the cell.

At the pH of the small intestine (pH 5.0-7.0, Kararli, 1995) NBS is largely in the unionized form. However, CHPP has a basic nitrogen with a pK_a of 5.58 and therefore will not be totally unionised at small intestinal pH's below pH 6.0. In theory, unionized drugs pass through biological membranes more easily than ionized drugs (Gibaldi and Kanig, 1965). This was demonstrated by Streisand *et al.* (1995) with fentanyl, increasing the apparent permeability coefficient 3- to 5-fold as the pH of the fentanyl buccal solution increased. Both PKC inhibitors are candidate drugs for oral administration with high lipophilicity, no charge at small intestinal pH values above pH 6.0, and low hydrogen bonding potential. They appear to satisfy the requirements for oral absorption, except Log D may be too large. However, highly lipophilic drugs can be absorbed across the epithelium and secreted into the lymphatic system to enter the systemic circulation by the thoracic duct. Although the low aqueous solubility will give rise to solubilization problems into formulations and dissolution into the aqueous environment of the GI tract lumen.

4.1.3 CACO-2/CO-SOLVENT ABSORPTION MODEL

To test these drugs in the Caco-2 absorption model, an adaptation of the general method to include the addition of ethanol was developed. This allowed sufficient drug to be completely solubilised for administration and facilitated transport of both NBS and CHPP without the risk of precipitation in the medium. Good correlation exists between oral absorption in humans and P_{app} values using the Caco-2 model (Artursson and Karlsson, 1991). In this case, the Caco-2 model will primarily be used to elucidate the mechanism of absorption and ways of enhancing absorption. The addition of ethanol as a co-solvent to the system will alter the transport characteristics and therefore the predictive value of the Caco-2 model. The *in vivo* absorption of CHPP following oral administration of CHPP formulations will be investigated to test the predictive value of the Caco-2 model.

4.2 EXPERIMENTAL

4.2.1 CACO-2 CELL CULTURE

All transport studies in this chapter were performed using 14 d Caco-2 monolayers unless otherwise stated. Caco-2 monolayers were considered a tight monolayer at this time and as these two drug candidates are highly lipophilic the mechanism of transport was thought likely to be by passive transcellular permeation. They were cultured on polycarbonate permeable Transwell™ supports as described previously (see section 2.3.3).

4.2.2 TRANSPORT AND TRANSEPITHELIAL ELECTRICAL RESISTANCE STUDIES

For the majority of transport studies and all transepithelial electrical resistance studies, transport buffer (TB) containing 2.9 % (v/v) ethanol (TB_{EtOH}) was used in both the apical and basolateral chambers, unless stated otherwise (see section 2.4).

The protocols for measuring transepithelial electrical resistance (see section 2.5), transepithelial transport (see section 2.6.2), cellular association (see section 2.7) and cytotoxicity assays (see section 2.8) are described in Chapter 2 materials and methods.

4.2.3 CHPP AND NBS ANALYSIS

In all Caco-2 NBS transport assays, permeability was quantified using radiolabelled NBS which was detected by LSC (see section 2.2.1). All samples from the Caco-2 transport assays were analysed by HPLC (see section 2.2.5). Rat plasma samples were prepared as described in section 2.11.3 and analysed by HPLC (see section 2.2.5).

4.2.4 *IN VIVO* STUDIES

The formulations administered to the rats are shown in Table 2.4. CHPP was dissolved in the required volume of either lactic acid, oleic acid, or melted Gelucire™ 44/14 followed by the other excipients before the addition of distilled water. Each formulation was then sonicated for 30 s in an ultrasonic water bath (Grant, UK) and either vortexed or roller mixed. The CHPP aqueous suspension was prepared by adding 75 mg CHPP to 3 ml 0.5 % (w/v) Klucel and dispersed with a Ultra Turrax® T8 homogeniser with low volume dispersing tool (0.5 -5 ml) for 30 s. This procedure was repeated for the preparation of the

CHPP oily suspension, 120 mg of CHPP was added to 3 ml sesame oil + 1 % (v/v) Tween 80 and dispersed as above. The formulation were then administered either by a gavage needle or intraduodenal administration as previously described (see section 2.11.2).

4.3. RESULTS

4.3.1 CO-SOLVENT ABSORPTION MODEL

The effect of ethanol on Caco-2 cell viability was assessed by measuring LDH activity release and MTT transformation to a coloured product by live Caco-2 cells in the presence of a range of ethanol concentration (0.1 %-20 % (v/v)). For LDH release, there was no significant difference from control cells (P=0.179). For the MTT transformation with 20 % (v/v) ethanol, part of the monolayer had detached from the plastic, this was shown by the formation of the coloured formazan product inside the Caco-2 cells before the solubilisation step. All other concentrations of ethanol produced the same level of formazan product as control cells. Therefore both LDH release and MTT transformation indicates ethanol had no effect on cell viability.

The effect of different ethanol concentrations on the Ap-to-Bl P_{app} of [^{14}C]mannitol across Caco-2 monolayers is shown in Figure 4.2. There was no significant difference in [^{14}C]mannitol P_{app} between 1 % (v/v) ethanol and control values. The [^{14}C]mannitol P_{app} for TB containing 2.9 % (v/v) ethanol (9.42 ± 0.96 cm s^{-1} x 10^{-7}) was significantly different from the control value (4.58 ± 0.40 cm s^{-1} x 10^{-7}), an increase of 2-fold. The addition of 5 % (v/v) ethanol to TB produced a 7.5-fold increase in [^{14}C]mannitol P_{app} (38.5 ± 6.07 cm s^{-1} x 10^{-7}). Indicating that above 2.9 % (v/v) ethanol in TB their was a loss of monolayer integrity as demonstrated by the increased permeability of [^{14}C]mannitol a paracellular pathway marker.

With the lack of apparent cytotoxicity and minimal increase in [^{14}C]mannitol P_{app}, 2.9 % (v/v) ethanol was used as the co-solvent concentration in TB_{EtOH}. This gave clear solutions of 50 μM CHPP and NBS for administration to Caco-2 monolayers.

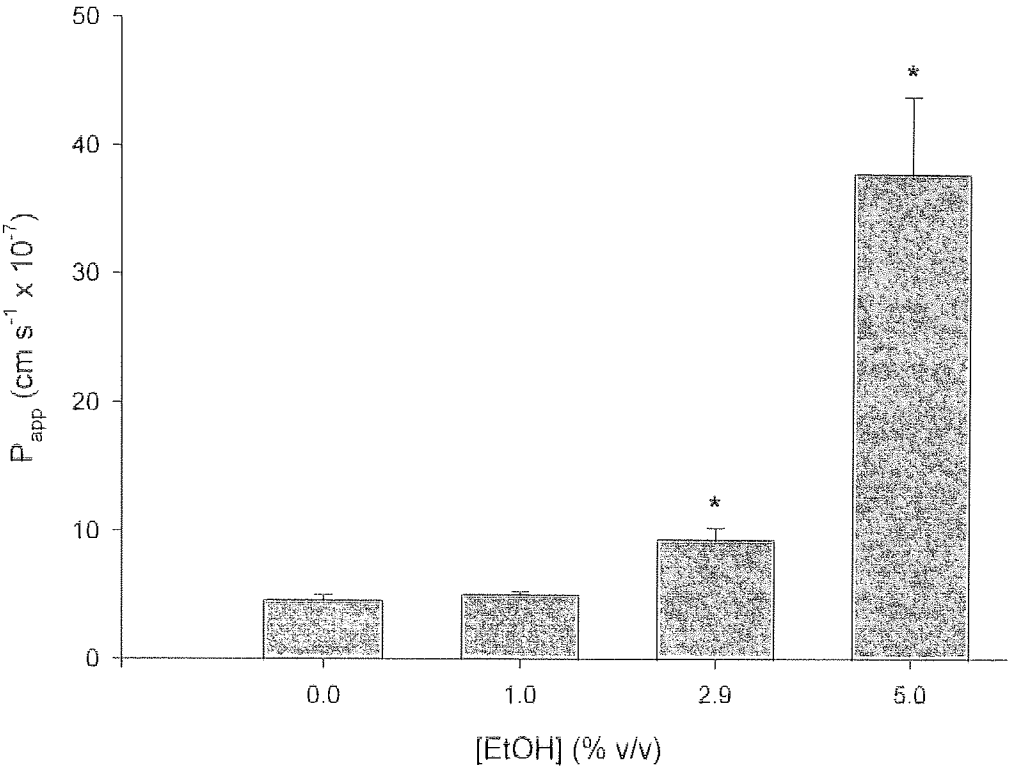

Figure 4.2 The effect of ethanol on the apical to basolateral transport of [^{14}C]mannitol across 14 d Caco-2 monolayers. Monolayers were washed with appropriate ethanol TB for 15 min at 37°C before [^{14}C]mannitol in appropriate ethanol TB was applied to the Ap surface. Transport kinetics were followed by sequential transfer of the inserts into fresh ethanol TB medium at 30, 60, 90, 120 and 180 min. The Ap-to-Bl [^{14}C]mannitol P_{app} was determined in the presence of a range of ethanol concentrations (0-5 % (v/v)). Data are presented as the mean values ± SEM (n=3). * Denotes significant difference from control value at $p<0.05$.

4.3.2 EFFECT OF NBS ON CACO-2 MONOLAYER INTEGRITY

Figure 4.3 shows the effect of apical NBS on Ap-to-Bl [^{14}C]mannitol P_{app} across 14 d Caco-2 monolayers. Below 50 μM NBS, there was no significant difference in [^{14}C]mannitol P_{app} compared with control values (9.42 ± 0.96 cm s^{-1} x 10^{-7}). The [^{14}C]PEG 4000 P_{app} value was 7.81 ± 0.41 cm s^{-1} x 10^{-8}, below 30 μM NBS, there was no significant difference in P_{app} values. At 30 μM NBS, there was a significant increase in [^{14}C]PEG 4000 P_{app}, with 30 μM (11.14 ± 0.40 cm s^{-1} x 10^{-8}) being 1.4-fold higher than control values (Figure 4.4). These data indicate the loss of Caco-2 monolayer barrier integrity with the addition of higher concentrations of NBS. However, no cellular cytotoxicity, as measured by LDH release (P=0.579) and MTT formation (P=0.636) over the concentration range 0-50 μM, could be seen. The reduced barrier function is also indicated by the 61 % decrease in TER (Figure 4.5, control). The loss of TER is still evident with apical pH 5.5, 5.0 mM sodium azide and 5.5 mM 2-deoxyglucose. In contrast, 5.0 mM La^{3+} and 100 μM ouabain significantly increased TER, 7.8- and 1.6-fold, respectively after 180 min (Figure 4.5).

4.3.3 NBS PERMEABILITY

The Ap-to-Bl transport of NBS across 14 d Caco-2 monolayers shows a linear dose-dependency over the concentration range 9.4-19.2 μM (Figure 4.6). However, at 59.3 μM NBS the rate of NBS transport deviates below the line suggesting saturability of the the transport process. The P_{app} was calculated for the different NBS concentrations applied to Caco-2 monolayers and a significant decrease in P_{app} was found with 59.3 μM compared to the lowest concentration of NBS, 9.4 μM, radiolabelled NBS alone (Table 4.2).

The effects of apical pH 5.5 medium, 5.0 mM sodium azide (uncouples oxidative phosphorylation), 100 μM ouabain (Na^+/K^+ATPase inhibitor), and 5.5 mM 2-deoxyglucose (non-metabolised glucose analogue) transcellular transport inhibitors and 5.0 mM La^{3+}, a paracellular transport inhibitor, on the permeability of 50 μM NBS are shown in Figure 4.7. None of the conditions inhibited the transport of 50 μM NBS across 14 d Caco-2 monolayers.

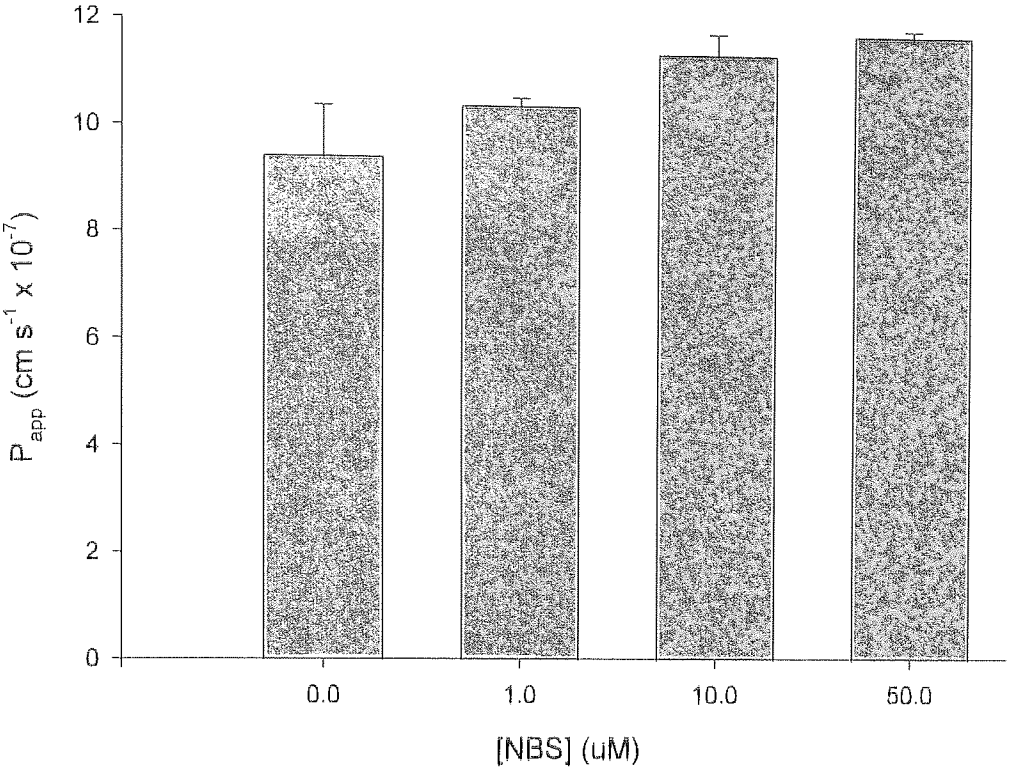

Figure 4.3 The effect of NBS on the apical to basolateral [^{14}C]mannitol apparent permeability coefficient (P_{app}) across 14 d Caco-2 monolayers. Monolayers were washed with TB for 15 min at 37°C before [^{14}C]mannitol and NBS in TB_{EtOH} were applied to the Ap surface. Transport kinetics were followed by sequential transfer of the inserts to fresh TB_{EtOH} at 30, 60, 90, 120 and 180 min. The Ap-to-Bl [^{14}C]mannitol P_{app} was determined in the presence of a range of NBS concentrations (0-50 μM). Data are presented as the mean values ± SEM (n=3). There was no significant difference from control values.

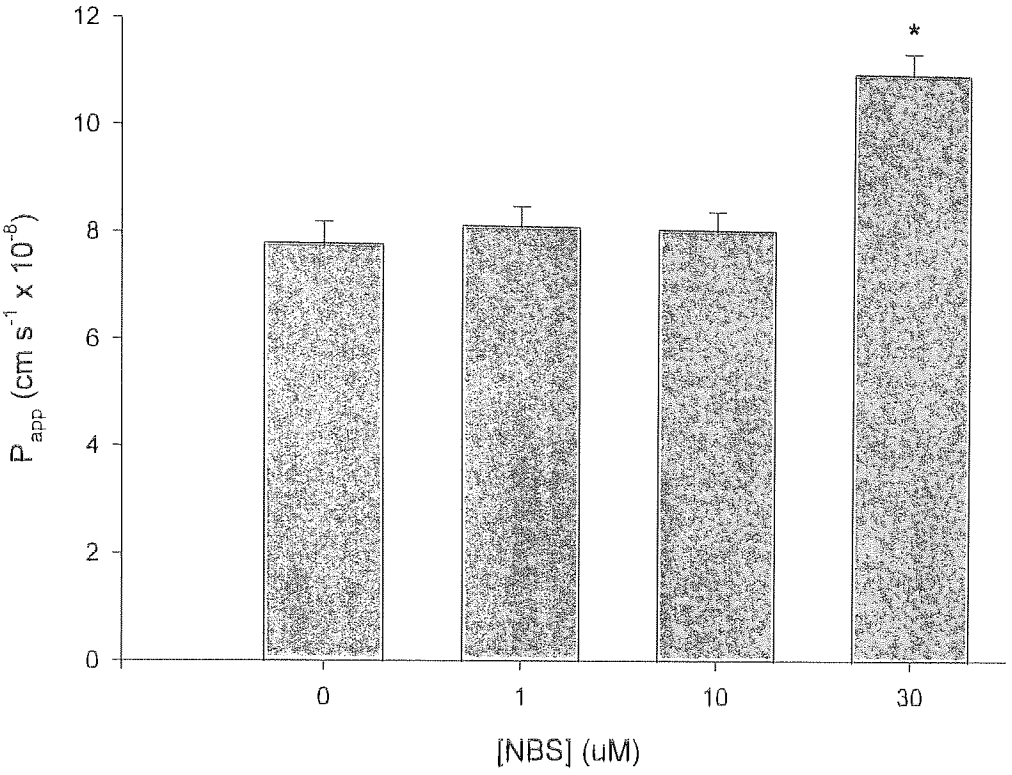

Figure 4.4 The effect of NBS on the apical to basolateral [^{14}C]PEG 4000 apparent permeability coefficient (P_{app}) across 14 d Caco-2 monolayers. Monolayers were washed with TB for 15 min at 37°C before [^{14}C]PEG 4000 and NBS in TB_{EtOH} were applied to the Ap surface. Transport kinetics were followed by sequential transfer of the inserts to fresh TB_{EtOH} at 30, 60, 90, 120 and 180 min. The Ap-to-Bl [^{14}C]PEG 4000 P_{app} was determined in the presence of a range of NBS concentrations (0-30 μM). Data are presented as the mean values ± SEM (n=3). * Denotes significant difference from control value at $p<0.05$.

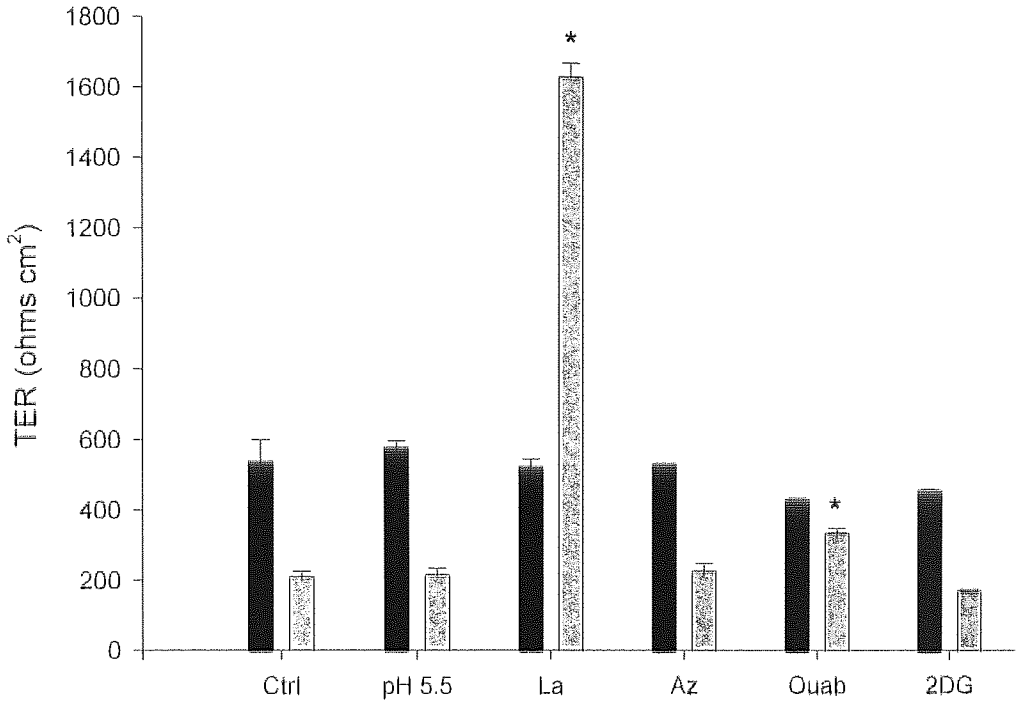

Figure 4.5 The effect of selected inhibitors and 50 μM NBS on transepithelial electrical resistance (TER) of Caco-2 monolayers cultured over 14 d. Monolayers were washed with TB for 15 min at 37°C before inhibitor and NBS in TB_{EtOH} were applied to the Ap surface. The TER of each monolayer was measured with an epithelial voltmeter using STX2 'chopstick' electrodes at the time points shown. TER at 0 min (black) and at 180 min (grey). Control (ctrl), Apical pH 5.5 (pH 5.5), 5 mM apical La^{3+} (La), 5 mM Azide (Az), 100 μM Ouabain (Ouab), 5.5 mM 2-deoxyglucose (2DG). Data are presented as mean values ± SEM (n=3). * Denotes significant difference from control value at $p<0.05$.

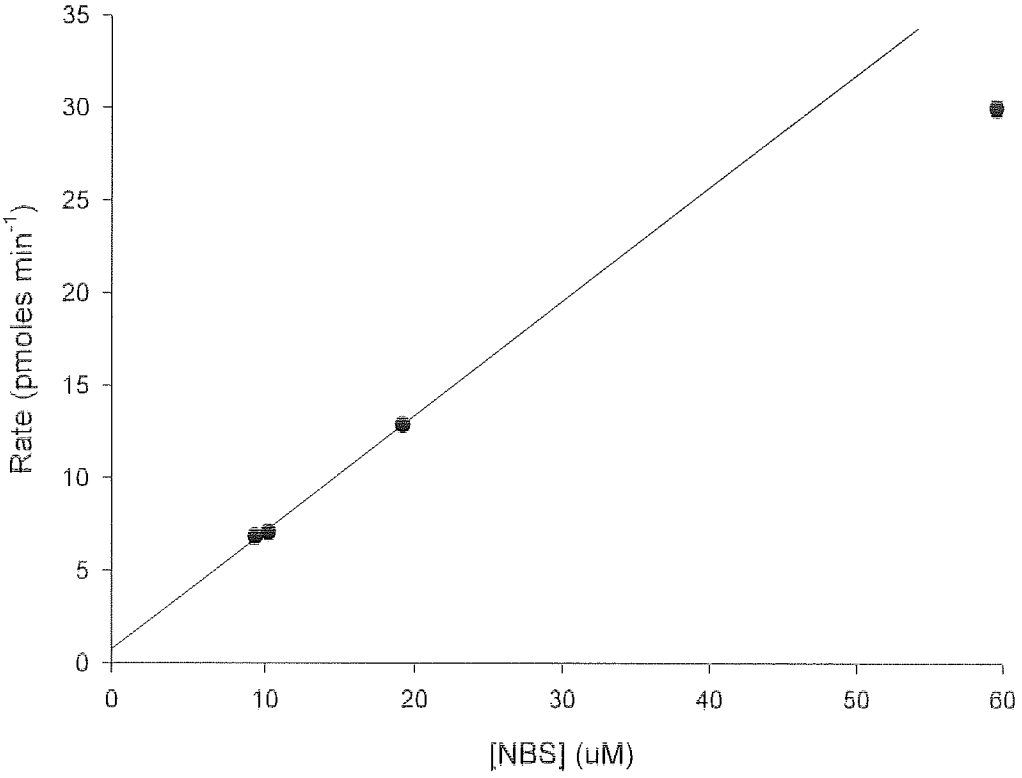

Figure 4.6 Concentration-dependent apical to basolateral transport of NBS across 14 d Caco-2 monolayers. Monolayers were washed with TB for 15 min at 37°C before NBS and [^{14}C]NBS in TB_{EtOH} were applied to the Ap surface. Transport kinetics were followed by sequential transfer of the inserts to fresh TB_{EtOH} at 30, 60, 90, 120 and 180 min. The Ap-to-Bl NBS transport rate was determined over a range of apical concentrations (9.4 to 59.3 μM). Data are presented as the mean values ± SEM (n=3).

Table 4.2 The apparent permeability of NBS following the addition of apical NBS to 14 d Caco-2 monolayers. Monolayers were washed with TB for 15 min at 37°C before NBS and [^{14}C]NBS in TB_{EtOH} were applied to the Ap surface. Transport kinetics were followed by sequential transfer of the inserts to fresh TB_{EtOH} at 30, 60, 90, 120 and 180 min. The Ap-to-Bl NBS P_{app} was determined over a range of apical concentrations (9.4 to 59.3 μM). Data are presented as the mean values ± SEM (n=3). * Denotes significant difference from 9.4 μM value at $p<0.05$.

[NBS] (μM)	**P_{app} ± SEM ($cm\ s^{-1} \times 10^{-6}$)**
9.4	2.59 ± 0.03
10.4	2.45 ± 0.02
19.2	2.39 ± 0.04
59.3	1.83 ± 0.03*

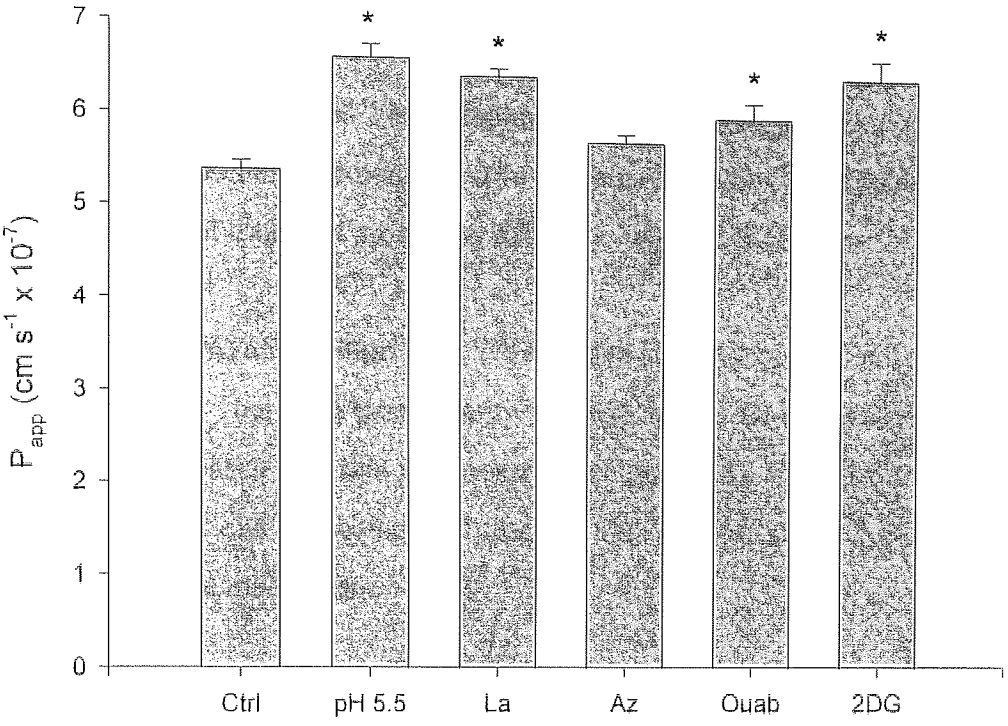

Figure 4.7 The effect of selected inhibitors on the apical to basolateral permeability of 50 μM NBS across 14 d Caco-2 monolayers. Monolayers were washed with TB for 15 min at 37°C in air before inhibitor and NBS in TB_{EtOH} were applied to the Ap surface. Transport kinetics were followed by sequential transfer of the inserts to fresh TB_{EtOH} at 30, 60, 90, 120 and 180 min. Control (ctrl), Apical pH 5.5 (pH 5.5), 5 mM apical La^{3+} (La), 5 mM Azide (Az), 100 μM Ouabain (Ouab), 5.5 mM 2-deoxyglucose (2DG). Data are presented as the mean values ± SEM (n=3). * Denotes significant difference from control value at $p<0.05$.

Sodium azide at 5.0 mM had no effect on NBS transport, apical pH 5.5, 5 mM La^{3+}, 100 μM ouabain and 5.5 mM 2-deoxyglucose significantly increased the permeability of NBS across Caco-2 monolayers, 1.23-, 1.19-, 1.11-, and 1.20-fold respectively.*

A further experiment combined 1 mM sodium azide and 50 mM 2-deoxyglucose to see if increased concentration of 2-deoxyglucose in combination with sodium azide would inhibit any energy dependent transport processes; this also, had no effect (Figure 4.8).

Budworth *et al.* (1996) and Beltran *et al.* (1997) have shown that NBS is an inhibitor of the P-gp efflux pump. Therefore permeability of NBS in the Bl-to-Ap direction would be expected to be increased and this was observed (Figure 4.8). This information with the above transport data one can concluded that the transport of NBS across Caco-2 cells is probably by a passive mechanism.

To investigate further the possible role of P-gp in NBS permeability 500 μM verapamil, a known P-gp inhibitor, was added to see if an increase in NBS permeability could be effected. However, in contrast verapamil produced a significant 26.9 % decrease in NBS permeability (Figure 4.8). Also tested was 3 % (w/v) Gelucire™ 44/14 which also produced a significant 51.8 % decrease in NBS permeability (Figure 4.8). Both these observations were surprising as the verapamil was expected to inhibit P-gp efflux and therefore increase NBS permeability. Whereas, Gelucire™ 44/14 was tested as a possible formulation for NBS to again increase NBS permeability.

4.3.4 EFFECT OF CHPP ON CACO-2 MONOLAYER INTEGRITY

There was no observed effect on Ap-to-Bl [^{14}C]mannitol P_{app} (13.90 ± 0.16 cm s^{-1} x 10^{-7}) below 10 μM CHPP. However, at 10 μM and above, CHPP caused a significant dose-dependent decrease in Ap-to-Bl [^{14}C]mannitol P_{app} from control values (Figure 4.9).

In contrast, at 10 μM and above, CHPP, there was a significant increase in Ap-to-Bl [^{14}C]PEG 4000 P_{app} (7.91 ± 0.25 cm s^{-1} x 10^{-8}) compared to control values (5.65 ± 0.64 cm s^{-1} x 10^{-8}) (Figure 4.10).

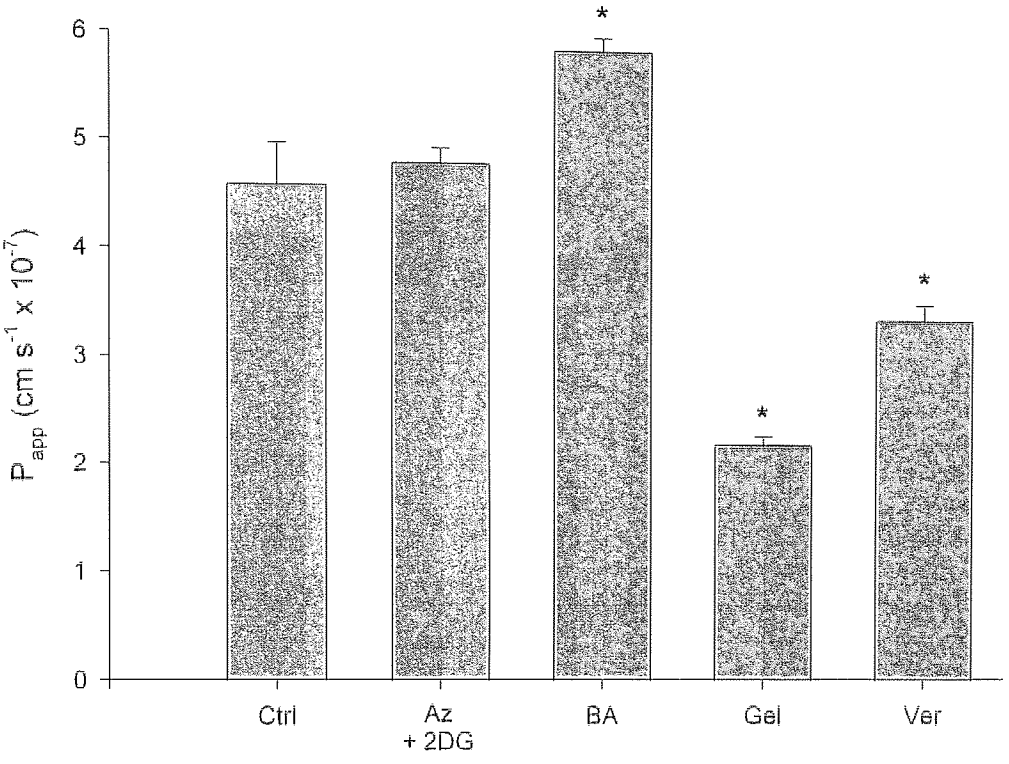

Figure 4.8 The effect of selected inhibitors on the apical to basolateral permeability of 50 μM NBS across 14 d Caco-2 monolayers. Monolayers were washed with TB for 15 min at 37°C in air before inhibitor and NBS in TB_{EtOH} were applied to the Ap surface. Transport kinetics were followed by sequential transfer of the inserts to fresh TB_{EtOH} at 30, 60, 90, 120 and 180 min. Control (ctrl), 1 mM sodium azide and 50 mM 2-deoxyglucose (Az + 2DG), Bl-to-Ap (BA), 3.0 % (w/v) Gelucire™ 44/14 (Gel), 500 μM Verapamil (Ver). Data are presented as the mean values ± SEM (n=3). * Denotes significant difference from control value at $p<0.05$.

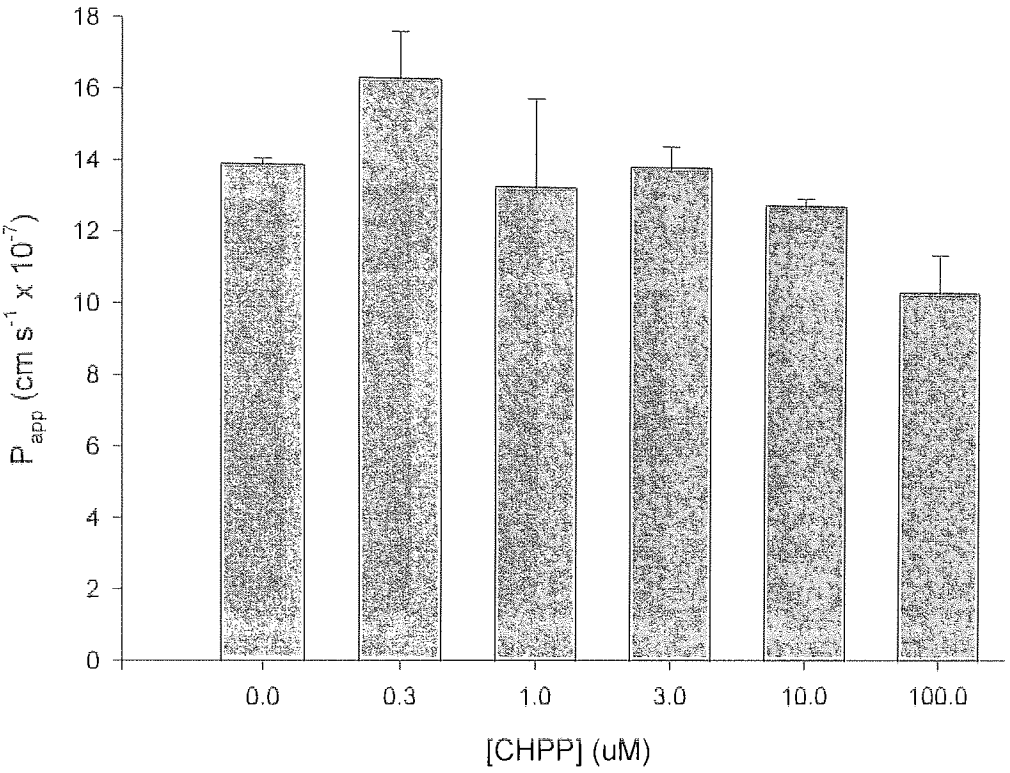

Figure 4.9 The effect of CHPP on the apical to basolateral permeability of [^{14}C]mannitol across 14 d Caco-2 monolayers. Monolayers were washed with TB for 15 min at 37°C before [^{14}C]mannitol and CHPP in TB_{EtOH} were applied to the Ap surface. Transport kinetics were followed by sequential transfer of the inserts to fresh medium at 30, 60, 90, 120 and 180 min. The Ap-to-Bl [^{14}C]mannitol P_{app} was determined in the presence of a range of CHPP concentrations (0-100 μM). Data are presented as the mean values ± SEM (n=3). * Denotes significant difference from control value at $p<0.05$.

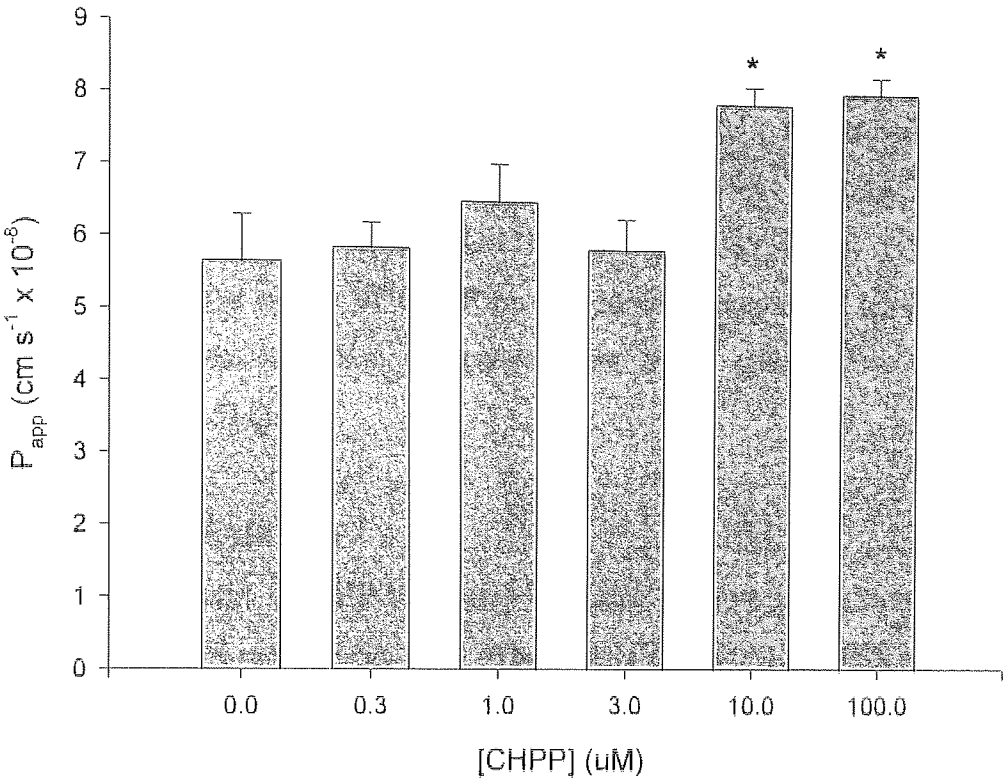

Figure 4.10 The effect of CHPP on the apical to basolateral permeability of [^{14}C]PEG 4000 across 14 d Caco-2 monolayers. Monolayers were washed with TB for 15 min at 37°C before [^{14}C]PEG 4000 and CHPP in TB_{EtOH} were applied to the Ap surface. Transport kinetics were followed by sequential transfer of the inserts to fresh medium at 30, 60, 90, 120 and 180 min. The Ap-to-Bl [^{14}C]PEG 4000 P_{app} was determined in the presence of a range of CHPP concentrations (0-100 μM). Data are presented as the mean values ± SEM (n=3). * Denotes significant difference from control value at $p<0.05$.

The alteration in tight junction integrity measured by the hydrophilic markers [^{14}C]mannitol and [^{14}C]PEG 4000 is reflected in the increased TER of Caco-2 monolayers at 180 min with 10 μM CHPP 319.76 ± 6.43 ohms cm^2 compared to control values 152.81 ± 5.15 ohms cm^2 (Figure 4.11). With the addition of ethanol as a co-solvent, barrier function is reduced over time as indicated by the 1.9-fold increase in [^{14}C]mannitol permeability (Figure 4.2) and a 63 % decrease in TER values (Control in Figure 4.11). However, in the presence of 10 μM CHPP, the 63 % decrease in TER is prevented, indicating a protective action of CHPP on the barrier function of Caco-2 monolayers. Also, CHPP was not cytotoxic as measured by LDH release (P=0.604) and MTT transformation (P=0.511).

4.3.5 CHPP PERMEABILITY

The Ap-to-Bl transport of CHPP across 14 d Caco-2 monolayer shows a linear dose-dependency over the range 3-50 μM. These data follow the model of Ficks law of diffusion indicating that the mechanism of absorption across Caco-2 monolayers is passive diffusion (Figure 4.12). With increasing concentration of CHPP inhibiting the loss of monolayer barrier integrity as measured by TER (Figure 4.11) and not inhibiting CHPP transport, this infers that the transcellular pathway is the route of permeability for CHPP. The P_{app} was calculated for all initial CHPP concentrations tested, and found to be constant over the range of concentrations tested on the Caco-2 monolayers (Table 4.3).

Analysis by HPLC of the 120 and 180 min basolateral samples and apical media taken at the end of the Caco-2 permeability experiment produced chromatograms with an extra peak (retention time 9.6 min) compared to unchanged parent drug CHPP (retention time 15.7 min) (Figure 4.13). This indicates the presence of a more polar metabolite after contact with and transport across Caco-2 monolayers.

4.3.6 *IN VIVO* CHPP PERMEABILITY

The plasma concentration profile, assayed by HPLC, following tail vein i.v. injection of 10 mg kg^{-1} CHPP in 10 % (v/v) lactic acid into an anaesthetised rat is shown in Figure 4.14. The half-life of CHPP was 28.4 ± 11.25 min. The data following oral or i.d. administered CHPP is presented in Table 4.4.

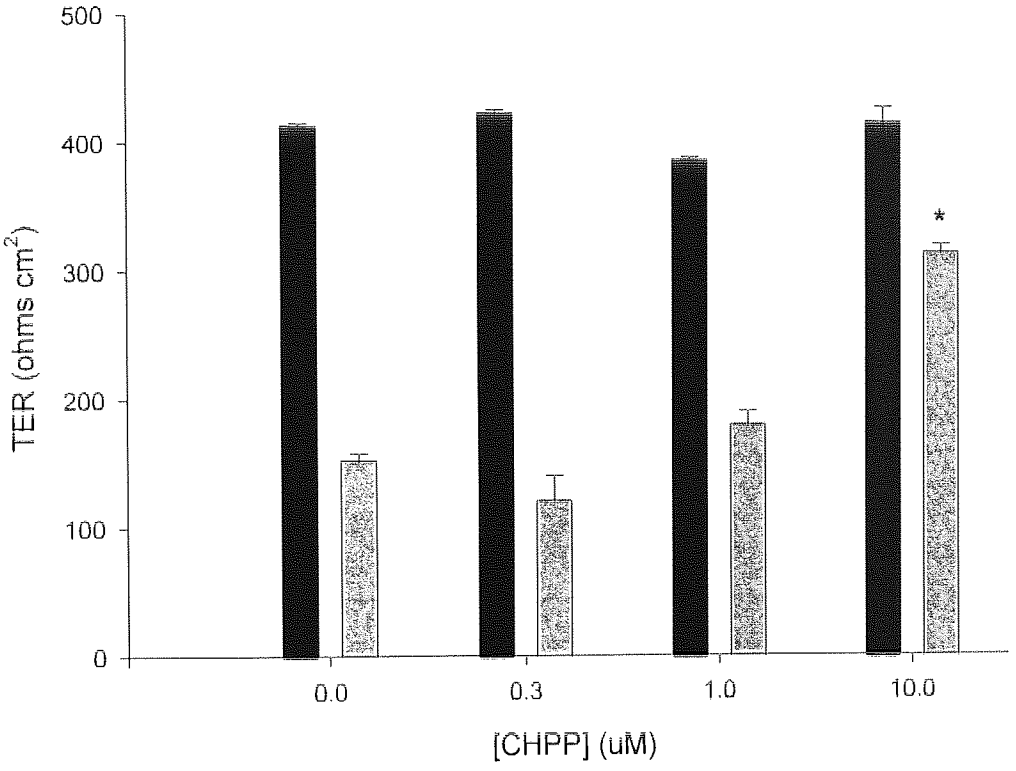

Figure 4.11 The effect of apical CHPP on transepithelial electrical resistance (TER) of Caco-2 monolayers cultured over 14 d. Monolayers were washed with TB for 15 min at 37°C before CHPP in TB_{EtOH} was applied to the Ap surface. The TER of each monolayer was measured with an epithelial voltmeter using STX2 'chopstick' electrodes at the time points shown. TER at 0 min (black) and at 180 min (grey). Data are presented as mean values ± SEM (n=3). * Denotes significant difference from control value at $p<0.05$.

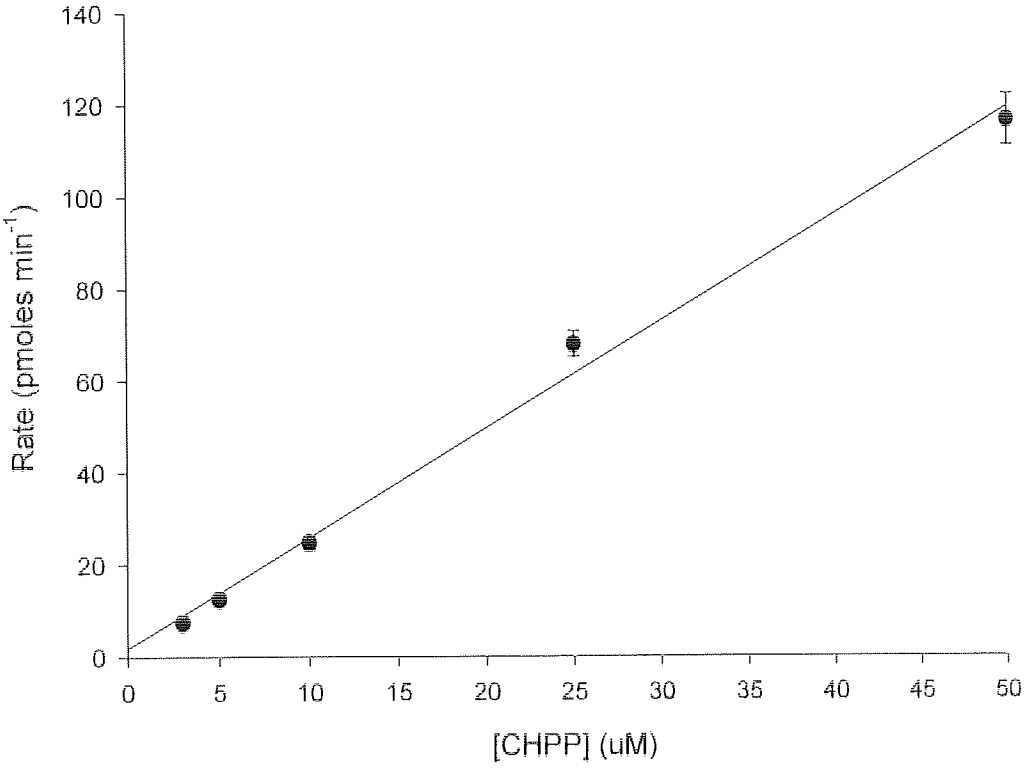

Figure 4.12 Concentration-dependent apical to basolateral transport of CHPP across 14 d Caco-2 monolayers. Monolayers were washed with TB for 15 min at 37°C before CHPP in TB_{EtOH} was applied to the Ap surface. Transport kinetics were followed by sequential transfer of the inserts to fresh TB_{EtOH} at 30, 60, 90, 120 and 180 min. The Ap-to-Bl CHPP transport rate was determined over a range of apical concentrations (3 to 50 μM). Data are presented as the mean values ± SEM (n=3). Error bars that cannot be seen are covered by the symbol.

Table 4.3 The apparent permeability of CHPP following the apical addition of CHPP to 14 d Caco-2 monolayers. Monolayers were washed with TB for 15 min at 37°C before CHPP in TB_{EtOH} was applied to the Ap surface. Transport kinetics were followed by sequential transfer of the inserts to fresh TB_{EtOH} at 30, 60, 90, 120 and 180 min. The Ap-to-Bl CHPP P_{app} was determined over a range of apical concentrations (3 to 50 μM). Data are presented as the mean values ± SEM (n=3).

[CHPP] (μM)	P_{app} ± SEM ($cm\ s^{-1} \times 10^{-6}$)
3	8.88 ± 0.43
5	8.92 ± 0.13
10	8.83 ± 0.30
25	9.73 ± 0.23
50	8.46 ± 0.23

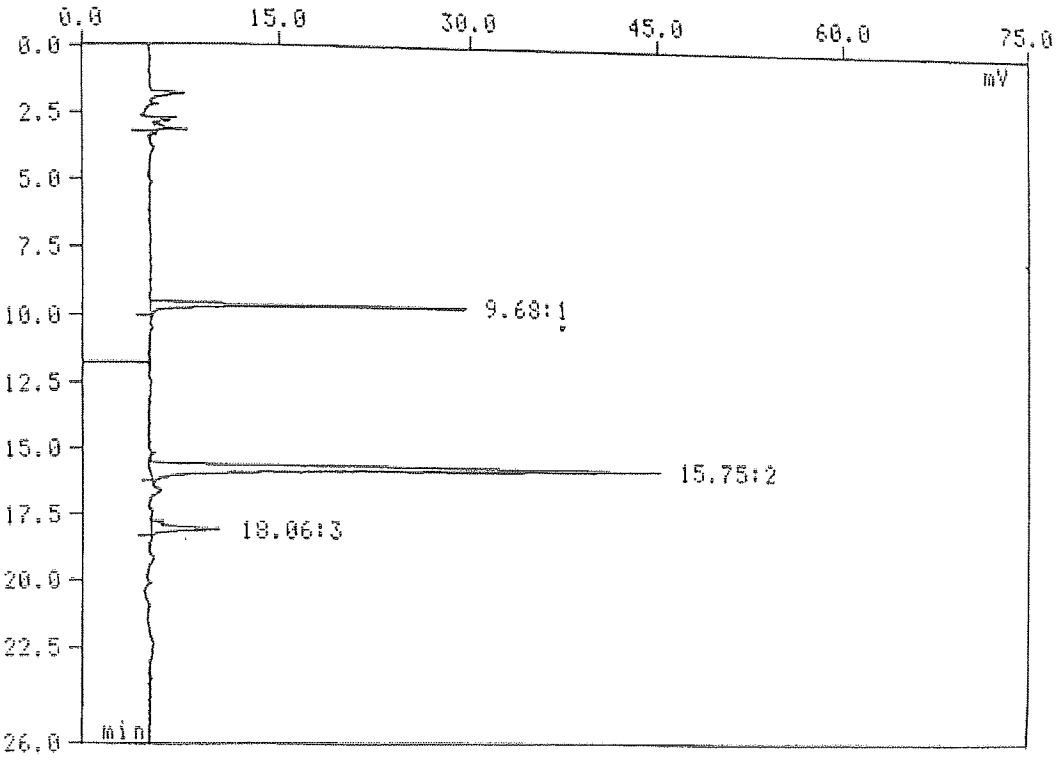

Figure 4.13 A typical chromatogram of TB_{EtOH} media containing CHPP (retention time 15.7 min) and possible metabolite after Ap-to-Bl transport of CHPP across 14 d Caco-2 monolayers. Monolayers were washed with TB for 15 min at 37°C before CHPP in TB_{EtOH} was applied to the Ap surface. Transport kinetics were followed by sequential transfer of the inserts to fresh TB_{EtOH} at 30, 60, 90, 120 and 180 min.

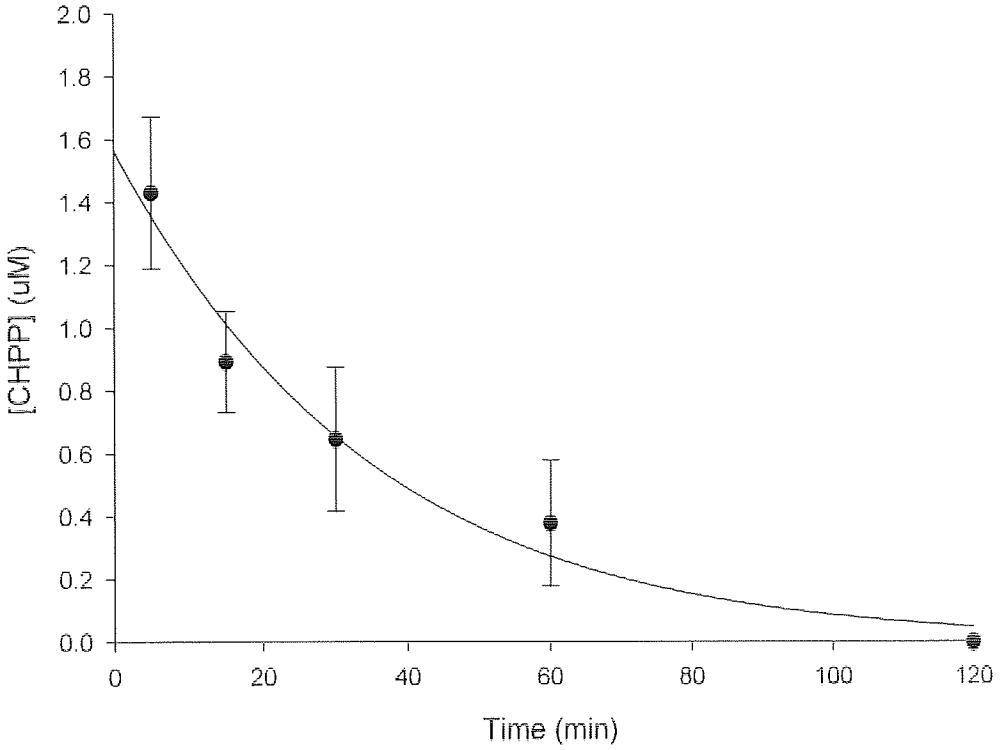

Figure 4.14 Plasma CHPP concentration after intravenous administration of a 10 mg kg^{-1} dose of CHPP. The fitted line ($y=1.566\ e^{-0.0266t}$) gives an initial concentration of 1.566 ± 0.9 μM and an elimination rate constant of 0.0266 ± 0.0091 s^{-1}. Results are presented as mean ± SEM (n=3).

Table 4.4 *In vivo* data following CHPP administration.

Formulation	Dose (mg kg^{-1})	n	Route	Plasma levels
3 % (v/v) Lactic acid	50	3	p.o	n.d.
0.5 % (w/v) Klucel HF	50	3	p.o	n.d.
0.5 % (w/v) Klucel HF	50	3	i.d.	<0.3μM
sesame oil + 1 % (w/v) Pluronic PE6800	50	3	p.o.	n.d.
oleic acid + 1 % (v/v) Tween 80	50	3	p.o.	n.d.
SEDDS	50	3	p.o	n.d.
3 % (w/v) Gelucire™ 44/14	20	3	p.o	n.d.

SEDDS, Self-emulsifying drug delivery system; p.o., Per os; i.d., intraduodenal; n.d., not detected.

The data show that there were no detectable levels of CHPP in rat plasma after 50 mg kg^{-1} CHPP dosed p.o. in the various formulations; an aqueous solution (50 mg kg^{-1} in 3 % (v/v) lactic acid), an aqueous suspension (50 mg kg^{-1} in 0.5 % (w/v) Klucel HF), an oily suspension (50 mg kg^{-1} in sesame oil + 1 % (w/v) Pluronic PE6800) or an oily solution (oleic acid + 1 % (v/v) Tween 80). Also, when CHPP was formulated into an emulsion, either melted into Gelucire™ 44/14 or a SEDDS formulation, there were no detectable plasma levels of CHPP. Increasing the dosing volume from 0.2 ml per 100 g body weight to 1 ml per 100 g body weight did not produce detectable CHPP plasma levels following p.o. administration.

The above formulations administered orally and CHPP plasma levels assayed by HPLC, indicates that discernible absorption has not taken place or the amount of CHPP absorbed into the blood is below the sensitivity of the HPLC method or metabolised. However, when CHPP is administered i.d. it is seen to be absorbed from the small intestine with detectable levels in rat plasma but at all time points, the level of drug is below the limit of quantification of the HPLC system which is 6.9 ng per injection volume *i.e.* below the bottom standard 0.3 μM. With all formulations administered orally, plasma levels of CHPP were not detected. Although absorption was detected with i.d. administration, this was of little consequence as the bioavailability was estimated to be below 1 %. This indicates that the formulation strategies used on CHPP did not give any advantage for increased absorption.

4.4 DISCUSSION

4.4.1 PROTEIN KINASE C INHIBITOR PERMEABILITY

Artursson and Karlsson (1991) demonstrated a correlation between the oral absorption of compounds in humans and derived P_{app} values using the Caco-2 model. Compounds that were completely absorbed had P_{app} values of $> 1 \times 10^{-6}$ cm s^{-1}. Compounds which were not completely absorbed had P_{app} values between 1×10^{-6} cm $s^{-1}$and 1×10^{-7} cm s^{-1}. The apparent permeability values below 1×10^{-7} cm s^{-1} represent compounds that are poorly absorbed in humans following oral administration. The P_{app} for 10 μM CHPP and 10 μM NBS was $8.83 \pm 0.30 \times 10^{-6}$cm s^{-1},and $2.39 \pm 0.04 \times 10^{-6}$cm s^{-1} respectively. These values for 10 μM CHPP and NBS predict complete absorption *in vivo*.

The Caco-2 permeability studies indicate that both compounds, at concentrations up to 50 μM, are passively transported. This is corroborated with no inhibitory effect of 1.0 mM azide and 50.0 mM 2-deoxyglucose.

Caco-2 cells have been reported to overexpress P-gp (Hunter *et al.*, 1991). Therefore, for NBS, which has been reported to be a P-gp inhibitor (Budworth *et al.*, 1996; Beltran *et al.*, 1997) the addition of a P-gp substrate verapamil, should increase the permeability of NBS if P-gp is reducing NBS permeability. This was found not to be the case, in fact there was a significant 25 % decrease in NBS permeability across Caco-2 monolayers (Figure 4.5).

This may be explained by competition for a common binding site in P-gp by both NBS and verapamil as proposed by Seelig (1998). The suggestion being, molecular recognition elements are formed by two (type I unit) or three electron donor groups (type II unit) with a fixed spatial separation. Type I units consist of two electron donor groups with a spatial separation of 2.5 ± 0.3 Å. Type II units contain either two electron donor groups with a spatial separation of 4.6± 0.6 Å or three electron donor groups with a spatial separation of the outer two groups of 4.6 ± 0.6 Å. Verapamil contains type I units and NBS could contain type I units and therefore compete for P-gp substrate binding sites leading to reduced transport.

Although the Caco-2 data predicted high absorption, this was not observed in the *in vivo* experiments. The lack of correlation between the *in vitro* Caco-2 permeability data and *in vivo* absorption of CHPP could be possibly explained by any one of the following of reasons:-

1) *in vivo* absorption went undetected by HPLC analysis of rat plasma samples because the drug level was below the limit of quantification, (0.3 μM).

2) CHPP is taken up into the plasma membrane of the absorbing enterocyte and because of its increased Log D, does not partition into the cytosolic or the portal circulation, aqueous environment. This may well be the case *in vivo* where there is a large reserve of membrane. Unlike the Caco-2 absorption model, which only has a small finite amount of membrane available with a relatively steep Ap-to-Bl CHPP gradient across the Caco-2 monolayer.

3) rapid metabolism of CHPP by first-pass metabolism at the intestinal wall or in the liver. There is some evidence to support this as both Caco-2 cells and *in vivo* data indicate that metabolism is taking place. With Caco-2 monolayers this was seen with the production of a polar metabolite with a decreased retention time of 9.6 min (Figure 4.13) in the HPLC chromatogram, although this metabolite was not observed *in vivo*.

4) interaction in GI tract lumen *i.e.* binding to mucus or fibre within the intestine making CHPP unavailable for absorption.

5) P-gp efflux; the GI tract, as well as Caco-2 cells have been shown to express P-gp (Thiebaut *et al.*, 1987; Hunter *et al.*, 1991), therefore the lack of CHPP *in vivo* absorption could be due to P-gp efflux of CHPP and its metabolite from intestinal enterocytes. This may well be taking place, but as detectable absorption of both CHPP and metabolite was not observed it would have to be investigated further.

6) dissolution problems; with CHPP having a Log D of 4.1 even when dissolved into various formulation (Table 4.4) its dissolution into the aqueous environment of the GI lumen is unfavourable. In the case of 3 % (v/v) lactic acid, CHPP could precipitate and is thus unavailable for absorption. When formulated into an oily solution, *e.g.* oleic acid + 1 % (v/v) Tween 80, then the raised Log D of CHPP favours the lipophilic environment of the formulation and does not partition into the aqueous environment of the GI lumen and therefore not available for absorption. Even with CHPP melted into Gelucire™ 44/14 or formulated into a SEDDS formulation, with both forming emulsions. CHPP will still favour the lipophilic environment of the emulsion droplets and micelles instead of the aqueous GI lumen, unless the CHPP emulsion is brought into close proximity either to partition or be transported across the apical membrane of the absorbing enterocyte.

However, with CHPP, its lack of aqueous solubility at intestinal pH needed formulations that were compliant for testing *in vivo*. Four formulation approaches were attempted, to overcome the physicochemical properties of CHPP; an aqueous solution (50 mg kg^{-1} in 3 % lactic acid), an aqueous suspension (50 mg kg^{-1} in 0.5 % Klucel HF), an oily suspension (40 mg kg^{-1} in sesame oil + 1 % Pluronic PE6800) or an oily solution (oleic acid + 1 % Tween 80). Also, when CHPP was formulated into an emulsion, either melted into Gelucire™ 44/14 or a SEDDS formulation there were no detectable plasma levels of CHPP. The formulations administered per os indicate that discernible absorption had not taken place, or the amount of CHPP absorbed into rat plasma is below the sensitivity of the HPLC method. This suggests that CHPP will not be an effective oral anti-tumour agent *in vivo* in experimental models of cancer. Although, in the rat studies, the level of detection

was such that concentrations of CHPP could well be above the 100 nM IC_{50} in i*n vitro* antiproliferative assays for many human tumour cells cannot be excluded and may still be sufficient to attain anti-tumour activity, this will need to be investigated further.

4.4.2 CO-SOLVENT MODEL

The ethanol co-solvent model gives a 2-fold increase in mannitol and PEG 4000 permeability compared to monolayers without ethanol. If this increased permeability, with the co-solvent model, was to hold true for all Caco-2 monolayer drug permeability, a correction factor would be needed to predict human absorption from the correlation curve of human absorption versus Caco-2 P_{app} and this would potentially move compounds to the left (Figure 4.15).

In both cases, the native Caco-2 absorption model and the co-solvent model, predict complete absorption of CHPP. In contrast, the potential shift in the correlation curve of the co-solvent model predicts variable permeability for NBS. The effect of 2.9 % (v/v) ethanol on the Caco-2 monolayer result in the loosening of tight junctions. As evidenced by the time-dependent loss of TER and the increased [^{14}C]mannitol and [^{14}C]PEG 4000 P_{app} values across Caco-2 monolayers.

However, the co-solvent model seems to hold true because even with increased paracellular permeability, the PKC inhibitor NBS is unaffected by the paracellular inhibitor La^{3+} which would indicate that the main permeability pathway is the transcellular pathway. If ethanol is having an effect on Caco-2 cells, it is not apparent from this study. The addition of transcellular transport inhibitors had no inhibitory effect and there was no significant difference in the Bl-to-Ap permeability of NBS, if anything a stimulatory effect indicating that the co-solvent model was metabolically active and possibly trying to efflux the PKC inhibitors.

4.4.3 PROTEIN KINASE C INHIBITOR EFFECTS ON CACO-2 MONOLAYERS

It has already been shown that Caco-2 cells have a complement of PKC isoforms, namely predominantly PKC-α and -ζ with minimal detectable amounts of PKC-β and -ε by

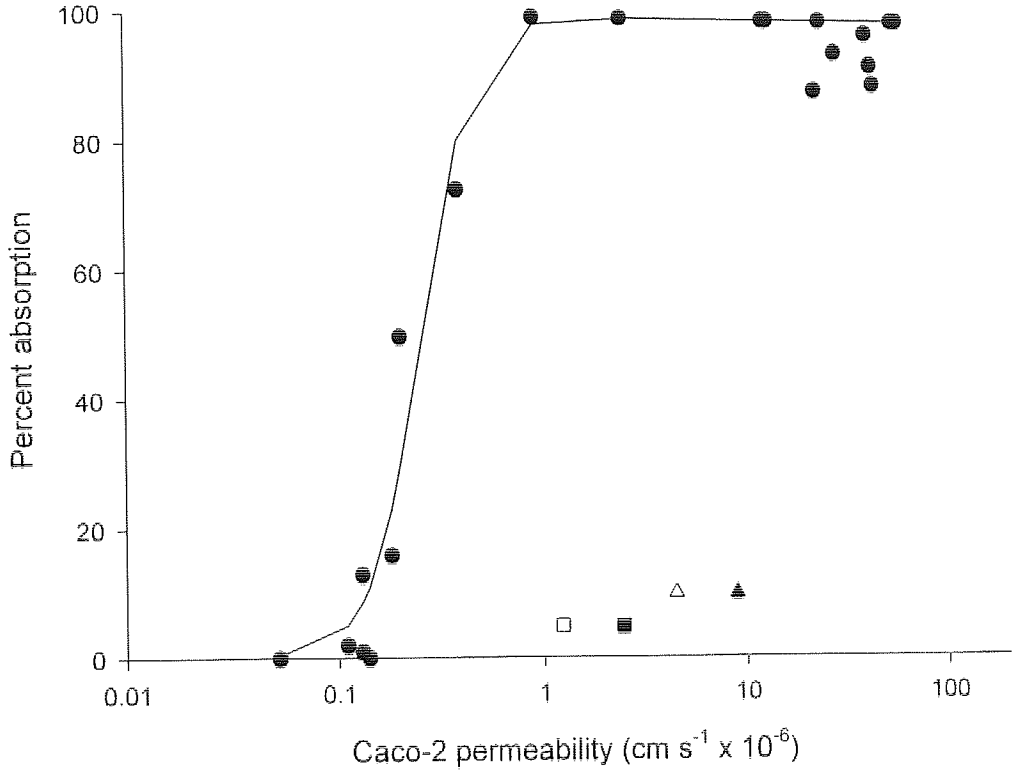

Figure 4.15 Correlation between absorbed fraction in humans after oral administration (percent absorption) versus permeability in Caco-2 monolayers. Data obtained form Artursson and Karlsson (1991) (● and solid line). P_{app} of NBS (■), and CHPP (▲) measured in the co-solvent model. Their potential shift when the co-solvent model is accounted for (open symbols).

Western blotting (Bissonnette *et al.*, 1994). In Caco-2 monolayers, stimulation of PKC by phorbol esters increases mannitol permeability with a reciprocal decrease in TER and this is blocked by the PKC inhibitor staurosporine (Stenson *et al.*, 1993). This response is also seen in the pig kidney epithelial cell line LLC-PK_1 (Mullin *et al.*, 1998a) where the increased paracellular permeability gave as much as a 20-fold increase in transepithelial flux of biologically active insulin (Mullin *et al.*, 1998b). Citi (1992), using the renal MDCK cell line, demonstrated the same response, this time using Ca^{2+} removal and the protein kinase inhibitor H7 at 50 μM to block the TER changes.

The effect of CHPP and NBS is to inhibit PKC which is known to regulate intracellular Ca^{2+} concentration which in turn can regulate tight-junction resistance and permeability (Tai *et al.*, 1996). Therefore, they should increase TER and decrease both [^{14}C]mannitol and [^{14}C]PEG 4000 permeability. NBS, a PKC inhibitor, and CHPP, a specific PKC-α inhibitor, show differential effects on Caco-2 monolayer permeability to the paracellular marker [^{14}C]mannitol and TER. With NBS their was no significant effect on [^{14}C]mannitol permeability and TER (Figures 4.3, and 4.7). Whereas, with CHPP as would be expected there was a decrease in [^{14}C]mannitol permeability and an increase in TER (Figures 4.9 and 4.11). However, [^{14}C]PEG 4000 permeability actually increases with higher concentration of both inhibitors (Figures 4.4 and 4.10). This gives rise to contradictory evidence on the state of the Caco-2 tight junctions, with TER and [^{14}C]mannitol permeability returning to normal, indicating tight junctions, but the increased [^{14}C]PEG 4000 permeability possibly indicating toxic concentrations of the PKC inhibitors in Caco-2 monolayers. Although, this is not indicated by the cytotoxicity assays, LDH release and MTT transformation.

Lactate dehydrogenase and MTT are gross manifestations of cell death and not the more sensitive intracellular events alluded to by Kokoska *et al.* (1998) and Banan *et al.* (1998). Kokoska *et al.* (1998) exposed Caco-2 cells to ethanol which elicited a concentration-dependent increase in intracellular Ca^{2+} concentration. This effect was highly related to cellular injury measured by a fluorescent probe entering cells *via* damaged membranes to produce enhanced fluorescence. Further, Banan *et al.*, (1998) demonstrated Caco-2 exposure to ethanol concentrations, greater than or equal to 2.5 % (v/v), increases microtubule breakdown and, with this, a marked decrease in cellular viability as measured by trypan blue exclusion. Thus, it is likely that disruption of the plasma membrane by ethanol, could lead to alterations in calcium flux eventually giving rise to cytotoxic intracellular Ca^{2+} concentrations, leading to loosening of tight junctions and cellular death. This may be reversed by CHPP, but not by NBS. The result gained with NBS is in contrast with Rochat *et al.* (1993) who showed that ATP depletion due to oxidative stress or PKC activity was not responsible for the increase in mannitol permeability, as the increase was not inhibited by NBS. However, NBS inhibited the mannitol permeability that was caused by phorbol 12,13-dibutyrate, a phorbol ester that activates PKC.

4.5 CONCLUSION

On first inspection of CHPP and NBS physicochemical parameters, they would be expected to undergo absorption to a reasonable degree. The Caco-2/co-solvent model predicts that CHPP and NBS could be expected to be orally available by passive absorption. For NBS there is a dose-dependent increase of NBS permeability that is not inhibited by metabolic inhibitors and therefore passive transport is being limited by a non-specific passive mechanism. The Caco-2/co-solvent absorption model does not seem to predict the lack of *in vivo* absorption of the two PKC inhibitors. However, the lack of correlation may result from other inhibitory absorption mechanisms and possibly highlight further investigations into the potential development problems with the compounds. The Caco-2/co-solvent model demonstrates that PKC-α inhibitor, CHPP, may be involved in cytoprotection and permeability regulation of the tight junctions following exposure to 2.9 % (v/v) ethanol.

CHAPTER FIVE CACO-2 TRANSEPITHELIAL TRANSPORT OF HUMAN CALCITONIN

5.1 INTRODUCTION

For the purpose of this chapter, very small synthetic peptides *e.g.* di- and tri-peptide type compounds such as angiotensin-converting-enzyme inhibitors and renin inhibitors are excluded from the class of therapeutic compounds considered as peptides and proteins. These low molecular weight compounds that possess a peptide linkage do not present the same biopharmaceutical problems that are encountered with the larger molecules in this class.

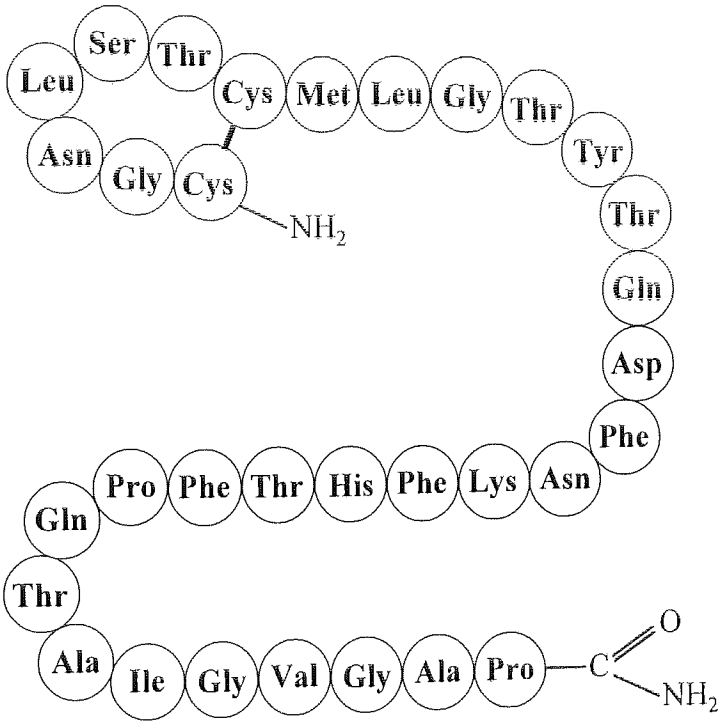

Figure 5.1 Amino acid primary structure of human calcitonin

5.1.1 HUMAN CALCITONIN (hCT)

Human calcitonin is a 32 amino acid polypeptide chain, molecular weight 3418 Da, with a 7-member disulphide ring at the N-terminus and an amidated proline C-terminus (Figure 5.1). In humans it is secreted from the parafollicular C-cells of the thyroid gland, producing a hypocalcaemic and hypophosphataemic effect in the body. This is achieved through the binding of hCT to its receptors; on osteoclasts, inhibiting their activity and subsequent calcium release from bone, and on the cells lining the proximal tubule

stimulating calcium renal excretion and possibly reducing calcium GI absorption (Plosker and McTavish, 1996). The clinical usefulness of calcitonin has focused on the treatment of bone disease with accelerated bone resorption that requires long-term therapy such as Paget's disease, hypercalcaemia and osteoporosis (Body, 1995).

5.1.2 OSTEOPOROSIS THERAPY

Osteoporosis is an exaggerated inbalance in the normal remodelling of bone. Where bone resorption by osteoclasts is greater than bone formation by osteoblasts (Figure 5.2).

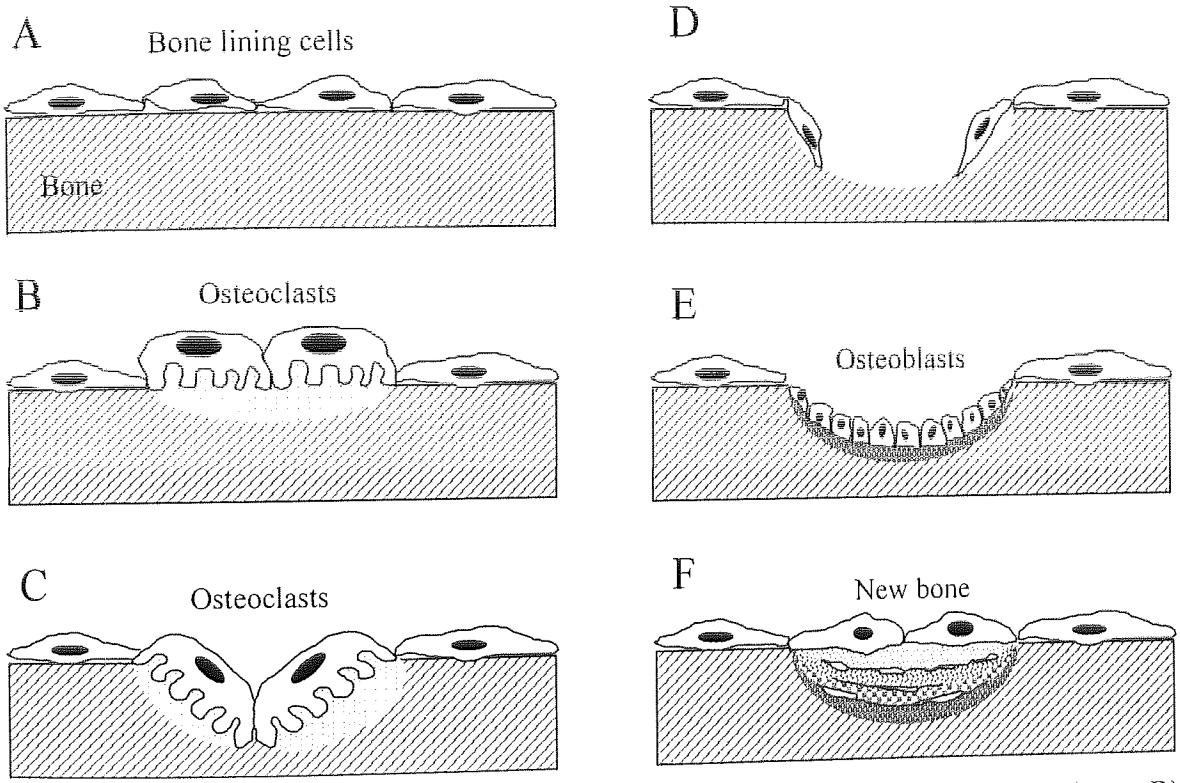

Figure 5.2 Sequence of events in normal bone remodelling. A) Normal quiescent bone; B) Osteoclasts attach themselves to bone and form the characteristic ruffled border: C) Osteoclasts proceed to dissolve the bone forming a depression or pit; D) Reversion, osteoclasts leave behind a pit where osteoblasts migrate into; E) The osteoblasts lay down new bone into the pit; F) The formation of new bone: in healthy young bone, all the bone is replaced, but in ageing, bone formation does not quite replace all the bone excavated.

Age related osteoporosis is found in both men and women. However, postmenopausal osteoporosis is becoming an increasingly significant syndrome with 1 in 4 women being affected over the age of 65. This bone loss is exaggerated in women with low peak bone mass and the rapid loss which occurs when oestrogen is withdrawn after the menopause.

The loss of bone occurs to the point at which fractures occur particularly in the spine, wrist and hip. This loss can be prevented by hormone replacement therapy (HRT) which also reduces the risk of heart disease. For women who cannot tolerate HRT or are contraindicated *e.g.* high risk for breast cancer, calcitonin is an obvious alternative therapeutic agent for the prevention and treatment of osteoporosis.

Plosker and McTavish (1996) have recently reviewed the effect of intranasal salmon calcitonin (sCT) administration in a large number of randomised studies. Intranasal sCT was administered for 1 to 5 years, usually 50 to 200 IU d^{-1}, plus oral calcium supplements to recently postmenopausal women for the prevention of osteoporosis. The bone mineral density or content of the lumbar spine increased by approximately 1 to 3 % from baseline, compared with reductions of about 3 to 6 % among women receiving oral calcium supplements only. Even with the improved compliance of intranasal sCT administration, an orally administered form would increase the clinical utility of calcitonin and improve patient compliance for chronic therapy.

5.1.3 CHRONIC ADMINISTRATION

For chronic delivery of peptides and proteins, a non-injectable delivery route would be preferred. Therefore, transmucosal routes such as the GI tract become the only alternative. However, the physical and chemical properties of all the calcitonins make them poor candidates for oral administration. Several molecular forms of calcitonin are marketed, hCT (Cibacalcine®) and sCT (Miacalcic®, Calsynar®) being the most often administered to humans. Salmon calcitonin is reported to be 40 to 50 times more potent than hCT and also lasts longer in the systemic circulation (Plosker and McTavish, 1996). This has been challenged recently by Cudd *et al.* (1995), who demonstrated that hCT has a tendency to aggregate and fibrillate whereas sCT does not. Their results show that when aggregation and fibrillation are avoided, both hCT and sCT are equipotent in the *in vitro* osteoclast resorption assay.

Although calcitonins have been proven to be safe (Wimalawansa, 1993) the parenteral route has limited acceptability. Subcutaneous or intramuscular injections sometimes give uncomfortable side effects, such as local irritation and systemic effects of flushing, nausea,

and epigastric cramps (Schipper *et al.*, 1995). With the introduction of intranasal sCT administration, compliance has been seen to improve (Plosker and McTavish, 1996). Although heterologous CTs give rise to the formation of antibodies, this occurs in some 50-70 % of patients treated with heterologous CT. The therapeutic relevance is still in debate (Tagliaro *et al.*, 1995; Grauer *et al.*, 1995) as absence of impairment of CT efficacy found in patients showing a specific immune response is surprising. It may explain the so-called CT escape phenomenon suggested by Takahashi *et al.* (1995). Where isolated osteoclasts, are induced by CT into immediate quiescence and gradual contraction of osteoclasts and inhibition of bone resorption. After 4-8 h, osteoclasts regain cytoplasmic motility and resumption of bone resorption. However, a more plausible explanation is the down regulation of osteoclast receptors to CT.

Administration of peptides and proteins as replacement or inhibition therapies requires chronic administration. Compliance decreases in patients undergoing daily injections required for chronic therapy, although, for life-threatening diseases like diabetes mellitus, the pain of frequent insulin injections is tolerated. For these reasons, researchers are trying to develop alternative formulations that overcome the barriers of oral administration (see section 1.3).

5.1.4 HUMAN CALCITONIN DEGRADATION

Peptides are susceptible to chemical and physical degradation and pre-systemic enzymatic degradation is still one of the major barriers to oral bioavailability of peptide and proteins. For hCT this means deamidation, oxidation, reduction of disulphide bridges and aggregation (Cholewinski *et al.*, 1996).

Tozaki *et al.* (1997) demonstrated that hCT degradation in rat caecal contents, a 33 % (w/v) suspension had a half-life of 2.5 min and this could be extended with the addition of aprotinin (3.2-fold) and Camostat (6.4-fold). Hastewell *et al.* (1995) demonstrated that this strategy might also work in humans with 16000 U aprotinin inhibiting hCT degradation in human faecal extracts and extending the half-life of 0.1 mg ml^{-1} hCT by 1.7-fold. With hCT, the predicted enzyme degradation sites are confirmed and do produce the expected fragments (except in congenital cases) (Lang *et al.*, 1996). For example, hCT in contact

with nasal mucosae shows that degradation is initiated by tryptic and chymotryptic endopeptidase activity which cuts in the mid section residues Phe^{16} to Phe^{19}. Salmon CT is less susceptible to degradation, with fewer recognised tryptic and chymotryptic sites and this is borne out by the results. Both Lang *et al.* (1996) and Camilleri *et al.* (1991) have reported that sCT was degraded to four fragments by trypsin. These data suggest that hCT has susceptibility to both trypsin and chymotrypsin whereas sCT is probably degraded by tryptic activity. This was confirmed by Dohi *et al.* (1993) who showed a slightly different pattern in nasal homogenates, although the predicted degradation fragments were observed. Oral delivery of hCT with numerous labile peptide bonds available for degradation in the GI tract presents a considerable challenge.

The enzymatic barrier of the GI tract and strategies to overcome it have been reviewed by Lee and Yamamoto (1990). In brief, three main strategies to overcome this barrier are outlined below with examples specifically related to hCT:-

a) chemical modification of the enzyme labile bonds. For example, acyl derivatives of hCT in homogenates of intestinal mucosae significantly prolonged hCT half-life by approximately 10.9-fold and 3.4-fold in small intestine and colon, respectively (Fujita *et al.*, 1996). Although the structures of small peptides may be modified rather easily to improve enzymatic stability and membrane permeability by passive diffusion or peptide transporter, modification of protein structure is often difficult to achieve without sacrificing certain activity. However, modification can be made if the modified and inactive protein can be reversibly and quantitatively converted back to its active form.

b) the addition of enzyme inhibitors to stop degradation which increases the amount of peptide available for transport (Tozaki *et al.*, 1997; Hastewell *et al.*, 1995; Ungell and Andreasson, 1990). The effect of proteolytic inhibitors are different in different regions of the GI tract. Many protease inhibitors have been tested with varying degrees of success (Lee and Yamamoto, 1990; Wang 1996) and are usually carried out on a case by case basis depending on the primary structure of the peptide or protein although folding will determine if labile bonds are accessible for hydrolysis.

c) encapsulation of the macromolecule which separates and therefore protects it from degradative enzymes until the particles reach their site of absorption, where the macromolecule is released (Damgè *et al.*, 1990, Eldridge *et al.*, 1990, Saffran *et al.*, 1990). This was investigated by Lowe and Temple (1994) for hCT. Using polyacrylamide nanoparticles loaded with hCT, they demonstrated decreased proteolytic degradation *in vitro*. *In vivo,* the plasma pharmacokinetic profiles were consistent with increased survival time of hCT in the intestine, with higher plasma concentrations of the peptide at the later time points. The nanocapsules enhanced hCT absorption but did not reach significance. Encapsulation of protein is a very important class of oral protein drug delivery systems, simply because of their ability to control the release of proteins at a particular site and protect effectively from enzymatic degradation (Wang, 1996). However, inconsistent and inefficient absorption of encapsulated protein as shown with hCT (Lowe and Temple, 1994) is partly due to particulate-related factors such as size, hydrophobicity, charge and polymeric composition.

5.1.5 HUMAN CALCITONIN ORAL DELIVERY

It has been shown that hCT crosses the GI epithelium of rat and man, entering the body intact and showing biological action (Hastewell *et al.*, 1992; Beglinger *et al.*, 1992). The absolute bioavailability of intracolonic administered hCT in the rat for doses 0.1, 1.0 and 5.0 mg kg^{-1} were 0.2 %, 0.9 % and 0.5 % respectively. However, this is even less in the small intestine; a 2 mg kg^{-1} dose had bioavailabilities of < 0.1 %. Baudys *et al.* (1996) confirmed these data when CT was formulated with either dodecyl maltoside or SDS. However, with their best formulation of Capmul/0.01 % (v/v) acetic acid, 9/1 administered to the colon they achieved a bioavailability of 4.6 %. This has been confirmed by Fujita *et al.* (1996) who, instead of measuring bioavailability, measured pharmacological availability of hCT following administration to the small and large intestine. They found the pharmacological availability after administration to the small and large intestine was, 0.29 ± 0.10 % and 0.79 ± 0.24 %, respectively.

Antonin *et al.* (1992) first demonstrated that hCT could be absorbed across the distal colon of man with bioavailabilities of up to 0.22 %. Three out of 8 volunteers showed no measurable plasma hCT levels, due to the failure of a micro-enema to clear the distal colon

of faecal material. The re-calculated bioavailability for the remaining 5 volunteers was 0.118 ± 0.028 %. Including the 3 non-responders, the bioavailability was 0.076 ± 0.026 %. Antonin *et al.* (1996) followed up their study of colonic hCT absorption by repeating the previous study in loop stoma patients. Direct dosing of hCT into the transverse colon achieved a C_{max} of 1242 ± 346 pg ml^{-1} and a bioavailability of 0.22 ± 0.06 %. Compared to the bioavailability of the responders in their previous study, the transverse colon is a better site than the descending colon, possibly due to the luminal contents being more fluid. Even though Beglinger *et al.* (1992) demonstrated hCT bioavailability ranging from 0.01 to 2.7 % in 6 volunteers, with bioavailabilities for 5 of the volunteers being 0.034 ± 0.015 % and only one volunteer reaching a bioavailability of 2.7 %. This has shown again that hCT absorption can occur from an unflushed descending colon.

The low availability of hCT, less than 1 %, is the same for most peptides and proteins delivered to the GI tract, due to extensive pre-systemic clearance and low intrinsic membrane permeability. In addition to the strategies to decrease the enzymatic barrier, (see section 5.1.4), there are numerous approaches to improve absorption of peptide and proteins in the literature (Swenson et al., 1994; Fix, 1996; Wang, 1996), some of these have been investigated for hCT. To improve hCT absorption, Hastewell *et al.*, (1995) increased the local concentration of hCT dosed to the descending colon, improving absorption compared to the 5 responders in the above study (Antonin *et al.*, 1992). The group also coadministered the high concentration dose with aprotinin, a protease inhibitor, but, unexpectedly, the bioavailabilities decreased to 0.11 ± 0.03 %. Their explanation was that high concentration of hCT with aprotinin caused precipitation of the hCT. They speculated that the hCT could have precipitated in the instrument and therefore delivered to the colon in an unabsorbable form, or the luminal contents could have had a similar effect. To enhance hCT absorption, Hastewell *et al.* (1994) used a mixed micelle system with 40 mM monoolein:sodium taurocholate which gave 11.8, 9.2, and 6.4-fold enhanced colonic absorption in rats of hCT, HRP and PEG 4000, respectively. With no acute toxicity seen at the light microscopy level. However, for assessment of therapeutic use the long term toxicity of absorption enhancers needs to be investigated.

5.1.6 PATHWAYS

The molecular weight-sensitive transport of peptides and proteins was postulated to occur paracellularly *via* the tight junctional pathway (McMartin, 1989). However, large hydrophilic, charged peptides and proteins do cross the epithelium, travelling either by a specific receptor-mediated endocytosis with saturable binding and transepithelial transport (Marcon-Genty *et al.*, 1989) or a non-specific diffusional pathway by either transcellular or paracellular pathway. The evidence of the molecular weight cut-off for transport of peptides and proteins suggests that the tight junctional paracellular pathway is involved. This is a continuous hydrophilic pathway suitable for peptides and proteins. The transcellular route has been demonstrated for di- and tri-peptides *via* carrier-mediated transport. Burton *et al.* (1991) have shown that peptides of up to 10 amino acid residues cross by the transcellular pathway through desolvation and intra- and inter-molecular hydrogen bonding. Proteins have been demonstrated to cross by receptor-mediated and fluid-phase vesicular transcytosis (section 1.2.1.3).

Hastewell *et al.* (1992) in their study of hCT delivery to rat colon demonstrated that transport was rapid and a significant amount was *via* the transcellular pathway as shown by intracellular immunohistochemical staining. In their follow up study to enhance hCT absorption and marker molecules, HRP a 40 kDa glycosylated protein and PEG 4000, a transcellular pathway for enhanced absorption, was again demonstrated by intracellular immunohistochemical localisation of HRP (Hastewell *et al.*, 1994). Only recently, hCT has been demonstrated to be associated with vesicles using fluorescently labelled hCT and measuring the intracellular fluorescence with confocal laser scanning microscopy (Lang *et al.*, 1998). They speculate that as much as 25 % of hCT transport is *via* this pathway and the rest by the paracellular pathway. Further evidence using trapped-labelled CT indicated that intact and degradation products are enclosed within membrane-bound vesicles of rat kidneys. With hCT moving from a cell membrane fraction at 2 min to a lysosomal fraction between 5 and 15 min. The kinetics of renal degradation of CT indicate that substantial amounts of endocytosed CT is degraded before the hormone reaches the lysosome (Hysing *et al.*, 1991).

The mechanism of hCT intestinal absorption is, as yet, unclear due to two pieces of evidence:-

a) demonstration of hCT associated with vesicles indicating that hCT transport can be *via* a transcytotic vesicular pathway.

b) the apparent molecular weight cut-off of approximately 1000 Da for absorption of macromolecules across the GI epithelium, indicating the paracellular pathway. In this chapter, using the Caco-2 absorption model, the pathways involved in hCT absorption will be investigated to determine the predominant pathway for intact hCT.

5.2 EXPERIMENTAL

5.2.1 CELL CULTURE

For all studies, 21 d Caco-2 monolayers grown on polycarbonate Transwell™ inserts, passage number 87-100, were used. They were cultured as described previously (see section 2.3.3).

5.2.2 PREPARATION OF HUMAN CALCITONIN FORMULATIONS

A stock solution of hCT was prepared in 0.01 % (v/v) acetic acid. This was diluted in transport buffer (TB) to give the desired concentration of hCT, plus the addition of transport markers or inhibitors when required. If an inhibitor stock solution was in either ethanol or DMSO then the concentration of solvent in the final dose was <0.1 % (v/v). The equimolar concentrations of monoolein and sodium taurocholate, in the mixed-micelle enhancer preparations, were added to TB and then vortex mixed followed by sonication in a sonicating water bath for 2 min. All dosage forms were clear.

5.2.3 TRANSPORT EXPERIMENTS

Human calcitonin in TB was applied to either the apical or basolateral chamber in the presence or absence of a 21 d Caco-2 monolayer. Both Ap-to-Bl and Bl-to-Ap transport kinetics were followed as described previously (see section 2.6.2.7). Caco-2 monolayer hCT degradation followed the protocol as described previously (see section 2.10). To determine hCT binding in the presence and absence of Caco-2 monolayers, the protocol described in section 2.9 was followed.

5.3 RESULTS

5.3.1 TRANSPORT OF HUMAN CALCITONIN ACROSS CACO-2 MONOLAYERS

The concentration-dependent transport of hCT across Caco-2 monolayers was determined using the hCT RIA. The Ap-to-Bl and Bl-to-Ap flux of hCT across 21 d Caco-2 monolayers shows no significant difference over the concentration range 0.1-5.0 mg hCT ml^{-1} suggesting a linear dose-dependency indicating that hCT is transported passively in both directions (Figure 5.3). The apparent permeability coefficient (P_{app}) for Ap-to-Bl and Bl-to-Ap hCT transepithelial transport at the various doses, 0.1 to 5.0 mg ml^{-1}, are shown in Table 5.1. The P_{app} of [^{125}I]hCT across blank filters is 16.3 ± 0.08 cm s^{-1} x 10^{-6} with 3.84± 0.26 % of the dose binding to the filter insert (see section 2.6.1).

5.3.2 THE EFFECT OF HUMAN CALCITONIN ON CACO-2 MONOLAYER INTEGRITY

The transepithelial flux of both [^{14}C]mannitol and [^{14}C]PEG 4000 together with TER measurements, were used to check Caco-2 monolayers integrity when exposed to hCT. Using [^{14}C]mannitol as a marker for the paracellular pathway, the effect of apical and basolateral hCT on Caco-2 monolayers was investigated. The comparison of Ap-to-Bl (2.97 ± 0.39 cm s^{-1} x 10^{-7}) and Bl-to-Ap (2.96 ± 0.76 cm s^{-1} x 10^{-7}) P_{app} showed no significant difference (Figure 5.4). The Ap-to-Bl transport of [^{14}C]mannitol was significantly increased with 1 mg ml^{-1} apical hCT the P_{app} was 6.23 ± 0.36 cm s^{-1} x 10^{-7}. Whereas, in the Bl-to-Ap direction, there was no significant difference in [^{14}C]mannitol P_{app} values with the addition of basolateral 0.1 and 1.0 mg ml^{-1} hCT (Figure 5.4).

To test if substrate load increased the flux of a non-absorbed marker, perhaps through solvent drag, the transepithelial transport of [^{14}C]PEG 4000 was measured across Caco-2 monolayers. Increasing hCT concentrations, 0.1 to 5.0 mg ml^{-1}, did not significantly effect the P_{app} of [^{14}C]PEG 4000, 1.5 ± 0.24 cm s^{-1} x 10^{-8} (P=0.53). Also, the addition of 0.1 or 1.0 mg ml^{-1} hCT to the apical chamber has no significant effect on TER (Figure 5.5).

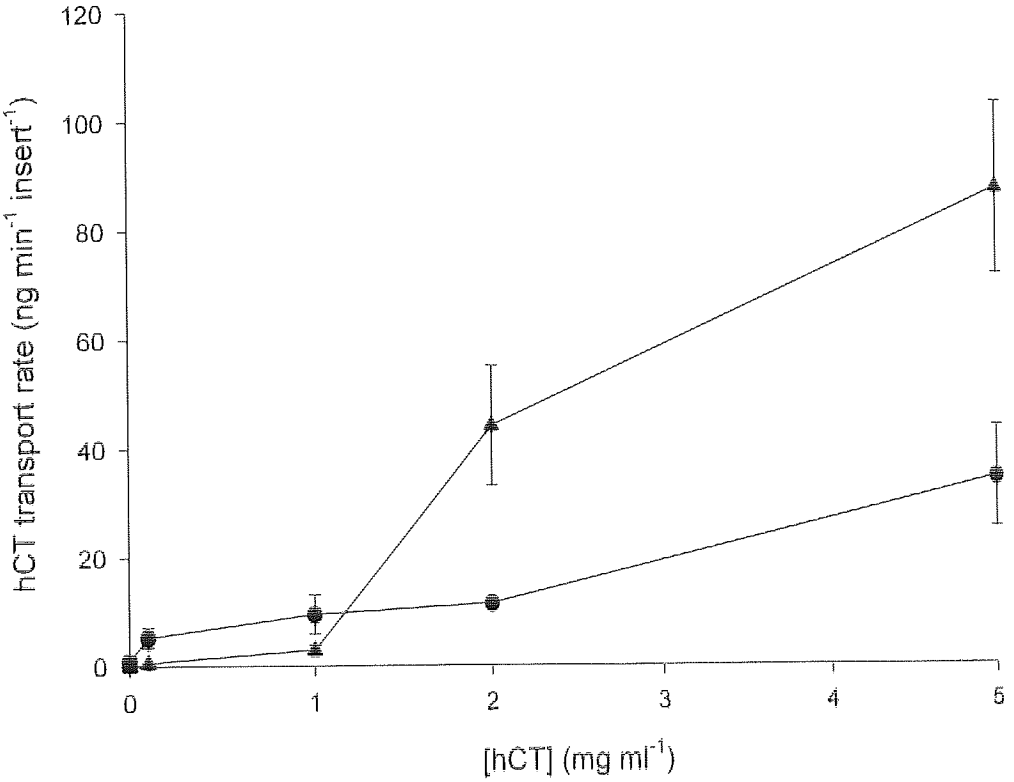

Figure 5.3 Concentration-dependent transport kinetics of human calcitonin. Monolayers were washed with TB for 15 min at 37°C before hCT was applied to either their Ap or Bl surface over a range of hCT concentration (0.1 mg ml^{-1} to 5 mg ml^{-1}). Transport kinetics were followed by sequential transfer of the inserts to fresh medium at 30, 60, 90, 120 and 180 min. The levels of hCT in TB were analysed by the hCT RIA. Ap-to-Bl ▲; Bl-toAp ●. Data are presented as mean values ± SEM (n=5).

Table 5.1 Apparent permeability coefficient (P_{app}) for human calcitonin apical to basolateral and basolateral to apical transport at various concentrations, 0.1 to 5.0 mg ml^{-1}. The levels of hCT in either the apical or basolateral medium were analysed by the hCT RIA. Data are presented as mean values ± SEM (n=5).

Dose ($mg\ ml^{-1}$)	**Ap-to-Bl P_{app}** ($cm\ s^{-1} \times 10^{-8}$)	**Bl-to-Ap P_{app}** ($cm\ s^{-1} \times 10^{-8}$)
0.1	2.09 ± 0.82	18.77 ± 6.60
1.0	1.05 ± 0.31	3.36 ± 1.27
2.0	7.87 ± 1.96	2.05 ± 0.18
5.0	6.41 ± 1.16	2.53 ± 0.68

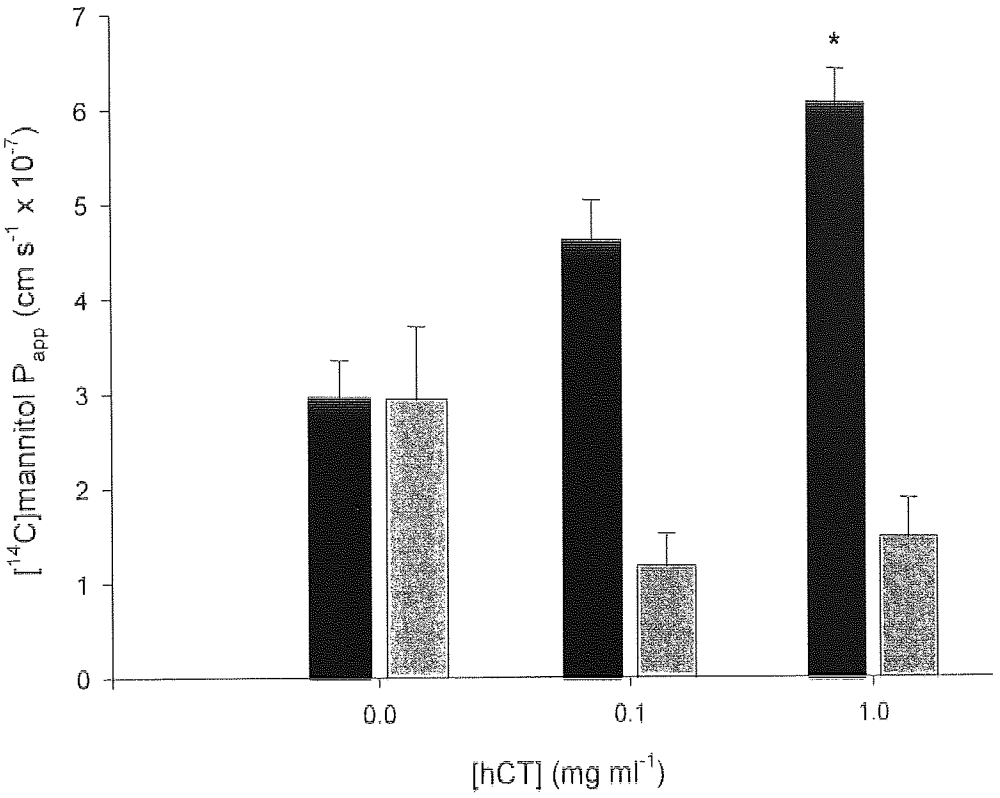

Figure 5.4 The effect of human calcitonin on [^{14}C]mannitol apparent permeability coefficient (P_{app}) across 21 d Caco-2 monolayers. Monolayers were washed with TB for 15 min at 37°C before [^{14}C]mannitol and hCT were applied to either their Ap or Bl surface. Transport kinetics were followed by sequential transfer of the inserts to fresh medium or replacement with fresh apical medium at 30, 60, 90, 120 and 180 min. Ap-to-Bl (black bar); Bl-to-Ap (grey bar). Data are presented as mean values ± SEM (n=6). * Denotes a significant difference from control values at $p<0.05$.

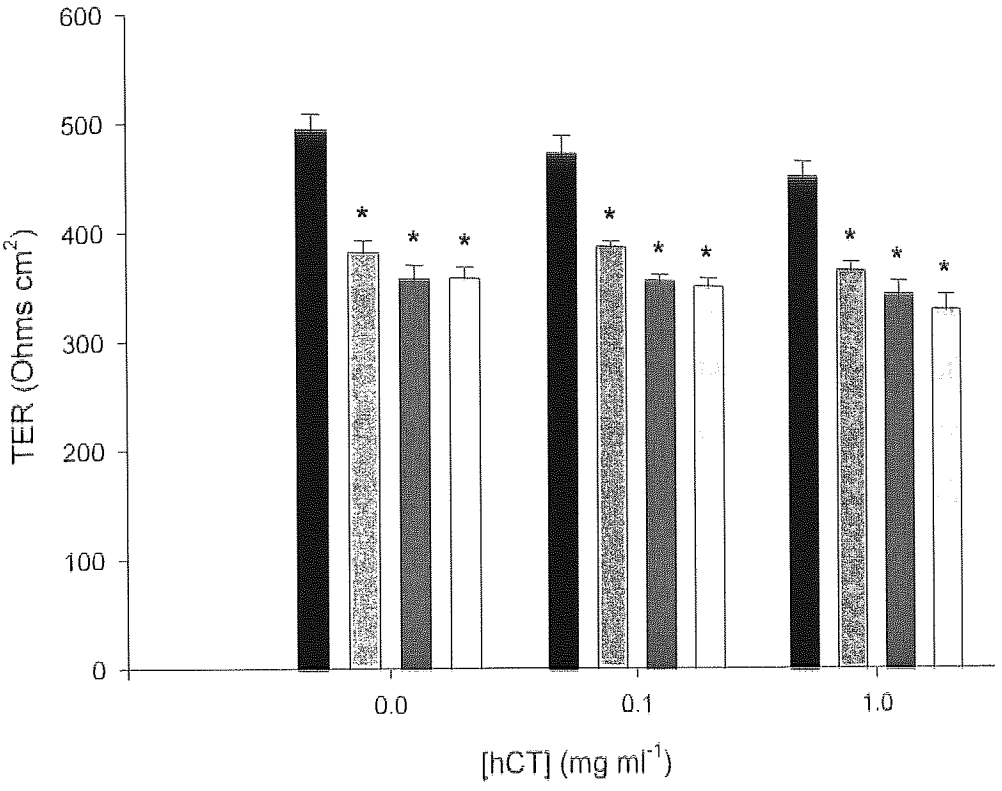

Figure 5.5 The effect of apical human calcitonin on transepithelial electrical resistance (TER) of 21 d Caco-2 monolayers. Monolayers were washed with TB for 15 min at 37°C before hCT was applied to the Ap surface. The TER of each monolayer was measured with an epithelial voltmeter using STX2 'chopstick' electrodes at the time points shown. TER at 0 min (black bar); 60 min (medium grey bar); 120 min (dark grey bar); 180 min (light grey bar). Data are presented as mean values ± SEM (n=6). * Denotes a significant difference from 0 min values at $p<0.05$.

5.3.3 INHIBITION OF HUMAN CALCITONIN TRANSPORT ACROSS CACO-2 MONOLAYERS

To investigate the mechanism of hCT transepithelial transport, further work was carried out at a hCT concentration of 0.1 mg ml^{-1}. The levels of hCT in Caco-2 cell homogenates and TB were analysed by the hCT IRMA (see section 2.2.7). The P_{app} for Ap-to-Bl hCT was calculated from the steady-state flux achieved after 30 min from the start of the experiment. The P_{app} for hCT in the Ap-to-Bl direction was 0.79 ± 0.07 cm s^{-1} x 10^{-8} with the percentage of the dose that underwent transepithelial transport in 180 min being 0.03 % ± 0.003 %. Transport in the Bl-to-Ap direction was 3-fold higher giving a P_{app} of 2.43 ± 0.29 cm s^{-1} x10^{-8} (0.12 ± 0.02 % of the dose transported) (Figure 5.6). The Bl-to-Ap uptake (4098.1 ± 62.5 pg $insert^{-1}$) also increased 3-fold over the Ap-to-Bl uptake (1299.6 ± 15.5 pg $insert^{-1}$) (Figure 5.7).

To see if active transport mechanisms were responsible for hCT transepithelial transport, the metabolic poison sodium azide and the non-metabolisable sugar substrate 2-deoxyglucose were used to inhibit energy production in the Caco-2 monolayer. Also, monensin, an inhibitor of receptor-mediated endocytosis (Brown *et al.*, 1983), and colchicine, a compound that inhibits microtubule assembly were used. The combination of 1 mM sodium azide and 50 mM 2-deoxyglucose or 500 μM colchicine increased hCT permeability across Caco-2 monolayers however they did not reach significance. Whereas, 50 μM monensin significantly increased hCT P_{app} 1.8-fold (Table 5.2). In all three cases this was due to an initial increase in the rate of hCT transport followed by a decrease in the rate of transport to control values (Figure 5.8). The only exception was that of 2 mM La^{3+}, which inhibited hCT P_{app} by 96.2 % ± 0.8 % to 0.03 ± 0.007 cm s^{-1} x 10^{-8}. (Table 5.2).

The hCT cell content following incubation with the potential transport inhibitors for 180 min, is shown in Figure 5.7. The addition of any of the inhibitors administered to the apical surface of Caco-2 monolayers made no significant difference on hCT uptake after 180 min. Suggesting that La^{3+} and the other inhibitors have no effect on uptake. However,

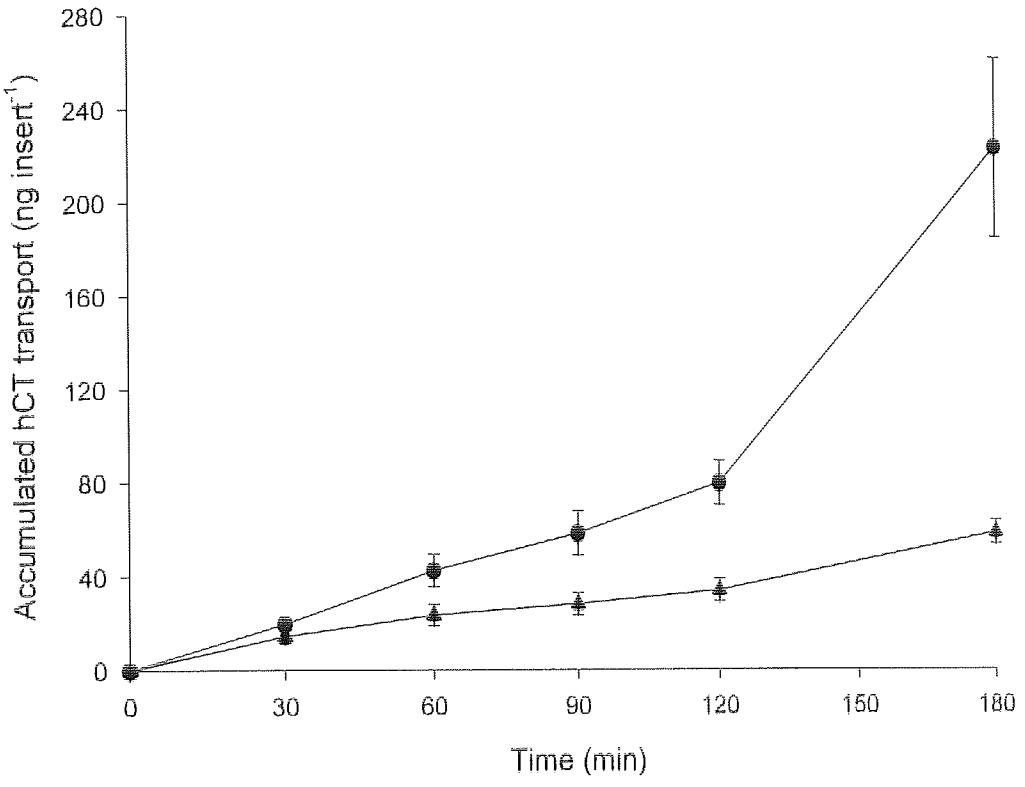

Figure 5.6 The polarity on 0.1 mg ml^{-1} human calcitonin transport across 21 d Caco-2 monolayers. Monolayers were washed with TB for 15 min at 37°C before hCT was applied to either the Ap or Bl surface. Transport kinetics were followed by sequential transfer of the inserts to fresh medium or replacement with fresh apical medium at the time points shown. The levels of hCT in TB were analysed by the hCT IRMA. Ap-to-Bl ▲; Bl-toAp ●. Data are presented as mean values ± SEM (n=3).

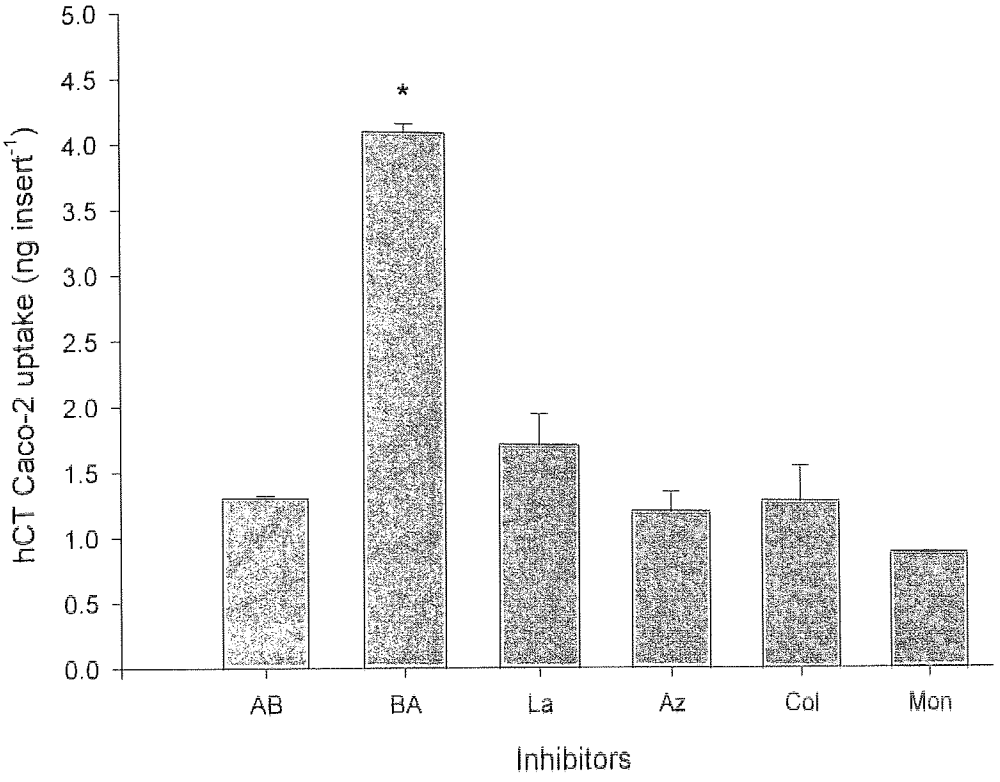

Figure 5.7 The effect of apically administered inhibitors on human calcitonin Caco-2 monolayer uptake after apical to basolateral transport of 0.1 mg ml^{-1} human calcitonin across 21 d Caco-2 monolayers. Monolayers were washed with TB for 15 min at 37°C before hCT was applied to either the Ap or Bl surface or inhibitor and hCT were applied to the Ap surface. Transport kinetics were followed by sequential transfer of the inserts to fresh medium or replacement with fresh apical medium at 30, 60, 90, 120 and 180 min. The inserts were washed 3 times with ice-cold PBS-N_3 before incubating with lysis buffer for 20 min at room temperature 20-22°C. The levels of hCT in Caco-2 cells were analysed by the hCT IRMA. Control, Ap-to-Bl (AB); Bl-to-Ap (BA); 2 mM apical La^{3+} (La); 1 mM Azide + 50 mM, 2-deoxyglucose (Az+2DG); 500 μM, Colchicine (Col); 50 μM, monensin (Mon). Data are presented as mean values ± SEM (n=3). * Denotes a significant difference from control values at $p<0.05$.

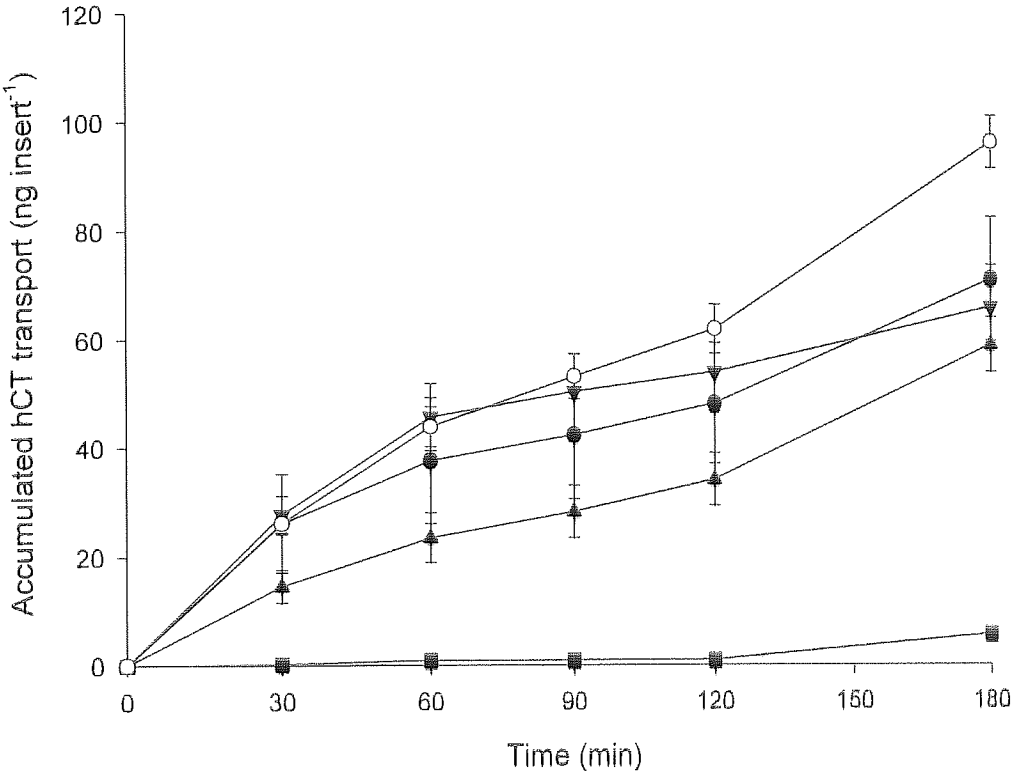

Figure 5.8 The effect of selected inhibitors on apical to basolateral transport of 0.1 mg ml^{-1} human calcitonin across 21 d Caco-2 monolayers. Monolayers were washed with TB for 15 min at 37°C before inhibitor and hCT were applied to the Ap surface. Transport kinetics were followed by sequential transfer of the inserts to fresh medium at the time points shown. The levels of hCT in TB were analysed by the hCT IRMA. Control, Ap-to-Bl (▲); 2 mM, apical La^{3+} (■); 1 mM Azide + 50 mM, 2-deoxyglucose (▼); 500 μM, Colchicine (●); 50 μM, monensin (○). Data are presented as mean values ± SEM (n=3).

Table 5.2 Apparent permeability coefficient (P_{app}) for apical to basolateral transport of 0.1 mg ml^{-1} human calcitonin with the addition of either inhibitors or enhancers to the apical chamber. The levels of hCT in TB were analysed by the hCT IRMA. Data are presented as mean values ± SEM (n=3). * Denotes a significant difference from control Ap-to-Bl values at $p<0.05$.

	Ap-to-Bl P_{app} ($cm\ s^{-1} \times 10^{-8}$)	**% control**
Control	0.79 ± 0.07	100.0
2 mM La^{3+}	0.03 ± 0.007*	3.8
1 mM Azide + 50 mM 2-deoxyglucose	1.07 ± 0.17	136.0
500 μM Colchicine	0.90 ± 0.10	114.6
50 μM Monensin	1.45 ± 0.12*	184.1
Control	0.53 ± 0.03	100
Aprotinin 1 mg ml^{-1}	1.63 ± 0.05*	310.3
Aprotinin 10 mg ml^{-1}	1.35 ± 0.07*	256.5
pH 5.5 Ap medium	0.96 ± 0.05*	182.8
20 mM mixed micelle	1.13 ± 0.03*	214.4
40 mM mixed micelle	0.66 ± 0.06	124.5

50 μM monensin increases Ap-to-Bl transport and 2 mM La^{3+} inhibits Ap-to-Bl transport of hCT across Caco-2 monolayers.

5.3.4 ENHANCEMENT OF HUMAN CALCITONIN TRANSPORT ACROSS CACO-2 MONOLAYERS

The transport of hCT across Caco-2 monolayers was increased 1.8-fold when the apical pH was reduced to pH 5.5. The P_{app} of the control for this experiment was 0.53 ± 0.03 cm s^{-1} x10^{-8} increasing to 0.96 ± 0.05 cm s^{-1} x 10^{-8} for pH 5.5. With a 1.5-fold increase in the amount transported, expressed as % dose over 180 min, 0.0125 % and 0.0183 % for control (Ap pH 7.2) and Ap pH 5.5, respectively (Table 5.2).

Aprotinin is a serine protease inhibitor that has been used to inhibit degradation and therefore to increase transport of various proteins (Ungell and Andreasson, 1990; Yamamoto *et al.*, 1994; Bai and Chang, 1996). It was chosen as a possible enhancer of hCT transport. Also chosen for investigation was the mixed-micelles enhancer system shown to be effective *in vivo* (Hastewell *et al.*, 1994). Two concentrations of aprotinin were investigated 1.0 and 10 mg ml^{-1} in the apical media (Table 5.2).

The Ap-to-Bl transport of hCT, with 1 mg ml^{-1} apical aprotinin, revealed a P_{app} of 1.63 ± 0.05 cm s^{-1} x 10^{-8}, a 3.1-fold increase above control levels. At 10 mg ml^{-1} aprotinin hCT P_{app} was again increased but only 2.6-fold to 1.35 ± 0.07 cm s^{-1} x10^{-8}. The mixed-micelle system of equimolar concentrations (20 mM or 40 mM) of sodium taurocholate and monoolein was less effective in enhancing Ap-to-Bl transport of hCT. The 20 mM mixed-micelles increased the rate of transport by 2.1-fold to a P_{app} of 1.13 ± 0.03 cm s^{-1} x10^{-8}, whereas, the 40 mM mixed-micelles did not significantly increase the rate of Ap-to-Bl hCT transport above that of control levels (Table 5.2). The hCT Caco-2 cell uptake following this transport experiment, was not significantly different from the control values (P=0.052).

5.3.5 DEGRADATION OF HUMAN CALCITONIN

5.3.5.1 TIME COURSE OF HUMAN CALCITONIN DEGRADATION

A time-course of the apical degradation of hCT by Caco-2 monolayers was investigated. At 2, 5, and 10 min, the amount of degraded hCT was 45.9 % ± 8.9 %, 61.3 % ± 14.4 %,

and 62.0 % ± 13.5 % respectively of the dose, 200 μg hCT per insert at 0 min. This was further reduced after 60 min to only 37.4 % ± 4.3 % of the dose. Whereas, hCT in contact with the basolateral surface lost approximately 80 % of the dose, 300 μg hCT per insert at 0 min *i.e.* 20 % of the dose remained, after 60 min (Figure 5.9).

The kinetics of hCT uptake into Caco-2 monolayers from either the Ap and Bl surfaces are shown in Figure 5.10. The uptake from the basolateral surface is saturated after 2 min, the earliest time point. Whereas the uptake from the apical surface indicates an increased level at 5 min, which did not reach significance, and thereafter a constant cell content of around 700 pg insert^{-1} is maintained.

5.3.5.2 INHIBITION OF APICAL HUMAN CALCITONIN DEGRADATION

Four protease inhibitors and the 40 mM mixed-micelle enhancer formulation were tested for their effect on the degradation of 0.1 mg ml^{-1} hCT. The protease inhibitors were incubated with hCT on the apical surface of Caco-2 monolayers for 10 min. After 10 min the control without inhibitor had lost 46.7 % ± 0.3 % of the dose (Figure 5.11). This was in agreement with the previous result from the time-course study (see section 5.3.5.1). None of the protease inhibitors significantly inhibited the degradation of 0.1 mg ml^{-1} hCT. In contrast, the 40 mM mixed micelle system increased hCT degradation when in contact with the Caco-2 monolayer, however, it did not reach significance (P=0.062) (Figure 5.11).

The hCT content of control Caco-2 monolayers after 10 min exposure to 0.1 mg ml^{-1} was 416.05 ± 201.8 pg insert^{-1}, again consistent with the previous time course experiment (see section 5.3.5.1). Only chymostatin and the mixed-micelle system significantly increased hCT cell uptake, whereas, the other inhibitors, aprotinin, leupeptin, antipain did not reach significance (Figure 5.12).

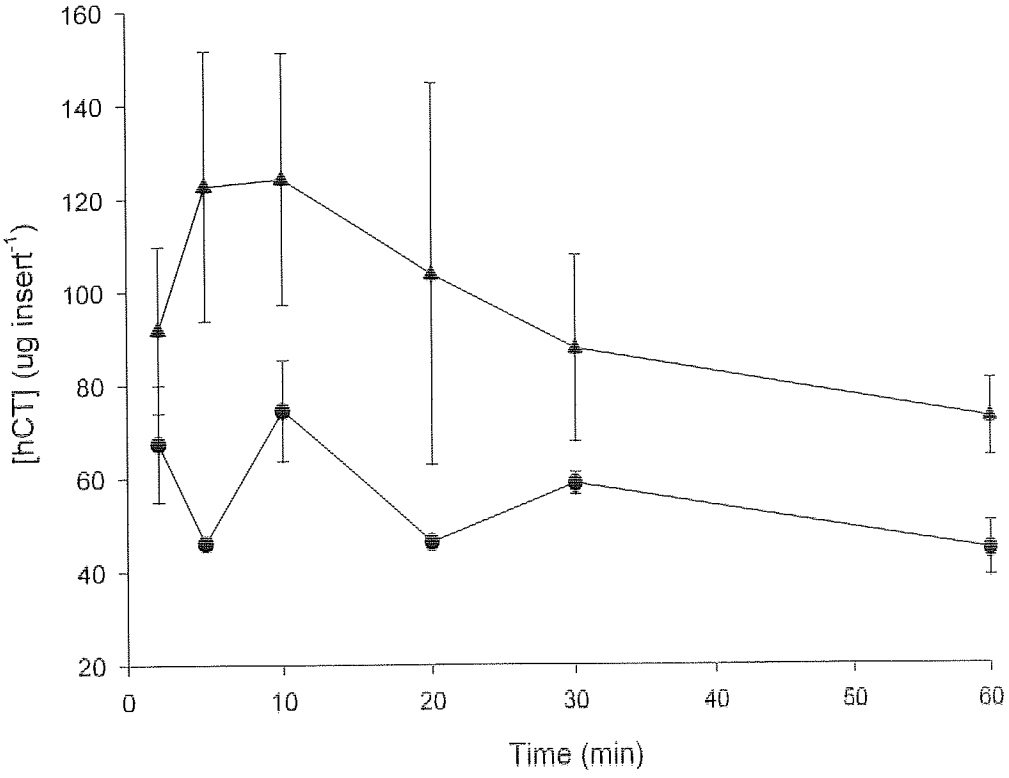

Figure 5.9 Donor chamber degradation kinetics of 0.1 mg ml^{-1} human calcitonin in contact with 21 d Caco-2 monolayers. Monolayers were washed with TB for 15 min at 37°C before 0.1 mg ml^{-1} hCT in TB was applied to either the Ap (2 ml) or Bl (3 ml) surface. Degradation kinetics were followed by removal of the insert into an empty cluster plate and the apical or basolateral TB removed at the time points shown. The levels of hCT in TB were analysed by the hCT IRMA. Apical ▲; Basolateral ●. Data are presented as mean values ± SEM (n=3).

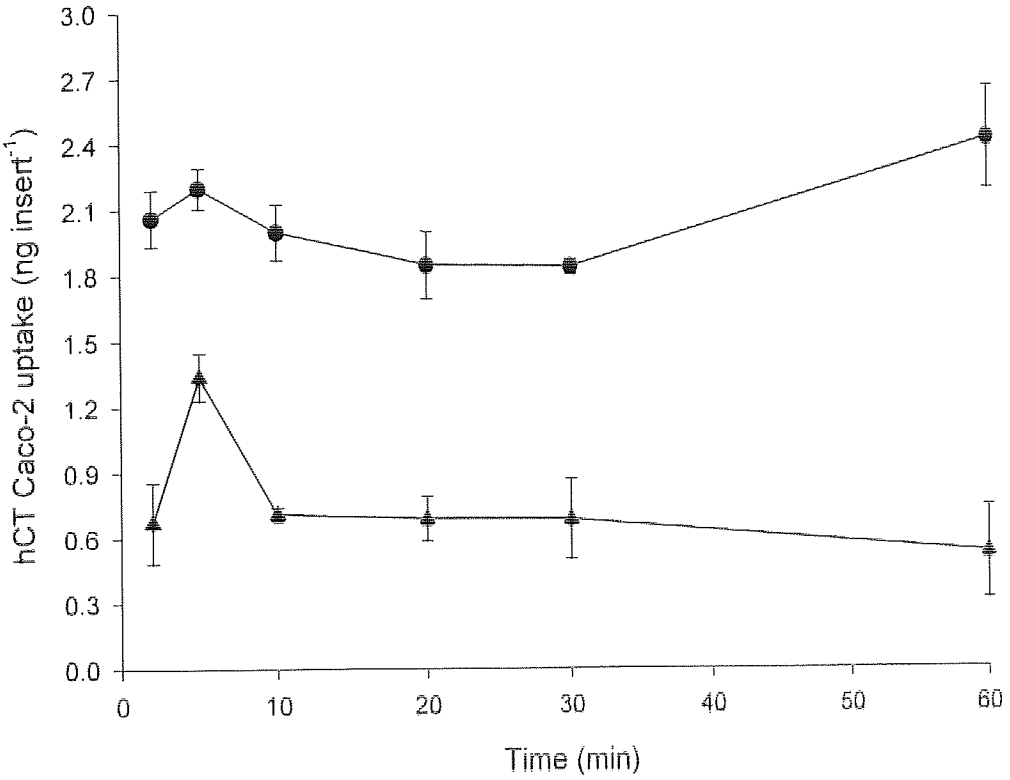

Figure 5.10 Caco-2 uptake kinetics of human calcitonin after administration of 0.1 mg ml^{-1} human calcitonin to either the apical or basolateral chamber. Monolayers were washed with TB for 15 min at 37°C before 0.1 mg ml^{-1} hCT in TB was applied to either the Ap (2 ml) or Bl (3 ml) surface. Uptake kinetics were followed by removal of the insert into an empty cluster plate and the apical TB removed at the time points shown. The inserts were washed 3 times with ice-cold PBS-N_3 before incubating with lysis buffer for 20 min at room temperature 20-22°C. The levels of hCT in monolayer homogenates were analysed by the hCT IRMA. Apical ▲; Basolateral ●. Data are presented as mean values ± SEM (n=3).

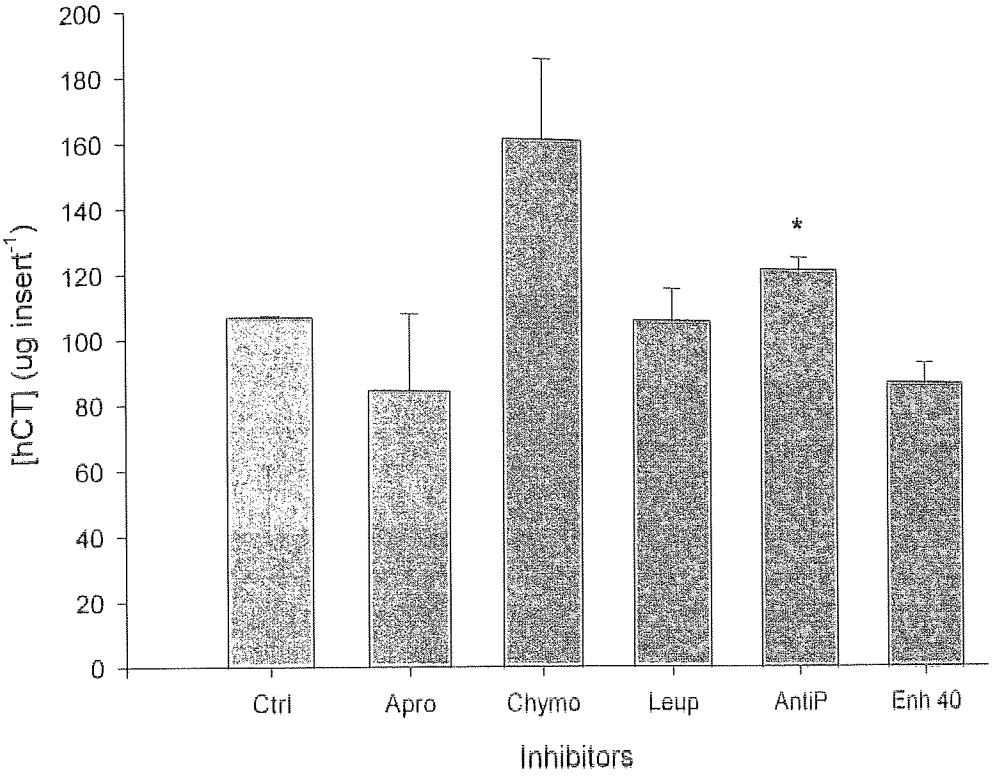

Figure 5.11 The effect of selected inhibitors on apical degradation of 0.1 mg ml^{-1} human calcitonin in contact with 21 d Caco-2 monolayers. Monolayers were washed with TB for 15 min at 37°C before inhibitor and hCT were applied to the Ap surface. The inhibition of degradation was followed by removal of the insert at 10 min into an empty cluster plate and the apical medium removed. The levels of hCT in the apical medium were analysed by the hCT IRMA. Control (Ctrl); 10 mg ml^{-1} aprotinin (Apro); 1 mg ml^{-1} chymostatin (Chymo); 3.6 mg ml^{-1} leupeptin (Leup); 3.6 mg ml^{-1} antipain (Antip); and 40 mM mixed micelle enhancer (Enh 40). Data are presented as mean values ± SEM (n=3). * Denotes a significant difference from control values at $p<0.05$.

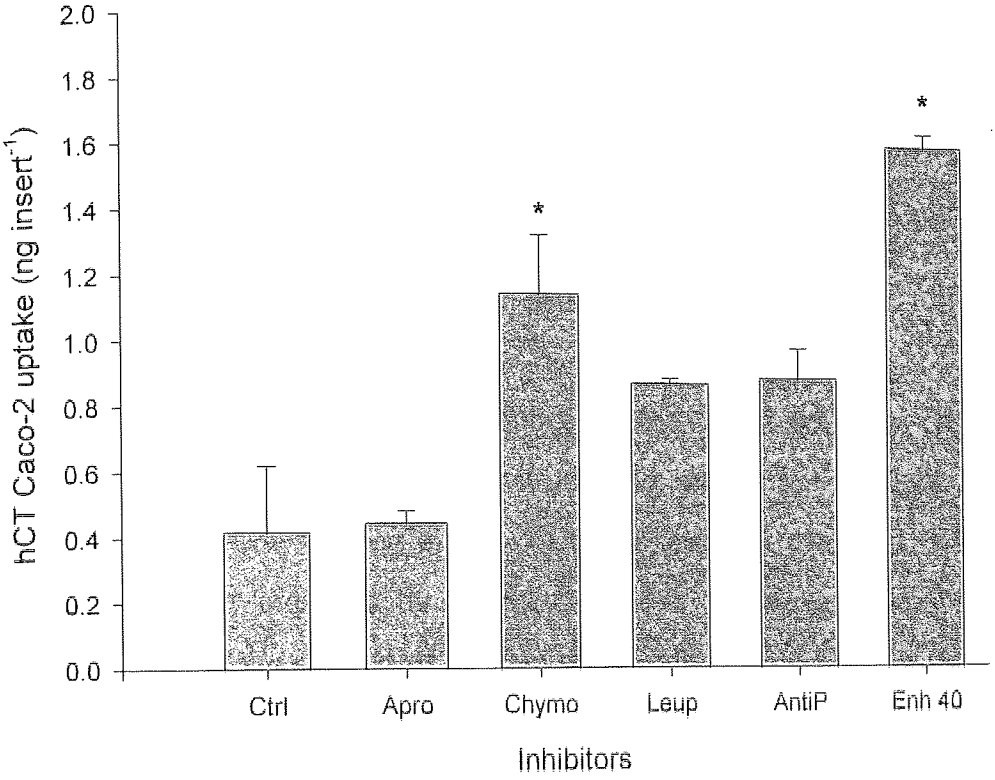

Figure 5.12 The effect of selected inhibitors on human calcitonin Caco-2 uptake after 10 min contact with apical 0.1 mg ml^{-1} human calcitonin and inhibitors. Monolayers were washed with TB for 15 min at 37°C before inhibitors and hCT in TB were applied to the Ap surface. Following a 10 min incubation at 37°C in air cell content was measured by removal of the insert into an empty cluster plate and the apical TB removed. The inserts were washed 3 time with ice-cold PBS-N_3 before incubating with lysis buffer for 20 min at room temperature 20-22°C. The levels of hCT in monolayer homogenates were analysed by the hCT IRMA. Control (Ctrl); 10 mg ml^{-1} aprotinin (Apro); 1 mg ml^{-1} chymostatin (Chymo); 3.6 mg ml^{-1} leupeptin (Leup); 3.6 mg ml^{-1} antipain (AntiP); and 40 mM mixed micelle enhancer (Enh 40). Data are presented as mean values ± SEM (n=3). * Denotes a significant difference from control values at $p<0.05$.

To see if the inhibitors had an effect on transport, the basolateral medium was also analysed for hCT. The control inserts transport 5646.9 ± 293.6 pg insert^{-1} in 10 min; again this is in keeping with the time course experiment. As can be seen in Figure 5.13, only the 40 mM mixed-micelle system significantly improved the transepithelial transport of hCT to 11823.1 ± 489.3 pg insert^{-1} in 10 min.

5.4 DISCUSSION

Although the oral route would give the best patient compliance, the chronic administration of hCT in the treatment of, for example, postmenopausal osteoporosis is limited by its oral bioavailability in man which is <1 % (Antonin *et al.*, 1992; Beglinger *et al.*, 1992; Antonin *et al.*, 1996). Evidence so far indicates that hCT absorption is a mixture of transcellular and paracellular pathways (Lang *et al.*, 1998; Hastewell *et al.*, 1994). The 25 % transcellular transport indicated by Lang *et al.* (1998) to be vesicular in nature and therefore transcytosed *via* either RME or fluid-phase endocytosis is probable. In this work, the transepithelial pathway of hCT absorption across Caco-2 monolayers has been investigated.

5.4.1 HUMAN CALCITONIN EFFECT ON CACO-2 MONOLAYERS

The transport of hCT across Caco-2 monolayers occurred in the absence of any changes in TER indicating no change in paracellular permeability or monolayer integrity. However, monolayer integrity as measured by Ap-to-Bl or Bl-to-Ap [^{14}C]mannitol permeability did not confirm this (Figure 5.4). Apical application of 1.0 mg ml^{-1} hCT had a significant effect on [^{14}C]mannitol permeability, with a significant increase in [^{14}C]mannitol flux. The hypothesis of Pappenheimer and Reiss (1987) who suggested that increased nutrient absorption, in this case amino acids from the hydrolysis of hCT, brings about increased solvent drag across the tight junctions which may explain the increased mannitol permeability *via* the tight-junctions. This does not explain the unchanged PEG 4000 permeability, indicating either size restricts its passage through the paracellular pathway or there is little effect of solvent drag on the possible transcellular pathway of PEG 4000. This could be comfirmed by mesauring Caco-2 monolayer elelctrophysiological parameters, in particular short-circuit current. Another possibility is that hCT with its

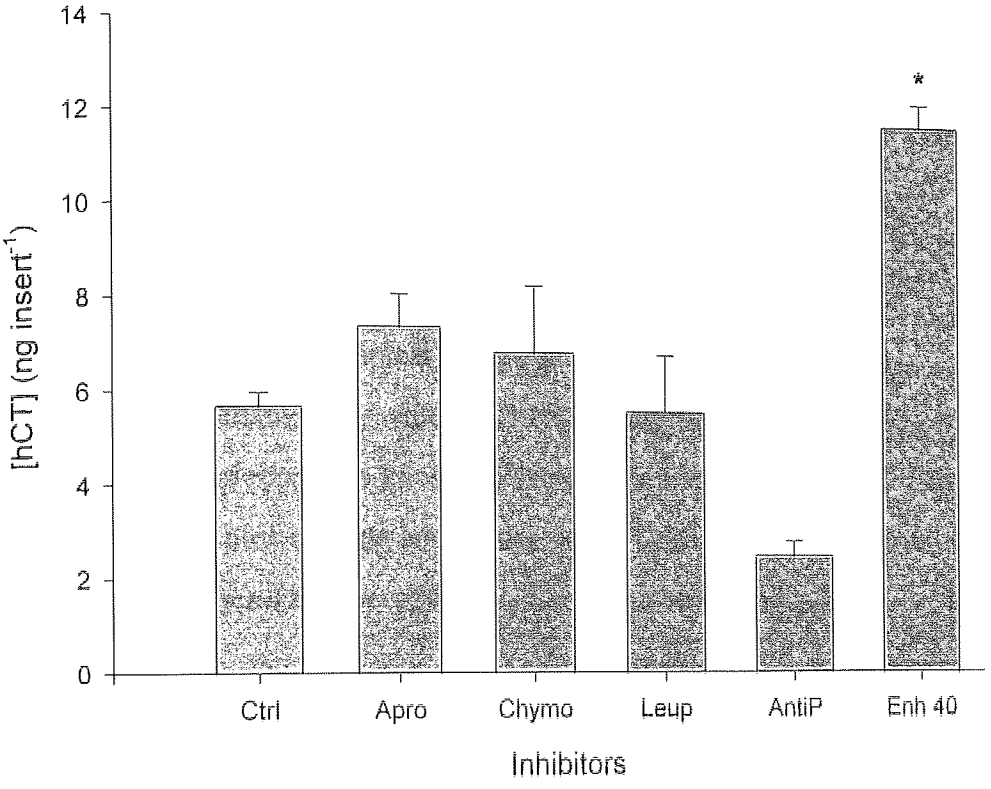

Figure 5.13 The effect of selected inhibitors on apical to basolateral transport of 0.1 mg ml^{-1} human calcitonin across 21 d Caco-2 monolayers. Monolayers were washed with TB for 15 min at 37°C before inhibitor and hCT were applied to the Ap surface. Transport was measured after 10 min by removal of the insert into an empty cluster plate and the basolateral medium collected. The levels of hCT in the basolateral medium was analysed by the hCT IRMA. Control (Ctrl); 10 mg ml^{-1} aprotinin (Apro); 1 mg ml^{-1} chymostatin (Chymo); 3.6 mg ml^{-1} leupeptin (Leup); 3.6 mg ml^{-1} antipain (AntiP); and 40 mM mixed micelle enhancer (Enh 40). Data are presented as mean values ± SEM (n=3). * Denotes a significant difference from control values at $p<0.05$.

partial amphiphilic α-helix structure which causes it to fibrillate may cause a similar action in Caco-2 tight junction disrupting their integrity.

Apical hCT had no effect on the transepithelial permeability of [^{14}C]PEG 4000 (Figure 5.5), a molecule of similar size to hCT. However, because of its M_r and linear configuration it is thought to travel *via* the paracellular pathway. But Iqbal *et al.* (1993) have shown that PEG permeates across a lipid barrier suggesting that 13.4 μM PEG 4000 administered to Caco-2 monolayers may permeate *via* the transcellular pathway. No specific-binding of hCT to the apical surface of Caco-2 monolayers was demonstrated (see section 2.9). The mechanism by which hCT causes the changes in mannitol permeability is unknown. Human calcitonin is known to increase in intracellular cAMP and Ca^{2+} when hCT binds to its receptor in bone and kidney cells (Wada *et al.*, 1996; Muff *et al.*, 1994). However, in this study no hCT receptors were reported on Caco-2 cells.

5.4.2 HUMAN CALCITONIN ACROSS CACO-2 MONOLAYERS

Data show that hCT is transported across Caco-2 monolayers (Figures 5.3 and 5.7). The transport of hCT was found not to be saturable with increasing concentrations of either apical or basolateral hCT and therefore is indicative of a passive mechanism. Bl-to-Ap hCT transport was 3-fold above Ap-to-Bl hCT transport (see section 5.3.3). This agrees with studies on cow milk protein uptake in rat jejunum (Stern and Walker, 1984), and with transport of intact HRP in Caco-2 monolayers, which was saturable and energy-dependent. (Heyman *et al.*, 1990).

Human calcitonin applied to the apical chamber at 0.1 mg ml^{-1} has an Ap-to-Bl P_{app} of $0.787 \pm 0.074 \times 10^{-8}$ cm s^{-1}; this is similar to PEG 4000, and compares with that of mannitol, a paracellular marker. This suggests that hCT is passively absorbed. To establish whether the transepithelial flux of hCT across Caco-2 epithelia was transcellular rather than paracellular, the monolayers were subjected to transcellular transport inhibitors. The metabolic inhibitors azide with 2-deoxyglucose and colchicine a microtubule-assembly inhibitor did not significantly effect hCT transport across Caco-2 monolayers. Whereas, monensin, a RME inhibitor, significantly increased hCT transport (Figure 5.8 and Table 5.2). These findings are unexpected as other authors have reported macromolecular

transport to be decreased in response to metabolic inhibition (Walker *at al.*, 1972). Metabolic inhibition has previously been shown to decrease uptake of both intact HRP and β-lactoglobulin (Heyman *et al.*, 1982; Marcon-Genty *et al.*, 1989).

Therefore the mechanism of hCT transport across Caco-2 monolayers is not through an energy requiring process as observed above. However, hCT could still be transported through either the paracellular pathway or *via* intra-membrane transport. With the addition of La^{3+}, hCT transport was reduced by 96.2 %± 0.8 % (Figure 5.8). This is unlikely to be totally paracellular pathway inhibition, as the addition of La^{3+} inhibited HRP transport across Caco-2 monolayers by 98.0 % ± 11.7 % indicating a possible vesicular pathway. This may well be the case, however, the reduction could be due to La^{3+} interacting with charged polar head groups of phospholipids in the plasma membrane stabilizing the plasma membrane and making it less fluid for transport and reducing vesicular membrane recycling. However, this may not effect hCT interactions with the cell membrane as indicated by the lack of an effect on hCT cell uptake in the presence of 2 mM La^{3+} (Figure 5.7). Also, these findings may reflect the lack of complete inhibition provided by these treatments or, alternatively, may indicate the involvement of another mechanism for the uptake of macromolecular molecules.

5.4.3 DEGRADATION OF HUMAN CALCITONIN

The enterocyte brush-border contains many hydrolases to degrade peptides (section 1.3.1). Also, enterocytes continually form endocytotic vesicles at the microvillus base, and proteins are taken up in both membrane-bound and soluble fractions. It has been postulated that, after internalisation, the endocytotic vesicles fuse with lysosomal vesicles and the majority of proteins are degraded, but a fraction of protein escapes and is transported intact. This may be due to incomplete breakdown of the protein after lysosomal fusion or a set of vesicles do not fuse with the lysosomal system and are transcytosed.

Bile salts inhibit brush border membrane and cytosolic proteolytic hydrolysis, and therefore may be useful for reducing intestinal degradation of peptide drugs. Although bile salts have stronger inhibitory effects on soluble rather than membrane-bound activity (Bai, 1994c).

The cytosolic proteosome which has multicatalytic chymotrypsin-like, trypsin-like and cucumsin-like activities are strongly inhibited by leupeptin, chymostatin and aprotinin (Bai and Chang 1995). The significance of lysomomal peptidases or the proteosome in limiting the absorption of hCT is unknown, since it is unclear whether hCT enters the lysosomes or the cytosol during transport through enterocytes.

In this study, Caco-2 monolayers have shown they are capable of degrading hCT, this is in keeping with other studies using different therapeutic proteins. From the studies carried out with apical hCT administration, 50 % degradation occurs within 2 min and 63 % at 60 min (Figure 5.11). The fast initial phase is in keeping with reports of the very fast degradation *in vivo*, whereas the slower phase may be a problem of increasing the unstirred water layer as hCT is degraded into smaller peptides. Basolateral degradation, surprisingly, is half as much again with over 80 % of the initial dose missing. This may well be due to the increased transport and cell degradation of hCT *via* the basolateral surface. Efforts to minimise binding to the plastic cluster-plate and filter were aided by the addition of 0.1 % (w/v) BSA to solubilise hCT.

The difference in cellular kinetics following apical or basolateral application of hCT is in keeping with the increased transport in the Bl-to-Ap direction. Caco-2 monolayer uptake following basolateral administration of hCT reaches a steady-state within 2 min, the first time-point. The levels of hCT Caco-2 cell uptake are approximately 3-fold higher than levels following apical administration. Also, apical administration of hCT may give rise to a peak at 5 min which fall to steady-state levels of approximately 700 pg insert^{-1} (Figure 5.12).

The effect of various protease inhibitors on hCT degradation and transport by Caco-2 monolayers was investigated. None of the protease inhibitors significantly inhibited apical degradation of hCT. The 40 mM mixed-micelle system significantly increased apical degradation. This may possibly be due to the displacement of hCT from BSA and dispersion of hCT fibrils. These data are surprising, considering the amount of hCT degradation carried out by the brush-border of the Caco-2 monolayers. Inhibition of the brush-border endopeptidases by aprotinin, and chymostatin has been successful in Caco-2

monolayers with other proteins that display tryptic and chymotryptic sensitivity (Bai and Chang 1995). The use of a lysosomal peptidase inhibitor leupeptin suggests that serine and thiol brush-border peptidases do not figure in apical degradation. With antipain a microbial cysteine peptidase inhibitor, which also has anti-trypsin activity, shows no significant inhibition of apical hCT degradation (Figure 5.13).

All the inhibitors except aprotinin increase the hCT Caco-2 cell uptake although chymostatin, leupeptin and antipain do not reach significance (Figure 5.14). This increased hCT cell content does not follow through with increased transepithelial transport of hCT. Only the 40 mM mixed micelle system significantly produced increased absorption of hCT across Caco-2 monolayers, with antipain significantly reducing the absorption of hCT (Figure 5.15). This indicates that although the inhibitors increase uptake of hCT into Caco-2 monolayers they do not necessarily increase transport across Caco-2 monolayers, because of it.

5.4.4 ENHANCEMENT OF HUMAN CALCITONIN TRANSPORT

The transepithelial transport of hCT was shown to be increased in the presence of 1 and 10 mg ml^{-1} aprotinin (Table 5.2). The mixed micelle enhancer system was also tried, at the lower concentration of 20 mM which significantly increased the absorption of hCT compared to the control, whereas the 40 mM mixed micelle system did not (Table 5.2). This is unexpected as the 40 mM mixed micelle system increased hCT transport in the degradation study over 10 min. The difference between the two experiments is the length of time the cells were exposed to hCT, 10 min and 180 min. Also, in the transport experiment, the 40 mM mixed micelle system did not increase transport, whereas the 20 mM mixed micelle system gave a 2.1-fold increase. The enhancement by mixed-micelle system of hCT absorption across Caco-2 monolayers is in agreement with Hastewell *et al.* (1994 and 1995). The effect of a more acidic pH on hCT absorption across Caco-2 monolayers may be due to more than one mechanism of action. The lowered pH is sub-optimal for brush-border proteases and therefore will lower their activity. This will increase the amount of hCT available for transport. Also, the lower apical pH may inhibit the tendancy hCT has to aggregate and fibrillate (Cudd *et al.*, 1995) again increasing the amount available for transport.

5.5 CONCLUSION

The results obtained in this study of the interaction of hCT with Caco-2 monolayers support the conclusion that a passive mechanism is involved in hCT transport. The metabolic or vesicular inhibitors (*i.e.* sodium azide with 2-deoxyglucose, colchicine and monensin) showed no effect on hCT transport. In contrast, La^{3+}, the passive transepithelial inhibitor, reduced hCT transport to approximately 10 % of total hCT transport. The degradation and enhancement studies indicate that hCT is also transcellularly transported, with protease inhibitors increasing hCT uptake although not transport. The mixed micelle system, increases hCT degradation, uptake and transport indicating it has a positive effect on hCT availability.

These results suggest that hCT movement across the intestinal cell line Caco-2's occurs *via* passive transcellular processes with increased availability of hCT and access to the plasma membrane having a significant effect on hCT transport.

CHAPTER SIX GENERAL DISCUSSION

6.1 La^{3+} AS A TOOL

The hypothesis that La^{3+} ions inhibit the paracellular pathway has been established in Caco-2 monolayers. This agrees with Sostman and Simon (1991) and Bryant and Moore (1995) who used La^{3+} as a tight-junction blocking agent. Qualitatively similar effects were observed by Machen *et al.* (1972) with decreased ion flow and increased epithelial resistance after mucosal administration of La^{3+} to rabbit ileum. The main effects of apical application of La^{3+} to Caco-2 monolayers were: a dose-dependent inhibition of D-mannitol with 63.0 % ± 1.37 % inhibition of D-mannitol permeability with 2 mM La^{3+} and a 1.5-fold increase in TER. These dominant effects are proposed to reflect the inhibition of the paracellular pathway.

The paracellular pathway inhibition was not repeated with other selected cations. The majority of those investigated either had no effect, or increased mannitol permeability (Table 3.3). However, Zn^{2+} did inhibit mannitol permeability but by only 20 %. This has been shown to be inhibition of nutrient transporters and explains the low inhibition of mannitol (Lugea *et al.*, 1995; Rodriguez-Yoldi *et al.*, 1996). Also, the fact that La^{3+} does not totally inhibit mannitol permeability across Caco-2 monolayers implies that mannitol has a substantial transcellular transport component. The effect of various Ca^{2+} channel inhibitors and the Ca^{2+} ionophore A23178 were used to elucidate if La^{3+} was infact creating the paracellular pathway inhibition by affecting Ca^{2+} cellular flux. This was not observed, as the reverse was evident with all the Ca^{2+} effectors tested indicating that blocking Ca^{2+} influx *via* Ca^{2+} channels led to increased permeability. This suggests that intracellular Ca^{2+} plays an important role in regulating the tight junction. The interplay of intracellular Ca^{2+} concentrations and the fluxes from the intra- and extracellular stores could be an important factor in regulating tight junction function (Martinez-Palomo *et al.*, 1971). This could be tested by adding La^{3+} and measuring intracellular Ca^{2+} concentration in Caco-2 monolayers, however, to my knowledge this is not feasible.

However, as La^{3+} was not observed to interact through Ca^{2+} effectors in Caco-2 monolayers, the possibility that it may be interacting with other protein carrier-mediated

systems or channels, which can influence the paracellular pathway were investigated. Therefore, other inhibitors were tested which established that La^{3+} was not interacting with them. These included, sodium and Cl^- channels in the apical membrane, and the Na^+/K^+ATPase, and $Na^+/K^+/2Cl^-$ cotransporter in the basolateral membrane. The glucose carrier-mediated proteins, the Na^+-dependent glucose transporter and the facilitative glucose transporters in the basolateral membrane. All the inhibitors tested either had no effect or increased mannitol permeability. Therefore, with the above evidence it is assumed that 2 mM La^{3+} applied apically is inhibiting the paracellular pathway with no obvious toxic effects.

The effect of apical 2 mM La^{3+} was tested on a series of compounds, some with well known characterised transport mechanisms and three unknowns, CHPP, NBS and hCT (Table 6.1). Two known carrier-mediated molecules, D-glucose and sodium taurocholate, were poorly inhibited by La^{3+}, their activity being 91.1 % ± 1.6 % and 91.0 % ± 3.2 % of the control value respectively. However, when sodium taurocholate was tested at a 333 molar excess, *i.e.* 1 mM, inhibition was 97.1 % ± 0.33 % indicating that the compound has a paracellular component, which may well account for the small inhibition seen at sub K_t concentration. Also tested was the vesicularly transported 40 kDa protein HRP, at 0.5 mg ml^{-1}, 2 mM apical La^{3+} inhibited it by 92.9 % ± 1.14 %. This indicates that La^{3+} may well also be having a membrane stabilising effect which inhibits vesicular internalisation. This scale of inhibition was repeated for 0.1 mg ml^{-1} hCT which was inhibited by 96.2 % ± 0.8 %, indicating either a possible large vesicular transcellular pathway component for hCT transport, as indicated by the HRP result or hCT transport is *via* a membrane route. This is in agreement with reports on both molecules having or being associated with vesicular transcellular transport pathways (Heyman *et al.*, 1990: Lang *et al.*, 1998). The level of inhibition by La^{3+} indicates that the majority of the dose for both compounds is transported by the transcellular pathway. However, the paracellular marker PEG 4000 did not decrease in permeability with increasing concentrations of La^{3+} indicating PEG 4000 in Caco-2 monolayers is not a good marker for the paracellular pathway. This may well be the case as others have questioned its use as a paracellular marker, arguing that PEG 4000 is a relatively flexible lipophilic molecule that may diffuse across the intestinal epithelium transcellularly (Iqbal *et al.*, 1993). Taurocholate concentrations, above 20 mM increased

PEG 4000 permeability, indicating that a transcellular pathway is probable, through taurocholate acting as a membrane fluidiser and therefore acting as a non-specific absorption enhancer for PEG 4000.

The two test drugs NBS and CHPP, both shown to be passively transported, were unaffected by 2 mM La^{3+} indicating that they are passively transported by the transcellular pathway. This was corroborated with La^{3+} having no effect on transepithelial permeability of testosterone, a drug known to be absorbed by the transcellular pathway.

Table 6.1 The effect of 2 mM apical La^{3+} on the apparent permeability coefficient (P_{app}) of various compounds across Caco-2 monolayers.

Compound	Control P_{app} (cm s^{-1})	2 mM La^{3+} P_{app} (cm s^{-1})	% Control
D-mannitol	$1.46 \pm 0.14 \times 10^{-7}$	$0.54 \pm 0.02 \times 10^{-7}$	37.0 % ± 1.37 % *
PEG 4000	$2.05 \pm 0.12 \times 10^{-8}$	$1.98 \pm 0.12 \times 10^{-8}$	96.6 % ± 5.9 %
100 μM Testosterone	$2.06 \pm 0.23 \times 10^{-5}$	$3.27 \pm 1.58 \times 10^{-5}$	158.7 % ± 76.7 %
5.5 mM D-glucose	$1.24 \pm 0.03 \times 10^{-5}$	$1.13 \pm 0.02 \times 10^{-5}$	91.1 % ± 1.6 %
3 μM Taurocholate	$1.89 \pm 0.06 \times 10^{-6}$	$1.72 \pm 0.06 \times 10^{-6}$	91.0 % ± 3.2 %
0.5 mg ml^{-1} HRP	$0.88 \pm 0.25 \times 10^{-9}$	$0.06 \pm 0.01 \times 10^{-9}$	7.1 % ± 1.14 % *
0.1 mg ml^{-1} hCT	$0.79 \pm 0.07 \times 10^{-8}$	$0.03 \pm 0.01 \times 10^{-8}$	3.8 % ± 0.88 % *
50 μM CHPP	$8.46 \pm 0.23 \times 10^{-6}$	ND	
50 μM NBS	$5.31 \pm 0.15 \times 10^{-7}$	$6.45 \pm 0.20 \times 10^{-7}$	121.5 ± 3.77 % *

ND = not determined; * denotes significant difference from control value at $p<0.05$.

6.2 CACO-2 CELLS AS A MODEL OF THE HUMAN DISTAL ILEUM

A knowledge of permeability barriers, transport pathways, and transport mechanisms of the human GI tract is important for the development and optimisation of drugs intended for oral absorption, see Chapter 1. The phenotypic heterogeneity of Caco-2 cells arises from their primary colonic carcinoma origin with colonic and foetal distal ileal phenotypic characteristics. The region of the normal human GI tract represented by the Caco-2 absorption model still remains unclear. Caco-2 monolayers have been shown to have

amino acid and glucose transporters found in the normal human small intestine along with taurocholate and intrinsic factor-Cbl transport pathways (Wilson *et al.*, 1990; Dix *et al.*, 1990) unique to the distal ileum. However, Caco-2 cells represent the only cell line known to express the foetal markers lactase and sucrase-isomaltase (van Beers *et al.*, 1995). Furthermore, Caco-2 monolayers have increased TER value equivalent to their colonic origins.

Pappenheimer and Reiss (1987) proposed the controversial theory, that increased solvent drag across the tight junctions, brought about a substantial increase in nutrient absorption *via* the paracellular pathway after a meal. Further work, has shown that luminal nutrients appear to be a potent stimuli for the alteration of tight junction permeability, and this response appears to be restricted to those nutrients requiring sodium-coupled active transport for their absorption (Pappenheimer and Volpp, 1992). However, the proportion that is absorbed depends on the concentration of D-glucose in the lumen postprandially and the relative magnitude of transport by both the sodium-dependent glucose carrier and the paracellular route at this concentration. Sadowski and Meddings (1993) calculate that 13 % of total glucose transport is transported by the paracellular route at a luminal glucose concentration of 30 mM. This was corroborated by Madara and his co-workers, who demonstrated using oligopeptides of approximately 1900 Da, penetrating tight junctions selectively at sites dilated by the luminal presence of D-glucose. The same oligopeptide tracers did not penetrate tight junctions when glucose was not present (Atisook and Madara, 1991). Fricker and Drewe (1995), using Caco-2 cells, demonstrated a 2.3-fold increase in the permeability of Octreotide, a somatostatin analog, with the addition of 20 mM D-glucose. However in this study it was found that increasing apical glucose concentrations (5.5-100 mM) on Caco-2 monolayers did not produce the increase in transepithelial transport predicted by Pappenheimer and Reiss (1987), with no increase in the paracellular pathway transport markers, [^{14}C]mannitol and [^{14}C]PEG 4000 or a decrease in TER expected with loosening of the tight junctions (Chapter 3).

In contrast, Artursson *et al.* (1996) propose that the larger surface area of the cell membrane, compared to the paracellular space in the intestine, will compensate for the

differences in partitioning of a hydrophilic drug. As a result they suggest that hydrophilic drugs could be transported in equal amounts by transcellular and paracellular pathways.

In both cases this may well be true, as increased solvent drag across the epithelium would result in more drug being absorbed across the epithelium. However as to whether this is regulated is still an open question. Using the Caco-2 absorption model may not be the best model to investigate this phenomena in view of the fact that apically 100 mM glucose did not drive enhanced transepithelial transport of the marker molecules D-[^{14}C]mannitol and [^{14}C]PEG 4000 or reduce TER (Chapter 3). Thus the Caco-2 transport system may not mimic the *in vivo* situation when considering fluid handling in the small intestine, as Caco-2 monolayers have increased TER values equivalent to their colonic origin.

6.3 CACO-2 ABSORPTION MODEL

Many research groups have expounded their *in vitro* model for predicting drug absorption in the GI tract and reported the close correlation to the *in vivo* situation. However, Yamashita *et al.* (1997) has pointed out that drug permeation through Caco-2 monolayers, which consist of an epithelial cell layer and a supporting filter, is essentially the same process as that of *in vivo* drug absorption. *i.e.* drug permeation across the GI epithelium supported on a basement membrane.

However, a major concern of the usefulness of Caco-2 monolayers is their reproducibility between research groups and therefore the prediction and *in vivo* correlation. Artursson *et al.* (1996) demonstrated qualitative similar correlation between absorbed fraction in humans and permeability in Caco-2 monolayers obtained in four different laboratories. But the data were not directly comparable due to quantitative differences in the permeability of the Caco-2 monolayers. The heterogeneous nature of the Caco-2 cell line parent population, along with selection pressures resulting from different protocols to maintain stock cultures, can cause research groups to develop their own sub-population, by clonal selection, within the parent population (Woodcock *et al.*, 1991). Recently qualitative and quantitative differences in Caco-2 populations have started to appear in the scientific literature with investigation into the changes associated with time in culture and passage number (Yu *et al.*, 1997; Briske-Anderson *et al.*, 1997).

In addition to the heterogeneity of the Caco-2 cell line it is important to minimise the influence of diffusion apparatus on permeability. The development of different diffusion chambers to minimise the influence of the unstirred water layer on drug transport kinetics across Caco-2 monolayers is important. However, they can detract from the relative simplicity and rapidity of the Caco-2 absorption model. Also the type of support can influence the transport of a compound. It is important to select an appropriate culture-insert, the polycarbonate permeable-support displays uniformly low ligand binding (Nicklin *et al.*, 1992a; Yu and Sinko, 1997). Furthermore, since transport rates for compounds are device-dependent, standardisation of apparatus along with techniques used for transport studies, is required if inter-laboratory data extrapolation is desired. Automated procedures for screening of drug transport in Caco-2 absorption model using robotics and 3 day fully differentiated cells increases their acceptability as a model for the GI tract absorption screen (Kuhfeld *et al.*, 1994; Chong *et al.*, 1997). Caco-2 monolayers are being used to screen the permeability of combinatorial libraries for compounds that are likely to be transported across the intestinal mucosa. This will greatly enhance the discovery of orally available drugs (Taylor *et al.*, 1997; Stevenson *et al.*, 1995).

6.4 CACO-2 ABSORPTION SCREEN

To predict human GI tract absorption and elucidate their mechanism of absorption, the Caco-2 absorption model was chosen. Numerous research groups and pharmaceutical companies are also using the Caco-2 absorption model in trying to evaluate the structure activity relationship of absorption (reviewed by Artursson *et al.*, 1996). In this study the absorption of two classes of poorly absorbed drugs were investigated; highly lipophilic low molecular weight synthetic organic compounds CHPP and NBS and a high molecular weight, hydrophilic, polypeptide, hCT. Both, CHPP and NBS travel by passive diffusion transcellularly and hCT *via* a mixture of vesicular transcellular and paracellular pathways (Chapter 4 and 5). The distinction of the pathways was enabled by the use of La^{3+} as a new tool for inhibiting paracellular transport (Chapter 3).

In Chapter 4 the Caco-2 absorption model was used in conjunction with a co-solvent (2.9 % (v/v) ethanol) to predict the *in vivo* absorption of CHPP and NBS, two PKC inhibitors, and elucidate their mechanism of absorption. Taking into account the effect of the co-

solvent on the Caco-2 monolayers, complete absorption was predicted. However, when this was tested *in vivo* with CHPP, no absorption of the parent drug was observed. The Caco-2 monolayers did produce an extra peak, a more polar metabolite, upon HPLC analysis of basolateral samples after 120 min and in apical samples at the end of the experiment, indicating the possible metabolism of the parent compound. However, this metabolite was not seen on i.v. or oral administration to rats, suggesting CHPP is metabolised differently in rats versus human Caco-2 cells, or the different route of administration (i.v. or oral) of CHPP may give rise to different drug metabolism. This needs to be investigated further to see if the metabolite is active and whether CHPP is absorbed unchanged and what fraction is metabolised by the intestine and liver.

Whereas, complete absorption was predicted for CHPP and NBS this was not the case for hCT. The Caco-2 hCT permeability as measured by P_{app} indicated incomplete absorption, which has been observed *in vivo* (Hastewell *et al.*, 1992: Hastewell *et al.*, 1995). However, using the Caco-2 absorption model to elucidate the pathway of hCT transport proved difficult to accomplish. Evidence has pointed to two pathways, paracellular and transcellular vesicular transcytosis, in both cases there will be limited transport of hCT, because of its size and number of vesicles transcytosed, respectively. With the addition of 2 mM La^{3+} to Caco-2 monolayers inhibiting 0.1 mg ml^{-1} hCT transport by 96.2 % ± 0.8 % indicates that hCT transport across Caco-2 monolayers is predominantly *via* the vesicular transcellular pathway as displayed by the similar inhibition of the vesicular transported protein HRP.

In using the Caco-2 absorption model to screen compounds for absorption and study structure absorption activity, their mechanisms of absorption will possibly be elucidated. Some may take advantage of the active nutrient transporters in the apical membrane of mature, fully differentiated Caco-2 cells. Several acidic drugs including salicylic acid and its analogues (Fisher, 1981) and the HMG-CoA reductase inhibitor, pravastatin, are thought to be absorbed *via* the monocarboxylic acid transporters (Tamai *et al.*, 1995). Phosphate transport across intestinal brush-border membranes is mediated by sodium ion and pH-sensitive mechanisms. The antiviral agent, forcarnet (Ritschel *et al.*, 1985) and the antibacterial agent, fosfomycin (Ishizawa *et al.*, 1990), each contain a phosphate moiety

within the molecule, allowing it to be absorbed *via* the phosphate transporter. Carrier-mediated transport of several water-soluble vitamins, including nicotinic acid, folic acid, ascorbic acid, biotin, choline and pantothenic acid, has also been demonstrated. Methotrexate is absorbed *via* the folic acid transporter (Zimmerman *et al.*, 1986), but it is not known whether the other vitamin transporters function in the absorption of structurally analogous drugs.

The di-/tripeptide carrier transports di- and tripeptides of different amino acid composition and is relatively tolerant of many structural modifications unlike the amino acid carriers. Quai and co-workers (1972) first demonstrated the active transport of the orally active β-lactam antibiotic, cephalexin, across isolated rat jejunum. Another group of bioactive compounds the angiotensin-converting enzyme inhibitors, exhibit oral bioavailabilities greater than would be expected from size and physicochemical characteristics. It was found that some of these peptide-like drugs had an affinity for the peptide transport system and was an important determinant of their therapeutic efficacy (Hu and Amidon, 1988; Friedman and Amidon, 1989). Other examples of drugs observed to use the di-/tripeptide carrier mediate transport system include β-lactam and cephalosporin antibiotics (Nakashima *et al.*, 1984; Kramer *et al.*, 1990), thyrotropin-releasing hormone analogues (Yokohama *et al.*, 1984) and renin inhibitors (Kleemann *et al.*, 1992).

Russell-Jones *et al.* (1986) have demonstrated using the oral delivery of Cbl conjugated to either lutenizing hormone releasing hormone (LHRH) or bovine serum albumin (BSA), it is possible to get the required biological response. With Cbl-Lys-6, LHRH stimulation of ovulation in developing follicles of mice, and with Cbl-BSA an immune reaction to the BSA as evidenced by a significant serum antibody response. Although receptor-mediated uptake of Cbl conjugates indicate a possible pathway for macromolecular delivery, it is not proven. Also, free Cbl in the GI tract would compete for finite number of Cbl-intrinsic factor receptors with expression on the cell surface down regulated when the cell has sufficient Cbl.

The Caco-2 cell line is now widely used to investigate a variety of intestinal functions; differentiation and derivation of morphology phenotype, cellular sorting, synthesis of macromolecules, *e.g.*, lipoproteins, metabolism, assessment of the effect of pharmaceutical

excipients, and the absorption of nutrients and drugs across the intestinal epithelium *via* the various absorption pathways.

6.5 FUTURE WORK

Following this initial study into the use of La^{3+} as a paracellular inhibitor in Caco-2 monolayers, further studies would need to be carried out to ascertain whether it works *in vivo*. Also, the exact mechanism of action of the paracellular block by La^{3+} would be of great interest, as this knowledge would give us increased understanding of intercellular tight junctions. Some possibilities could be, La^{3+} binding to the negatively charged proteoglycans and glycoproteins lining the tight junction, replacing Ca^{2+} in the binding of E-cadherins, and binding to occludin the tight junction protein. All reducing tight junction permeability by possibly forming more stable binding interactions that would increase pore closure. In conjunction with the results of the co-solvent model, suggesting intracellular signalling events, such as intracellular Ca^{2+} concentrations and/or PKC activation, regulate the permeability of the tight junctions, would give further insights into tight junction regulation. This was highlighted by the investigation into the permeability of the two candidate PKC inhibitors. The first, CHPP, a PKC-α inhibitor, reversed the loss of tight junctional integrity, as measured by TER, in the presence of 2.9 % (v/v) ethanol. Whereas, NBS, a PKC inhibitor, had no effect, implying that PKC-α is selectively activated by the presence of ethanol and this activity is inhibited by CHPP. Indicating changes in cytoskeletal arrangement altering intracellular calcium concentration or intracellular signalling *via* PKC has an effect on tight junction regulation and permeability.

Ethanol is a pharmaceutically accepted excipient and causes, in Caco-2 monolayers, increased permeability. This raises the question of the use of excipients in drug formulations to be tested in Caco-2 monolayers. Work has been reported on the use of Caco-2 monolayers in discovering the mode of action of various permeability enhancers (Hochman *et al.*, 1994; Nerurkar *et al.*, 1996). But could Caco-2 monolayers be used to screen absorption enhancers to improve drug permeability? Caco-2 monolayers seem to be more sensitive to the effects of enhancers compared to *in vivo* where the cell monolayer has the protective mucus layer and the support of the intestinal mucosae. An improvement of the Caco-2 absorption model has been to co-culture Caco-2 cells with mucus secreting HT-

29 cells. However, this has been accomplished with varying degrees of success (Wikman-Larhed and Artursson, 1995; Walter *et al.*, 1996) although wide spread acceptance has not been forthcoming. With the added barrier of mucus, the sensitivity issue may be diminished thus allowing formulation screening.

6.6 CONCLUSION

La^{3+} has been demonstrated to be an inhibitor of paracellular pathway transport in the Caco-2 absorption model as observed by the decreased D-mannitol permeability and increased TER. This was not repeated with other cations or selected channel and transporter inhibitors. La^{3+} did not inhibit the passive transcellular transport of testosterone. It also did not inhibit the permeability of PEG 4000 which highlighted its use as a paracellular marker. Also there was minimal inhibition of transcellular carrier-mediated permeability of glucose or taurocholate. However, there was > 90 % inhibition of HRP a protein transported across Caco-2 monolayers and the GI tract epithelium by fluid-phase vesicular transcytosis, indicating that La^{3+} may also inhibit the transcellular pathway.

The elucidation and characterisation of CHPP, NBS and hCT transport was partially accomplished. For CHPP and NBS, permeability across the Caco-2 monolayers is by transcellular passive diffusion. However, for hCT it is not clear cut as the rate versus concentration graph indicates passive diffusion or fluid-phase vesicular transcytosis. With La^{3+} inhibiting hCT permeability > 90 % suggests a similar mechanism to HRP *i.e.* transported *via* a vesicular transcytotic pathway, which needs to be confirmed. Therefore La^{3+} may have to be used with care as an inhibitor of the paracellular pathway

The Caco-2 absorption model is an important methodology into discovering more about the function and regulation of intestinal absorption processes. Through the elucidation and characterisation of CHPP and NBS passive permeability across Caco-2 monolayers it was predicted using the relationship put forward by Artursson and Karlsson (1991) that complete absorption *in vivo* of the two compounds would take place. However, there was a lack of *in vitro*/*in vivo* correlation, with no CHPP *in vivo* absorption. The evidence from the Caco-2 studies indicate that CHPP was metabolised which may explain the lack of correlation, further investigation is necessary to elucidate this lack of correlation. Also, in

this study the Caco-2 model of the human small intestine is also questioned as it may not mimic the fluid absorption found in the small intestine.

REFERENCES

Addison, J.M., Burston, D. and Matthews, D.M. (1972) Evidence for active transport of the dipeptide glycylsarcosine by hamster jejunum in vitro. Clin. Sci. 43, (6), 907-911.

Alcorn, C.J., Simpson, R.J., Leahy, D. and Peters, T.J. (1991) *In vitro* studies of intestinal drug absorption. Determination of partition and distribution coefficients with brush border membrane vesicles. Biochem. Pharmacol. 42, 2259-2264.

Alcorn, C.J., Simpson, R.J., Leahy, D.E. and Peters, T.J. (1993) Partition and distribution coefficients of solutes and drugs in brush border membrane vesicles. Biochem. Pharmacol. 45, (9), 1775-1782.

Aldini, R., Montagnani, M., Roda, A., Hrelia, S., Biagi, P. L. and Roda, E. (1996) Intestinal absorption of bile acids in the rabbit: Different transport rates in jejunum and ileum. Gastroenterology 110, 459-468.

Alvarez-Hernandez, X., Madigosky, S.R., Stewart, B. and Glass, J. (1994a) Iron status effects Aluminium uptake and transport by Caco-2 cells. J. Nutr. 124, 1574-1580.

Alvarez-Hernandez, X., Smith, M. and Glass, J. (1994b) Regulation of iron uptake and transport by transferrin in Caco-2cells an intestinal cell line. Biochim. Biophys. Acta 1192, 215-222.

Amidon, G.L., Leesman, G.D. and Elliott, R.L. (1980) Improving intestinal absorption of water-insoluble compounds: A membrane metabolism strategy. J. Pharm. Sci. 69, (12), 1363-1368.

Anderson, J.M. and van Itallie, C.M. (1995) Tight junctions and the molecular basis for regulation of paracellular permeability. Am. J. Physiol. 269, (Gastrointest. Liver Physiol. 32): G467-G475.

Andrejauskas-Buchdunger, E. and Regenass, U. (1992) Differential inhibition of the epidermal growth factor-, platelet-derived growth factor-, and protein kinase C-mediated signal transduction pathways by the staurosporine derivative CGP 41251. Cancer Res. 52, (19), 5353-5358.

Antonin, K.H., Saano, V., Bieck, P., Hastewell, J., Fox, R., Lowe, P. and Mackay, M. (1992) Colonic absorption of human calcitonin in man. Clin. Sci. 83, 627-631.

Antonin, K.H., Rak, R., Bieck, P.R., Preiss, R., Schenker, U., Hastewell, J., Fox, R. and Mackay, M. (1996) The absorption of human calcitonin from the transverse colon of man. Int. J. Pharm. 130, 33-39.

Artursson, P. (1990) Epithelial transport of drugs in cell culture. I: A model for studying the passive diffusion of drugs over intestinal absorptive (Caco-2) cells. J. Pharm Sci. 79, (6), 476-482.

Artursson, P. (1991) Cell cultures as models for drug absorption across the intestinal mucosa. Crit. Rev. Ther. Drug Carrier Syst. 8, 305-330.

Artursson, P. and Magnusson, C. (1990) Epithelial transport of drugs in cell culture II: Effect of extracellular calcium concentration on the paracellular transport of drugs of different lipophilicities across monolayers of intestinal epithelial (Caco-2) cells. J. Pharm. Sci. 79, 595-600.

Artursson, P. and Karlsson, J. (1991) Correlation between oral drug absorption in humans and apparent drug permeability coefficients in human intestinal epithelial (Caco-2) cells. Biochem. Biophys. Res. Comm. 175, (3), 880-885.

Artursson, P., Ungell, A.L. and Lofroth, J.E. (1993) Selective paracellular permeability in two models of intestinal absorption: Cultured monolayers of human intestinal epithelial cells and rat intestinal segments. Pharm. Res. 10, (8), 1123-1129.

Artursson, P., Lindmark, T., Davis, S.S. and Illum, L. (1994) Effect of chitosan on the permeability of monolayers of intestinal epithelial cells (Caco-2). Pharm. Res. 11, (9), 1358-1361.

Artursson, P., Palm, K. and Luthman, K. (1996) Caco-2 monolayers in experimental and theoretical predictions of drug transport. Adv. Drug Del. Revs. 22, 67-84.

Atisook, K. and Madara, J.L. (1991) An oligopeptide permeates intestinal tight junction at glucose-elicited dilatations. Gastroenterology 100, 719-724.

Bai, J.P.F. and Chang, L.L. (1995) Transepithelial transport of Insulin: I. Insulin degradation by insulin-degrading enzyme in small intestinal epithelium. Pharm. Res. 12, (8), 1171-1175.

Bai, J.P.F. and Chang, L.L. (1996) Effects of enzyme inhibitors and insulin concentration on transepithelial transport of insulin in rats. J. Pharm. Pharmacol. 48, 1078-1082.

Bai, J.P.F. (1994b) Subcellular distribution of proteolytic activities degrading bioactive peptides and analogues in the rat small intestinal and colonic enteroyctes. J. Pharm. Pharmacol. 46, 671-675.

Bai, J.P.F. (1994d) Stability of neurotensin and acetylneurotensin 8-13 in brush-border membrane, cytosol, and homogenate of rat small intestine. Int. J. Pharm. 112, 133-141.

Bai, J.P.F. (1994a) Distribution of brush-border membrane peptidases along the rat intestine. Pharm. Res. 11, 897-900.

Bai, J.P.F. (1994c) Effects of bile salts on brush-border and cytosolic proteolytic activities of intestinal enterocytes. Int. J. Pharm. 111, 147-152.

Balda, M.S. (1991) Intracellular signals and the tight junction, in: The Tight Junction (M. Cereijido, ed.), CRC Press, Boca Raton, Fla. 121-137.

Balda, M.S., Gonzalez-Mariscal, L., Contreras, R.G. and Cereijido, M. (1991) The assembly and sealing of tight junctions: Participation of G-proteins, phospholipase C, protein kinase C and calmodulin. J. Membr. Biol. 122, 193-202.

Balda, M.S., Gonzalez-Mariscal, L., Matter, K., Cereijido, M. and Anderson, J.M. (1993) Assembly of the tight junction: The role of diacylglycerol. J. Cell Biol. 123, (2), 293-302.

Banan, A., Smith, G. S., Rieckenberg, C. L., Kokoska, E. R. and Miller, T. A. (1998) Protection against ethanol injury by prostaglandin in human intestinal cell line: Role of microtubules. Am. J. Physiol. 274 (Gastrointest. Liver Physiol. 37): G111-G121.

Baudys, M., Mix, D. and Kim, S.W. (1996) Stabilization and intestinal absorption of human calcitonin. J. Contr. Rel. 39, 145-151.

Beglinger, C., Born, W., Muff, R., Drewe, J., Dreyfuss, J.L., Bock, A., Mackay, M. and Fischer, J.A. (1992) Intracolonic bioavailability of human calcitonin in man. Eur. J. Clin. Pharmacol. 43, (5), 527-531.

Beltran, P.J., Fan, D., Fidler, I.J. and O'Brian, C. A. (1997) Chemosensitization of cancer cells by the staurosporine derivative CGP 41251 in association with decreased P-glycoprotein phosphorylation. Biochem. Pharmacol. 53, (2), 245-247.

Bentzel, C.J., Hainau, B., Ho, S., Huis, W., Edelman, A., Anagnostopoulus, T. and Benedetti, E.L. (1980) Cytoplasmic regulation of tight-junction permeability: Effect of plant cytokinins. Am. J. Physiol. 239, C75-C89.

Bentzel, C.J., Palant, C.E. and Fromm, M. (1991) Physiological and pathological factors affecting the tight junction, in: The Tight Junction (M. Cereijido, ed.), CRC Press, Boca Raton, Fla. 151-173.

Bissonette, M., Tien, X. -Y., Niedziela, S. M., Hartmann, S. C., Frawley Jnr., B. P., Roy, H. K., Sitrin, M. D., Perlman, R. L. and Brasitus, T. A. (1994) 1, 25$(OH)_2$ vitamin D_3 activates PKC-α in Caco-2 cells: a mechanism to limit secosteroid-induced rise in $[Ca^{2+}]_i$. Am. J. Physiol. 267 (Gastrointest. Liver Physiol. 30): G465-475.

Blais, A., Bissonette, P. and Berteloot, A. (1987) Common characteristics for Na+-dependent sugar transport in Caco-2 cells and human fetal colon. J. Membr. Biol. 99, 113-125.

Body, J.J. (1995) Calcitonin for prevention and treatment of postmenopausal osteoporosis. Clin. Rheum. 14, (3), 18-21.

Bomsel, M., Prydz, K., Parton, R.G., Gruenberg, J. and Simons, K. (1989) Endocytosis in filter-grown Madin-Darby canine kidney cells. J. Cell Biol. 109, 3243-3258.

Borchardt, R.T., Lane, H.E., Hirst, B.H., Smith, P.L., Audus, K.L. and Tsuji, A. (1995) Application of cell culture systems to the study of drug transport and metabolism. In: Pharmacological Sciences: Perspectives for Research and Therapy in the Late 1990's, (A.C. Cuello Ed.), Birkhauser Verlag, CH-4010, Basel.

Boulenc, X., Bourrie, M., Fabre, I., Roque, C., Joyeux, H., Berger, Y. and Fabre, G. (1992) Regulation of cytochrome P450IA1 expression in a human intestinal cell line, Caco-2. J. Pharmacol. Exp. Ther. 263, (3), 1471-1478.

Briske-Anderson, M.J., Finley, J.W. and Newman, S.M. (1997) The influence of culture time and passage number on the morphological and physiological development of Caco-2 cells. P.S.E.B.M. 214, 248-257.

Brittain, H.G., Richardson, F.S. and Martin, R.B. (1976) Terbium (III) emission as a probe of calcium (II) binding sites in proteins. J. Am. Chem. Soc. 98, (25), 8255-8260.

Bronk, J.R. and Hastewell, J.G. (1987) The transport of pyrimidines into tissue rings cut from rat small intestine. J. Physiol. Lond. 382, 457-488.

Brown, M.S. Anderson, R.G.W. and Goldstein, J.L. (1983) Recycling receptors: The round trip itinerary of migrant membrane proteins. Cell. 32, 663-667.

Bryant, B.P. and Moore, P.A. (1995) Factors affecting the sensitivity of the lingual trigeminal nerve to acids. Am. J. Physiol. 268, (Regulatory Integrative Comp. Physiol. 37): R58-R65.

Budworth, J., Davies, R., Malkhandi, J., Gant, T.W., Ferry, D.R. and Gescher, A. (1996) Comparison of staurosporine and four analogues: Their effects on growth, rhodamine 123 retention and binding to P-glycoprotein in multi drug-resistant MCF-7/Adr cells. Br. J. Cancer. 73, (9), 1063-1068.

Burton, P.S., Conradi, R.A. and Hilgers, A.R. (1991) Transcellular mechanism of peptide and protein absorption: passive aspects. Adv. Drug Del. Revs. 7, 365-386.

Burton, P.S., Conradi, R.A., Hilgers, A.R., Ho, N.F.H. and Maggiora, L.L. (1992) The relationship between peptide structure and transport across epithelial cell monolayers. J. Contr. Rel. 19, 97-98.

Caillard, I. and Tome, D. (1995) Transport of β-lactoglobulin and α-lactalbumin in enterocyte-like Caco-2 cells. Reprod. Nutr. Dev. 35, (2), 179-188.

Caldwell, J., Gardner, I. and Swales, N. (1995) An introduction to drug disposition: The basic principles of absorption, distribution, metabolism, and excretion. Tox. Path. 23, (2), 102-114.

Camilleri, P., Okafo, G.N., Southan, C. and Brown, R. (1991) Analytical and micropreparative capillary electrophoresis of the peptides from calcitonin. Anal. Biochem. 198, (1), 36-42.

Caponigro, F., French, R.C. and Kaye, S.B. (1997) Protein Kinase C: A worthwhile target for anticancer drugs? Anticancer Drugs. 8, (1), 26-33.

Carafoli, E. (1991) Calcium pump of the plasma membrane. Physiol. Revs. 71, (1), 129-153.

Carlsson, O., Nielsen, S., Zakaria, E.R. and Rippe, B. (1996) In vivo inhibition of transcellular water channels (aquaporin-1) during acute peritoneal dialysis in rats. Am. J. Physiol. 271, (Heart Circ. Physiol. 40): H2254-H2262.

Caro, I., Boulenc, X., Rousset, M., Meunier, V., Bourrie, M., Julian, B., Joyeux, H., Roques, C., Berger, Y., Zweibaum, A. and Fabre, G. (1995) Characterization of a newly isolated Caco-2 clone (TC-7), as a model of transport processes and biotransformation of drugs. Int. J. Pharm. 116, 147-158.

Caspary, W.F. (1992) Physiology and pathophysiology of intestinal absorption. Am. J. Clin. Nutr. 55, 299S-308S.

Cereijido, M., Meza, I. and Martinez-Palomo, A. (1981) Occluding junctions in cultured epithelial monolayers. Am. J. Physiol. 240, C96-C102.

Cereijido, M., Gonzalez-Mariscal, L., Avila, G.A. and Contreras, R.G. (1988) Tight junctions. CRC Crit. Rev. Anat. Sci. 1, 171-192.

Chabre, O., Conklin, B.R., Lin, H.Y., Lodish, H.F., Wilson, E., Ives, H.E., Catanzariti, L., Hemmings, B.A. and Bourne, H.R. (1992) A recombinant calcitonin receptor independently stimulates 3', 5'-cyclic adenosine monophosphate and Ca2+/inositol phosphate signaling pathways. Mol. Endrocrinol. 6, (4), 551-556.

Chandler, C.E., Zaccaro, L.M. and Moberly, J.B. (1993) Transepithelial transport of cholyltaurine by Caco-2 cell monolayers is sodium dependent. Am. J. Physiol. 264, (Gastrointest. Liver Physiol. 27): G1118-G1125.

Chantret, I., Barbat, A., Dussaulx, E., Brattain, M.G. and Zweibaum, A. (1988) Epithelial polarity, villin expression, and enterocytic differentiation of cultured human colon carcinoma cells: A survey of twenty cell lines. Cancer Res. 48, (7), 1936-1942.

Chantret, I., Rodolosse, A., Barbat, A., Dussaulx, E., Brot-Laroche, E., Zweibaum, A. and Rousset, M. (1994) Differential expression of sucrose-isomaltase in clones isolated from early and late passages of the cell line Caco-2: Evidence for glucose-dependent negative regulation. J. Cell Sci. 107, 213-225.

Cheema, M.S., Marriott, C. and Beeson, M.F. (1984) The diffusion of water and drugs through mucus layers. In: Proceedings, 2nd International Congress of Biopharmaceutics and Pharmacokinetics, Salamanca, 555-563.

Chin, K.V., Pastan, I. and Gottesman, M.M. (1993) Function and regulation of the human multidrug resistance gene. Adv. Cancer Res. 60, 157-179.

Cholewinski, M., LÜckel, B. and Horn, H. (1996) Degradation pathways, analytical characterization and formulation strategies of a peptide and a protein calcitonine and human growth hormone in comparison. Pharmaceutica Acta Helvetiae 71, 405-419.

Chong, S., Dando, S.A. and Morrison, R.A. (1997) Evaluation of Biocoat intestinal epithelium differentiation environment (3-day cultured Caco-2 cells) as an absorption screening model with improved productivity. Pharm. Res. 14, (12), 1835-1837.

Chovath, B., Sedlak, J. and Novotny, L. (1994) The protein kinase C inhibitor, CGP 41 251, reverses decreased daunomycin uptake in a human drug-resistant ovarian carcinoma cell line. Int. J. Cancer. 59, (6), 852-853.

Citi, S. (1992) Protein kinase inhibitors prevent junction dissociation induced by low extracellular calcium in MDCK epithelial cells. J. Cell. Biol. 117, (1), 169-178.

Cogburn, J.N., Donovan, M.G. and Schasteen, C.S. (1991) A model of human small intestinal absorptive cells. 1. Transport Buffer. Pharm. Res. 8, (2), 210-216.

Coleman, R. and Kan, K.S. (1990) Oestradiol 17-β-glucuronide and tight junctional permeability increase. Biochem. J. 266, 622.

Collado, E.F., Fabra-Campass, S., Peris-Ribera, J.G., Casada, V.G., Martin Villocire, A. and Pia-Delfina, J.M. (1988) Absorption-partition relationships for a true homologous series of xenobiotics as a possible approach to study mechanisms of surfactants in absorption. II. Aromatic amines in rat small intestine. Int. J. Pharm. 44, 187-196.

Collett, A., Sims, E., Walker, D., He, Y-L., Ayrton, J., Rowland, M. and Warhurst, G. (1996) Comparison of HT29-18-C_1 and Caco-2 cell lines as models for studying intestinal paracellular drug absorption. Pharm. Res. 13, (2), 216-221.

Conradi, R.A., Hilgers, A.R., Ho, N.F.H. and Burton, P.S. (1991) The influence of peptide structure on transport across Caco-2 cells. Pharm. Res. 8, 1453-1460.

Conradi, R.A., Wilkinson, K.F., Rush, B.D., Hilgers, A.R., Ruwart, M.J. and Burton, P.S. (1993) *In vitro/in vivo* models for peptide oral absorption: Comparison of Caco-2 cell permeability with rat intestinal absorption of renin inhibitory peptides. Pharm. Res. 10, (12), 1790-1792.

Contreras, R.G., Miller, J.H., Zamora, M., Gonzalez,-Mariscal, L. and Cereijido, M. (1992) Interaction of calcium with plasma membrane of epithelial (MDCK) cells during junction formation. Am. J. Physiol. 263, (Cell Physiol. 32), C313-C318.

Cudd, A., Arvinte, T., Gaines Das, R.E., Chinni, C. and MacIntyre, I. (1995) Enhanced potency of human calcitonin when fibrillation is avoided. J. Pharm. Sci. 84, (6), 717-719.

Damgè, C., Michel, C., Aprahamian, M., Couvreur, P. and Devissaguet, J.-P. (1990) Nanocapsules as carriers for oral peptide delivery. J. Contr. Rel. 13, 233-239.

Dan, N. and Cutler, D.F. (1994) Transcytosis and processing of intrinsic factor-cobalamin in Caco-2 cells. J. Biol. Chem. 269, (29), 18849-18855.

Daniels, R.S., Downie, J.C., Hay, J.J., Knossow, M., Shehel, J.J., Wang, M.L. and Wiley, D.C. (1985) Fusion mutants of the influenza virus haemagglutinin glycoprotein. Cell 40, 431-439.

Dantzig, A.H. and Bergin, L. (1990) Uptake of the cephalosporin, cephalexin, by a dipeptide transport carrier in the human intestinal cell line, Caco-2. Biochim. Biophys. Acta. 1027, (3), 211-217.

Dantzig, A.H., Duckworth, D.C. and Tabas, L.B. (1994) Transport mechanisms responsible for the absorption of loracarbef, cefixime, and cefuroxime axetil into human intestinal Caco-2 cells. Biochim. Biophys. Acta. 1191, 7-13.

Deen, P.M.T., Nielsen, S., Bindels, R.J.M. and van Os, C.H. (1997) Apical and basolateral expression of aquaporin-1 in transfected MDCK and LLC-PK cells and functional evaluation of their transcellular osmotic water permeabilities. Pflügers Arch. Eur. J. Physiol. 433, 780-787.

Denker, B.M. and Nigam, S.K. (1998) Molecular structure and assembly of the tight junction. Am. J. Physiol. 274, (Renal Physiol. 43): F1-F9.

Desia, M.A. and Vadgama, P. (1991) Estimation of effective diffusion coefficients of model solutes through gastric mucus: Assessment of a diffusion chamber technique based on spectrophotometric analysis. Analyst. 116, 1113-1116.

Diamond, J.M. (1962) The mechanism of solute transport by the gall-bladder. J. Physiol. 161, 474.

Diamond, J. (1991) Evolutionary design of intestinal nutrient absorption: Enough but not too much. News Physiol. Sci. 6, 92-96.

Dix, C.J., Hassan, I.F., Obray, H.Y., Shah, R. and Wilson, G. (1990) The transport of vitamin B_{12} through polarized monolayers of Caco-2 cells. Gastroenterology 98, 1272-1279.

Dohi, M., Nishibe, Y., Makino, Y. and Suzuki, Y. (1993) Proceed. Intern. Symp. Control. Rel. Soc. P;9, Kyoto, Japan.

Donovan, M.D., Flynn, G.L. and Amidon, G.L. (1990) Absorption of polyethylene glycols 600 through 2000: The molecular weight dependence of gastrointestinal and nasal absorption. Pharm. Res. 7, 863-868.

Doluisio, J.T., Billups, N.F., Dittert, L.W., Sugita, E.T. and Swintosky, J.V. (1969) Drug absorption I: An in situ rat gut technique yielding realistic absorption rates. J. Pharm. Sci. 58, 1196-1200.

Doluisio, J.T., Crouthamel, W.G., Tan, G.H., Swintosky, J.V. and Dittert, L.W. (1970) Drug Absorption. III. Effect of membrane storage on the kinetics of drug absorption. J. Pharm. Sci. 59, (1), 72-76.

Duffey, M.E., Hainau, B., Ho, S. and Bentzel, C.J. (1981) Regulation of epithelial tight junction permeability by cAMP. Nature 294, 451-453.

Dyer, J., Beechey, R.B., Gorvel, J.P., Smith, R.T., Wootton, R. and Shirazi-Beechey, S.P. (1990) Glycyl-L-proline transport in rabbit enterocyte basolateral-membrane vesicles. Biochem. J. 269, (3), 565-571.

Eldridge, J.H., Hammond, C.J., Meulbroek, J.A., Staas, J.K., Gilley, R.M. and Tice, T.R. (1990) Controlled vaccine release in the gut-associated lymphtoid tissues. I. Orally administered biodegradable microsperes target the Peyer's patches. J. Contr. Rel. 11, 205.

Elsenhans, B., Blume, R., Lembcke, B. and Caspary, W.R. (1983) A new class of inhibitors for *in vitro* small intestinal transport of sugars and amino acids in the rat. Biochim. Biophys. Acta. 727, (1), 135-143.

Fasano, A., Baudry, B., Pumplin, D.W., Wasserman, S.S., Tall, B.D., Ketley, J.M. and Kaper, J.B. (1991) *Vibrio cholerae* produces a second entertoxin, which affects intestinal tight junctions. Proc. Natl. Acad. Sci. USA. 88, 5242-5246.

Féger, J., Gil-Falcon, S. and Lamaze, C. (1994) Cell receptors: Definition, mechanisms and regulation of receptor-mediated endocytosis. Cell. Mol. Biol. 40, 1039-1061.

Fisher, R.B. (1981) Active transport of salicylate by rat jejunum. Quart. J. Exp. Physiol. 66, 91-98.

Fix, J.A. (1996) Strategies for delivery of peptides utilizing absorption-enhancing agents. J. Pharm. Sci. 85, (12), 1282-1285.

Fogh, J., Fogh, J.M. and Orfeo, T. (1977) One hundred and twenty-seven cultured human tumor cell lines producing tumors in nude mice. J. Natl. Cancer Inst. 59, 221-225.

Fricker, G. and Drewe, J. (1995) Enteral absorption of octreotide: Modulation of intestinal permeability by distinct carbohydrates. J. Pharmacol. Exp. Ther. 274, (2), 826-832.

Friedman, D.I. and Amidon, G.L. (1989) Passive and carrier-mediated intestinal absorption components of two angiotensin converting enzyme (ACE) inhibitor prodrugs in rats: Enalapril and fosinopril. Pharm. Res. 6, (12), 1043-1047.

Fromter, E. and Diamond, J. (1972) Route of passive ion permeation in epithelia. Nature New Biol. 235, 9-13.

Fujita, T., Fujita, T., Morikawa, K., Tanaka, H., Iemura, O., Yamamoto, A. and Muranishi, S. (1996) Improvement of intestinal absorption of human calcitonin by chemical modification with fatty acids: Synergistic effects of acylation and absorpton enhancers. Int. J. Pharm. 134, 47-57.

Gallati, H. and Pracht, I. (1985) Horseradish peroxidase: Kinetic studies and optimization of the peroxidase activity determination with the substrates H_2O_2 and 3,3',5,5'-tetramethylbenzidine. J. Clin. Chem. Clin. Biochem. 23, (8), 453-460.

Gan, L-S, Niederer, T., Eads, C. and Thakker, D. (1993) Evidence for predominantly paracellular transport of thyrotrpin-releasing hormone across Caco-2 cell monolayers. Biochim. Biophys. Res. Comm. 197, (2), 771-777.

Gan, L-S. L., Yanni, S. and Thakker, D.R. (1998) Modulation of the tight junctions of the Caco-2 cell monolayers by H_2-antagonists. Pharm. Res. 15, (1), 53-57.

Gardner, M.L.G. (1988) Gastrointestinal absorption of intact proteins. Ann. Rev. Nutr. 8, 329-350.

Gibaldi, M. and Kanig, J. (1965) Absorption of drugs through the oral mucosa. J. Oral. Ther. Pharmacol. 1, 440-450.

Giuliano, A.R. and Wood, R.J. (1991) Vitamin D-regulated calcium transport in Caco-2 cells: Unique in vitro model. Am. J. Physiol. 260, (Gastrointest. Liver Physiol. 23): G207-G212.

Godefroy, O., Huet, C., Ibarra, C., Dautry-Varsat, A. and Louvard, D. (1990) Establishment of polarized endocytosis in differentiable intestinal HT29-18 subclones. New Biol. 2, (10), 875-886.

Gonzalez-Mariscal, L., Contreras, R.G., Bolivar, J.J., Pounce, A., Chavez de Ramirez, B. and Cereijido, M. (1990) Role of calcium in tight junction formation between epithelial cells. Am. J. Physiol. 259, C978-C986.

Gonzalez-Mariscal, L., Chavez de Ramirez, B. and Cereijido, M. (1985) Tight junction formation in cultured epithelial cells (MDCK) J. Membr. Biol. 86, 113-125.

Goodwin, T.J., Schroeder, W.F., Wolf, D.F. and Moyer, M.P. (1993) Proc. Soc. Exp. Biol. Med. 202, 181.

Grauer, A., Ziegler, R. and Raue, F. (1995) Clinical significance of antibodies against calcitonin. Exp. Clin. Endocrinol. 103, 345-351.

Greger, J.L. and Sutherland, J.E. (1997) Aluminium exposure and metabolism. Crit. Rev. Clin. Lab. Sci. 34, (5), 439-474.

Gumbiner, B. (1987) Structure, biochemistry and assembly of epithelial tight junctions. Am. J. Physiol. 253, C749-C758.

Gumbiner, B. and Simons, K. (1987) The role of uvomorulin in the formation of epithelial occluding junctions. In: Junctional complexes of epithelial cells. Stoker, M. (Ed.), Ciba Foundation Symposium 125, Wiley, Chichester, 168-186.

Gumbiner, B., Stevenson, B. and Grimaldi, A. (1988) The role of the cell adhesion molecule uvomorulin in the formation and maintenance of the epithelial junctional complex. J. Cell Biol. 107, 1575-1787.

Halline, A.G., Davidson, N.O., Skarosi, S.F., Sitrin, M.D., Tietze, C., Alpers, D.H. and Brasitus, T.A. (1994) Effects of 1, 25-dihydroxyvitamin D_3 on prolifieration and differentiation of Caco-2 cells. Endocrinology. 134, (4), 1710-1717.

Hanson, P.J. and Parsons, D.S. (1976) The utilization of glucose and production of lactate by *in vitro* preparations of rat small intestine: Effects of vascular perfusion. J. Physiol. 255, (3), 755-795.

Hartmann, F., Owen, R. and Bissell, D.M. (1982) Characterization of isolated epithelial cells from rat small intestine. Am. J. Physiol. 242, (2), G147-G155.

Hashimoto, K., Takeda, K., Nakayama, T. and Shimizu, M. (1995) Stabilization of the tight junction of the intestinal Caco-2 cell monolayer by milk whey proteins. Biosci. Biotech. Biochem. 59, (10), 1951-1952.

Hashimoto, N., Fujioka, T., Hayashi, K., Odaguchi, K., Toyoda, T., Nakamura, M. and Hirano, K. (1994) Renin inhibitors: Relationship between molecular structure and oral absorption. Pharm. Res. 11, 1443-1451.

Hashimoto, K. and Shimizu, M. (1993) Epithelial properties of human intestinal Caco-2 cells cultured in a serum-free medium. Cytotechnology. 13, (3), 175-184.

Hastewell, J., Lynch, S., Williamson, I., Fox, R. and Mackay, M. (1992) Absorption of human calcitonin across the rat colon *in vivo*. Clin. Sci. 82, 589-594.

Hastewell, J., Lynch, S., Fox, R., Williamson, I., Skelton-Stroud, P. and Mackay, M. (1994) Enhancement of human calcitonin absorption across the rat colon *in vivo*. Int. J. Pharm. 101, 115-120.

Hastewell, J., Antonin, K.H., Fox, R. and Mackay, M. (1995) The colonic absorption of human calcitonin: The effects of increasing local concentration and co-administration with a protease inhibitor. Int. J. Pharm. 126, 245-251.

Hecht, G., Pothoutakis, C., LeMont, J.T. and Madara, J.L. (1988) *Clostridium* difficile toxin A perturbs cytoskeletal structure and tight junction permeability of cultured human intestinal epithelial monolayers. J. Clin. Invest. 82, 1516-1524.

Herold, G., Jungwirth, R., Rogler, G., Geerling, I. and Strange, E.F. (1995) Influence of cholesterol supply on cell growth and differentiation in cultured enterocytes (Caco-2) Digestion. 56, 57-66.

Heyman, M., Ducroc, R., Desjeux, J.F. and Morgat, J.L. (1982) Horseradish peroxidase transport across adult rabbit jejunum *in vitro*. Am. J. Physiol. 242 (Gastrointest. Liver Physiol. 5), G558-G564.

Heyman, M., Grasset, E., Ducroc, R. and Desjeux, J.F. (1988) Antigen absorption by the jejunal epithelium of children with cow's milk allergy. Pediatr. Res. 24, 197-202.

Heyman, M., Crain-Denoyelle, A.M., Nath, S.K. and Desjeux J.F. (1990) Quantification of protein transcytosis in the human colon carcinoma cell line Caco-2. J. Cell. Physiol. 143, 391-395.

Hidalgo, I.J., Raub, T.J. and Borchardt, R.T. (1989) Characterization of the human colon carcinoma cell line (Caco-2) as a model system for intestinal epithelial permeability. Gastroenterology 96, 736-749.

Hidalgo, I.J. and Borchardt, R.T. (1990) Transport of large neutral amino acid (phenylalanine) in a human intestinal epithelial cell line: Caco-2. Biochim. Biophys. Acta, 1028, 25-30.

Hilgers, A.R., Conradi, R.A. and Burton, P.S. (1990) Caco-2 cell monolayers as a model for drug transported across the intestinal mucosa. Pharm. Res. 7, (9), 902-910.

Hill, A.E. and Shachar-Hill, B. (1993) A mechanism for isotonic fluid flow through the tight junctions of Necturus gallbladder epithelium. J. Membr. Biol. 136, 253-262.

Hillgren, K.M., Kato, A. and Borchardt, R.T. (1995) *In vitro* systems for studying intestinal drug absorption. Med. Res. Revs. 15, 83-109.

Ho, N.F.H., Merkle, H.P. and Higuchi, W.I. (1983) Quantitative, mechanistic and physiologically realistic approach to the biopharmaceutical design of oral drug delivery systems. Drug Dev. Ind. Pharm. 9, (7), 1111-1184.

Hochman, J. and Artursson, P. (1994) Mechanisms of absorption enhancement and tight junction regulation. J. Contr. Rel. 29, 253-267.

Hochman, J.H., Fix, J.A. and LeCluyse, E.L. (1994) *In vitro* and *in vivo* analysis of the mechanism of absorption enhancement by palmitoylcarnitine. J. Pharmacol. Exp. Ther. 269, (2), 813-822.

Howell, S., Kenny, A.J. and Turner, A.J. (1992) A survey of membrane peptidases in two human colonic cell lines, Caco-2 and HT-29. Biochem. J. 284, 595-601.

Hu, M. and Amidon, G.L. (1988) Passive and carrier-mediated intestinal absorption components of captopril. J. Pharm. Sci. 77, (12), 1007-1011.

Hu, M. and Borchardt, R.T. (1990) Mechanism of L-α-methyldopa transport through a monolayer of polarized human intestinal epithelial cells (Caco-2). Pharm. Res. 7, (12), 1313-1319.

Hu, M. and Borchardt, R.T. (1992) Transport of a large neutral amino acid in a human intestinal epithelial cell line (Caco-2): uptake and efflux of phenylalanine. Biochim. Biophys. Acta. 1135, (3), 233-244.

Hughes, D.R.L. (1988) The influence of intestinal mucus on drug absorption. PhD Thesis, Brighton Polytechnic, Brighton, CNNA.

Hughson, E.J. and Hopkins, C.R. (1990) Endocytic pathways in polarized Caco-2 cells: Identification of an endosomal compartment accessible from both apical and basolateral surfaces. J. Cell Biol. 110, 337-348.

Hunter, J., Hirst, B.H. and Simmons, N.L. (1991) Epithelial secretion of vinblastine by human intestinal adenocarcinoma cell (hct-8 and t84) layers expressing p-glycoprotein. Br. J. Cancer 64, 437-444.

Hunter, J., Hirst, B.H. and Simmons, N. L. (1993) Drug absorption limited by P-glycoprotein-mediated secretory drug transport in human intestinal epithelial Caco-2 cell layers. Pharm. Res. 10, 743-749.

Hussain, A.A. (1998) Intranasal drug delivery. Adv. Drug Del. Revs. 29, 39-49.

Hysing, J., Gordeladze, J.O., Christensen, G. and Tolleshaug, H. (1991) Renal uptake and degradation of trapped-label calcitonin. Biochem. Pharmacol. 41, (8), 1119-1126.

Iglesias, J., Gonzalez-Pacanowska, D. and Garcia-Peregrin, E. (1988) Mevalonate 5-pyrophosphate decarboxylase in isolated villus and crypt cells of chick intestine. Lipids 23, (4), 291-294.

Ikegami, Y., Yano, S. and Nakao, K. (1996a) Antitumor effect of CGP41251, a new selective protein kinase C inhibitor, on human non-small cell lung cancer cells. Jpn. J. Pharmacol. 70, (1) 65-72.

Ikegami, Y., Yano, S. and Nakao, K. (1996b) Effects of the new selective protein kinase C inhibitor 4'-N-benzoyl staurosporine on cell cycle distribution and growth inhibition in human small cell lung cancer cells. Arzneimittelforschung. 46, (2), 201-204.

Inui, K.I., Yamamoto, M. and Saito, H. (1992) Transepithelial transport of oral cephalosporins by monolayers of intestinal epithelial cell line Caco-2: Specific transport systems in apical and basolateral membranes. J. Pharmacol. Exp. Ther. 261, 195-201.

Iqbal, T.H., Lewis, K.O. and Cooper, B.T. (1993) Diffusion of poly(ethylene glycol)-400 across lipid barriers *in vitro*. Clin. Sci. 85, 111-115.

Ishizawa, T., Tsuji, A., Tamai, I., Terasaki, T., Hosoi, K. and Kukatsu, S. (1990) Sodium and pH dependent carrier-mediated transport of antibiotic, fosfmycin, in the rat intestinal brush-border membrane. J. Pharmacobio-Dyn. 13, 292-300.

Juliano, R.L. and Ling, V. (1976) A surface glycoprotein modulating drug permeability in chinese hamster ovary cell mutants. Biochem. Biophys. Acta. 455, 152-162.

Jumarie, C., Herring-Gillam, E., Beaulieu, J.-F. and Malo, C. (1996) Triiodothyronine stimulates the expression of sucrase-isomaltase in Caco-2 cells cultured in serum-free medium. Exp. Cell Res. 222, 319-325.

Kararli, T.T. (1989) Gastrointestinal absorption of drugs. Crit. Rev. Ther. Drug Carrier Syst. 6, (1), 39-86.

Kararli, T.T. (1995) Comparison of the gastrointestinal anatomy, physiology, and biochemistry of humans and commonly used laboratory animals. Biopharm. Drug Dispos. 16, 351-380.

Karlsson, J., Kuo, S.M., Ziemniak, J. and Artursson, P. (1993) Transport of celiprolol across human intestinal epithelial (Caco-2) cells: Mediation of secretion by multiple transporters including P-glycoprotein. Br. J. Pharmacol. 110, (3), 1009-1016.

Killion, J.J., Beltran, P., O'Brian, C.A., Yoon, S, S., Fan, D., Wilson, M.R. and Fidler, I.J. (1995) The antitumor activity of doxorubicin against drug-resistant murine carcinoma is enhanced by oral administration of a synthetic staurosporine analogue, CGP 41251. Oncol. Res. 7, (9), 453-459.

Kim, D.C., Burton, P.S. and Borchardt, R.T. (1993) A correlation between the permeability characteristics of a series of peptides using an *in vitro* cell culture model (Caco-2) and those using an in situ perfuses rat ileum model of the intestinal mucosa. Pharm. Res. 10, (12), 1710-1714.

Kimmich, G.A. (1990) Isolation of intestinal epithelial cells and evaluation of transport functions. Methods Enzylmol. 192, 324-340.

King, T.P., Pusztai, A. and Clarke, E.M. (1980) Immunocytochemical localisation of ingested kidney bean (Phaseolus vulgaris) lectins in rat gut. J. Histochem. 12, 201-208.

Kleemann, H.W., Heitsch, H., Henning, R., Kramer, W., Kocher, W., Lerch, U., Linz, W., Nickel, W.U., Ruppert, D. and Urbach, H. et al (1992) Renin inhibitory pentols showing improved enteral bioavailability. J. Med. Chem. 35, (3), 559-567.

Knipp, G.T., Ho, N.F.H., Barsuhn, C.L. and Borchardt, R.T. (1997) Paracellular diffusion in Caco-2 cell monolayers: Effect of perturbation on the transport of hydrophilic compounds that vary in charge and size. J. Pharm. Sci. 86, (10), 1105-1110.

Kokoska, E. R., Smith, G. S., Deshpande, Y., Rieckenberg, C. L. and Miller, T. A. (1998) Adaptive cytoprotection induced by ethanol in human intestinal cells: Role of prostaglandins and calcium homeostasis. Annals of Surgery 228, (1) 123-130.

Kolars, J.C., Schmiedlin-Ren, P., Schuetz, J.D., Fang, C. and Watkins, P.B. (1992) Identification of rifampicin-inducible P450IIIA4 (CYP3A4) in human small bowel enterocytes. J. Clin. Invest. 90, 1871-1888.

Kolbeck, R.C. and Speir, W.A. Jr. (1986) The influence of lanthanum on the subcellular distribution of calcium in the perfused dog heart. J. Mol. Cell Cardiol. 18, (7), 733-738.

Kotze, A.F., Lueben, H.L., de Leeuw, B.J., de Boer, B. G., Verhoef, J.C. and Junginger, H.E., (1998) Comparison of the effect of different chitosan salts and *N*-trimethyl chitosan chloride on the permeability of intestinal epithelial cells (Caco-2). J. Contr. Rel. 51, 35-46.

Kramer, W., Dechent, C., Girbig, F., Gutjahr, U. and Neubauer, H. (1990) Intestinal uptake of dipeptides and beta-lactam antibiotics. I. The intestinal uptake system for dipeptides and beta-lactam antibiotics is not part of a brush border membrane peptidase. Biochim. Biophys. Acta. 1030, (1), 41-9.

Kremski, V.C., Varani, L., DeSaive, C., Miller, P. and Nicolini, C (1977) Crypt cell isolation in the small intestine of the mouse. J. Histochem. Cytochem. 25, (7), 554-559.

Kurfeld, M.T., Hinshaw, M.E., Stratford, R.E. and Zynger, J. (1994) An automated *in vitro* permeability screen using robotics. Pharm. Res. 11, S-39.

Lacaz-Vieira, F. (1997) Calcium site specificity: Early Ca^{2+}related tight junction events. J. Gen. Physiol. 110, 727-740.

Lacaz-Vieira, F., Kachar, B. (1996) Tight junction dynamics in the frog urinary bladder. Cell Adhes. Comm. 4, 53-68.

Lane, T.A., Lamkin, G.E. and Wancewicz, E.V. (1990) Protein kinase C inhibitors block the enhanced expression of intercellular adhesion molecule-1 on endothelial cells activated by interleukin-1, lipopolysaccharide and tumor necrosis factor. Biochem. Biophys. Res. Comm. 172, (3), 1273-1281.

Lang, S., Rothen-Rutishauser, B., Perriard, J-C., Schmidt, M.C. and Merkle, H.P. (1998) Permeation and pathways of human calcitonin (hCT) across excised bovine nasal mucosa. Peptides. 19, (3), 599-607.

Lang, S.R., Staudenmann, W., James, P., Manz, H-J., Kessler, R., Galli, B., Moser, H-P., Rummelt, A. and Merkle, H.P. (1996) Proteolysis of human calcitonin in excised bovine nasal mucosa: Elucidation of the metabolic pathway of liquid secondary ionization mass spectrometry (LSIMS) and matrix assisted laser desorption ionization mass spectrometry (MALDI). Pharm. Res. 13, (11), 1679-1685.

Langer, G.A., Frank, J.S. and Nudd, L.M. (1979) Correlation of calcium exchange, structure, and function in myocardial tissue culture. Am. J. Physiol. 237, (2), H239-H246.

Lash, L.H. and Jones, D.P. (1984) Renal glutathione transport. Characteristics of the sodium-dependent system in the basal-lateral membrane. J. Biol. Chem. 259, (23), 14508-14514.

Lee, V.H.L. and Yamamoto, A. (1990) Penetration and enzymatic barriers to peptide and protein absorption. Ad. Drug Del. Revs. 4, 171-207.

Leese, H.J. and Mansford, K.R. (1971) The effect of insulin deficiency on the trransport and metabolism of glucose by rat small intestine. J. Physiol. Lond. 212, (3), 819-838.

Leo, A.J., Hansch, C. and Elkins, D. (1971) Partition coefficients and their uses. Chem. Rev. 71, 525-616.

Levine, R.R., McNary, W.F., Kornguth, P.J. and LeBlanc, R. (1970) Histological reevaluation of everted gut technique for studying intestinal absorption. Eur. J. Pharmacol. 9, (2), 211-219.

Loehry, C.A., Axon, A.T.R., Hilton, P.J., Hider, R.C. and Creamer, B. (1970) Permeability of the small intestine to substances of different molecular weight. Gut. 11, 466-470.

Lowe, P.J. and Temple, C.S. (1994) Calcitonin and insulin in isobutylcyanoacrylate nanocapsules: Protection against proteases and effect on intestinal absorption in rats. J. Pharm. Pharmacol. 46, 547-552.

Lu, S., Gough, A.W., Bobrowski, W.F. and Stewart, B.H. (1996) Transport properties are not altered across Caco-2 cells wit heightened TEER despite underlying physiological and ultrastructural changes. J. Pharm. Sci. 85, (3), 270-273.

Lucas, M.L. and Blair, J.A. (1978) The magnitude and distribution of the acid microclimate in proximal jejunum and its relation to luminal acidification. Proc. R. Soc. Lond. B. Biol. Sci. 200, (1138), 27-41.

Lucas, M.L., Schneider, W., Haberich, F.J. and Bair, J.A. (1975) Direct measurement by pH-microelectrode of the pH microclimate in rat proximal jejunum. Proc. R. Soc. Lond. B. Biol. Sci. 192, (1106), 39-48.

Lugea, A., Barber, A. and Ponz, F. (1995) Effect of Zinc on D-galactose and L-phenylalanine uptake in rat intestine in vitro. J. Physiol. Biochem. 51, (3), 139-146.

Lutz, K.L. and Siahaan, T.J. (1997) Molecular structure of the apical junction complex and its contribution to the paracellular barrier. J. Pharm. Sci. 86, (9), 977-984.

Ma, T.Y., Hollander, D., Riga, R. and Bhalla, D. (1993) Autoradiographic determination of permeation pathway of permeability probes across intestinal and tracheal epithelia. J. Lab. Clin. Med. 122, 590-600.

MacAdam, A. (1993) The effect of gastro-intestinal mucus on drug absorption. Adv. Drug Del. Revs. 11, 201-220.

Machen, T.E. and Diamond, J.M. (1972) The mechanism of anion permeation in Thorium-treated gallbladder. J. Membr. Biol. 8, 63-69.
Machen, T.E., Erlij, D. and Wooding, F.B.P. (1972) Permeable junctional complexes: The movement of lanthanum across rabbit gallbladder and intestine. J. Cell Biol. 54, 302-312.

Mackay, M., Williamson, I. and Hastewell, J. (1991) Cell biology of epithelia, Adv. Drug Del. Revs. 7, 313-338.

Mackay, M., Phillips, J. and Hastewell, J. (1997) Peptide drug delivery: Colonic and rectal absorption. Adv. Drug Del. Revs. 28, 253-273.

Madara, J.L. (1987) Intestinal absorptive cell tight junctions are linked to the cytoskeleton. Am. J. Physiol. 253, C171-C175.

Madara, J.L. (1988) Tight junction dynamics: Is paracellular transport regulated? Cell 53, 497-498.

Madara, J.L. (1989) Loosening tight junctions-Lessons from the intestine. J. Clin. Invest. 83, 1089-94.

Madara, J.L. (1991) Dynamics of intestinal epithelial tight junctions. Curr. Top. Membr. 38, 175-185.

Madara, J.L. and Dharmsathaphorn, K. (1985) Occluding junction structure-function relationships in a cultured epithelial monolayer. J. Cell Biol. 101, 2124-2133.

Madara, J.L. and Pappenheimer, J.R. (1987) Structural basis for physiological regulation of paracellular pathways in intestinal epithelia. J. Membr. Biol. 100, (2), 149-164.

Madara, J.L. and Stafford, J. (1989) Interferon-y directly affects barrier function of cultured intestinal epithelial monolayers. J. Clin. Invest. 83, 724-727.

Madara, J.L. and Carlson, S. (1991) Supraphysiologic L-tryptophan elicits cytoskeletal and macromolecular permeability alterations in hamster small intestinal epithelium *in vitro*. J. Clin. Invest. 87, 454-462.

Madara, J.L., Barenberg, D. and Carlson, S. (1986) Effects of cytochalasin-D on occluding junctions of intestinal absorptive cells: further evidence that the cytoskeleton may influence paracellular permeability and junctional charge selectivity. J. Cell Biol. 102, 2125-2136.

Madara, J.L., Moore, R. and Carlson, S. (1987) Alteration of intestinal tight junction structure and permeability by cytoskeletal contraction. Am. J. Physiol. 253, C854-861.

Mahraoui, L., Rodolosse, A., Barbat, A., Dussaulx, E., Zweibaum, A. and Rousset, M. (1994) Presence and differential expression of SGLT1, GLUT1, GLUT2, GLUT3 and GLUT5 hexose-transporter mRNAs in Caco-2 cell clones in relation to cell growth and glucose consumption. Biochem. J. 298, 629-633.

Mandel, L.J., Bacallo, R. and Zampighi. (1993) Uncoupling of the molecular 'fence' and paracellular 'gate' functions in epithelial tight junctions. Nature 361, 552-555.

Marcon-Genty, D., Tome, D., Kheroua, O., Dumontier, A.M., Heyman, M. and Desjeux, J.F. (1989) Transport of β-lactoglobulin across the rabbit ileum *in vitro*. Am. J. Physiol. 256 (Gastrointest. Liver Physiol. 19), G943-G948.

Martin, Y.C. (1981) A practitioner's perspective of the role of quantitative structure-activity analysis in medicinal chemistry. J. Med. Chem. 24, 229-237.

Martinez-Palomo, A., Erlij, D. and Bracho, H. (1971) Localization of permeability barriers in the frog skin epithelium. J. Cell Biol. 50, 277-287.

Martinez-Palomo, A., Meza, I., Beaty, G. and Cereijido, M. (1980) Experimental modulation of occluding junctions in a cultured transporting epithelium. J. Cell Biol. 87, 746-754.

McMartin, C. (1989) Molecular sieving, receptor processing and peptidolysis as major determinants of peptide pharmacokinetics *in vivo*. Biochem. Soc. Trans. 17, 931-934.

McRoberts, J.A. and Riley, N.E. (1992) Regulation of T84 cell monolayer permeability by insulin-like growth factors. Am. J. Physiol. 262, C207-C213.

Meyer, T., Regenass, U., Fabbro, D., Alteri, E., Rosel, J., Muller, M., Caravatti, G. and Matter, A. (1989) A derivative of staurosporine (CGP 41251) shows selectivity for protein kinase C inhibition and in vitro anti proliferative as well as in vivo anti-tumor activity. Int. J. Cancer. 43, (5), 851-856.

Meza, I., Iberra, G., Sabanero, M., Martinez-Palomo, A. and Cereijido, M. (1980) Occluding junctions and cytoskeletal components in a cultured transporting epithelium. J. Cell Biol. 87, 746.

Meza, I., Sabanero, M., Stefani, E. and Cereijido, M. (1982) Occluding junctions in MDCK cells: Modulation of transepithelial permeability by the cytoskeleton. J. Cell Biochem. 18, 407.

Middleton III, H.M. (1990) Uptake of riboflavin by rat intestinal mucosa *in vitro*. J. Nutr. 120, (6), 588-593.

Milovic, V., Stein, J., Ruppert, S., Zeuzem, S. and Caspary, W.F. (1994) Preparation of basolateral membrane vesicles from rat enterocytes: Influence of different gradient media. Physiol. Res. 43, (2), 75-81.

Moeller, T. (1963) The chemistry of the lanthanides. Reinhold Publishing Corporation, New York.

Mohrmann, I., Mohrmann, M., Biber, J. and Murer, H. (1986) Sodium-dependent transport of Pi by an established intestinal epithelial cell line (Caco-2). Am. J. Physiol. 250, G323-G330.

Mosmann, T. (1983) Rapid colorimetric assay for cellular growth and survival: Application to proliferation and cytotoxic assays. J. Immunol. Meth. 65, 55-63.

Mostov, K.E. and Simister, N.E. (1985) Transcytosis. Cell. 43, (2), 389-390.

Moyer, M.P. (1983) Culture of human gastrointestinal epithelial cells. Proc. Soc. Exp. Biol Med. 174, (1), 12-15.

Muff, R., Kaufmann, M., Born, W. and Fischer, J.A. (1994) Calcitonin inhibits phosphate uptake in opossum kidney cells stabley transfected with a porcine calcitonin receptor. Endocrinol. 134, (3), 1593-1596.

Mullins, J.G., Beechey, R.B., Gould, G.W., Campbell, F.C. and Shirazi-Beechey, S.P. (1992) Characterization of the ileal Na+/bile salt co-transporter in brush border membrane vesicles and functional expression in Xenopus laevis oocytes. Biochem. J. 285, 785-790.

Mullin, J.M. and O'Brien, T.G. (1986) Effects of tumor promotors on LLC-PK_1 renal epithelial tight junctions and transepithelial fluxes. Am. J. Physiol. 251, C597-C602.

Mullin, J.M. and Snock, K.V. (1990) Effect of tumor necrosis factor on epithelial tight junctions and transepithelial permeability. J. Cancer Res. 50, 2172-2176.

Mullin, J.M., Kampherstein, J.A., Laughlin, K.V., Clarkin, C.E., Miller, R.D., Szallasi, Z., Kachar, B., Soler, A.P. and Rosson, D. (1998a) Overexpression of protein kinase C-delta increases tight junction permeability in LLC-PK1 epithelia. Am. J. Physiol. 275, C544-C554.

Mullin, J. M., Ginanni, N. and Laughlin, K. V. (1998b) Protein kinase C activation increases transepithelial transport of biological active insulin. Cancer Res. 58, 1641-1645.

Murer, H., Hopfer, U. and Kinne, R. (1976) Sodium/proton antiport in brush-border membrane vesicles isolated from rat small intestine and kidney. Biochem. J. 154, 597-604.

Nakashima, E., Tsuji, A., Mizuo, H. and Yamana, T. (1984) Kinetics and mechanism of in vitro uptake of amino-beta-lactam antibiotics by rat small intestine and relation to the intact-peptide transport system. Biochem. Pharmacol. 33, (21), 3345-3352.

Nerurkar, M.M., Burton, P.S. and Borchardt, R.T. (1996) The use of surfactants to enhance the permeability of peptides through Caco-2 cells by inhibition of an apically polarized efflux system. Pharm. Res. 13, (4), 528-534.

Neutra, M. and Louvard, D. (1989) Differentiation of intestinal cells in vitro. In Modern Cell Biology: Functional Epithelial Cells in Culture. ed. Matlin, K. S. and Valentich, J. D. 363. New York: A. R. Liss.

Nicklin, P.L. and Irwin, W.J. (1991) Thyrotropin-releasing hormone transport across monolayers of human intestinal absorptive (Caco-2) cells *in vitro*. J. Pharm. Pharmacol. 43, 103P.

Nicklin, P., Irwin, B., Hassan, I., Williamson, I. and Mackay, M. (1992a) Permeable support type influences the transport of compounds across Caco-2 cells. Int. J. Pharm. 83, 197-209.

Nicklin, P.L., Irwin, W.J., Hassan, I.F. and Mackay, M. (1992b) Proline uptake by monolayers of human intestinal absorptive (Caco-2) cells in vitro. Biochim. Biophys. Acta. 1104, 283-292.

Nicklin, P.L., Irwin, W.J., Hassan, I.F. and Mackay, M. (1995) Development of a minimum-calcium caco-2 monolayer model: Calcium and magnesium ions retard the transport of pamidronate. Int. J. Pharm. 123, (2), 187-197.

Nishizuka, Y. (1992) Intracellular signalling by hydrolysis of phospholipids and activation of protein kinase C. Science 258, (5082), 607-614.

Nook, T., Doelker, E. and Bori, I. (1988) Intestinal absorption kinetics of various model drugs in relation to partition coefficients. Int. J. Pharm. 43, 119-129.

Oguchi, S., Walker, W.A. and Sanderson, I.R. (1995) Iron saturation alters the effect of lactoferrin on the proliferation of differentiation of human enterocytes (Caco-2 cells) Biol. Neonate 67, 330-339.

Olsnes, S., Refsnes, K. and Phil, A. (1974) Mechanism of action of the toxic lectins abrin and ricin. Nature 249, 627-631.

Pappenheimer, J.R. and Reiss, K.Z. (1987) Contribution of solvent drag through intercellular junctions to absorption of nutrients by the small intestine of the rat. J. Membr. Biol. 100, (2), 123-136.

Pappenheimer, J.R. and Volpp, K. (1992) Transmucosal impedance of small intestine: Correlation with transport of sugars and amino acids. Am. J. Physiol. 263, C480-C493.

Penaud, J.F., Decroix, M.O. Arnaud, P., Magne, D., Gobert, J.G. and Chaumeil, J.C. (1996) In vitro study of cyclosporin absorption: vehicles and intestinal immaturity. Int. J. Pharm. 142, 1-8.

Peters, W.H. and Roelofs, H.M. (1989) Time-dependent activity and expression of glutathione S-transferases in the human colon adrenocarcinoma cell line Caco-2. Biochem. J. 264, (2), 613-616.

Pinches, S.A., Gribble, S.M., Beechey, R.B., Ellis, A., Shaw J.M. and Shirazi-Beechey, S.P. (1993) Preparation and characterization of basolateral membrane vesicles from pig and human colonocytes: The mechanism of glucose transport. Biochem. J. 294, 529-534.

Pinto, M., Robine-Leon, S., Appay, M.D., Kedinger, M., Triadou, N., Dussaulx, E., Lacroix, B., Simon Assman, P., Haffen, K., Fogh, J. and Zweibaum, A. (1983) Enterocyte-like differentiation and polarization of the human colon carcinoma cell line Caco-2 in culture. Biol. Cell 47, 323-330.

Pitelka, D.R., Taggart, B.N. and Hamamoto, S.T. (1983) Effects of extracellular calcium depletion on membrane topography and occluding junctions of mammary epithelial cells in culture. J. Cell Biol. 96, 613-524.

Plosker, G.L. and McTavish, D. (1996) Intranasal salcatonin (salmon calcitonin): A review of its pharmacological properties and role in the management of postmenopausal osteoporosis. Drugs and Aging 8, (5), 378-400.

Plumb, J.A., Burston, D., Baker, T.G. and Gardner, M.L.G. (1987) A comparison of the structural integrity of several commonly used preparations of rat small intestine *in vitro*. Clin. Sci. 73, 53-59.

Poelma, F.G. and Tukker, J.J. (1987) Evaluation of a chronically isolated internal loop in the rat for the study of drug absorption. J. Pharm. Sci. 76, (6), 433-436.

Powis, D.A., Clark, C.L.and O'Brien and K.J. (1994) Lanthanum can be transported by the sodium-calcium exchange pathway and directly triggers catecholamine release from bovine chromaffin cells. Cell Calcium 16, 377-390.

Procter, D.S. (1973) Oesophageal carcinoma. S. Afr. Med. J. 47, (8), 348-351.

Quai, J.F. (1972) Transport interaction of glycine and cephalexin in rat jejunum. Physiologist 15, 241.

Ranaldi, G., Islam, K. and Sambuy, Y. (1992) Epithelial cells in culture as a model for the intestinal transport of antimicrobial agents. Antimicrob. Agents Chemother. 36, 1374-1381.

Rasmussen, H., Zawalich, K.C., Ganesan, S., Calle, R. and Zawalich, W.S. (1990) Physiology and pathophysiology of insulin secretion. Diabetes Care 13, (6), 655-666.

Read, N.W., Barber, D.C., Levin, R.J. and Holdsworth, C.D. (1977) Unstirred layer and kinetics of electrogenic glucose absorption in the human jejunum in situ. Gut 18, (11), 865-876.

Represa, A., Deloulme, J.C., Sensenbrenner, M., Ben-Ari, Y. and Baudier, J. (1990) Neurogranin: Immunocytochemical localization of a brain-specific protein kinase C substrate. J. Neurosci. 10, (12), 3782-3792.

Riley, S.A., Warhurst, G., Crowe, P.T. and Turnberg, L.A. (1991) Active hexose transport across cultured human Caco-2 cells: Characterisation and influence of culture conditions. Biochim. Biophys. Acta, 1066, 175-182.

Ritschel, W.A. (1991) Targeting in the gastrointestinal tract: new approaches. Methods Find Exp. Clin. Pharmacol. 13, (5), 313-336.

Ritschel, W.A., Grummich, K.W. and Hussain, S.A. (1985) Pharmacokinetics of PFA (trisodium phosphonoformate) after I.V. and P.O. administration to beagle dogs and rabbits. Methods Find. Exp. Clin. Pharmacol. 7, 41-48.

Rochat, T., Burkhard, C., Finci-Cerkez, V. and Meda, P. (1993) Oxidative stress causes a protein kinase C-independent increase of paracellular permeability in an in vitro epithelial model. Am. J. Respir. Cell Mol. Biol. 9, 496-504.

Rodriguez-Yoldi, M. C., Mesonero, J. E. and Rodriguez-Yoldi, M. J. (1996) Effect of Zinc on aminopeptidase N activity and L-threonine transport in rabbit jejunum. Biol. Trace Elem. Res. 53, 213-223.

Rosenberg, D.W. and Leff, T. (1993) Regulation of cytochrome P_{450} in cultured human colonic cells. Arch. Biochem. Biophys. 300, (1), 186-192.

Rossi, A., Poverini, R., Di Lullo, G., Modesti, A., Modica, A. and Scarino, M.L. (1996) Heavy metal toxicity following apical and basolateral exposure in the human intestinal cell line Caco-2. Tox. in Vitro 10, 27-36.

Rubas, W., Villagran, J., Cromwell, M., McLeod, A., Wassenberg, J. and Mrsny, R. (1995) Correlation of solute flux across Caco-2 monolayers and colonic tissue *in vitro* S.T.P. Pharma. Sci. 5, 93-97.

Rubas, W., Jezyk, N. and Grass, G.M. (1993) Comparison of the permeability characteristics of a human colonic epithelial Caco-2 cell line to colon of rabbit, monkey and dog intestine and human drug absorption. Pharm. Res. 10, 113-118.

Rubin, L.L., Hall, D.E., Porter, S., Barbu, K., Cannon, C., Horner, H.C., Janatpour, M., Liaw, C.W., Manning, K., Morales, J., Tanner, L.I., Tomaselli, K.J. and Bard, F. (1991) A cell culture model of the blood-brain barrier. J. Cell Biol. 115, 1725-1735.

Russell-Jones, G.J. (1996) The potential use of receptor-mediated endocytosis for oral drug delivery. Adv. Drug Del. Revs. 20, 83-97.

Russell-Jones, G.J., de Aizpurua, H.J., Howe, P.A. and Rand, K.N. (1986) Oral Vaccines: PCT/AU86/00135/86-N2 (Granted).

Sadowski, D.C. and Meddings, J.B. (1993) Luminal nutrients alter tight-junction permeability in the rat jejunum: an *in vivo* perfusion model. Can. J. Physiol. Pharmacol. 71, 835-839.

Saffran, M., Kumar, G.S., Neckers, D.C., Pena, J., Jones, R.H. and Field, J.B. (1990) Biodegradable azopolymer coating for oral delivery of peptide drugs. Biochem. Soc. Trans. 18, (5), 752-754.

Sanyal, S.N., Jamba, L. and Channan, M. (1992) Effect of the antiprotozoal agent metronidazole (Flagyl) on absorptive and digestive functions of the rat intestine. Ann. Nutr. Metab. 36, (4), 235-243.

Sarosiek, J., Slomiany, A., Takagi, A. and Slomiany, B.L. (1984) Hydrogen ion diffusion in dog gastric mucus glycoprotein: Effect of associated lipid and co-valently bound fatty acids. Biochem. Biophys. Res. Comm. 118, 523-531.

Schanker, L.S., Tocco, D.J., Brodie, B.B. and Hogben, C.A.M. (1985) Absorption of drugs from the rat small intestine. J. Pharmacol. Exp. Ther. 123, 81-88.

Schatzki, P.F. (1971) The passage of radioactive lanthanum from the biliary to the vascular system. Z. Zellforsch. 119, 451-459.

Schipper, N.G.M., Verhoef, J.C., Romeijn, S.G. and Merkus, F.W.H.M. (1995) Methylated β-cyclodextrins are able to improve the nasal absorption of salmon calcitonin. Calcif. Tissue Int. 56, 280-282.

Schneeberger, E.E. and Lynch, R.D. (1992) Structure, function and regulation of cellular tight junctions. Am. J. Physiol. 262, (6), L647-L661.

Schnittler, H.J., Wilke, A., Gress, T., Suttorp, N. and Drenckhahn, D. (1990) Role of actin and myosin in the control of paracellular permeability in pig, rat, and human vascular endothelium. J. Physiol. 431, 379-491.

Seelig, A. (1998) A general pattern for substrate recognition by P-glycoprotein. Eur. J. Biochem. 251, 252-261,

Sergent-Engelen, T., Halleux, C., Ferrain, E., Hanot, H., Legras, R. and Schneider, Y.J. (1990) Improved cultivation of polarized animal cells on culture inserts with new transparent polyethylene terephthalate or polycarbonate microporous membranes. Biotechnol. Tech. 4, 89-94.

Sergent-Engelen, T., Delistrie, V. and Schneider, Y.J. (1993) Phase I and II biotransformations in living Caco-2 cells cultivated under serum-free conditions. Selective apical excretion of reaction products. Belg. Biochem. Pharmacol. 46, (8), 1393-1401.

Shasby, D.M., Winter, M. and Shasby, S. (1988) Oxidant and conductance of cultured epithelial cell monolayers: inositol phospholipid hydrolysis. Am. J. Physiol. 225, C781-C788.

Shaw, R.D., Li, B.U.K., Hamilton, J.W., Shug, A.L. and Olsen, W.A. (1983) Carnitine transport in rat small intestine. Am. J. Physiol. 245, (3), G376-G381.

Shimada, T. and Hoshi, T. (1988) Na+-dependent elevation of the acidic cell suface pH (microclimate pH) of rat jejunal villus cells induced by cyclic nucleotides and phorbol ester: possible mediators of the regulation of the Na+/H+ antiporter. Biochim. Biophys. Acta. 937, (2), 328-334.

Shimanda, T., Yamazaki, H., Mimura, M., Inui, Y. and Guengerich, F.P. (1994) Interindividual variations in human liver cytochrome P-450 enzymes involved in the oxidation of drugs, carcinogens and toxic chemicals: studies with liver microsomes of 30 Japanese and 30 caucasians. J. Pharmacol. Exp. Ther. 270, 414-423.

Shurety, W. and Luzio, J.P. (1995) Differential modulation of apical and basolateral endocytosis in Caco-2 cells. Biochem. Soc. Trans. 23, (2), 184S.

Sillen, L.G. and Martell, A.E. (1964) Stability constants of metal-ion complexes. The Chemical Society, Burlington House, London.

Skou, J.C. and Norby, J.G., Na^+-K^+ATPase: Structure and kinetics. Academic Press, 1979, London.

Sostman, A.L. and Simon, S.A. (1991) Trigeminal nerve responses in the rat elicited by chemical stimulation of the tongue. Archs Oral Biol. 36, (2), 95-102.

Snyder, E.E., Buoscio, B.W. and Falke, J.J. (1990) Calcium (II) site specificity: Effect of size and charge on metal ion binding to an EF-hand-like site. J. Biochem. 29, 3937-3943.

Steinman, R.M., Mellman, I.S., Muller, W.A. and Cohn, Z.A. (1983) Endocytosis and the recycling of plasma membrane. J. Cell. Biol. 96, (1), 1-27.

Stenson, W. F., Easom, R. A., Riehl, T. E. and Turk, J. (1993) Regulation of paracellular permeability in Caco-2 cell monolayers by protein kinase C. Am. J. Physiol. 265 (Gastrointest. Liver Physiol. 28): G955-G962.

Sterchi, E.E. (1981) The distribution of brush border peptidases along the small intestine of the adult human. Pediatr. Res. 15, (5), 884-885.

Sterchi, E.E. and Woodley, J.F. (1980) Peptide hydrolases of the human small intestinal mucosa: Distribution of activities between brush border membranes and cytosol. Clin. Chim. Acta. 102, (1), 49-56.

Stern, M. and Walker, W.A. (1984) Food proteins and gut mucosal barrier. I. Binding and uptake of cow's milk proteins by adult rat jejunum *in vitro*. Am. J. Physiol. 9, G556-G562.

Stevenson, C.L., Augustijns, P.F. and Hendren, R.W. (1995) Permeability screen for synthetic peptide combinatorial libraries using Caco-2 cell monolayers and LC/MS/MS. Pharm. Res. 12, S-94.

Stewart, B.H., Chan, O.H., Lu, R.H., Reyner, E.L., Schmid, H.L., Hamilton, H.W., Steinbaugh, B.A. and Taylor, M.D. (1995) comparison of intestinal permeabilities determined in multiple *in vitro and in situ* models: relationship to absorption in humans. Pharm. Res. 12, (5), 693-699.

Streisand, J.B., Zhang, J., Niu, S., McJames, S. and Natte, R. (1995) Buccal absorption of fentanyl is pH-dependent in dogs. Anesthesiology. 82, 759-764.

Strocchi, A. and Levitt, M.D. (1991) A reappraisal of the magnitude and implications of the intestinal unstirred layer. Gastroenterology. 101, (3), 843-847.

Surendran, N., Nguyen, L.D., Giuliano, A.R. and Blanchard, J. (1995) Enhancment of calcium transport in the Caco-2 cell monolayer model. J. Pharm. Sci. 84, (4), 410-414.

Swenson, E.S., Milisen, W.B. and Curatolo, W. (1994) Intestinal permeability enhancement: Efficacy, acute local toxicity, and reversibility. Pharm. Res. 11, 1132-1142.

Switzer, M.E. (1978) The lanthanide ions as probes of calcium ion binding sites in biological systems. Sci. Prog. 65, (257), 19-30.

Tagliaro, F., Dorizzi, R and Luisetto, G. (1995) Effect of antibodies to calcitonin on the pharmacokinetics and the pharmacodynamics of the hormone. Horm. Metab. Res. 27, 31-34.

Tai, Y. -H., Flick, J., Levine, S. A., Madara, J. L., Sharp, G. W. G. and Donowitz, M. (1996) Regulation of tight junction resistance in T_{84} monolayers by elevation in intracellular Ca^{2+}: A protein kinase C effect. J. Membr. Biol. 149, 71-79.

Takahashi, S., Goldring, S., Katz, M., Hilsenbeck, S., Willliams, R. and Roodman, G.D. (1995) Downregulation of calcitonin receptor mRNA expression by calcitonin during human osteoclast-like cell differentiation. J. Clin. Invest. 95, 167-171.

Tamai, I., Takanaga, H., Maeda, H., Ogihara, T., Yoneda, M. and Tsuji, A. (1995) Proton-cotransport of pravastatin across intestinal brush-border membrane. Pharm. Res. 12, 1727-1732.

Tanaka, Y., Taki, Y., Sakane, T., Nadai, T., Sezaki, H. and Yamashita, S. (1995) Characterization of drug transport through tight-junctional pathway in Caco-2 monolayer: Comparison with isolated rat jejunum and colon. Pharm. Res. 12, (4), 523-528.

Tarpey, P.S., Vayro, S., Shirazi-Beechey, S.P. and Beechey, R.B. (1992) Na(+)-dependent orthophosphate and D-glucose symporters of the sheep parotid acinar cell: Expression in Xenopus oocytes. Biochem. Soc. Trans. 20, (4), 328S.

Taylor, C.W. and Broad, L.M. (1998) Pharmacological analysis of intracellular Ca^{2+} signalling: Problems and pitfalls. TiPS 19, 370-375.

Taylor, E.W., Gibbons, J.A. and Braeckman, R.A. (1997) Intestinal absorption screening of mixtures from combinatorial libraries in the Caco-2 model. Pharm. Res. 14, (5), 572-577.

Thiebaut, F., Tsuruo, T., Hamada, H., Gottesman, M.M., Pastan, I. and Willingham, M.C. (1987) Cellular localization of the multidrug-resistance gene product P-glycoprotein in normal human tissues. Proc. Natl. Acad. Sci. U.S.A. 84, 7735-7738.

Thomson, A.B. and Dietschy, J.M. (1977) Derivation of the kinetics that describe the effects of unstirred waters layers on the kinetic parameters of active transport processes in the intestine. J. Theor. Biol. 64, 277-294.

Thwaites. D.T., Hirst, B.H. and Simmons, N.L. (1993) Passive transepithelial absorption of thyrotropin-releasing hormone (TRH) via a paracellular route in cultured intestinal and renal epithelial cell lines. Pharm. Res. 10, (5), 674-681.

Tien, X-Y., Katnik, C., Qasawa, B.M., Sitrin, M.D., Nelson, D.J. and Brasitus, T.A. (1993) Characterization of the 1,25-dihydroxycholecalciferol-stimulated calcium influx pathway in Caco-2 cells. J. Membr. Biol. 136, 159-168.

Tomita, M., Hayashi, M., Horie, T., Ishizawa, T. and Awazu, S. (1988) Enhancement of colonic drug absorption by the transcellular permeation route. Pharm. Res. 5, (12), 786-789.

Tozaki, H., Emi, Y., Horisaka, E., Fujita, T., Yamamoto, A. and Muranishi, S. (1997) Degradation of insulin and calcitonin and their protection by various protease inhibitors in rat caecal contents: Implications in peptide delivery to the colon. J. Pharm. Pharmacol. 49, 164-168.

Turner, N.C., Martin, G.P. and Marriott, C (1985) The influence of native porcine gastric mucus gel on hydrogen ion diffusion: the effects of potentially ulcerogenic agents. J. Pharm. Pharmacol. 37, 776-780.

Ungell, A. and Andreasson, A. (1990) The effect of enzymatic inhibition versus increased paracellular route of transport of vasopressin peptides. J. Contr. Rel. 13, 313.

Ussing, H.H. and Zerahn, K. (1951) Active transport of sodium as the source of electric current in the short-circuited isolated frog skin. Acta. Physiol. Scand. 23, 110-127.

Utz, I., Hofer, S., Regenass, U., Hilbe, W., Thaler, J., Grunicke, H. and Hofmann, J. (1994) The protein kinase C inhibitor CGP 41251, a staurosporine derivative with antitumor activity reverses multidrug resistance. Int. J. Cancer. 57, (1), 104-110.

van Beers, E.H., Al, R.H., Rings, E.H.H.M., Einerhand, W.C., Dekker, J. and Buller, H.A. (1995) Lactase and sucrase-isomaltase gene expression during Caco-2 cell differentiation. Biochem. J. 308, 769-775.

van Bree, J.B.M.M., de Boer, A.G., Danhof, M., Ginsel, L.A. and Breimer, D.D. (1988) Characterization of an "in vitro" blood-brain barrier: Effects of molecular size and lipophilicity on cerebrovascular endothelial transport rates of drugs. J. Pharmacol. Exp. Ther. 247, 1233-1239.

van Hoogdalem, E.J., de-Boer, A.G. and Breimer, D.D. (1989) Intestinal drug absorption enhancement: An overview. Pharmacol. Ther. 44, (3), 407-443.

Wacher, V.J., Wu, C.-Y. and Benet, L.Z. (1995) Overlapping substrate specificities and tissue distribution of cytochrome P_{450} 3A and P-glycoprotein: implications for drug delivery and activity in cancer chemotherapy. Mol. Carcinog. 13, 129-134.

Wacher, V.J., Salphati, L. and Benet L.Z. (1996) Active secretion and enterocytic drug metabolism barriers to drug absorption. Adv. Drug Del. Revs. 20, 99-112.

Wada, S., Udagawa, N., Nagata, N., Martin, T.J. and Findlay, D.M. (1996) Physiological levels of calcitonin regulate the mouse osteoclast calcitonin receptor by a protein kinase Alpha-mediated mechanism. Endocrinol. 137, (1), 312-320.

Walker, W.A., Cornell, R., Davenport, L.M. and Isselbacher, K.J. (1972) Macromolecular absorption. Mechanism of horseradish peroxidase uptake and transport in adult and neonatal rat intestine. J. Cell Biol. 54, 195-205.

Walter, E. and Kissel, T. (1994) Transepithelial transport and metabolism of thyrotropin-releasing hormone (TRH) in monolayers of a human intestinal cell line (Caco-2): Evidence for an active transport component? Pharm. Res. 11, (11), 1575-1580.

Walter, E. and Kissel, T. (1995) Heterogeneity in the human intestinal cell line Caco-2 leads to differences in transepithelial transport. Eur. J. Pharm. Sci. 3, 215-230.

Walter, E., Janich, S., Roessler, B.J., Hilfinger, J.M. and Amidon, G.L. (1996) HT29-MTX/Caco-2 cocultures as an in vitro model for the intestinal epithelium: *In vitro-in vivo* correlation with permeability data from rats and humans. J. Pharm. Sci. 85, (10), 1070-1076.

Wang, W. (1996) Oral protein drug delivery. J. Drug Target. 4, (4), 195-232.

Watkins, P.B. (1994) Non-invasive tests of CYP3A enzymes. Pharmacogenetics 4, 171-184.

Watkins, P.B., Wrighton, S.A., Schuetz, E.G. and Guzelian, P.S. (1987) Identification of glucocorticoid-inducible cytochromes P_{450} in the intestinal mucosa of rats and man. J. Clin. Invest. 80, 1029-1036.

Welsh, M.J., Shasby, D.M. and Husted, R.M. (1985) Oxidants increase paracellular permeability in a cultured epithelial cell line. J. Clin. Invest. 76, (3), 1155-1168.

Whittembury, G. and Rawlins, F.A. (1971) Evidence of a paracellular pathway for ion flow in the kidney proximal tubule: Electromicroscopic demonstration of lanthanum precipitate in the tight junction. Pflügers Arch. 330, 302-309.

Wien, E.M. and van Campen, D.R. (1991) Ferric iron absorption in rats: relationship to iron status, endogenous sulfhdryl and other redox components in the intestinal lumen. J. Nutr. 121, 825-831.

Wikman-Larhed, A and Artursson, P. (1995) Co-cultures of human intestinal goblet (HT29-H) and absorptive (Caco-2) cells for studies of drug and peptide absorption. Eur. J. Pharm. Sci. 3, 171-183.

Wils, P., Legrain, S., Frenois, E. and Scherman, D. (1993) HT-29-18C1 intestinal cells: A new model for studying the epithelial transport of drugs. Biochim. Biophys. Acta. 1177, 134-138.

Wils, P., Warnery, A., Phung-Ba, V. Legrain, S. and Scherman, D. (1994) High lipophilicity decreases drug transport across intestinal epithelial cells. J. Pharmacol. Exp. Ther. 269, (2), 654-658.

Wilson, G., Hassan, I. F., Dix, C.J., Williamson, I., Shah, R., Mackay, M. and Artursson, P. (1990) Transport and permeability properties of human Caco-2 cells: an *in vitro* model of the intestinal epithelial cell barrier. J. Contr. Rel. 11, 25-40.

Wilson, T.H. and Wiseman, G. (1954) The use of sacs of everted small intestine for the study of the transference of substances from the mucosal to the serosal surface.J. Physiol. 123, 116-125.

Wimalawansa, S.J. (1993) Long- and short-term side effects and safety of calcitonin in man: A prospective study. Calcif. Tissue Int. 52, 90.

Winne, D. and Verheyen, W. (1990) Diffusion coefficient in native mucus gel of the rat small intestine. J. Pharm. Pharmacol. 42, 517-519.

Wolfe, D.L., Forland, S.C. and Benet, L.S. (1973) Drug transfer across intact rat intestinal muscosa following surgical removal of serosa and muscularis externa. J. Pharm. Sci. 62, (2), 200-205.

Woodcock, S., Williamson, I., Hassan, I. and Mackay, M. (1991) Isolation and characterization of clones from the Caco-2 cell line displaying increased taurocholic acid transport. J. Cell Sci. 98, 323-332.

Woodley, J.F. (1994) Enzymatic barriers for GI peptide and protein delivery. Clin. Revs. Ther. Carrier Syst. 11, (2&3), 61-95.

Yokohama, S., Yoshioka, T., Yamashita, K. and Kitamori, N. (1984) Intestinal absorption mechanisms of thyrotropin-releasing hormone. J. Pharmacobiodyn. 7, (7), 445-451.

Yamamoto, A., Taniguchi, T., Rikyuu, K., Tsuji, T., Fujita, T., Murakami, M. and Muranishi, S. (1994) Effects of various protease inhibitors on the intestinal absorption and degradation of insulin in rats. Pharm. Res. 11, (10), 1496-1500.

Yamashita, S., Tanaka, Y., Endoh, Y., Taki, Y., Sakane, T., Nadai, T. and Sezaki, H. (1997) Analysis of drug permeation across Caco-2 monolayer: Implication for predicting *in vivo* drug absorption. Pharm. Res. 14, (4), 486-491.

Yap, A.S., Mullin, J.M. and Stevenson, B.R. (1998) Molecular analyses of tight junction physiology: Insights and paradoxes. J. Membr. Biol. 163, 159-167.

Yu, H. and Sinko, P.J. (1997) Influence of the microporous substratum and hydrodynamics on resistances to drug transport in cell culture systems: Calculation of intrinsic transport parameters. J. Pharm. Sci. 86, (12), 1448-1457.

Yu, H., Cook, T.J. and Sinko, P.J. (1997) Evidence for diminished functional expression of intestinal transporters in Caco-2 cell monolayers at high passages. Pharm. Res. 14, (6), 757-762.

Zimmerman, J., Salhub, J. and Rosenberg, I.H. (1986) Role of sodium ion in transport of folic acid in the small intestine. Am. J. Physiol. 251, G218-G222.

APPENDIX 1 ABBREVIATIONS

Amino acids in polypeptide sequences are abbreviated as follows:

Ala	Alanine	Glu	Glutamic acid
Arg	Arginine	Gln	Glutamine
Asn	Asparagine	Gly	Glycine
Asp	Aspartic acid	His	Histidine
Cys	Cysteine	Ile	Isoleucine
Leu	Leucine	Ser	Serine
Lys	Lysine	Thr	Threonine
Met	Methionine	Trp	Tryptophan
Phe	Phenylalanine	Tyr	Tyrosine
Pro	Proline	Val	Valine

$1,25(OH)_2D_3$	1,25-dihydroxycolecalciferol
Å	Angstrom
ACE	Angiotensin converting enzyme
ANOVA	Analysis of variance
Ap	Apical
ATP	Adenosine triphosphate
ATPase	Adenosine triphosphatase
BBMV	Brush border membrane vesicles
Bl	Basolateral
BLMV	Basolateral membrane vesicles
BSA	Bovine serum albumin
cAMP	Cyclic adenosine monophosphate
Cbl	Cobalamin
CHPP	N-(3-chlorphenyl)-4-[2-(3-hydroxypropylamino)-4-pyridyl]-2-pyrimidinamin
C_i	Substrate concentration
CPM	Counts per minute
CT	Calcitonin
CYP3A	Cytochrome P_{450} Sub 3A
DIDS	4,4'-Diisothiocyanatostilbene-2,2'-disulphonic acid
DMEM	Dulbecco's modification of Eagle's medium
DMSO	Dimethyl sulphoxide
DNA	Deoxyribonucleic acid
DPM	Decays per minute
EDTA	Ethylenediaminetetraacetic acid
EGF	Epidermal growth factor
FBS	Foetal bovine serum
GI	Gastro-intestinal
GLUT-1 to 5	Facilitative hexose transporters
h	Hour
hCT	Human calcitonin
HBSS	Hanks balanced salt solution
HEPES	N-[2-hydroxyethyl]piperazine-N'-[2-ethanesulphonic acid]
hPTH	Human parathyroid hormone

HMG-CoA	3-hydroxy-3-methyl-glutaryl coenzyme A
HPLC	High performance liquid chromatography
HRP	Horseradish peroxidase
HRT	Hormone replacement therapy
HSA	Human serum albumin
IC_{50}	Concentration at 50% inhibition
i.d.	Intraduodenal
IGF	Insulin growth factor
i.m.	Intramuscular
INF-γ	Interferon-gamma
IRMA	Immunoradiometric assay
i.v.	Intravenous
J_i	Total flux
J_{max}	Maximum transport rate
kDa	kilodaltons
K_m	Substrate concentrtion at half V_{max}
K_t	Substrate concentration half J maximum
LDH	Lactate dehydrogenase
LHRH	Lutenizing hormone releasing hormone
Log D	Partition coefficient at specific pH
Log P	Partition coefficient
LSC	Liquid scintillation counter
MDCK	Madin-Darby canine kidney
MDR-1	Multi-drug resistance-1
MeCN	Acetonitrile
MES	2-[N-Morpholino]ethane-sulphonic acid
M_r	Relative molecular mass
mRNA	Messenger ribosenucleic acid
MTT	3-[4,5-dimethylthiazol-2yl]-2,5-diphenyltetrazolium bromide
NADH	Nicotinamide adenine dinucleotide reduced form
NBS	N-benzoyl-staurosporine
NEAA	Non essential amino acids
P_{app}	Apparent permeability coefficient
PBS	Phosphate buffered saline
PBS-N_3	Phosphate buffered saline with 0.04% w/v sodium azide
PEG's	Polyethylene glycols
Per os	By mouth
P-gp	P-glycoprotein
pK_a	Log acid dissociation constant
PKC	Protein kinase C
PMSF	Phenylmethylsulphonyl fluoride
PS	Penicillin and streptomycin
RME	Receptor mediated endocytosis
RNA	Ribonucleic acid
sCT	Salmon calcitonin
SDS	Sodium dodecyl sulphate
SEDDS	Self emulsifying drug delivery system
SEM	Standard error of the mean
SGLT-1	Sodium dependent glucose transporter

t	Time
TB	Transport buffer
$TB_{CHOLINE}$	Transport buffer with sodium substitution with choline chloride
TB_{EtOH}	Transport buffer with ethanol
$TB_{GLUCOSE}$	Glucose free transport buffer
TB_{NOBSA}	Transport buffer with no bovine serum albumin
TER	Transepithelial electrical resistance
TGF-β	Transforming growth factor-beta
TNF	Tissue necrosing factor
μCi	Microcurries
V_{max}	Maximal velocity